MAY 0 4 1990

671-F

I 72.12/2: 88-0046/v.2

OCS Study
MMS 88-0046

Gulf of Mexico Physical Oceanography Program Final Report: Year 3

Volume II: Technical Report

ORIGINAL
COMPLETED

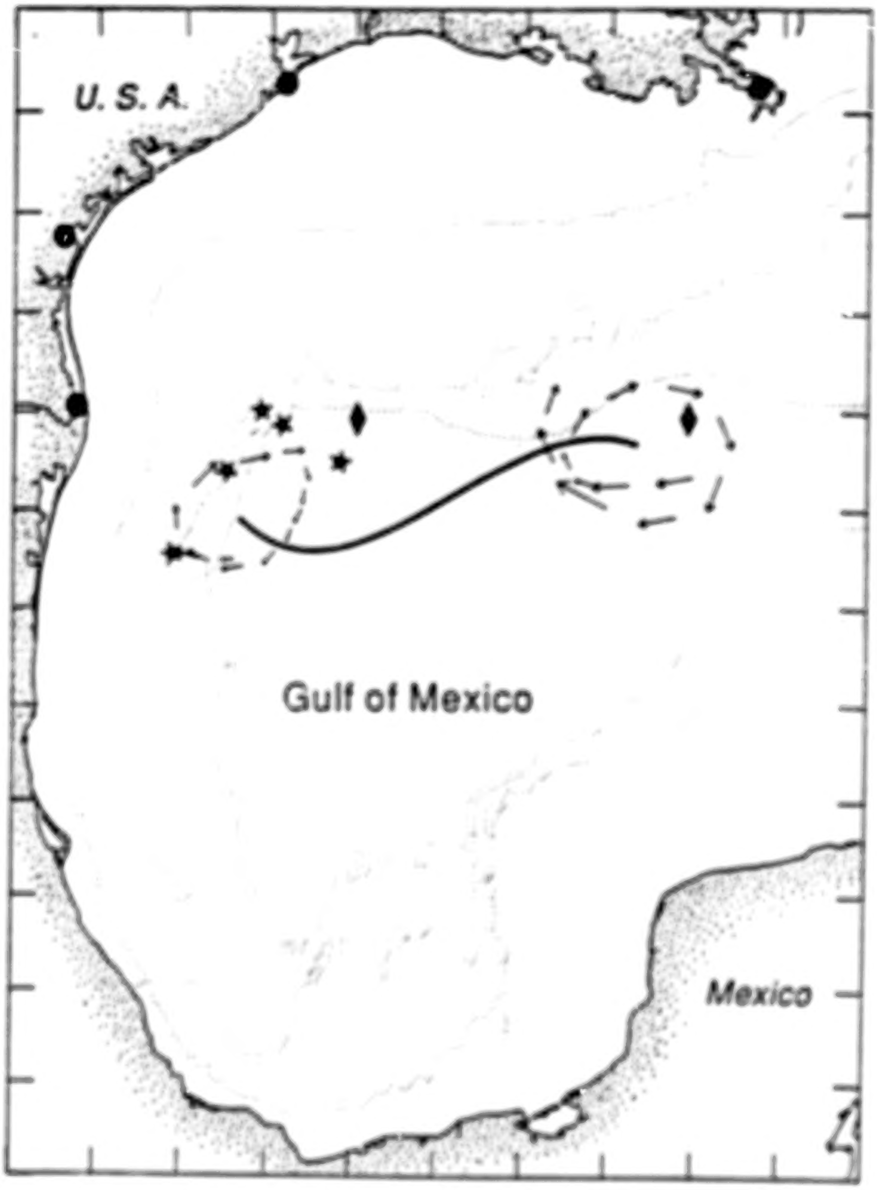

U.S. Department of the Interior
Minerals Management Service
Gulf of Mexico OCS Region

OCS Study
MMS 88-0046

Gulf of Mexico Physical Oceanography Program Final Report: Year 3

Volume II: Technical Report

Author

Science Applications International Corporation

Prepared under MMS Contract
14-12-0001-29158
by
Science Applications International Corporation
Raleigh, North Carolina 27606

Program Manager:
Evans Waddell, Ph.D.
Science Applications International Corporation
Raleigh, North Carolina 27606

Project Officer:
Murray L. Brown, Ph.D.
Minerals Management Service
Gulf of Mexico OCS Regional Office

Published by

U.S. Department of the Interior
Minerals Management Service
Gulf of Mexico OCS Regional Office

New Orleans, Louisiana
September 1988

BLANK PAGE

DISCLAIMER

This report was prepared under contract between the Minerals Management Service (MMS) and Science Applications International Corporation. This report has been technically reviewed by the MMS and approved for publication. Approval does not signify that contents necessarily reflect the views and policies of the Service, nor does mention of trade names or commercial products constitute endorsement or recommendation for use. It is, however, exempt from review and compliance with MMS editorial standards.

REPORT AVAILABILITY

Extra copies of the report may be obtained from the Public Information Unit (Mail Stop OPS-3-4) at the following address:

U.S. Department of the Interior
Minerals Management Service
Gulf of Mexico OCS Regional Office
1201 Elmwood Park Boulevard
New Orleans, Louisiana 70123-2394

Attention: Public Information Unit (OPS-3-4)

(Telephone Number: (504) 736-2519)

CITATION

Science Applications International Corporation, 1988, Gulf of Mexico physical oceanography program, final report: year 3. Volume II; technical report, OCS Report/MMS 88-0046, U.S. Dept. of the Interior, Minerals Mgmt. Service, Gulf of Mexico OCS Regional Office, New Orleans, LA. 241 pp.

BLANK PAGE

TABLE OF CONTENTS

Section | Page

Table of Contents v
List of Figures ix
List of Tables xxiii
Acknowledgements xxv

I. INTRODUCTION

1.1 Program Objectives 1

1.2 Program Background 1

1.3 Program Elements and Participants 1

1.3.1 Key Observations 1
1.3.2 Key Scientific Personnel 3

1.4 Report Organization 3

1.5 References for Chapter I 4

II. DATA ACQUISITION

2.1 Introduction 5

2.2 Drifter and Associated Data 5

2.2.1 Introduction 5
2.2.2 Separation of Eddy B from the Loop Current 9
2.2.3 Westward Movement of Eddy B 9
2.2.4 Interactions in the Western Gulf of Mexico 11

2.3 Hydrography 11

2.3.1 Introduction 11
2.3.2 Cruise Summaries 11

2.3.2.1 R/V PELICAN 11
2.3.2.2 B/O ALTAIR 13

2.3.3 Shipboard Operations 13

2.3.3.1 Equipment 13
2.3.3.2 Sampling Procedures 20

2.3.4 AXBT Survey 22

2.3.4.1 Introduction 22
2.3.4.2 Field Procedures 23

2.3.5 Ship-of-Opportunity (SOOP) Data 26

TABLE OF CONTENTS

Section | Page

2.3.5.1 Introduction 26
2.3.5.2 Equipment 26
2.3.5.3 SOOP Sections and Data Products 26

2.4 Satellite Imagery 26

2.5 Subsurface Currents 30

2.5.1 Introduction 30
2.5.2 Mooring Locations 30
2.5.3 Mooring Design 33
2.5.4 Aanderaa Current Meters 33
2.5.5 Deployment Period and Data Return 34

2.6 References for Chapter II 34

III. DATA ANALYSIS 38

3.1 Introduction 38

3.2 Drifting Buoys 38

3.2.1 Introduction 38
3.2.2 Kinematic Parameters and Procedures 38
3.2.3 Flow Field Estimation 39

3.3 Survey Data 40

3.3.1 CTD and XBT Data Calibration 40
3.3.2 Estimation of Dynamic Heights from XBT Data 41

3.4 Satellite Imagery 44

3.5 Subsurface Currents 44

3.6 References for Chapter III 44

IV. TECHNICAL DISCUSSION 49

4.1 Introduction 49

4.2 General Chronology 49

4.3 Eddy Separation and Initial Movement 60

4.3.1 Introduction 60
4.3.2 Separation of Eddy B 68

4.3.2.1 SST and Path Data 68
4.3.2.2 Loop Current vs. Eddy Kinematics 75

TABLE OF CONTENTS

Section Page

4.3.2.3 Kinematics Before and After an Eddy Detachment 75

4.3.3 Initial Eddy Configuration 83

4.3.3.1 Temperature and Salinity 83
4.3.3.2 Nutrients 83
4.3.3.3 Velocity 83

4.3.4 Westward Translation after Separation (Northern Route) 90

4.3.4.1 SST and Path Data 90
4.3.4.2 Eddy-Related Processes 90

4.3.5 Receiving Field 100

4.3.5.1 Time Domain Description 101
4.3.5.2 Statistical Characteristics of the Velocity Field 109
4.3.5.3 Frequency Domain Description 116

4.3.5.3.1 Autospectra 117
4.3.5.3.2 Rotary Spectra 119
4.3.5.3.3 Vertical and Horizontal Coherence 123

4.4 Eddy-Slope Interaction and Cyclone Intensification in the Western Gulf 133

4.4.1 Introduction 133
4.4.2 Sea-Surface Temperature and Surface Processes 138
4.4.3 Surface Currents and Dynamics in the Western Gulf 152

4.4.3.1 SST and Path Data 152
4.4.3.2 Interaction with Eddy A 154

4.4.4 Hydrographic Characterizations 160

4.4.4.1 AXBT Survey (November 1985) 160
4.4.4.2 B/O ALTAIR Hydrographic Cruise (January 23 to February 5, 1986) 166

4.4.4.2.1 Temperature 166
4.4.4.2.2 Salinity 166
4.4.4.2.3 Nutrients 174
4.4.4.2.4 The Question of Interaction between Eddy A and Eddy B 182

4.4.5 Subsurface Currents 182

4.4.5.1 Time Domain Description 182
4.4.5.2 Basic Characteristics of the Velocity Fields 185
4.4.5.3 Frequency Domain Description 190

TABLE OF CONTENTS

Section Page

4.4.5.3.1 Autospectra 190
4.4.5.3.2 Rotary Spectra 190
4.4.5.3.3 Vertical and Horizontal Coherence 194

4.5 Eddy Reflection and Dissipation 203

4.5.1 Introduction 203
4.5.2 Surface and Near-Surface Currents 203

4.5.2.1 Sea-Surface Temperature and Surface Processes........... 203
4.5.2.2 SST and Path Data 206

4.5.3 Temperature Fields 212

4.6 Eddy-Eddy Interaction (May 1985 and Onward)................. 212

4.6.1 Introduction 212
4.6.2 Surface Currents 216

4.6.2.1 Interaction with Eddy C 216

4.6.3 Temperature Fields 221

4.6.3.1 Consolidation of Eddies B and C 221
4.6.3.2 Western Gulf of Mexico XBT Surveys in 1987 221

4.7 References for Chapter IV 239

LIST OF FIGURES

Figure No.	Caption	Page
1.2-1.	Study area for the Gulf of Mexico Physical Oceanography Program	2
2.2-1.	Trajectory for: (a) Drifter 3378 and (b) Drifter 5495. The presence of Eddy A was detected at ~93°W when Drifter 5495 began making anticyclonic loops	6
2.2-2.	Trajectory for: (a) Drifter 3334 from mid-June through mid-September 1985 and Drifter 3378 from mid-July through September 1985 (also shown is the location of Eddy A during August and September 1985) and (b) Drifter 3379	7
2.3-1.	Cruise track of the R/V PELICAN and the location of all CTD and XBT stations occupied for the period from October 21-24, 1985	12
2.3-2.	Cruise track of the R/V PELICAN and the path of Hurricane Juan for the period from October 21 -31, 1985	15
2.3-3a-b.	Cruise track of the B/O ALTAIR for the period from January 22 through February 6, 1986 and the location of all: (a) CTD and XBT stations and (b) S-4 20-meter depth current measurement stations	16
2.3-3c.	Cruise track of the B/O ALTAIR for the period from January 22 through February 6, 1986 and the location of all plankton tow stations	17
2.3-4.	Schematic of CTD system used during: (a) the first hydrographic cruise aboard the R/V PELICAN (October 21-29, 1985) and (b) the second hydrographic cruise aboard the B/O ALTAIR (January 22 through February 6, 1986)	21
2.3-5.	Flight track and the location of all AXBT and AXCP stations for the Year 3 aerial survey for the period from November 11-13, 1985	24
2.3-6.	Examples of cruise tracks for typical MMS Ship of Opportunity data sets obtained in the western Gulf	28
2.3-7.	Examples of data products generated for each SOOP cruise: (a) surface parameters and (b) vertical temperature	29

LIST OF FIGURES

Figure No.	Caption	Page
2.5-1.	Mooring locations in the western Gulf of Mexico for Year 3 of the MMS-sponsored Gulf of Mexico Physical Oceanography Program	31
2.5-2.	Time line of the deployment periods and data return for each current meter level for instruments deployed in the western Gulf of Mexico Physical Oceanography Program	35
3.3-1.	Data plots and regression fits of CTD minus XBT depth differences for the same isotherms versus T-7 XBT isotherm depths for the October 1985 and January 1986 cruises	42
3.3-2.	Composite T-S plot of all CTD data collected during the October 1985 R/V PELICAN cruise	43
3.3-3.	Composite T-S plot of all CTD data collected during the January 1986 B/O ALTAIR cruise	45
3.3-4.	T-S diagram of Station 20 in the center of Eddy B from October 1986	46
3.3-5.	Plot of the dynamic heights and the difference between true and synthetic dynamic heights derived from XBT data for 150-650 decibars for the R/V PELICAN cruise in October 1985	47
4.2-1.	Partial trajectory for Drifter 3378 and the locations of the five current meter moorings (P, Q, R, S and T)	51
4.2-2.	Trajectory of Drifter 3378 during the month of October 1985	52
4.2-3.	Topography of the 8°C temperature surface based on CTD and XBT data from the R/V PELICAN survey and XBT data from the B/O ALTAIR	53
4.2-4.	Vertical temperature section to 800m based on R/V PELICAN CTD data	54
4.2-5.	Trajectory of Drifter 3378 during the month of November 1985	56
4.2-6.	Topography of the 8°C temperature surface based on the AXBT survey	57

LIST OF FIGURES

Figure No.	Caption	Page
4.2-7.	Trajectory of Drifter 3378 during the months of December 1985 and January 1986	58
4.2-8.	Topography of the 8°C temperature surface based on CTD and XBT data from the B/O ALTAIR survey	59
4.2-9.	Trajectory of Drifter 3378 during the months of February and March 1986	61
4.2-10.	Trajectory of Drifter 3378 during the month of April 1986	62
4.2-11.	Topography of the 8°C temperature surface based on all SOOP XBT data collected by the B/O ALTAIR during the period from April 27 to May 14, 1986	63
4.2-12.	Trajectory of Drifter 3379 during the months of March and April 1986	64
4.2-13.	Trajectory of Drifter 3379 during the months of May and June 1986	65
4.2-14.	Trajectory of Drifter 3379 during the months of July and August 1986	66
4.2-15.	Topography of the 8°C temperature surface based on all SOOP XBT data collected by the HO-2 during the period from August 17-22, 1986	67
4.3-1.	(a) Cruise tracks for SOOP XBT data collected during May 26-31, 1985. The vertical temperature structure is shown for data from: (b) the E.M. QUEENY cruise, May 26-27, 1985; (c) the STENA HISPANIA cruise, May 27-28, 1985; and (d) the STENA HISPANIA cruise, May 30-31, 1985	69
4.3-2.	SST data (°C) for June 18-24, 1985 with drifter trajectories shown	70
4.3-3.	(a) Cruise tracks for SOOP XBT data collected during June 26 through July 2, 1985. The vertical temperature structure is shown for data from: (b) the STENA HISPANIA cruise, June 26-28, 1985; (c) the STENA HISPANIA cruise, June 29-30, 1985; and (d) the E.M. QUEENY cruise, July 1-2, 1985	71
4.3-4.	SST data (°C) for June 29 through July 5, 1985 with drifter trajectories shown	72

LIST OF FIGURES

Figure No.	Caption	Page
4.3-5.	(a) Cruise tracks for SOOP XBT data collected during July 16-19, 1985. The vertical temperature structure is shown for data from: (b) and (c) the M/V NAT CO 6 cruise, July 16-19, 1985 and (d) the STENA HISPANIA cruise, July 16-17, 1985	73
4.3-6.	SST data (°C) for July 16-23, 1985 with drifter trajectories shown	74
4.3-7.	(a) Cruise track for SOOP XBT data collected by the STENA HISPANIA August 16-18, 1985 and (b) the vertical temperature structure	76
4.3-8a-b.	SST data (°C) for: (a) August 7-13, 1985 and (b) September 10-17, 1985 with drifter trajectories shown	77
4.3-8c.	SST data (°C) for September 17-24, 1985 with drifter trajectories shown	78
4.3-9.	Time histories of: (a) the filtered observed speed components for Eddy B and (b) the swirl speed components about the center of rotation for Eddy B	79
4.3-10.	Time history of: (a) the distance to the center of rotation of Eddy B as seen by Drifter 3378, (b) the rotational frequency of Eddy B and (c) the eccentricity and major axis orientation for Eddy B	80
4.3-11.	Time histories of: (a) the filtered observed speed components for Drifter 3354, (b) the swirl speed components about the center of rotation for the Loop Current and (c) the east/west and north/south distances for Drifter 3354 from the center of rotation in the Loop Current	81
4.3-12.	Time history of: (a) the rotational frequency within the Loop Current and (b) the Loop Current eccentricity (asterisk) and the orientation of the major axis (dashed line)	82
4.3-13.	Topography of the 8°C temperature surface based on all XBT data collected by the M/V NAT CO 6 during the period from July 16-19, 1985	84

LIST OF FIGURES

Figure No.	Caption	Page
4.3-14.	Vertical section of salinity along the R/V PELICAN CTD transect through Eddy B....................	85
4.3-15.	Composite T-S plot of all CTD data collected during the October 1985 R/V PELICAN cruise............	86
4.3-16.	Vertical section of Sigma-t to 1500m along the R/V PELICAN CTD transect through Eddy B................	87
4.3-17.	Vertical section of (a) dissolved oxygen, (b) silicate and (c) phosphate to 1500m along R/V PELICAN CTD transect through Eddy B................	88
4.3-18.	Vertical section of geostrophic velocities relative to 950m for the R/V PELICAN CTD transect through Eddy B..	89
4.3-19.	Stick-vector time series of 40-hour, low-passed currents recorded at Mooring R..........................	91
4.3-20.	SST data (°C) for September 25 through October 1, 1985 with drifter trajectories shown................	92
4.3-21.	SST data (°C) for October 23-29, 1985 with drifter trajectories shown	93
4.3-22.	Topography of the 8°C temperature surface based on all XBT data collected by the NAT CO 6 during the period from July 16-19, 1985.......................	95
4.3-23a.	SST data (°C) for November 6-12, 1985 with drifter trajectories shown.............................	97
4.3-23b-c.	SST data (°C) for (b) November 13-19, 1985 and (c) November 20-26, 1985, both with drifter trajectories shown..	98
4.3-23d-e.	SST data (°C) for: (d) December 11-17, 1985 and (e) December 22-28, 1985, both with drifter trajectories shown..	99
4.3-24.	(a) Vertical section of temperature along the line between Moorings T and P and (b) cruise track based on XBT data collected by the B/O ALTAIR during the period from October 18-19, 1985..	102
4.3-25.	Stick plots of 40-hour, low-passed currents at Mooring Q for the first deployment period..............	103

LIST OF FIGURES

Figure No.	Caption	Page
4.3-26.	Stick plots of 40-hour, low-passed currents at Mooring P for the first deployment period..............	104
4.3-27.	Stick plots of 40-hour, low-passed currents at Mooring S for the first deployment period..............	105
4.3-28.	Stick plots of 40-hour, low-passed currents at Mooring T for the first deployment period..............	106
4.3-29.	An illustration of the vector subtraction of the observed velocity on October 17, 1985 at Mooring R for the first deployment period.......................	108
4.3-30.	A subjectively drawn stream function field that is consistent with the pattern of observed currents at 100m on August 15, 1985.....................	110
4.3-31.	Forty-hour, low-passed temperature series at Mooring S from July 28 through September 27, 1985......	111
4.3-32.	Forty-hour, low-passed temperature series at Mooring Q from July 28 through September 27, 1985......	112
4.3-33.	Time-series plots of 40-hour, low-passed stick vectors, and 3-hour and 40-hour, low-passed U and V components and temperature for the first deployment period at Mooring P at 1000m................	113
4.3-34.	Mean values, over the record length, of velocity presented in vector form for the first deployment period: June 17 through October 20, 1985..................	115
4.3-35.	Spectra for Mooring R at 300m: U, V and temperature for the 107-day period beginning June 17, 1985..	118
4.3-36.	Spectra for Mooring R at 1500m: U, V and temperature for the 107-day period beginning June 17, 1985..	120
4.3-37.	Spectra for Mooring Q at 100m: U, V and temperature for the 107-day period beginning June 17, 1985..	121
4.3-38.	Spectra for Mooring Q at 1000m: U, V and temperature for the 107-day period beginning June 17, 1985..	122

LIST OF FIGURES

Figure No. Caption Page

4.3-39. Rotary spectra for Mooring P at 1000m for the 107-day period beginning June 17, 1985 124

4.3-40. Rotary spectra at 1000m for the first deployment period beginning June 18, 1985 for (a) Mooring S and (b) Mooring T 125

4.3-41. Vertical, cross-spectral coherence and phase at Mooring Q between 100m and 300m, and between 300m and 1000m: U, V and temperature for the 99-day period beginning June 21, 1985 126

4.3-42. Vertical, cross-spectral coherence and phase at Mooring Q between 1000m and 1500m: (a) U components of velocity and (b) V components for the 99-day period beginning June 21, 1985 127

4.3-43. Horizontal, cross-spectral coherence and phase at 1000m between Moorings Q and R: (a) U component of velocity and V components for the 99-day period beginning June 21, 1985 129

4.3-44. Horizontal, cross-spectral coherence and phase at 1500m between Moorings P and Q for U component of velocity (solid line) and V component of velocity (dashed line) for the 99-day period beginning June 21, 1985 130

4.3-45. Horizontal, cross-spectral coherence and phase at 1000m between Moorings P and S: (a) U component of velocity and (b) V component of velocity for the 99-day period beginning June 21, 1985 131

4.3-46. Rotary cross-spectral coherence and phase at 1000m between Moorings S and T: (a) inner coherence and phase and (b) outer coherence and phase 132

4.4-1. NOAA-9 SST (°C) analysis in the western Gulf of Mexico for November 19, 1985 134

4.4-2a. Analysis of the topography (m) of the 21°C temperature surface from AXBT data collected for the period of November 11-13, 1985 135

4.4-2b. Location of Transect Lines A through E 136

4.4-3. Path of ARGOS Drifter 3378 in the period of November 11-13, 1985 137

LIST OF FIGURES

Figure No. Caption Page

4.4-4. Vertical section of temperature (°C) along Line A from AXBT data collected for the period of November 11-13, 1985 139

4.4-5. NOAA-9 SST (°C) analysis in the western Gulf of Mexico for December 25, 1985 140

4.4-6. NOAA-9 SST (°C) analysis in the western Gulf of Mexico for January 13, 1986 141

4.4-7a. Location of hydrographic and XBT stations 143

4.4-7b. Analysis of the topography (m) of the 21°C temperature surface from data collected for the period of January 23 through February 5, 1986 144

4.4-8a. Path of Drifters 3353 (1), 5495 (2) and 3378 (3) in the period of December 1985 through January 1986 145

4.4-8b-c (b) Unit vectors depicting the flow field near the surface derived from the drifter data in Figure 4.4-8a and (c) isotachs of surface current speed (cm sec^{-1}) derived from the drifter data in Figure 4.4-8a 146

4.4-9. Simulated upper-layer flow field using a numerical model in the Gulf of Mexico for Experiment 68 (Wallcraft, 1986) in which an eddy encountered the western wall 149

4.4-10. The analysis of: (a) the vertical component of the relative vorticity and (b) the horizontal component of the divergence 150

4.4-11. Stylized representation of the path of Drifters 3378 and 3353 for the December 1985 through January 1986 period 151

4.4-12. Topography of the 8°C temperature surface from the AXBT survey of November 11-13, 1985 153

4.4-13a. SST data (°C) for January 7-13, 1986 with drifter trajectories shown 155

4.4-13b-c. SST data (°C) for: (b) January 15-21, 1986 and (c) January 22-28, 1986, both with drifter trajectories shown 156

LIST OF FIGURES

Figure No.	Caption	Page
4.4-14.	Surface dynamic topography (cm; with respect to 800m from the B/O ALTAIR survey of January 23 through February 5, 1986	157
4.4-15.	(a) Normal deformation rate, shear deformation rate and vorticity for Eddy B; (b) Time histories for the eccentricity and major axis orientation for Eddy B	158
4.4-16.	Divergence for Eddy A during the coalescing with Eddy B	159
4.4-17a.	Topography of the 8°C temperature surface based on the November 1985 AXBT survey	161
4.4-17b.	Topography of the 15°C temperature surface based on the November 1985 AXBT survey	162
4.4-17c.	Topography of the 21°C temperature surface based on the November 1985 AXBT survey	163
4.4-18.	Vertical section of temperature to 800m along Line A of the November 1985 AXBT survey	164
4.4-19.	Map of "synthetic" dynamic height at 150m relative to 650m based on the November 1985 AXBT temperatures and the T-S relation	165
4.4-20a.	Topography of the 8°C temperature surface based on XBT data collected during the January 1986 B/O ALTAIR cruise	167
4.4-20b.	Topography of the 15°C temperature surface based on XBT data collected during the January 1986 B/O ALTAIR cruise	168
4.4-20c.	Topography of the 21°C temperature surface based on XBT data collected during the January 1986 B/O ALTAIR cruise	169
4.4-21.	Vertical section of temperature to 800m along Line I of the January 1986 B/O ALTAIR cruise, passing through the centers of Eddy B and Eddy Z	171
4.4-22.	Vertical section of salinity to 1500m along Line I of the January 1986 B/O ALTAIR cruise	172

LIST OF FIGURES

Figure No.	Caption	Page
4.4-23.	Vertical section of salinity to 800m along: (a) Line D and (b) Line F of the January 1986 B/O ALTAIR cruise	173
4.4-24.	Salinity distribution at 200m during the January 1986 B/O ALTAIR cruise	175
4.4-25.	Composite T-S plot of all CTD data collected during the January 1986 B/O ALTAIR cruise	176
4.4-26a-b.	T-S diagram of: (a) Station 254 in the Loop Current from an eastern Gulf cruise in May 1984 and (b) Station 20 in the center of Eddy B in October 1986	177
4.4.26c.	T-S diagram of Station 176 in the center of Eddy B in January 1986	178
4.4-27a-b.	Vertical section of: (a) dissolved oxygen and (b) silicate to 1500m depth along Line I for January 1986	179
4.4-27c.	Vertical section of phosphate to 1500m depth along Line I for January 1986	180
4.4-28.	Composite plots of: (a) silicate versus sigma-t and (b) phosphate versus sigma-t for all data from the January 1986 B/O ALTAIR cruise	181
4.4-29.	Trajectory of Drifter 3353 from November 3, 1985 to February 4, 1986	183
4.4-30.	Stick plots of 40-hour, low-passed currents at 300m at Moorings Q and T for the second deployment period	184
4.4-31.	Stick plots of 7-day, low-passed currents at Moorings T (300m and 1000m), S (1000m), P (1000m and 1500m) and Q (300m and 1500m) for both deployment periods combined	186
4.4-32.	Plots of 7-day, low-passed temperature at Moorings T (300m and 1000m), S (1000m), P (1000m and 1500m) and Q (300m and 1500m) for both deployment periods combined	187

LIST OF FIGURES

Figure No.	Caption	Page
4.4-33.	Time-series plots of 40-hour, low-passed stick vectors, and 3-hour and 40-hour, low-passed U and V components and temperature for the second deployment period at Mooring P at 1000m.................	188
4.4-34.	Mean values, over the record length, of the U and V components of velocity presented in vector form for the second deployment period..................	191
4.4-35.	Spectra for Mooring Q at 300m and 1500m: U, V and temperature for the 171-day period beginning October 22, 1985......................................	192
4.4-36.	Rotary spectra emphasizing the inertial energy at 1000m for Moorings P, S and T using 3-hour, low-passed currents for the 171-day period beginning October 22, 1985............................	193
4.4-37.	Rotary spectra at 1000m for Mooring P using 40-hour, low-passed currents for the 186-day period beginning October 24, 1985............................	195
4.4-38.	Rotary spectra at 1000m for Mooring S using 40-hour, low-passed currents for the 186-day period beginning October 24, 1985............................	196
4.4-39.	Rotary spectra at 1000m for Mooring T using 40-hour, low-passed currents for the 186-day period beginning October 24, 1985............................	197
4.4-40.	Vertical, cross-spectral coherence and phase at Mooring T between 300m and 1000m: (a) U components of velocity, (b) V components of velocity and (c) temperature for the 184-day period beginning October 26, 1985	198
4.4-41.	Horizontal, cross-spectral coherence and phase at 1500m between Moorings Q and P: U, V and temperature for the 184-day period beginning October 26, 1985......................................	199
4.4-42.	Horizontal, cross-spectral coherence and phase at 1000m between Moorings S and T: U, V and temperature for the 184-day period beginning October 26, 1985......................................	200

LIST OF FIGURES

Figure No.	Caption	Page
4.4-43.	Rotary cross-spectral coherence and phase at 1000m between Moorings S and T: (a) outer coherence and phase and (b) inner coherence and phase........................	201
4.4-44.	Rotary cross-spectral coherence and phase at 1000m between Moorings P and T: (a) inner coherence and phase and (b) outer coherence and phase..	202
4.5-1.	NOAA-9 SST (°C) analysis in the western Gulf of Mexico for February 27, 1986........................	204
4.5-2.	(a) Location of stations for the SOOP transect performed in the period of February 13-14, 1986 and (b) vertical section of temperature (°C) from the data collected in (a)	205
4.5-3.	NOAA-9 SST (°C) analysis in the western Gulf of Mexico for March 28, 1986...........................	207
4.5-4.	Stylized representation of the paths of Drifters 3353 and 3378 during the period of February through March 1986.........................	208
4.5-5.	SST data (°C) for: (a) February 26 through March 4, 1986 and (b) March 12-18, 1986 with drifter trajectories shown................................	209
4.5-6.	SST data (°C) for: (a) March 19-25, 1986 and (b) April 16-22, 1986 with drifter trajectories shown..	210
4.5-7.	Togography of the 8°C temperature surface based on the April 26 to May 14, 1986 B/O ALTAIR XBT surveys...	211
4.5-8a.	Topography of the 15°C temperature surface based on the April 26 to May 14, 1986 B/O ALTAIR XBT surveys...	213
4.5-8b.	Topography of the 21°C temperature surface based on the April 26 to May 14, 1986 B/O ALTAIR XBT surveys...	214
4.5-9.	Vertical section of temperature to 800m between Station 1 and Station 28 of B/O ALTAIR XBT cruise AL-86-03 in April 1986.......................	215

LIST OF FIGURES

Figure No.	Caption	Page
4.6-1.	SST data (°C) for: (a) May 14-20, 1986 and (b) May 18-24, 1986 with drifter trajectories shown	217
4.6-2.	SST data (°C) for June 15-21, 1986 with drifter trajectories shown	218
4.6-3.	SST data (°C) for: (a) July 30 through August 5, 1986 and (b) August 13-19, 1986 with drifter trajectories shown	219
4.6-4.	Topography of the 8°C temperature surface based on August 17-22, 1986 HO-2 cruise.	220
4.6-5.	Topography of the 15°C temperature surface in late April and early May 1986 based on SOOP cruises AL-86-03, AL-86-04, AL-86-05 EJ-86-01, and EJ-86-02	222
4.6-6.	Cruise track for B/O ALTAIR cruise AL-86-06 in mid-July 1986	223
4.6-7.	Vertical section of temperature to 800m between Station 1 and Station 34 for B/O ALTAIR cruise AL-86-06 in mid-July 1986	224
4.6-8.	Cruise track for the HO-2 cruise and the location of all XBT stations occupied during the period from August 17-22, 1986	225
4.6-9a.	Topography of the 15°C temperature surface based on the August 1986 HO-2 cruise	226
4.6-9b.	Topography of the 21°C temperature surface based on the August 1986 HO-2 cruise	227
4.6-10.	Cruise track of the R/V JUSTO SIERRA and the location of all XBT stations occupied during the period from May 3 through June 11, 1987	229
4.6-11a.	Topography of the 15°C temperature surface based on XBT data for the May 1987 R/V JUSTO SIERRA cruise	230
4.6-11b.	Topography of the 21°C temperature surface based on XBT data for the May 1987 R/V JUSTO SIERRA cruise	231
4.6-12.	Cruise track of the R/V JUSTO SIERRA and the location of all XBT stations occupied during the period from October 14 through November 16, 1987	232

LIST OF FIGURES

Figure No.	Caption	Page
4.6-13a.	Topography of the 8°C temperature surface based on XBT data for the October 1987 R/V JUSTO SIERRA cruise	233
4.6-13b.	Topography of the 15°C temperature surface based on XBT data for the October 1987 R/V JUSTO SIERRA cruise	234
4.6-13c.	Topography of the 21°C temperature surface based on XBT data for the October 1987 R/V JUSTO SIERRA cruise	235
4.6-14.	Trajectory of Drifter 7234 from April 14 to June 19, 1987	236
4.6-15.	Trajectory of Drifter 5839 from June 10 to September 3, 1987	237
4.6-16.	Trajectory of Drifter 5837 from June 11 to September 1, 1987	238

LIST OF TABLES

Table No.	Caption	Page
2.2-1.	Drifters, their associated oceanographic structures, periods during which position data were collected, and symbols used for their trajectories on the SST charts	8
2.2-2.	A listing of cruises during which water temperature data were collected for Eddy B	10
2.3-1.	Station summary for the R/V PELICAN cruise for the period from October 21 through 29, 1985	14
2.3-2.	Sampling summary for the R/V PELICAN cruise for the period from October 21 through 29, 1985	14
2.3-3.	Station summary for the B/O ALTAIR cruise for the period from January 22 through February 6, 1986	18
2.3-4.	Sampling summary for the B/O ALTAIR cruise for the period from January 22 through February 6, 1986	19
2.3-5.	Station summary for the Year 3 aerial survey for the period from November 11 through 13, 1985	25
2.3-6.	MMS Ship of Opportunity data sets in the western Gulf of Mexico from June 1, 1985 through September 30, 1986	27
2.3-7.	MMS Ship of Opportunity sections in the eastern Gulf of Mexico from January 25, 1985 through September 30, 1986	27
2.5-1.	Mooring locations and nominal instrument depths in the western Gulf for Year 3 of the MMS-sponsored Gulf of Mexico Physical Oceanography Program	32
2.5-2.	Data return for moorings in the western Gulf for the period from June 11, 1985 through May 5, 1986	36
4.3-1.	Estimates for Eddy B of the vertical extent of the 8°C isotherm and of the volume of water between the 8°C and 15°C isothermal surfaces. These are used as indicators of the changes in the size of the eddy between various cruises	96
4.3-2.	Basic statistics of the U and V components of current and temperature over the available record lengths at Moorings P, Q, R, S and T for the first deployment period: June 17 through October 20, 1986	114

LIST OF TABLES

Table No.	Caption	Page
4.4-1.	Near-surface area estimates for Eddy B..................	147
4.4-2.	Areas (10^3 km^2) of Eddy B inside the given contours of the topography of the 8°C temperature surface.......	170
4.4-3.	Basic statistics of the U and V components of current and of temperature over the available record lengths at Moorings P, Q, S and T for the second deployment period: October 22, 1986 through May 1, 1986...........	189

ACKNOWLEDGEMENTS

Conducting an experiment as extensive and flexible as this one requires considerable coordination and effort from many people. Some of the key people and activities are described below. Please note that many others may have made substantial contributions to the project, and if they remain unidentified I hope they will accept my apologies and know the importance of their efforts to the overall success of the project.

As is mentioned in Chapter I, this program relied extensively on close and open cooperation between U.S. project principals and support personnel and participants from Mexico. Without this mutual support the project would have been substantially narrower in scope and insight. The processes of interest are active in portions of the ocean that are closely linked to both countries. In Mexico, Captain Alberto Vazquez had a lead role in logistics and other arrangements needed to coordinate working from Mexican Naval research vessels. This, however, was only possible with the support provided by Vice Admiral Gilberto Lopez-Lira, Director of Ocean Research in the Office of the Secretary, Mexican Navy. The captain of the B/O ALTAIR, Captain J. R. Alcala, provided support at sea during several of the project cruises.

The SOOP program was maintained only through the continued and longstanding diligence of P. deKernion. The provision of trajectory data from five oil industry ARGOS drifters deployed during the study period is gratefully acknowledged. These data were provided by G. Forristall of Shell Oil.

Much of the data processing was done by T. Martin and R. Weber. Their attention to detail and efficiency allowed SAIC to be responsive to the project requirements. Of special mention is the continued support of Dr. Peter Hamilton who was able to provide considerable technical leadership and to solve some sensitive analysis methodologies.

I would like to thank the field technical staff as a group for due diligence in what was often trying work. Their skill and perseverance were essential.

Finally, Dr. Murray Brown maintained flexibility and ongoing attention to the program, resulting in an awareness and understanding of evolving requirements that allowed him to make technical adjustments in the experimental design. Without Dr. Brown's continued involvement, the program would have had less success and would have been more limited in its results.

I. INTRODUCTION

1.1 Program Objectives

The Gulf of Mexico Physical Oceanography Program (GMPOP), a Minerals Management Service (MMS) study funded under contract with Science Applications International Corporation (SAIC), has as its objective the development of an improved understanding of primary Gulf circulation patterns and the mechanisms producing these patterns. It is expected that insights from this program will provide an expanded basis for making informed management decisions related to Outer Continental Shelf (OCS) oil and gas exploration, production and transportation in the Gulf of Mexico. This objective, in keeping with the OCS Lands Act, requires the Department of the Interior to conduct appropriate studies to evaluate the environmental impact of offshore oil and gas development.

1.2 Program Background

In 1982 a multi-year investigation into the physical oceanographic conditions related to or resulting from deep circulation patterns in the Gulf of Mexico was begun. This program has a phased, regional emphasis. Thus, the earlier two previous program reports describe three years of field measurements in the eastern Gulf and on the west Florida shelf (SAIC, 1986; SAIC, 1987). The present report describes measurements made during Program Year 3 in the central and western Gulf. The Year 3 goal was to document and describe the characteristics and circulation patterns in and related to eddies that detach from the Loop Current (LC) and migrate westward (Figure 1.2-1). The physical processes of interest do not respect political boundaries established or proposed for the Gulf basin, for example, national exclusive economic zones (EEZ). Because these processes directly affect U.S. and Mexican zones, many of the measurements of interest had to transcend these boundaries. Toward this end, a cooperative and joint effort was developed between this MMS-funded program and the Mexican Navy. It was only through this cooperation that an exceptional Program Year 3 data set was obtained.

Many individuals contributed to making this cooperative study program a success. Several key individuals are identified in the Acknowledgments for this program report.

1.3 Program Elements and Participants

1.3.1 Key Observations

To support the Program Year 3 objectives, a range of measurements was made. These measurements have been utilized by the scientific lead and support personnel to develop an integrated characterization of eddy-related features and patterns. Primary measurements included:

- Subsurface currents/temperature and pressure along and across isobaths in the west central and northwestern Gulf.
- A sequence of hydrographic surveys (ship- and plane-based) to document the 3-dimensional character and evolution of a LC eddy as it moved into the western Gulf.

BLANK

PAGE

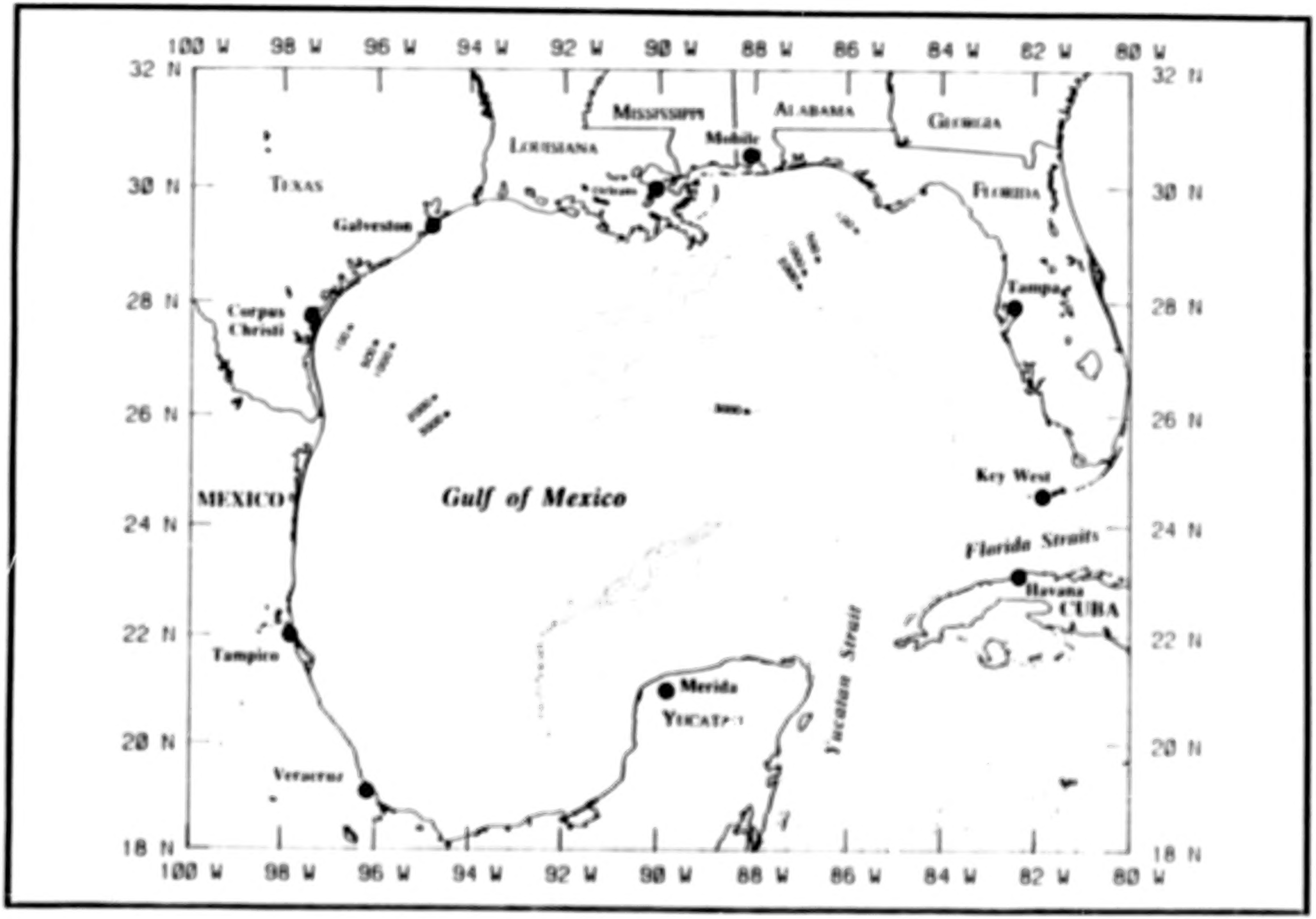

Figure 1.2-1. Study area for the Gulf of Mexico Physical Oceanography Program. This Year 3 Report focuses on Loop Current eddies in the central and western Gulf.

- Satellite-tracked drifters to provide information concerning the circulation patterns in and around eddies.

- Both regular, periodic and one-time ship-of-opportunity (SOOP) platforms used to release expendable temperature probes. These long-term observations provided valuable and cost-effective information regarding the temperature structure in both the presence and absence of eddies.

These data were, as appropriate, combined with marine winds and coastal winds and water level data. However, because the features and patterns of interest remained off the shelf and over the slope or in the deep Gulf, the effect on and utility of coastal data were often limited.

Several of the above data types provide a standard against which results of numerical models can be compared. Particularly relevant are drifter trajectories and subsurface currents.

1.3.2 Key Scientific Personnel

To extract important patterns and processes from the comprehensive, multivariate data set, a team of highly qualified scientists was established to work both independently and in collaboration. Presented alphabetically with their affiliation and primary areas of responsibility, they were as follows:

- Dr. David Brooks - Texas A&M University (TAMU), subsurface currents and hydrography.

- Mr. Frank Kelly - TAMU, subsurface currents and hydrography.

- Dr. James Lewis - SAIC, Lagrangian drifters.

- Dr. Fred Vukovich - Research Triangle Institute (RTI), satellite imagery.

Key support personnel were R. Wayland, J. Singer and C. Casagrande. Mr. Wayland was Data Manager and worked closely with the scientific team to provide data analysis, products and graphics in a timely manner. Mr. Singer was responsible for much of the program logistic support and served as Chief Scientist on some of the cruises as Chief Scientist. Mr. Casagrande was Chief Scientist the three subsurface current mooring cruises. Dr. E. Waddell is Program Manager for the GMPOP.

1.4 Report Organization

Since the present document reports on observations taken during a continuing program, many of the support procedures and methods are the same or similar to those used and described in previous reports. When this is the case, the redundant material will not be reproduced again in this report. Rather, the material in prior reports will be presented by reference to previous program documents.

In this report, Chapter I provides a brief overview of program elements. Chapter II describes data taken or used. Chapter III provides a description of methods by which data were analyzed in the synthesis process. Chapter IV gives a discussion of conditions and processes as deduced from the integrated program data set, i.e., the results.

1.5 References for Chapter I

Science Applications International Corporation. 1986. Gulf of Mexico physical oceanography program, final report, years 1 and 2. Volume II: technical report. MMS Contract No. 14-12-0001-29158, SAIC Report No. SAIC-86/1023. 378 pp.

Science Applications International Corporation. 1987. Gulf of Mexico physical oceanography program, final report, year 4. Volume II: technical report. MMS Contract No. 14-12-0001-29158, SAIC Report No. SAIC-87/1027. 226 pp.

II. DATA ACQUISITION

2.1 Introduction

Chapter II presents an overview of the extensive multivariate data set collected during the western Gulf program. The chapter objective is to provide a foundation by which the reader can understand the what, when, how and where of the program measurements. Pre-analysis corrections or adjustments are identified and discussed. When such adjustments are similar or the same as undertaken during previous program years, the reader will be referred to detailed discussions in these earlier reports. The discussion will not be reproduced here. Reading this chapter will provide the reader with a good understanding of the data base available to the program principals. The chapter is also organized so that each of the primary data or measurement types is discussed separately. Data taken during the program will be submitted to the National Oceanographic Data Center (NODC) and will be available from that source.

The integrated analyses of the data discussed below form the basis for the process syntheses developed in this report.

2.2 Drifter and Associated Data

2.2.1 Introduction

ARGOS Drifter 3378 was placed in a LC eddy identified as Eddy B which provided the primary Lagrangian data in this study (Figure 2.2-1a). Eddy B was tracked across the Gulf for a 10-month period during which time Drifters 5678 and 5683 were also entrained in the eddy's flow field. As it approached the Mexican coast, Eddy B interacted with a previously shed feature called Eddy A (Lewis and Kirwan, 1987; Figure 2.2-1b), which had several drifters (3353, 5495, and 5682) associated with it. Actually, Drifter 5495 had been seeded in Eddy B but was cast out early and became entrained in Eddy A (Figure 2.2-1b). A seventh drifter (3354) was entrained in the Loop Current at the time Eddy B was being shed (Lewis and Kirwan, 1987; Figure 2.2-2a); and an eighth drifter (3379) was seeded in a subsequent ring (Eddy C) in March 1986 (Figure 2.2-2b). Eddy B interacted with the younger Eddy C as the latter drifted into the western Gulf. Table 2.2-1 summarizes the drifter data sources.

The Lagrangian data are presented along with corresponding sea surface temperature (SST) data for the Gulf. Most SST maps represent average temperature structure over a 7-day period. In many cases (especially non-summer months), additional flow characteristics can be inferred from the SST contours. During warmer months the SST isotherms can be considered general estimates due to surface water heating and associated reduction of surface temperature gradients.

Water column parameters are used to infer changes in the size and extent of Eddy B. Specifically, the volume of water between the 8°C and 15°C isotherms was examined across the ring where the 8°C isotherm reaches upward to the depth of 550m. The spatial pattern of the 8°C isotherm depths helps describe the character of flow around the ring. The 8°C isotherm was chosen since this temperature surface is not affected by surface heating and cooling. Similarly, the 15°C isothermal surface is rarely affected by surface processes except in shallow shelf regions (water depth <100m). As for the consideration

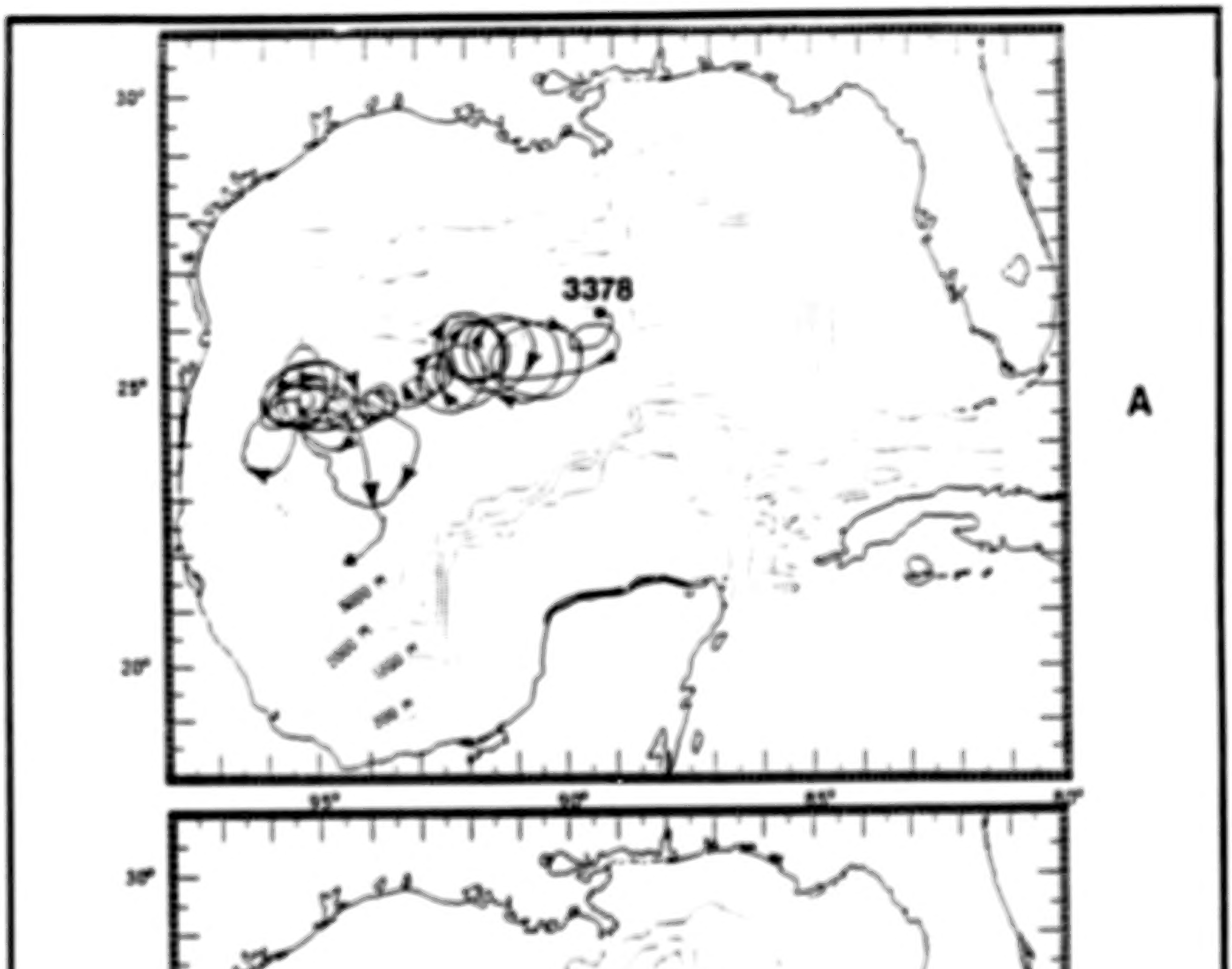

Figure 2.2-1. Trajectory for: (a) Drifter 3378 and (b) Drifter 5495. The presence of Eddy A was detected at ~93°W when Drifter 5495 began making anticyclonic loops. Depth contours are in meters. Squares denote the beginning positions of the drifter trajectories and triangles denote the end positions.

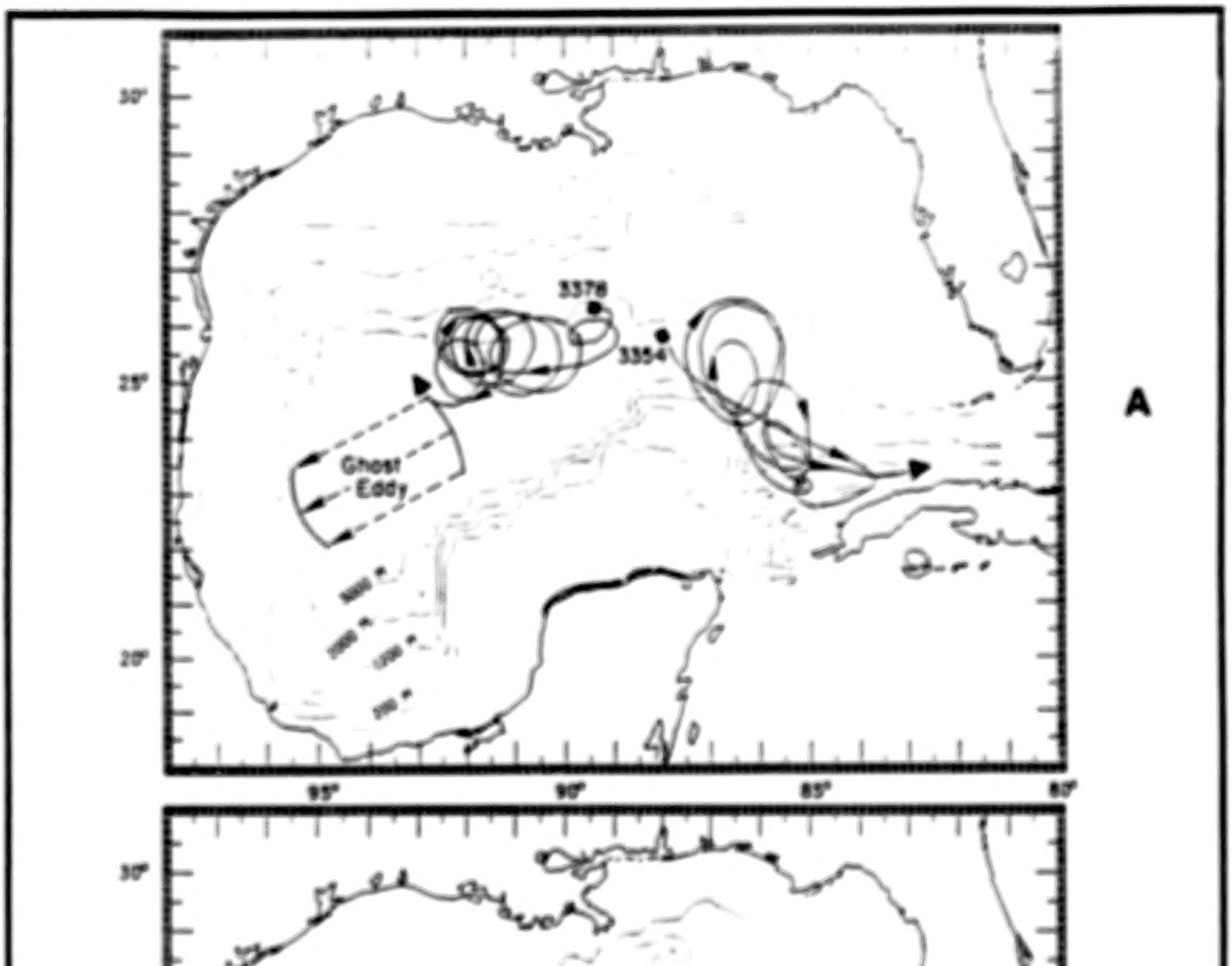

Figure 2.2-2. Trajectory for: (a) Drifter 3354 from mid-June through mid-September 1985 and Drifter 3378 from mid-July through September 1985 (also shown is the location of Eddy A during August and September 1985) and (b) Drifter 3379. Depth contours are in meters. Squares denote the beginning positions of the drifter trajectories and triangles denote the end positions.

Drifter Identification	Associated Anticyclone	Time in Gulf of Mexico	Symbol on SST Charts
3378*	Eddy B	Jul 18, 1985- Jun 26, 1986	▬▬▬▬
5495***	Eddy B, Eddy A	Jun 29, 1985- Jan 23, 1986	○○○○○○○
5680***	Not in a Ring	Jul 18, 1985- Sep 5, 1985	═══════
5682***	Eddy A	Aug 6, 1985- Oct 11, 1985	■○■○■○
3354**	Loop Current Anticyclone	Jun 18, 1985- Sep 15, 1985	□●□●□●
5683***	Eddy B	Aug 3, 1985- Nov 24, 1985	●●●●●●
5678***	Eddy B, Eddy C	Oct 23, 1985- Apr 30, 1986	□□□□□
3353**	Eddy B, Eddy A	Nov 3, 1985- May 22, 1986	■■■■■
3379*	Eddy C	Mar 7, 1986- Jan 22, 1987	▬●▬

*Polar Research Laboratory (PRL) TOD with 200m, weighted thermistor string.

**PRL Mini-TOD, 200m tether.

***Horizon Marine Drifter. Data provided by Shell Oil.

Table 2.2-1. Drifters, their associated oceanographic structures, periods during which position data were collected and symbols used for their trajectories on the SST charts.

of lateral extents bounded by where the 8°C isothermal surface reaches 550m, an inspection of expendable bathythermograph (XBT) data showed that the 8°C surface typically has its greatest slope at 550m. Thus, the 550m extent of the 8°C surface is used as an indicator of the eddy boundary. The hydrographic data collected for Eddy B are listed in Table 2.2-2.

The path information from a number of the drifters was analyzed to provide various kinematic data (Kirwan et al., 1987). These analyses are used to consider the changes of Eddy B during its lifetime. The changes include changes in swirl speed (rotary speed about the translating center of the ring), vorticity (related to angular velocity), period of rotation, ellipticity (eccentricity and orientation of the eddy axes), deformation (shape change rate) and size.

2.2.2 Separation of Eddy B from the Loop Current

Drifter 3354 was initially seeded in what appeared to be a newly formed eddy in June 1985. However, Eddy B had not totally broken free of the Loop Current at that time. Drifter 3354 was swept into the Loop Current proper and remained there for 3 months. Eddy B was reseeded with Drifter 3378 in July 1985. The interesting aspect of the co-existence of Drifters 3354 and 3378 from July to September 1985 is that both were entrained in anticyclones, one in the Loop Current and the other in Eddy B. This allows the processes within the Loop Current during and directly after the separation of Eddy B to be discussed.

Drifter 3354 was seeded at 25.9°N, 87.9°W on June 18, 1985. It was hoped that the drifter would remain in Eddy B, but it immediately left and moved southeastward ~525 kilometers and reached 23.2°N, 83.7°W by June 29, 1985. At this point, the drifter became entrained in a westward, anticyclonic flow field with a center of rotation at about 24.0°N, 85.5°W (Figure 2.2-2a). After two rotations (into mid-August), the drifter "suddenly" moved northwestward and made three additional rotations centered at about 25.5°N, 86.5°W. The drifter then left this flow pattern in mid-September 1985 and exited the Gulf through the Florida Straits.

Drifter 3378 was seeded in Eddy B at 26.4°N, 89.3°W on July 18, 1985. By that time the eddy had totally separated from the Loop Current. As shown in Figure 2.2-2a, Eddy B slowly moved westward, reaching approximately the 91°W meridian by mid-August. Recall that after mid-August the Loop Current (as determined by Drifter 3354) moved northwestward and remained there until at least mid-September. During that same 30-day period, Eddy B continued moving westward, reaching the 92.5°W meridian.

2.2.3 Westward Movement of Eddy B

As shown in Figure 2.2-1a, Eddy B reached 91°W by mid-August 1985. At that time, it moved west-northwest onto the continental slope where translation appears to cease for three revolutions. In mid-September 1985, Eddy B abruptly moved southward into deeper water. This movement occurred within one revolution of the eddy (~11 days). The eddy then translated westward, with the drifter moving closer to the eddy center (note the smaller loops between 92°W and 95°W in Figure 2.2-1a). The latter part of the trajectory (mid-November 1985 through May 1986) shows Eddy B interacting with the western shelf of the Gulf.

Available XBT Data	
Source	Date
M/V NAT CO 6	Jul 16-19, 1985
R/V PELICAN	Oct 22-27, 1985
AXBT Survey	Nov 11-13, 1985
B/O ALTAIR	Jan 23-Feb 5, 1986
B/O ALTAIR	Apr 26-May 14, 1986
HO-2	Aug 16-22, 1986

Table 2.2-2. A listing of cruises during which water temperature data were collected for Eddy B.

2.2.4 Interactions in the Western Gulf of Mexico

A drifter launched by the offshore industry in June 1985 eventually became entrained in the flow field of Eddy A (Figure 2.2-1b) which was centered at 23.5°N, 93°W at the beginning of August 1985. This eddy gradually moved southwestward across the deepest portion of the Gulf. By the end of September 1985, Eddy A was still rotating strongly at 23°N, 94.5°W.

Eddy A then moved westward onto the Mexican coast shelf at ~22.5°N. Figure 2.2-1b shows that the ring remained there until at least mid-December 1985. During that time, Eddy A took on a north-south eccentricity and moved northward. There was a considerable amount of interaction between Eddy A and Eddy B at the end of 1985; this interaction will be discussed in detail later.

The LC eddy which separated after Eddy B was Eddy C (Figure 2.2-2b). The beginnings of Eddy C can be seen in SST data as early as mid-November 1985. This eddy had been shed by mid-January 1986, and its flow field had entrained Drifter 5678 in April of that year. Eddy C was seeded with Drifter 3379 in early March 1986. The path of Drifter 3379 (Figure 2.2-2b) shows a southwestward movement through the deeper waters of the Gulf. However, in mid-May 1986, Eddy C interacted with the remnants of Eddy B, and the result was a curious east-west oriented, peanut-shaped path (Figure 2.2-2b) at ~24°N. Afterwards, Eddy C moved westward onto the Mexican shelf. Along the Mexican shelf, Drifter 3379 began making large, anticyclonic loops, approximately 4° in latitude and longitude.

2.3 Hydrography

2.3.1 Introduction

Between October 21, 1985 and February 6, 1986, two ship-based hydrographic surveys and one aerial expendable bathythermograph (AXBT) survey were conducted in the western Gulf of Mexico to study interaction of a Loop Current eddy (warm-core ring) with the western Gulf slope region. Such interaction, it is believed, contributes significantly to the regional transport and mixing processes.

Each of the ship-based surveys included conductivity/temperature/depth (CTD) and XBT measurements, near surface current measurements and the collection of water samples for the analysis of nutrients (nitrate, phosphate and silicate) and dissolved oxygen. Surface chlorophyll data were also collected, as were a few expendable current profiles (XCPs) during the initial hydrographic cruise. Aerial XCPs (AXCPs) were deployed as part of the AXBT survey. Each of the cruise and aerial survey sampling plans was adjusted in the field by combining the latest available satellite thermal imagery with the latest positions from ARGOS drifters entrained in the warm-core eddy. In addition, during each of the surveys vertical sections of temperature were plotted in real time to permit further adjustments in the survey as oceanographic conditions changed.

2.3.2 Cruise Summaries

2.3.2.1 R/V PELICAN

The first hydrographic cruise was between October 21 and 29, 1985 aboard the R/V PELICAN. The ship's track, indicating all CTD and XBT stations, is shown in Figure 2.3-1, and the cruise station and sampling summaries are presented

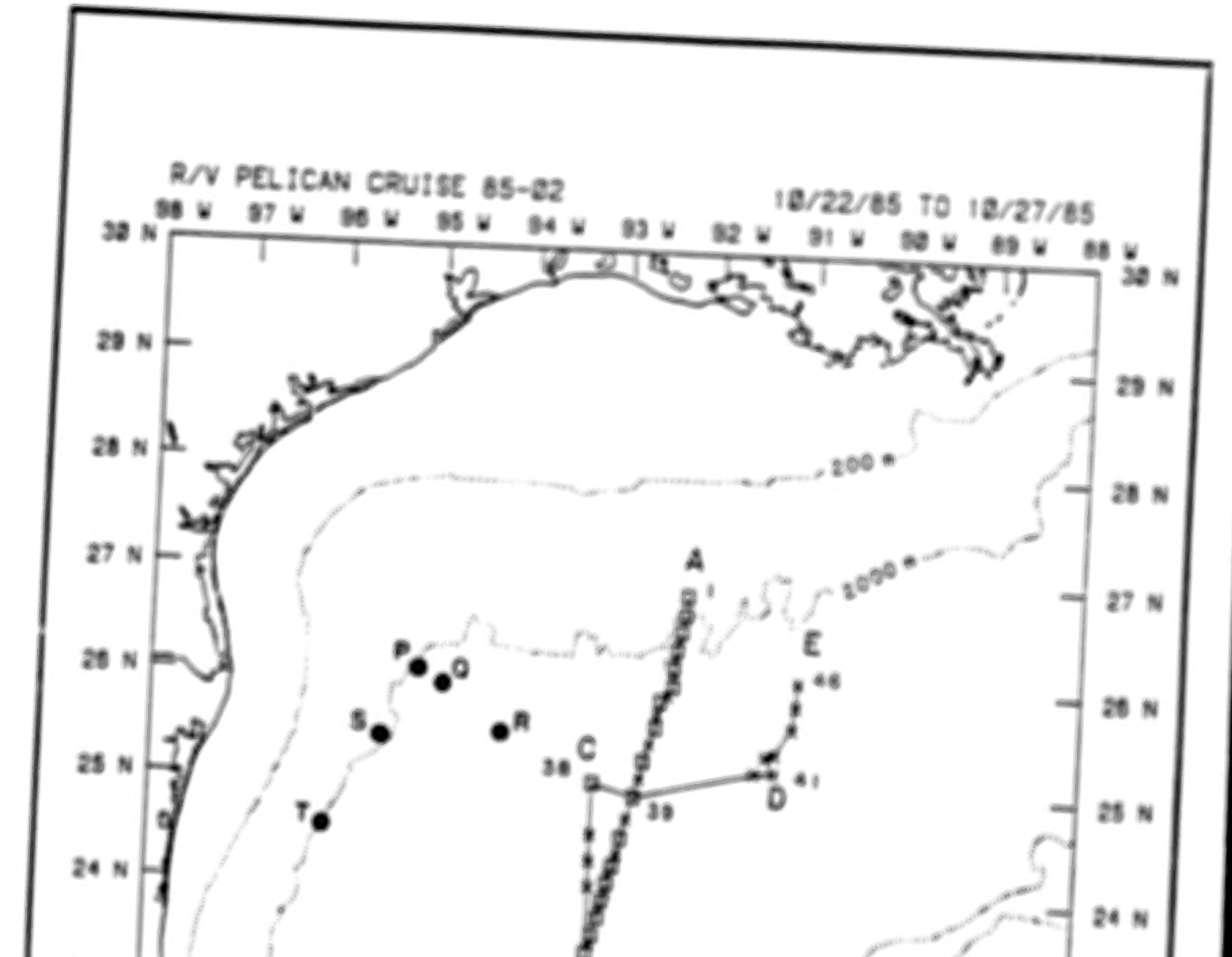

Figure 2.3-1. Cruise track of the R/V PELICAN and the location of all CTD and XBT stations occupied for the period from October 21-24, 1985.

in Tables 2.3-1 and 2.3-2. During this sampling period, adverse weather significantly affected the planned survey. Only one north-south section was run during which conditions were favorable. Following this, a second radial line was begun on October 25 from the eddy center to the east. However, operations were suspended shortly thereafter due to increasing winds (40-50 knots) and high seas (6-13 feet) which developed into Tropical Storm Juan on October 26 and Hurricane Juan on October 28. The remainder of the cruise period was spent attempting to avoid the hurricane and trying to make port (Figure 2.3-2). These efforts were further complicated by the persistence and unpredictability of the storm and by massive flooding in Cocodrie, Louisiana, the ship's home port.

2.3.2.2 B/O ALTAIR

The second hydrographic cruise took place from January 23 through February 6, 1986 aboard the B/O ALTAIR, a Mexican naval oceanographic research vessel. The ship's cruise track, indicating all CTD and XBT stations, all S-4 20m depth current measurement stations and all plankton tow stations, is shown in Figure 2.3-3. The cruise station and sampling summaries are presented in Tables 2.3-3 and 2.3-4.

During the cruise sampling period, weather conditions were dominated by mostly fair weather and ESE winds 10-20 knots, except for the passage of an intense cold front on January 26 accompanied by brisk NNW winds of 25 to 30 knots. This later event curtailed over-the-side oceanographic operations for about 12 hours and resulted in substitution of a number of XBT drops for CTD casts along one of the transects. Otherwise, the cruise was not adversely affected by the weather.

The sampling grid was designed to optimize measurements for the warm-core LC eddy as it interacted with the shelf-slope region. As such, eight parallel transect lines 30 nautical miles apart (labeled A through H from north to south) were oriented along 122°T. Grid points, separated by 20 nautical miles along each line, were designated as CTD stations, and XBTs were deployed midway between each CTD grid point. At all but three of the CTD stations, samples were collected for inorganic nutrient analysis and dissolved oxygen. As the survey progressed and the eddy structure became evident, several transects were cut short to save time by canceling stations at either end. Lines A, B, D, E, F and G were surveyed with the alternating CTD/XBT sequence described above. Line C was almost entirely surveyed with XBTs because high winds and seas prevented safe and practical operation of the CTD, and two of the CTDs on line H were replaced with XBTs to save time as the line appeared to parallel the dynamic topography of the southern perimeter of the eddy, showing little structure. Upon completion of the grid, Transect I was run due north along the 95.4°W meridian with XBTs deployed every 9 nautical miles.

2.3.3 Shipboard Operations

2.3.3.1 Equipment

During each of the cruises, a Neil Brown Mark IIIB CTD sensor package and a General Oceanics Model 1015 Mark V Rosette Multi-Bottle Sampler were used. The sampler was equipped with 12 five-liter Niskin bottles, two of which were outfitted with reversing thermometer racks. Each rack contained two protected and one unprotected reversing thermometer. The CTD was powered by a Model 1150 Data Terminal and controlled by a Hewlett Packard mini-computer system.

Section	Date (GMT)	Station Numbers
A-B	October 22-24	1C, 3C, 5X, 6C, 7X, 8C, 9X, 10C, 11X, 12C, 13X, 14C, 15X, 16C, 17X, 18C, 19X, 20C, 21X, 22C, 23X, 24C, 25X, 26C, 27X, 28C, 29X, 30C, 31X, 32C, 33X, 34C
B-C	October 25	34C, 35X, 36X, 37X, 38C
C-D	October 25-26	38C, 39C, 40X, 41X
D-E	October 26-27	41X, 42X, 43X, 44X, 45X, 46X

Table 2.3-1. Station summary for the R/V PELICAN cruise for the period from October 21 through 29, 1985.

Section	CTD	XBT	Nutrients	Oxygen	Salinity	Chlorophyll
A-B	17	15	133	133	15	15
(others)	2	10	19	19	2	2
TOTALS	19	25	152	152	17	17

Table 2.3-2. Sampling summary for the R/V PELICAN cruise for the period from October 21 through 29, 1985.

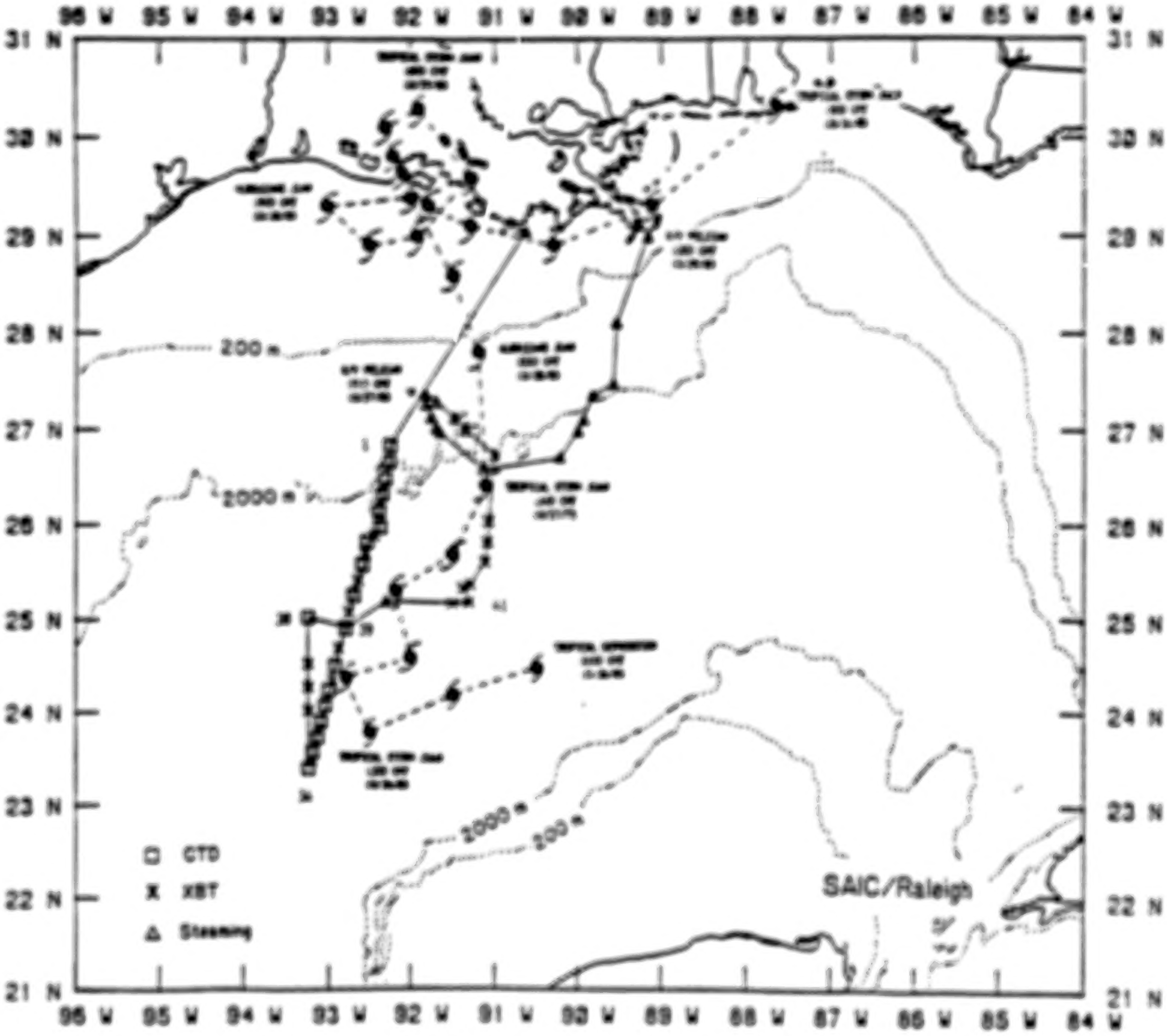

Figure 2.3-2. Cruise track of the R/V PELICAN and the path of Hurricane Juan for the period from October 21-31, 1985.

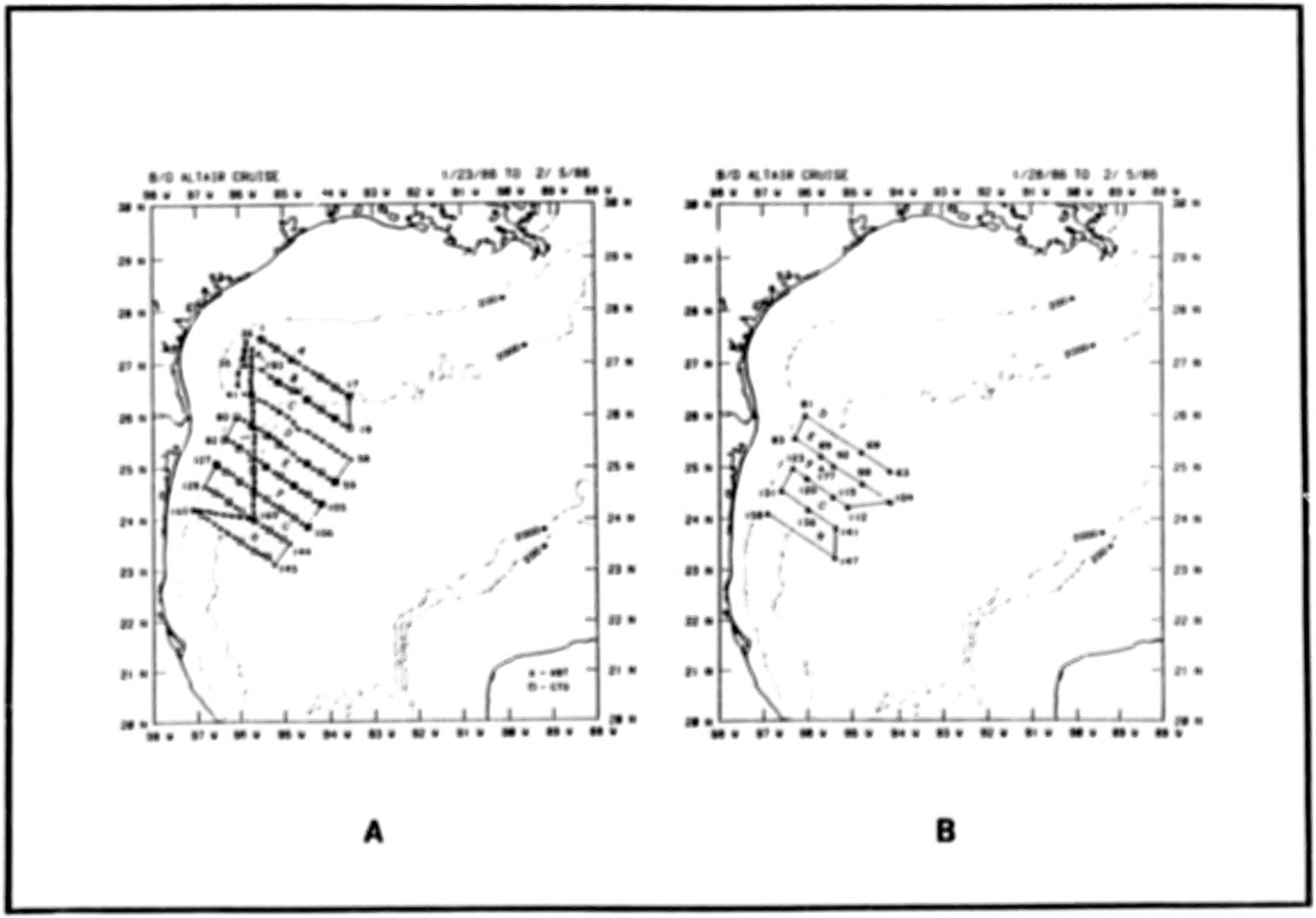

Figure 2.3-3a-b. Cruise track of the B/O ALTAIR for the period from January 22 through February 6, 1986 and the location of all: (a) CTD and XBT stations, (b) S-4 20-meter depth current measurement stations.

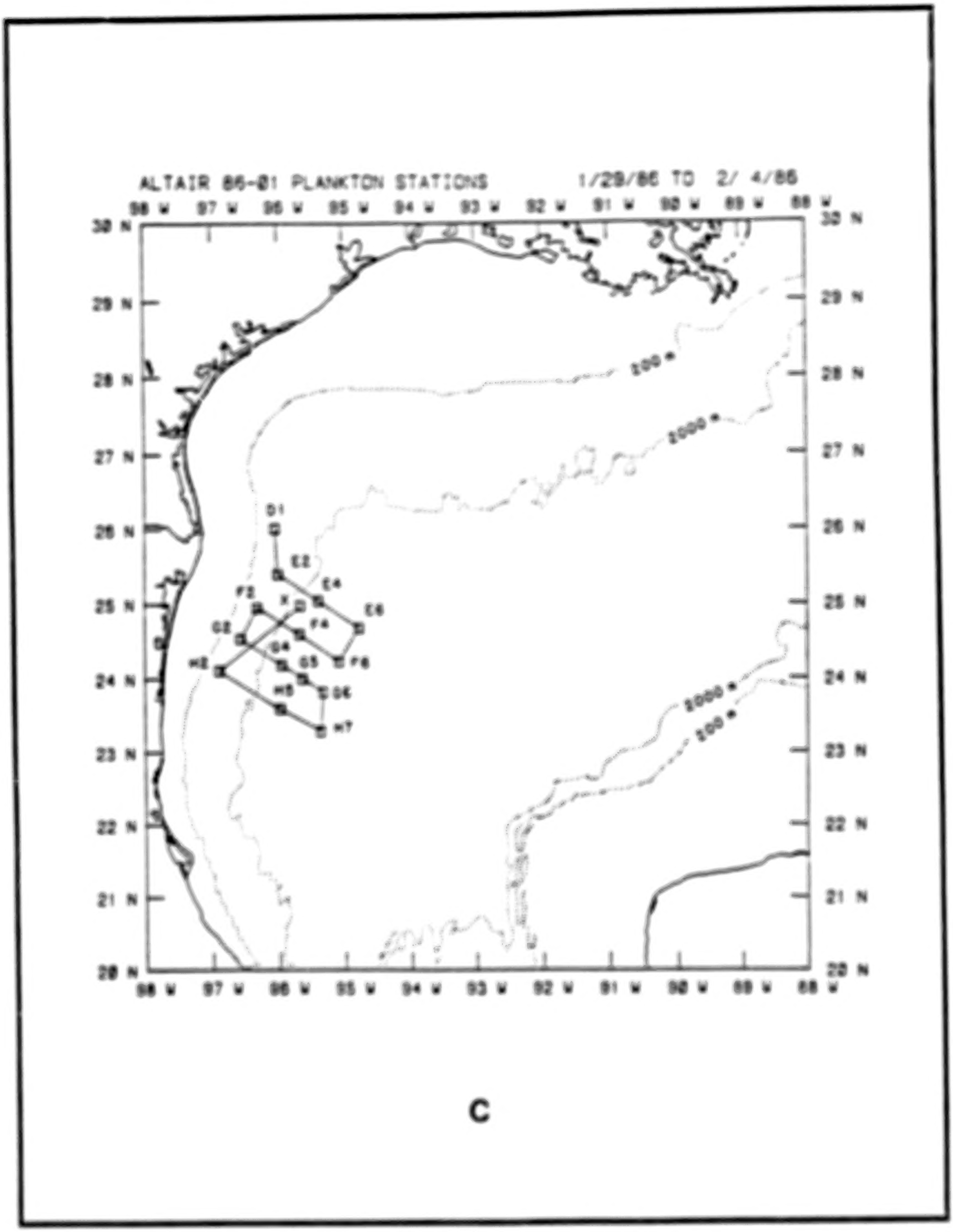

Figure 2.3-3c. Cruise track of the B/O ALTAIR for the period January 22 through February 6, 1986 and the location of all plankton tow stations.

Section	Date (GMT)	Station Numbers
A(A-A*)	January 23-24	1C(2X), 3X, 4C, 5X, 6C(7X), 8X, 9C(10X), 11X, 12C, 13X, 14C, 15X, 16C(17X)
B(B*-B)	January 25-26	19C, 20X, 21C(22X), 23X, 24C, 25X, 26C(27X), 28X, 29C, 30X, 31C(32X), 33X, 34X, 35X
(B-C)	January 26	36X, 37X, 38X, 39X, 40X
C(C-C*)	January 26-28	40X, 41X, 42C, 43X, 44X, 45X, 46X, 47X, 48X, 49X, 51X, 52X, 53X, 54X, 55X, 56X, 57X, 58X
D(D*-D)	January 28-29	59C(60X), 61X, 62C(63P), 64X, 65C(66X), 67X, 68C(69P), 70X, 71C(72X), 73X, 74C(75X), 76X, 77C(78X), 79X, 80C(81P)
E(E-E*)	January 30-31	82C(83P), 84X, 85C(86X), 87X, 88C(89P), 90X, 91C(92P,93X), 94X, 95C, 96X, 97C(98P, 99X), 100X, 101C, 102X, 103C(104P, 105X)
F(F*-F)	January 31- February 1	106C(107X), 108X, 109C, 110X, 111C(112P), 113X, 114C(115P), 116X, 117C, 118X, 119C(120P), 121X, 122C(123P), 124X, 125C(126X), 127X
G(G-G*)	February 1-3	128X, 129X, 130C(131P), 132X, 133C, 134X, 135C(136P), 137X, 138C, 139X, 140C(141P), 142X, 143C, 144X
H(H*-H)	February 3-4	145X, 146C(147P), 148X, 149C, 150X, 151C, 152X, 153X, 154X, 155X, 156X, 157C(158P), 159X, 160X
(H-G)	February 4	160X, 161X, 162X, 163X, 164X, 165X, 166X, 167X, 168X, 169X
I(I-I*)	February 4-5	169X, 170X 171X, 172X, 173X, 174X, 175X, 176C(177P), 178X, 179X, 180X, 181X, 182X, 183X, 184X, 185X, 186X, 187X, 188X, 189X, 190X, 191X, 192X, 193X

Table 2.3-3. Station summary for the B/O ALTAIR cruise for the period from January 22 through February 6, 1986.

Section	CTD	XBT	Current	Nutrients	Oxygen	Salinity	Plankton
(A-A*)	6	10	0	41	41	4	0
(B-B*)	6	11	0	50	50	6	0
(B-C)	0	4	0	0	0	0	0
(C-C*)	1	17	0	10	10	2	0
(D-D*)	8	12	3	76	16	10	1
(E-E*)	8	11	5	67	77	12	3
(F-F*)	8	10	4	75	75	16	3
(G-G*)	6	8	3	59	60	12	4
(H-H*)	4	10	2	40	40	7	3
(H-G)	0	8	0	0	0	0	0
(I-I*)	1	23	1	9	10	2	1
TOTALS	48	124	18	427	439	71	15

Table 2.3-4. Sampling summary for the B/O ALTAIR cruise for the period from January 22 through February 6, 1986.

An HP-9816S computer was used during the initial cruise, and data were stored on hard disk and 3-1/2 inch disks using an HP-9121D dual disk drive. Hard copies of the data were generated using an HP Think Jet printer and an HP-7470 plotter. A schematic of this configuration is presented in Figure 2.3-4a. During the second cruise an HP-85A computer was used and the data stored on SCOTCH data cartridges using the built-in cartridge drive. Back-up data logging capabilities were on a TEAC audio recorder and a TECHTRAN digital cassette recorder. Hard copies of the data were generated using the built-in thermal printer. A schematic of this configuration is presented in Figure 2.3-4b.

A BathySystems SA-810 digitizer and a Sippican MK-9 digital XBT system were used for XBT data acquisition. Each was controlled by an HP-85B computer and was equipped with an LM-3A hand-held launcher and 100 feet of cable. Data were stored on SCOTCH data cartridges.

Currents were measured using a Neil Brown Direct Reading Current Meter (DRCM) during the first cruise and an InterOcean S-4 current meter during the second. The DRCM data were processed through a Neil Brown CMDT Data Terminal and stored on an IBM compatible floppy disk using a COMPAQ computer. The S-4 data were stored internally in solid state memory and were later dumped and stored on an APPLE compatible floppy disk.

The SAIC Navigation and Data Acquisition System (NDAS) was used during the second cruise in conjunction with current measurements. It included a Northstar 6000 Loran-C receiver, a plotter, a printer, appropriate software, a mini-computer and CRT, and two disk drives.

2.3.3.2 Sampling Procedures

Once on station and after the vessel had come to a complete stop, the CTD/Rosette fish was lowered far enough into the water to keep it just below the surface. Bottom depth was checked, time and location recorded, data acquisition equipment activated and the cast begun. Since no bottom depths less than 180m were observed on either cruise, the fish was generally lowered to within 5-10m of the bottom for depths between 180 and 1500m, and to a maximum depth of 1500m for all deeper bottom depths. The lowering speed on the shelf and in the thermocline was around 30m per minute and was increased to speeds approaching 60m per minute below the thermocline at the deeper stations.

During the downcast, temperature and salinity were graphically displayed in real time as a function of depth on the CRT screen and as a digital readout of temperature, conductivity and depth on the 1150 Data Terminal. Once near bottom, the CTD/Rosette was stopped and held for 5 minutes at that level while the reversing thermometers equilibrated. During this time the sample depths for the upcast were selected. The upcast was identical to the downcast except that the fish was stopped at the selected depths, the Rosette bottles tripped and short CTD calibration soaks recorded.

The sample depths were selected based on the following general criteria:

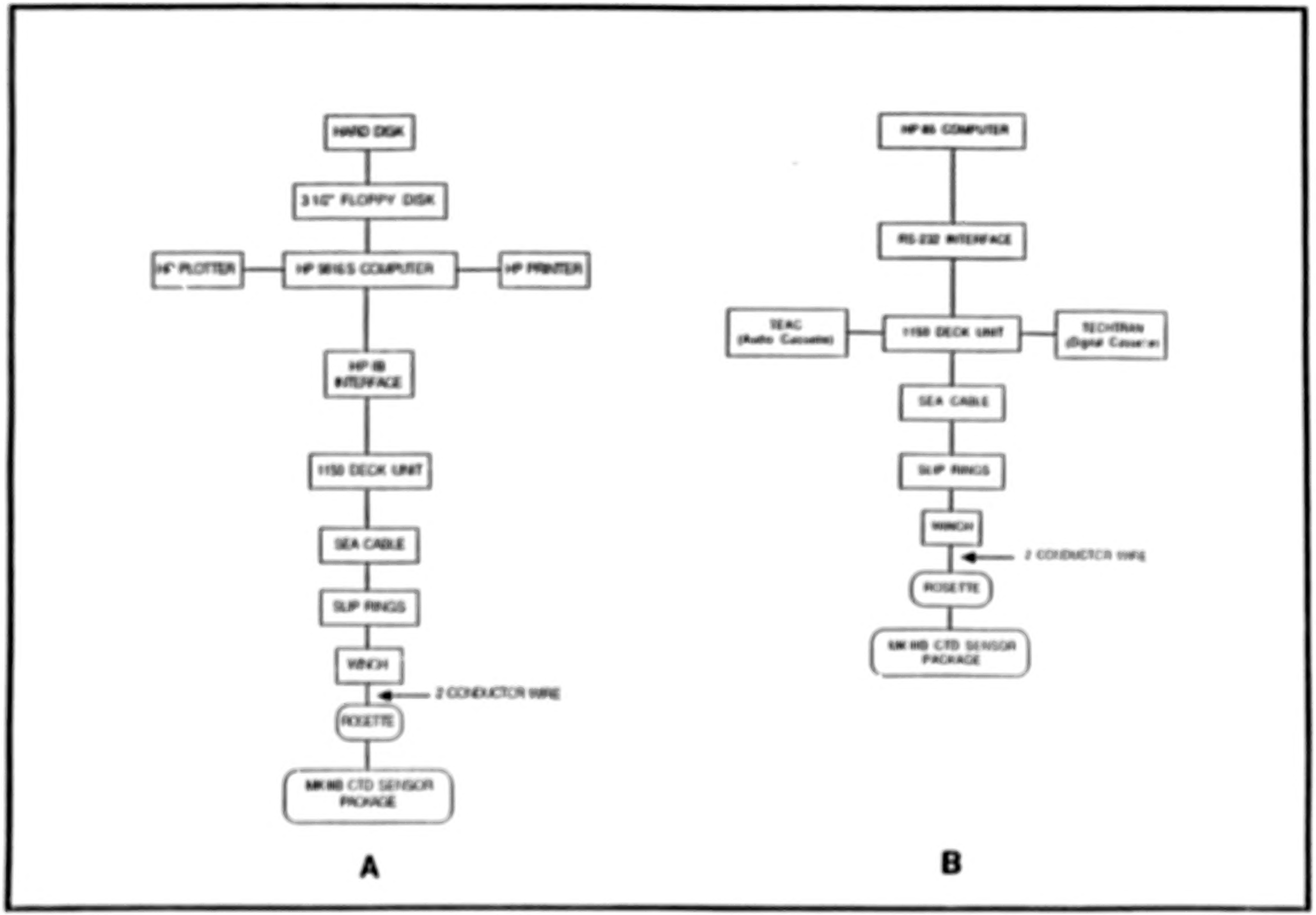

Figure 2.3-4. Schematic of CTD system used during: (a) the first hydrographic cruise aboard the R/V PELICAN (October 21-29, 1985) and (b) the second hydrographic cruise aboard the B/O ALTAIR (January 22 through February 6, 1986).

- Depths greater than 100m but less than 900m (12 depths maximum): 2, 50, 100, 150, 200, (250), 300, 400, 500, 600, 700, 800, bottom.

- Depths greater than 900m but less than 1500m (12 depths maximum): 2, 50, 100, 150, 200, 300, 400, (500), 600, (700), 800, (900), 1000, 1200, and bottom.

Occasionally, because of special situations or unusual structure, other depths were added and some were deleted.

After the near-surface bottle was tripped, the CTD fish was brought on board and secured and the CTD sensors rinsed in fresh water. Time and location were recorded and water samples drawn, beginning with dissolved oxygen and chlorophyll. Separate near-surface Niskin bottle trips were made at stations where chlorophyll samples were collected. Aliquots of these samples were filtered through 25-mm Whatman glass fiber filters and stored in a freezer for later extraction on shore by the fluorometric method of Yentsch and Menzel (1963) as described by Strickland and Parsons (1972). Oxygen samples were drawn after two rinses, and care was taken to avoid introducing air bubbles into the samples. Reagents were added, the ground glass stopper replaced, and the bottle shaken and stored. After 15 minutes, when the precipitate had settled, bottles were reshaken and stored in a dark laboratory where temperature fluctuations over the course of the day could be kept to a minimum. During the first cruise these samples were analyzed by the modified Winkler method described by Strickland and Parsons (1972) and during the second cruise by the micro-Winkler method of the Chesapeake Bay Institute. During both cruises, samples were generally run 6-12 hours after collection. Salinity samples were drawn into 250-ml linear-polyethylene or borosilicate bottles with leakproof caps and stored until analyzed by a Guildline conductive salinometer. Nutrient samples were drawn after two rinses into 125-ml polyethylene bottles during the first cruise and stored in a freezer for subsequent laboratory analysis by standard Alpkem Auto-analyzer methods. During the second cruise these samples were never frozen but were run at sea shortly after collection, again using an Alpkem Auto-analyzer. Finally, the reversing thermometers were read after equilibration to ambient temperature.

Immediately following CTD casts, at selected stations during both cruises and at depths of 10 or 20m, current measurements were made by a current meter suspended from a cable near the stern of the vessel. During the 15- to 30-minute measurement period, the ship was allowed to drift and Loran-C navigational updates were collected continuously.

At XBT stations, T-7 (760m) XBT probes were typically deployed while the ship was under way at speeds of up to 10 knots. However, 14 deployments were made during the second cruise coincident with CTD casts while the ship was on station.

2.3.4 AXBT Survey

2.3.4.1 Introduction

An aerial survey was made between November 11 and 13, 1985 as a supplement to the weather-shortened R/V PELICAN hydrographic survey made from October 21 through 29, 1985. The two types of air-deployed expendable probes included AXBTs to measure temperature and AXCPs to measure temperature and current.

Both type probes measured to depths approaching 760m. Seven AXCPs and 73 AXBTs were deployed along four lines (Lines A-D) which intersected (at 45° angles) approximately at the eddy center and extended outward away from this point some 120-160 nautical miles in each direction (Figure 2.3-5). A fifth and shorter section (Line E) was flown along the outer northwestern edge of the eddy in the vicinity of a current meter mooring (Mooring F). A station summary is presented in Table 2.3-5.

The sampling plan was designed to establish a series of transects that would completely map the eddy and cross each side approximately normal to the local frontal boundary. It was anticipated that the eddy was somewhat elliptical in shape with a major axis oriented in a NNE to SSW direction. This was based on an interpretation of data from the previous hydrographic cruise and from recent imagery provided by J. Hawkins of Naval Ocean Research and Development Activity (NORDA) and F. Vukovich. Station spacing was 10 nautical miles along the outer 50-60 nautical miles of each end of Lines A and B, and 15 nautical miles inward until 20 nautical miles from the grid center point (Station 90). A probe was also dropped at this center point position. Along Sections C and D, station spacing was 15 nautical miles inward from both ends until 20 nautical miles from the grid center point. The two stations on Line E were 30 nautical miles apart.

Four AXCPs were dropped in the northeastern quadrant of Line C, and three in the southwestern quadrant of Line D. One of the Line D probes failed completely, and temperature data from the remaining six are suspect. Of 73 AXBT probes dropped, 66 provided useful data, for a data return of 90%.

The plane, on-board equipment and personnel for the AXBT drops were provided by Aero Marine Surveys (AMS). Horizon Marine also participated, providing a technician and back-up analogue recorders on board for data acquisition when AXCPs were deployed. The AMS recorders were redundant in positioning (aerial LORAN-C), receiving and recording capability, and were specifically configured for aerial, expendable probe surveys.

2.3.4.2 Field Procedures

Using the latest available imagery and ARGOS drifter buoy locations from Drifters 3353 and 3378, a series of possible sampling schemes were evaluated and the final pattern selected (Figure 2.3-5). Prior to each daily flight, the pilot and two on-board operators were provided with the following:

- Station identification numbers
- Latitude and longitude for each station
- Type and frequency of the probe to be deployed at each station
- Direction and distance between successive stations

This information was used by the pilot to fly the proposed route and by the on-board personnel to assure that the correct probes were dropped at the selected locations. All flights originated in Harlingen, Texas, near Brownsville. Data from each profile were sent from the water surface to the plane by radio link over one of three available channels (12, 14 or 16), all of which could be received and recorded simultaneously. The observational information was contained in the modulation of the carrier frequency, and assigning a radio channel to a given station depended on consideration of station spacing, the ground speed of the plane, distance from a prior station and time required for completion of transmission from previously and

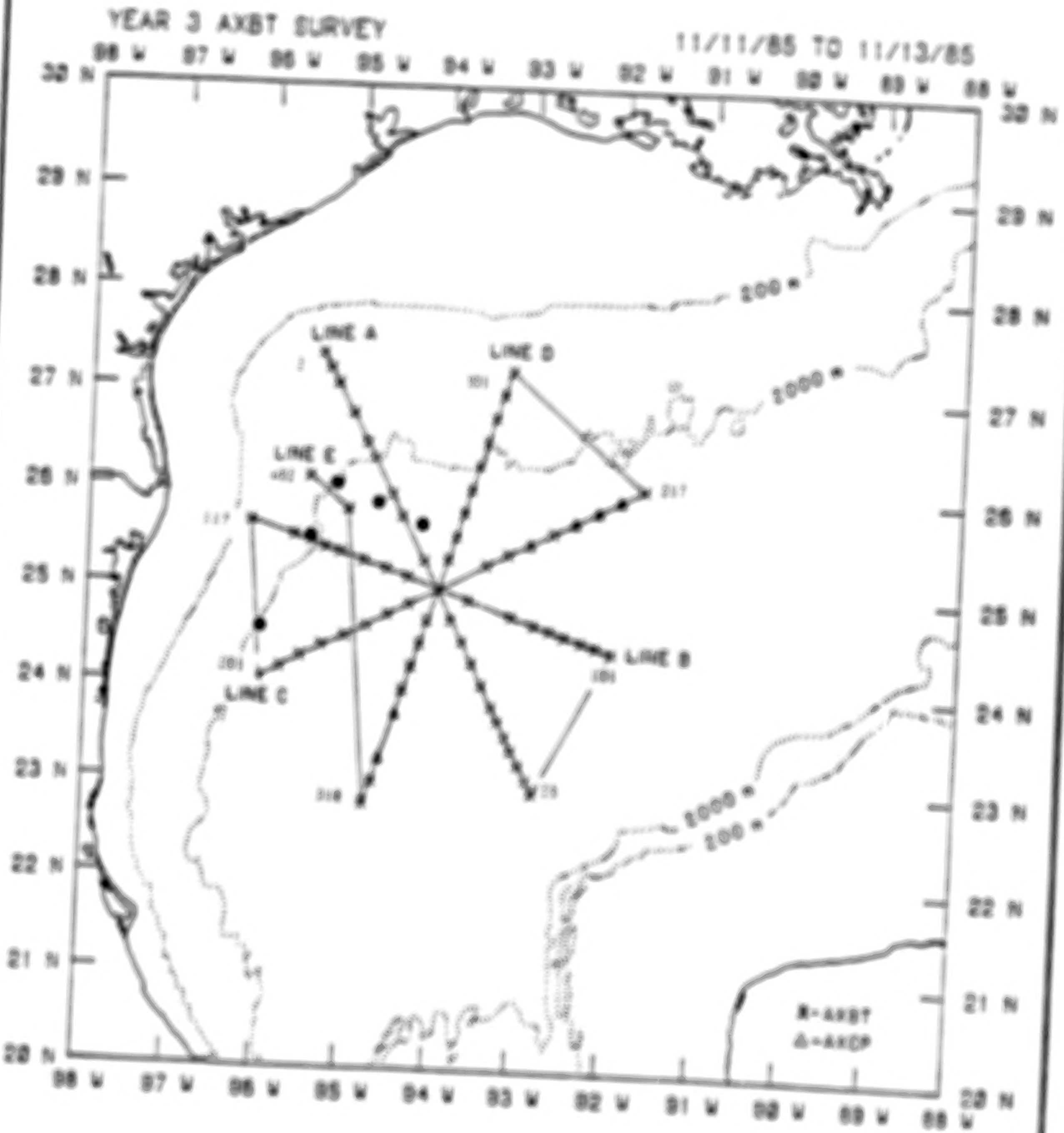

Figure 2.3-5. Flight track and the location of all AXBT and AXCP stations for the Year 3 aerial survey for the period from November 11-13, 1985.

Line	Date (GMT)	Station Numbers
A(A-AA)	November 11	2X, 3X, 4X, 6X, 8X, 9X, 11X, 12X,14X, 90X, 15X, 16X, 17X, 18X, 19X, 20X, 21X, 22X, 23X, 24X, 25X
B(B-BB)	November 11-12	101X, 102X, 103X, 104X, 105X, 106X, 107X, 109X, 90X, 110X, 111X, 112X, 113X, 114X, 115X, 116X, 117X
C(C-CC)	November 12	201X, 202X, 203X, 204X, 205X, 206X, 207X, 208X, 90X, 210X, 211X, 212P, 213X, 214P, 215P, 216P, 217X
D(D-DD)	November 12-13	301X, 302X, 303X, 304X, 305X, 306X, 307X, 308X, 309X, 90X, 310X, 311X, 312X, 313X, 314P, 316P, 317X, 318X
E(E-EE)	November 13	401X, 402X

Table 2.3-5. Station summary for the Year 2 aerial survey for the period from November 11-1[illegible]5

subsequently released probes. If position, timing and channel selection were not proper, proximate data links could broadcast simultaneously on the same channel (i.e., "on top" of one another), ruining data from both profiles. Prior to each flight, the daily station and probe frequency information was used by the ground support personnel to load and arrange probe canisters in on-board racks in the reverse order of deployment, that is, last loaded equals first deployed. To accommodate limited redeployments, an additional small storage rack contained several back-up probes (generally one in each broadcast frequency). Because of space limitations and the channel sequencing necessary, the order of probe release could not be altered once the flight began.

2.3.5 Ship-of-Opportunity (SOOP) Data

2.3.5.1 Introduction

As part of the field measurement program, SAIC sought out merchant and research vessels willing to deploy XBTs while passing through the study area. Three such vessels with irregular schedules and one line with a regular schedule were identified. The B/O ALTAIR and the HO-2, both Mexican naval oceanographic research vessels, and the EXXON JAMESTOWN, an oil industry tanker, provided opportunistic observations. These data sets are summarized in Table 2.3-6. A much more regular schedule was maintained by vessels operated by Coordinated Caribbean Transport (CCT), running between New Orleans and the Yucatan Straits. These data are summarized in Table 2.3-7 and were previously documented in the Year 4 report (SAIC, 1987).

2.3.5.2 Equipment

Data obtained from the B/O ALTAIR, the HO-2 and the CCT vessels were recorded on SCOTCH data cartridges by using a Sippican MK-9 XBT digitizer, an HP-85B mini-computer and an LM-3A handheld launcher. The data from the EXXON JAMESTOWN were digitized from graph plots obtained from a Sippican MK2A recorder with an LM-3A launcher. All vessels deployed T-7 (760m) probes.

2.3.5.3 SOOP Sections and Data Products

Examples of the cruise tracks from the B/O ALTAIR and the EXXON JAMESTOWN are presented in Figure 2.3-6. Data from these and the CCT vessels were routinely processed, generating 800m and 200m vertical section plots and a surface temperature plot along each track. Sample data products are presented in Figure 2.3-7.

2.4 Satellite Imagery

Sea-surface temperatures (SSTs), as derived from satellite imagery, had an important operational role and contributed significantly to the interpretation. RTI provided valuable GOES imagery during the planning of cruises and other field operations. RTI also used selected HRPT images (five at approximately one per month) to help explain and understand conditions and processes occurring as the primary eddy (Eddy B) interacted with the western wall of the Gulf. SAIC processed historical AVHRR imagery and made additional images available to the investigators to help visualize conditions in the Gulf basin at various clear-sky times throughout the study.

Ship	Dates	Cruise ID
ALTAIR	06/11/85 - 06/15/85	AL8501
ALTAIR	10/18/85 - 10/21/85	AL8502
ALTAIR	11/01/85 - 11/02/85	AL8503
ALTAIR	02/13/86 - 02/14/86	AL8602
ALTAIR	04/27/86 - 04/28/86	AL8603
ALTAIR	05/01/86 - 05/06/86	AL8604
ALTAIR	05/13/86 - 05/14/86	AL8605
ALTAIR	07/15/86 - 07/17/86	AL8606
ALTAIR	09/01/86 - 09/03/86	AL8607
EXXON JAMESTOWN	05/02/86 - 05/04/86	EJ8601
EXXON JAMESTOWN	05/06/86 - 05/07/86	EJ8602
HO-2	08/17/86 - 08/21/86	H28601

Table 2.3-6. MMS Ship of Opportunity data sets in the western Gulf of Mexico from June 1, 1985 through September 30, 1986.

Section	Ship	Dates	No. Trips
*I	NESTOR I	2/05/85 - 5/10/85	8
I	STENA HISPANIA	5/16/85 - 8/18/85	8
I	AMBASSADOR	9/05/85 - 9/27/86	35

* MMS section from New Orleans to the Yucatan Straits.

Table 2.3-7. MMS Ship of Opportunity section in the eastern Gulf of Mexico from January 25, 1985 through September 30, 1986.

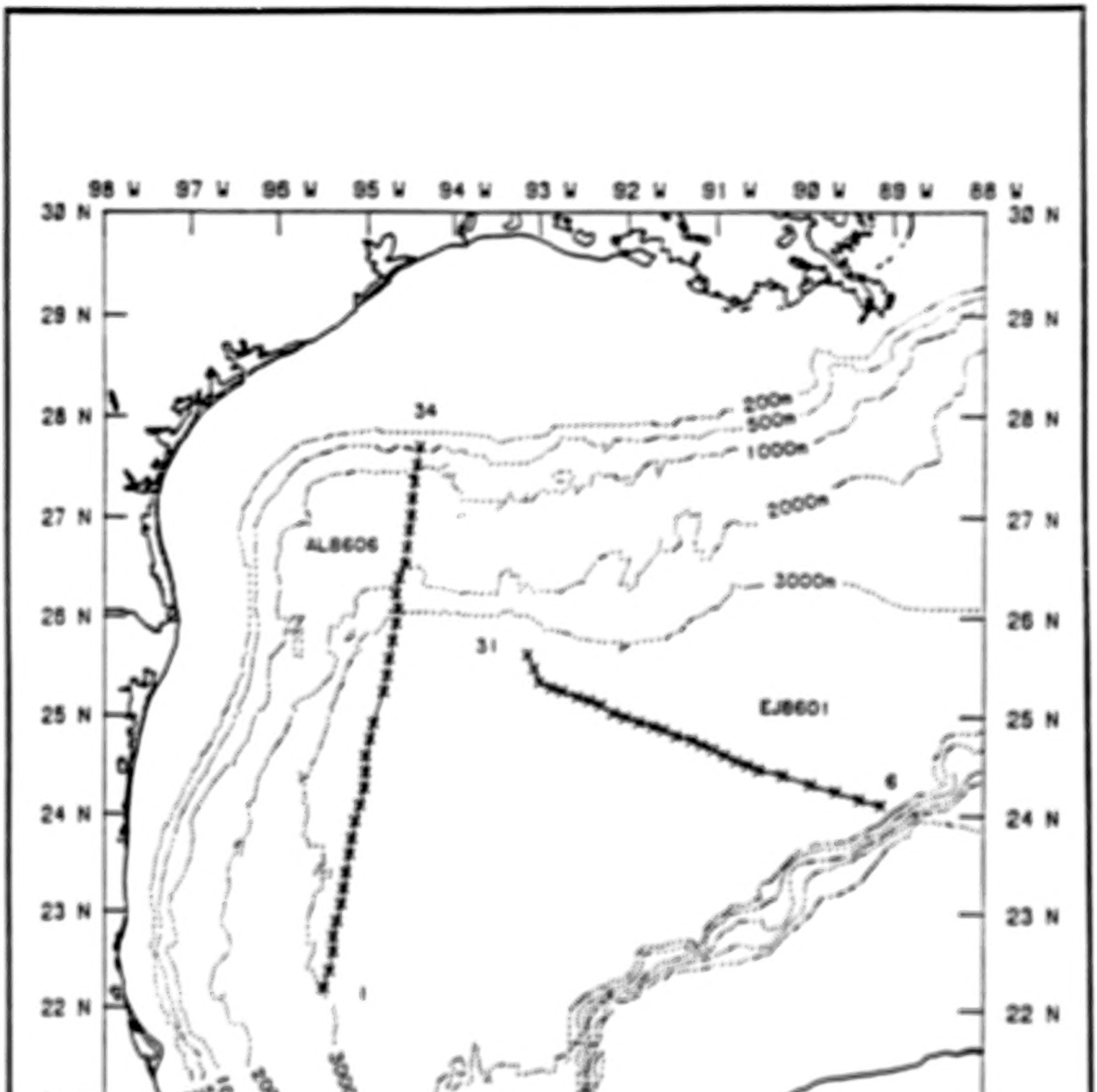

Figure 2.3-6. Examples of cruise tracks for typical MMS Ship of Opportunity data sets obtained in the western Gulf.

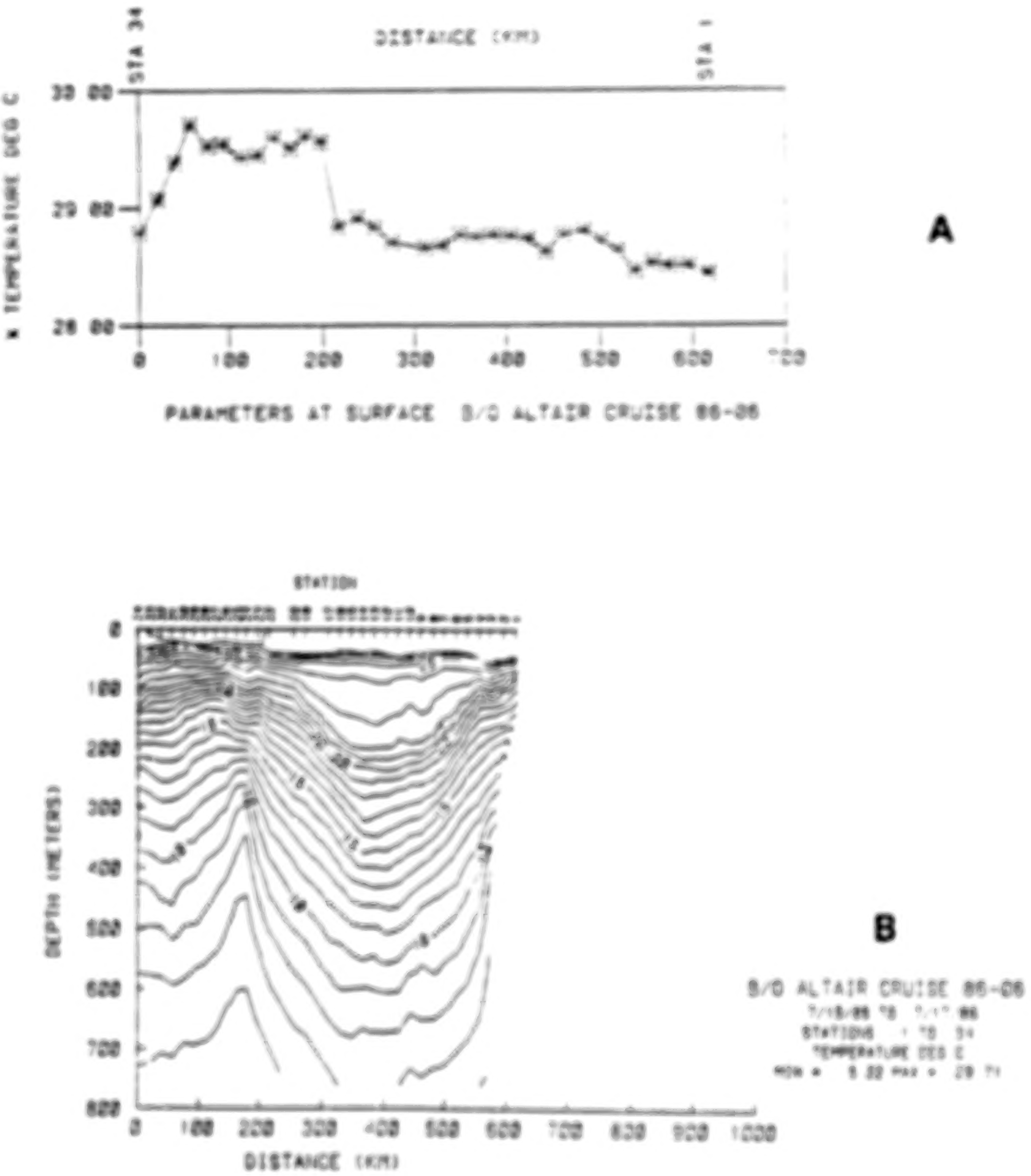

Figure 2.3-7. Examples of data products generated for each SOOP cruise: (a) surface parameters, and (b) vertical temperature.

In the Gulf, horizontal gradients of SST are sufficient to help define features and associated boundaries during the cooler months. Hence, imagery was most useful from approximately November 1985 through May 1986. During the summer months, surface waters have been warmed such that meaningful gradients could not be readily detected.

Procedures and methods used by RTI to evaluate the satellite thermal imagery were described in detail in the Years 1 and 2 program report. For more information on this topic the reader is referred to Chapter II (Section 2.3) of that report (SAIC, 1986).

2.5 Subsurface Currents

2.5.1 Introduction

Measurements of parameters such as current, temperature, pressure and conductivity are valuable inputs into the success of a field program. These data, along with hydrographic data, allow fundamental insights into circulation patterns and processes in the region being studied. In this case, the experimental design involved placing current meters at specific water depths in an array of tautline moorings which emphasized the outer slope. The purpose was to provide appropriate documentation of the 3-dimensional circulation associated with a Loop Current eddy as it interacted with the shelf-slope region.

2.5.2 Mooring Locations

Current meter data were collected from five moorings (P, Q, R, S and T) in the western Gulf of Mexico along two lines, one extending approximately along the 2000m isobath, oriented NNE to SSW (Moorings P, S, and T), and the other extending perpendicular offshore to the SE (Moorings P, Q, and R) from the northern end of the first line. The northernmost mooring (Mooring P) was common to both lines and located near 26°00'N, 95°07'W (Figure 2.5-1). The actual location of each mooring and the nominal instrument depths are presented in Table 2.5-1.

The general position of moorings and instruments was decided after a two-layer model was used to evaluate the length scale of possible radiated by-products resulting from an eddy interacting with the western slope. While not a precise approach, it provided an objective method of estimating possible wavelengths. In addition, the model results suggested that the decay process occurred more rapidly in the deeper layers so that current meters should be concentrated in the upper layers where organized flow patterns would persist longer. The decision to place the moorings in 2000m and deeper water was made because model results and limited observations indicated that the eddy flow field extended to considerable depth, and thus the interaction process began near the base of the slope.

The general geographic area for deployment was determined after several independent evaluations of eddy trajectories. This was tempered by a concern for conditions in the northwestern and northern portion of the Gulf. Placement of moorings south of 26°N was possible with the cooperation and assistance of the Mexican Navy.

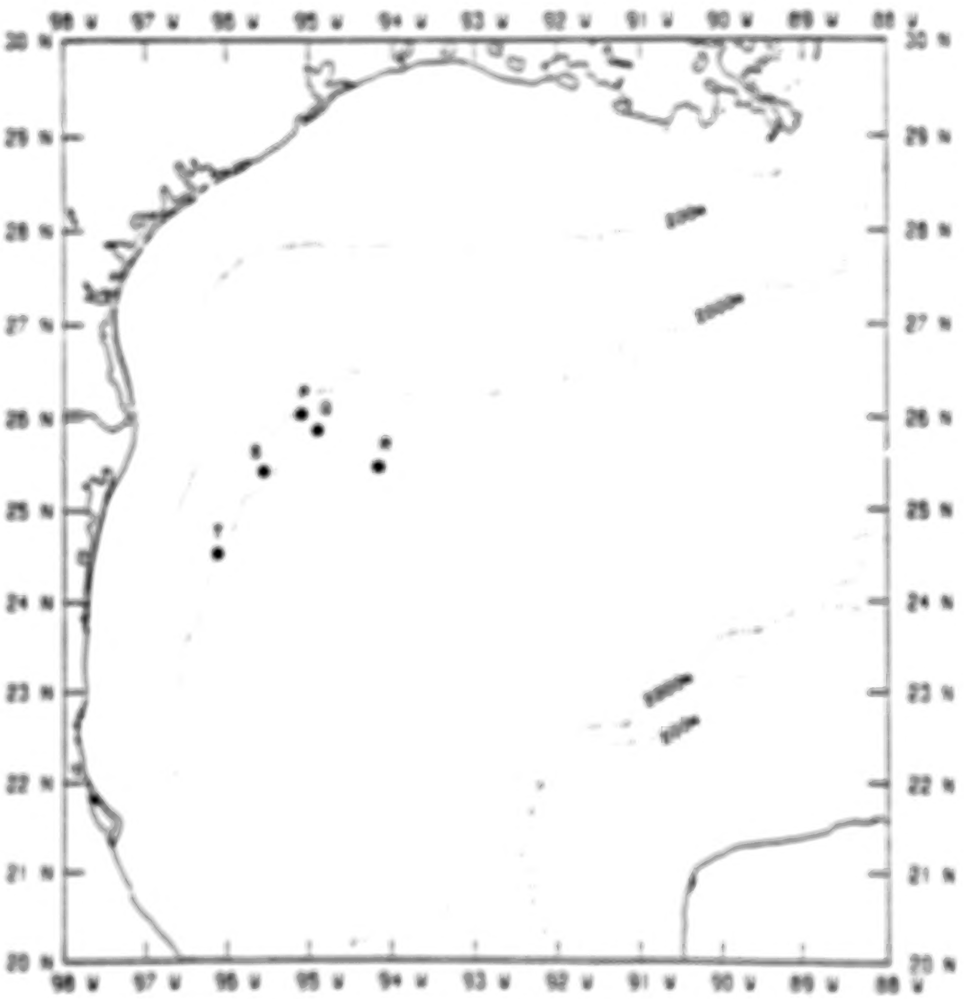

Figure 2.5-1. Mooring locations in the western Gulf of Mexico for Year 3 of the MMS sponsored Gulf of Mexico Physical Oceanography Program.

Mooring	Location Latitude	Longitude	Depth (m)	Nominal Instrument Depths(m)
P	26°00.8'N	95°07.3'W	2005	30, 230, 975, 1490
Q	25°52.3'N	94°52.8'W	3000	75, 275, 985, 1495
R	25°29.5'N	94°09.6'W	3505	180, 380, 1040, 1550, 2975
S	25°24.7'N	95°31.8'W	1500	75, 275, 980
T	24°33.2'N	96°07.1'W	2200	70, 270, 980

Table 2.5-1. Mooring locations and nominal instrument depths in the western Gulf for Year 3 of the MMS-sponsored Gulf of Mexico Physical Oceanography Program.

2.5.3 Mooring Design

Mooring design involved a process of successive iterations. The first step consisted of defining representative vertical current profiles likely to prevail at the deployment sites. This task required a review of existing literature relevant to the area of interest and of data sets collected in dynamically similar environments. Since no known data sets were identified for the specific mooring area, data from a number of dynamically similar environments were used as input to the mooring design computer program described below and for the definition of the static configuration of each mooring. The second step in the design consisted of defining a theoretical physical mooring configuration which, based on the experience of the design team, would be suitable for the environment in which it would be launched. In the third step, the adequacy of the mooring design defined in step two was checked by running the SAIC Static Buoy Analysis Program. This program is a finite element, stepwise linear integration, mooring simulation program that incorporates calibrated frictional and form drag coefficients. Outputs of this program include cable tensions, horizontal and vertical migration of the mooring, anchor weight requirements and tilt of the mooring in response to current flow. If some criterion (e.g., maximum allowable inclination) was violated, the mooring configuration was modified (step two) and step three repeated until the final configuration was such that the criteria on instrument inclination, reserve buoyancy and tensile loads were all met for the input current profiles selected in step one. The following additional design criteria were also met:

(1) The inclination angle of each current meter mooring segment was not to exceed 25° from the vertical.

(2) All instruments were shackled to glass or steel flotation sufficient to raise the instruments and associated hardware in the event of a mooring failure at any location along the mooring line.

(3) Insofar as possible, galvanized steel was used for the mooring components. Where this was not possible, dissimilar materials were isolated from one another.

(4) Paired, acoustically actuated release devices were used to attach/detach the anchor to/from the mooring to implement recovery of the instruments.

2.5.4 Aanderaa Current Meters

Aanderaa current meters were used. These instruments are self-contained recording current meters which record data on reel-to-reel magnetic tape. Data are recorded as 10-bit binary words in serial form. Six channels are available for the instrument ID, temperature, conductivity, pressure, current direction and current speed. Speed is measured by a rotor with a magnetic coupling through the instrument case and an electronic counter that sums the counts at the selected sampling rate. Direction is measured with a vane using a magnetic compass with a needle clamped on a potentiometer ring. The unit is powered by a 9-volt battery and has sufficient capacity for 10,000 samplings, where a sampling consists of a single recording of data from all six channels. The instrument is attached in-line through its two vertical spindles and is gimbal-mounted to permit up to a 25° mooring tilt without degrading the current speed measurement. It can measure speeds of up to 250 cm sec^{-1} and for periods up to 6 months at a 30-minute sampling rate, or 1 year at an hourly sampling rate.

These instruments were deployed at all levels on the five moorings. RCM-4s were deployed in the upper 1000m and RCM-5s at deeper depths. All were equipped to measure temperature, and the upper instrument on most moorings was equipped to measure pressure. Conductivity was also measured at 1 to 3 levels on each mooring in the upper 1000m of the water column.

2.5.3 Deployment Period and Data Return

All mooring work was conducted by SAIC from the B/O ALTAIR of the Mexican Navy. In June 1985 five moorings (P, Q, R, S and T) were deployed in depths of 2000, 3000, 3500, 1500 and 2200m, respectively. Four months later, in October, these moorings were rotated. At this time the upper instrument and flotation were found missing from Moorings P, Q and T. Considerable evidence suggests fishing activity damaged the moorings. In addition, rotors were missing and there was damage to the second instrument down (275m) of Moorings Q and S. The rotor was lost on the Mooring Q instrument, apparently at the time the mooring parted, and on the Mooring S instrument 2 months into the deployment period. Despite these problems, all three of the lost instruments were later recovered by fishing and oil interests and returned, resulting in a 90% data return for the initial deployment period.

Final mooring recovery was 6-1/2 months later in May 1986. At that time the upper instrument and flotation on each of Moorings S and T were missing, as were the upper two instruments and flotation on Mooring P and the upper four instruments and flotation on Mooring R (down to 1545m). Of the recovered instruments, one had flooded and a second had full tape transport, but no data could be found on the tape. None of the missing instruments has since been recovered.

A time line of the deployment periods and data return for each current meter level is presented in Figure 2.5-2. Table 2.5-2 summarizes the percent data return for each of these levels by parameter (current, temperature, pressure and conductivity when applicable). The overall data return for the two deployments was 63%, primarily due to the number of instrument losses apparently caused by offshore fishing.

2.6 References for Chapter II

Kirwan, A.D., Jr., J.K. Lewis, A.W. Indest, P. Reinersman and I. Quintero. 1987. Observed and simulated kinematic properties of Loop Current rings. J. Geophys. Res. (In press).

Lewis, J.K. and A.D. Kirwan, Jr. 1987. Genesis of a Gulf of Mexico ring as determined from kinematic analyses. J. Geophys. Res. (In press).

Science Applications International Corporation. 1986. Gulf of Mexico physical oceanography program, final report, years 1 and 2. Volume II: technical report. MMS Contract No. 14-12-0001-29158, SAIC Report No. SAIC-86/1023. 378 pp.

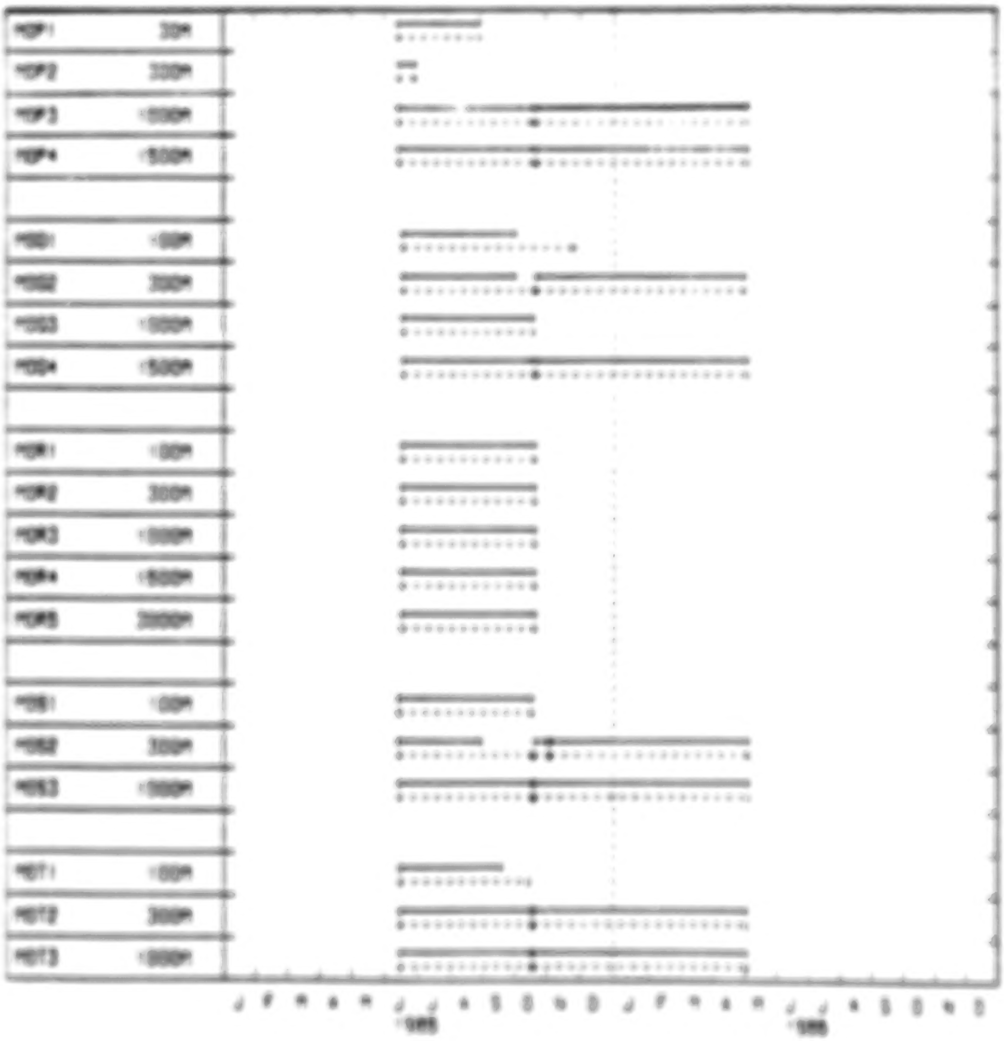

Figure 2.5-2. Time line of the deployment periods and data return for each current meter level for instruments deployed in the western Gulf of Mexico Physical Oceanography Program. The solid lines are for currents and the dashed lines are for temperature.

METER ID (DEPTH)	CURRENTS 1ST DEPLOY	CURRENTS 2ND DEPLOY	TEMPERATURE 1ST DEPLOY	TEMPERATURE 2ND DEPLOY	PRESSURE 1ST DEPLOY	PRESSURE 2ND DEPLOY	CONDUCTIVITY 1ST DEPLOY	CONDUCTIVITY 2ND DEPLOY
P1 (30m)	*62%	0%	62%	0%	62%	0%	62%	0%
P2 (230m)	12%	0%	12%	0%	============	============	============	0%
P3 (975m)	100%	100%	100%	100%	============	============	============	============
P4 (1490m)	100%	100%	100%	100%	============	============	============	============
Q1 (75m)	*87%	============	87%	============	87%	============	============	0%
Q2 (275m)	**87%	100%	87%	100%	============	============	87%	100%
Q3 (985m)	100%	0%	100%	0%	============	============	100%	0%
Q4 (1495m)	100%	100%	100%	100%	============	============	============	============
R1 (180m)	100%	0%	100%	0%	100%	0%	============	0%
R2 (280m)	100%	0%	100%	0%	============	============	100%	0%
R3 (1040m)	100%	0%	100%	0%	============	============	============	0%
R4 (1550m)	100%	0%	100%	0%	============	============	============	============
R5 (2375m)	100%	0%	100%	0%	============	============	============	============
S1 (75m)	100%	0%	100%	0%	============	0%	100%	0%
S2 (275m)	**62%	****100%	100%	****100%	============	============	============	============
S3 (980m)	100%	100%	100%	100%	============	============	============	============
T1 (70m)	***77%	0%	98%	0%	============	0%	98%	0%
T2 (270m)	100%	100%	100%	100%	============	============	============	============
T3 (980m)	100%	100%	100%	100%	============	============	============	============

Period 1: 06/11/85 - 10/21/85
Period 2: 10/21/85 - 05/05/86

* Instrument found drifting with flotation.

** Rotor missing when recovered.

*** Instrument found on beach with flotation.

**** Data collected at approximately 750 meters depth after first 8% of record as flotation was lost; speed o.k.; direction bad as instrument hanging upside down.

Table 2.5-2. Data return for moorings in the western Gulf for the period from June 11, 1985 through May 5, 1986.

Science Applications International Corporation. 1987. Gulf of Mexico physical oceanography program, final report, year 4. Volume II: technical report. MMS Contract No. 14-12-0001-29158, SAIC Report No. SAIC-87/1027. 226 pp.

Strickland, J.D.H. and T.R. Parsons. 1972. A practical handbook of seawater analysis. Fisheries Research Board of Canada, Ottawa. 310 pp.

Yentsch, C. and D.W. Menzel. 1963. A method for the determination of phytoplankton, chlorophyll, and phaeophytin by fluorescence. Deep-Sea Res. 10: 221-231.

III. DATA ANALYSIS

3.1 Introduction

Chapter III describes the various analyses used to present and/or identify physically meaningful processes or conditions. The different data discussed in Chapter II are handled in substantially different ways; therefore, this chapter is subdivided according to data type. As in Chapter II, if a thorough discussion of a data analysis procedure is available in prior program reports, it is not reproduced in this document. As appropriate, it may be described by reference to these prior reports or by reference with a brief summary discussion. Those analyses that are accepted as routine within the physical oceanographic community are not described in detail.

By separating discussion of the details of analysis methodologies from a discussion of the physically meaningful results, process characterization in Chapter IV includes only that material strictly relevant to understanding better the circulation in the study area.

3.2 Drifting Buoys

3.2.1 Introduction

Drifter trajectories were analyzed extensively. Since many of the analysis methods have been described in considerable detail in prior program reports, the reader is directed to these reports for that presentation. Some additional analyses schemes were developed for the present report. In particular, the numerical scheme which uses time histories of drifter trajectories to estimate ensembles of the surface current field is summarized in Section 3.2.3 below.

3.2.2 Kinematic Parameters and Procedures

The procedure for calculating the kinematic parameters for an eddy is based on an analysis of the curvature of a drifter trajectory section in the eddy. It is assumed that the kinematics of the eddy are essentially constant for a given section of the trajectory. Any variations in the drifter velocity are thus a result of the drifter encountering spatial variations in the flow field. From this, one may calculate the following for that section of the trajectory:

(U, V) - translation velocity of the eddy center,

(X, Y) - distance to the center of the eddy,

(u, v) - swirl velocity of the water around the center of the eddy,

f - vorticity (related to angular velocity),

D - divergence (rate of change of area),

N - normal deformation rate (shape change due to forces acting normal to the sides of the eddy), and

S - shear deformation rate (shape change due to forces acting parallel to the sides of the eddy).

The importance of the above parameters is considerable. From divergence, swirl velocities and distance to the eddy center, changes in the size of the upper layers of the eddy as well as the rate of these changes can be studied. This information provides valuable clues as to interactions of the eddy with topography and other oceanographic features.

Vorticity and divergence are critical dynamic parameters. From these and the position of the eddy, one may consider potential vorticity balance. Potential vorticity is a form of rotational balance, analogous to the change in the rate of spin of ice skaters as they pull their arms closer to their bodies. In the case of LC eddies, the spin rate is given by the vorticity (f) plus a parameter dependent on latitude. The divergence (D) gives the information pertaining to eddy width. An eddy that is becoming wider will typically begin to spin slower.

Finally, the normal and shear deformation rates (N and S) provide information on orientation and eccentricity. Large Gulf eddies are not always circular and often can be quite elliptical. Values of N and S can be mathematically manipulated to give the length of the major and minor axis of an ellipse fitting the path of the drifter. The spatial orientation of the ellipse can also be determined from N and S. Additional details on the kinematic parameters and the analysis methods can be found in Kirwan et al. (1984a; 1984b; 1987).

3.2.3 Flow Field Estimation

To develop the velocity field associated with the eddy that was located in the western Gulf, daily-averaged positions from the MMS Drifters 3353 and 3378 and from the offshore industry Drifter 3492 were integrated between December 1985 and January 1986. These data were used to obtain 24-hour displacements and daily-averaged velocity vectors. The velocities were carefully screened to remove the effects of changes occurring in the eddy within the 2-month period. A gravitational-weighted interpolation scheme was used to interpolate velocity components to each one-half degree latitude by one-half degree longitude using the screened velocity field. Analyses of unit vectors depicting the flow field direction near the surface and of contours of constant speed were developed using standard analysis routines.

The velocity components provided on the one-half degree latitude by one-half degree longitude grid were used to calculate the near-surface distribution of the vertical component of the relative vorticity (ζ) and of the horizontal component of the divergence (D). The vorticity and divergence were calculated using the following expressions:

$$\zeta = \frac{\partial v}{\partial x} - \frac{\partial u}{\partial y} \quad ; \text{ and}$$

$$D = \frac{\partial u}{\partial x} + \frac{\partial v}{\partial y}$$

These formulas were expressed in a finite difference form; that is,

$$\zeta_{(i,\,j)} \cong \frac{v(i+1,\,j) - v(i-1,\,j)}{2\Delta x} - \frac{u(i,\,j+1) - u(i,\,j-1)}{2\Delta y} \quad ;$$

and

$$D_{(i,\,j)} \cong \frac{u(i+1,\,j) - u(i-1,\,j)}{2\Delta x} + \frac{v(i,\,j+1) - v(i,\,j-1)}{2\Delta y} \quad ;$$

where i and j refer to the west-east and south-north grid locations respectively, Δx is the average distance in meters for a one-half degree longitude increment in the western Gulf and Δy is the average distance in meters for a one-half degree latitude increment in the western Gulf. Positive values of verticity reflect cyclonic verticity, and negative values, anticyclonic verticity. Positive values of D reflect divergence and negative values, convergence. Values of (ζ) and D were calculated at each i, j location possible on the grid and were then contoured.

3.3 Survey Data

3.3.1 CTD and XBT Data Calibration

Salinity (calculated from conductivity), temperature and depth data recorded by the CTD system, described in Section 2.3.3.1 (p. 13), were calibrated against data from the Rosette bottle casts. The XBT data were adjusted following comparison with calibrated CTD data from coincident or adjacent stations occupied during the cruises, and calibrations were performed for dissolved oxygen, nutrients and chlorophyll as part of the standard analytical procedures cited in Section 2.3.3.2 (p. 13).

The CTD salinity calibration data were obtained from the upcast bottle and CTD samplings in mixed layers, usually at the bottom, after the downcast. The salinities were run by the technical staffs at Old Dominion University and Texas A&M University on Guildline conductive salinometers. Temperature calibration data were obtained by comparing the CTD and the reversing thermometer readings from mixed layers, again usually at or near the bottom of the cast. The depth sensor was occasionally checked against wire out and, where appropriate, compared to the thermometric depth calculated from the unprotected and protected reversing thermometer readings. These comparisons revealed that no offsets or adjustments were required in the CTD salinity, temperature or depth data for the initial cruise aboard the R/V PELICAN because the differences were found to be within the range of the accuracy of the instruments used for the calibration check. For the second cruise aboard the B/O ALTAIR, however, a significant offset was detected in the temperature and calculated salinities. Subsequently, a post-cruise calibration check at the Northwest Regional Calibration Center revealed that the CTD temperature sensor was reading low by 0.049°C, that conductivity was reading high by 0.008 millimoles cm^{-1} and that pressure was within specifications. These calibration offsets which were consistent with the prior calibration were applied to the data in processing.

The XBT data from the two cruises were calibrated against CTD casts. Data from the January 1986 B/O ALTAIR cruise were calibrated by fitting to calibrated CTD data from 11 coincidental stations. This resulted in a depth adjustment of -4.2% in the data to compensate for the fact that the XBT isotherms were shallow by this amount. A similar correction (-4.5%) was applied to the XBT data from the October 1985 R/V PELICAN cruise because the isotherms from these XBTs were also significantly shallower than those observed in the adjacent calibrated CTD casts. Because coincidental CTD and XBT casts were not made during the October cruise, a comparison of 14 XBTs with the mean of the adjacent CTD casts on either side was made. This gave results similar to those observed during the January cruise. Scatter plots of the CTD minus XBT depth difference (for the compared isotherms) versus XBT isotherm depth for both cruises are presented in Figure 3.3-1.

3.3.2 Estimation of Dynamic Heights from XBT Data

The nature of the study of western Gulf eddies required rapid hydrographic surveys and the use of ships of opportunity. This necessarily restricted many of the surveys to mapping the temperature field using XBTs. It is advantageous, however, to obtain some measure of the density field so that dynamical quantities such as dynamic height can be calculated to give a picture of the geostrophic flow field. Below about 150 to 200m the temperature and salinity characteristics are remarkably consistent for Gulf waters. Two of the western Gulf hydrographic surveys, the R/V PELICAN PN-85-02 and B/O ALTAIR AL-86-01 cruises, included CTD stations. The R/V PELICAN survey (October 21 through 24, 1985) has a particularly useful, well-resolved CTD transect to depths of 1000m through the center of the major eddy which is the primary focus of this study (Figure 2.3-1, p. 14). The T-S diagram for the R/V PELICAN transect shows that for temperatures colder than 18°C there is a tight relation with little scatter. Between 18°C and 25°C the T-S curve has essentially two branches: the high salinity branch (>36.4 ppt) is associated with the subtropical underwater (SUW) core at about 100 to 150m depth in the center portion of the eddy, and the lower salinity branch (~36.0 ppt), which has more scatter, comes from water shallower than about 150m on the eddy edges (Figure 3.3-2).

The approach used to construct a synthetic salinity field from XBT casts is to use a reference CTD 150 to 650m station from the eddy center (Station 39 from PN-85-02), since water warmer than 17°C is found below 150m in the center of a warm eddy but is usually confined to depths shallower than 150m in cyclonic features and the outer parts of major eddies. Thus, for these latter stations the salinities are found from the lower half of the T-S curve, and the lower salinity branch is effectively excluded from the calculations. In the warmer eddy center the high salinity branch (22°C to 15°C, 36.0 to 36.7 ppt) is utilized automatically by using the reference station from the eddy

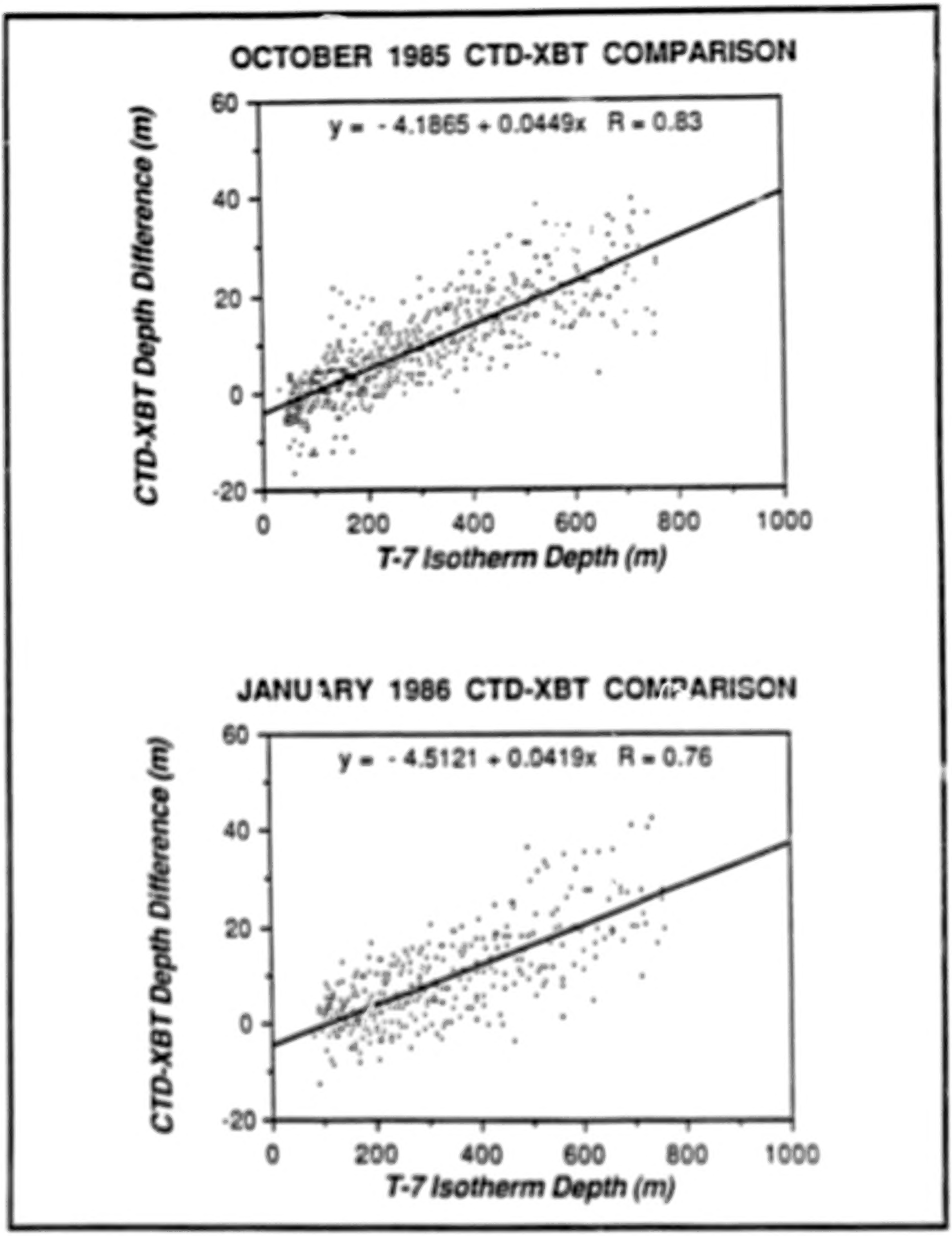

Figure 3.3-1. Data plots and regression fits of CTD minus XBT depth differences for the same isotherms versus T-7 XBT isotherm depths for the October 1985 and January 1986 cruises.

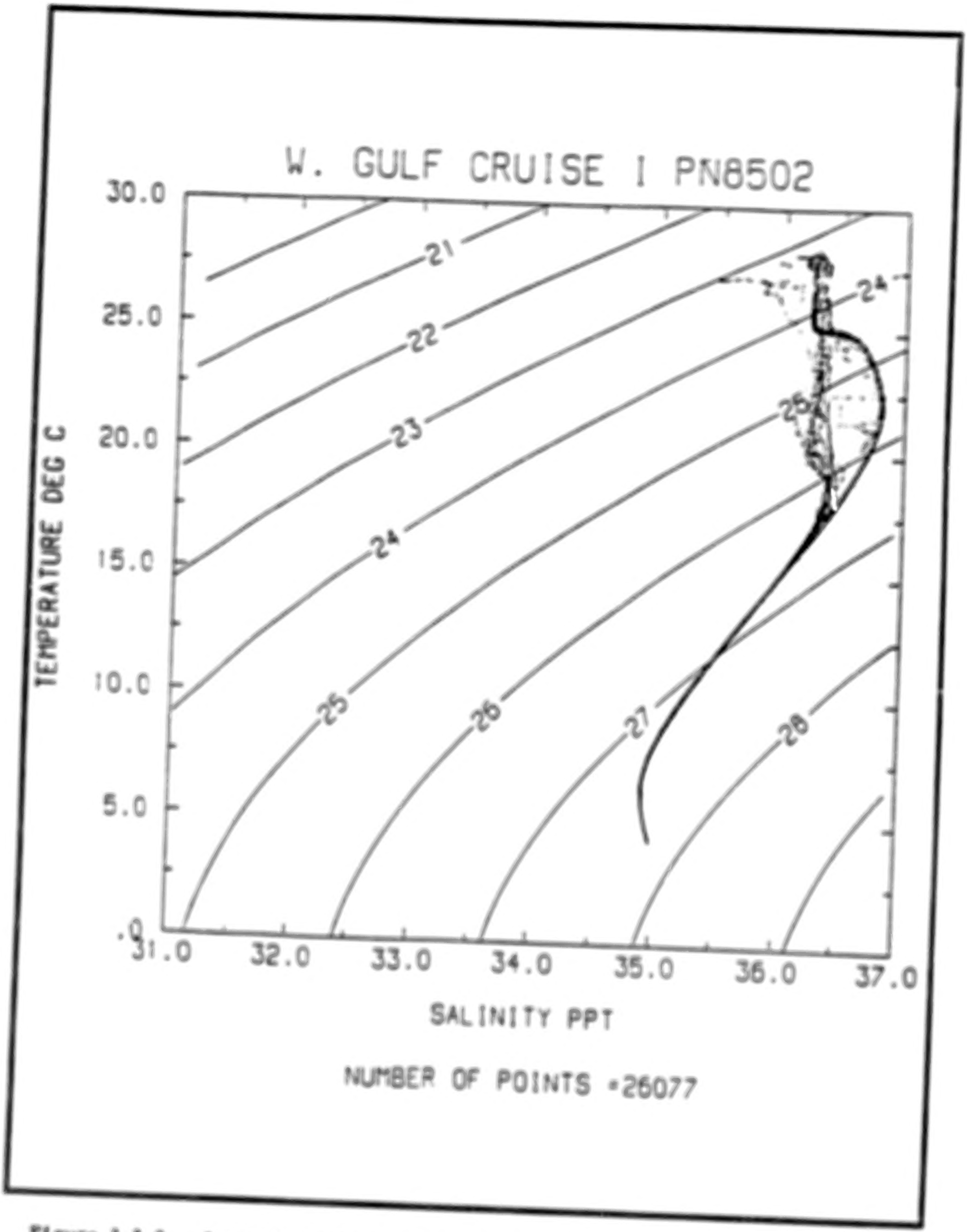

Figure 3.3-2. Composite T-S plot of all CTD data collected during the October 1985 R/V PELICAN cruise.

water mass containing SUW. This method may not work as well if the SUW mass is eroded by mixing. However, this did not occur in this set of surveys as comparison with the T-S curve from the B/O ALTAIR AL-86-01 cruise, 3 months later, shows (Figure 3.3-3). There the high salinity branch between 22°C and 5°C is practically identical to the R/V PELICAN T-S curve over the same temperature range (Figure 3.3-4).

The procedure for each temperature value from an XBT cast between the depths of 150 and 650m (650m is the deepest common depth of the XBT cast) is to search the reference cast from the bottom up for the same temperature value and then use the corresponding salinity value interpolated between observations as necessary. The procedure was checked by calculating dynamic heights from the CTD stations for the R/V PELICAN cruise, using the actual observations and using synthetic salinities (temperatures from the CTD) derived from the reference station. The dynamic heights and the difference between the true and synthetic dynamic heights are given in Figure 3.3-5. The maximum absolute error is 1.8 dynamic cm. A similar check was performed for the B/O ALTAIR AL-86-01 CTD stations with equally satisfactory results.

3.4 Satellite Imagery

Details of the processing and analysis of satellite data are identical to those reported in the Years 1 and 2 report (SAIC, 1986). Reference should be made to Section 3.3 of this earlier report for a detailed discussion of real-time processing, post-processing and the actual analysis of these data.

3.5 Subsurface Currents

Subsurface currents/temperature time series were analyzed using techniques which have been described in detail in previous final reports in the sequence of MMS Gulf Physical Oceanography Programs. The methodologies are all completely verified and most are standard within the physical oceanographic community. All field data taken as part of this program have been incorporated into the program data base maintained by SAIC. All analysis and graphics routines used for the time series analysis, time and frequency domain are coupled to the database to help assure accuracy and veracity of the procedures. A detailed discussion of the time series analysis procedures is contained in Chapter III of the Final Report for Program Years 1 and 2. (See References for further information).

3.6 References for Chapter III

Kirwan, A.D., Jr., W.J. Merrell, Jr., J.K. Lewis and R.E. Whitaker. 1984a. Lagrangian observations of an anticyclonic ring in the western Gulf of Mexico. J. Geophys. Res. 89(C3): 3417-3424.

Kirwan, A.D., Jr., W.J. Merrell, Jr., J.K. Lewis, R.E. Whitaker and R. Legeckis. 1984b. A model for the analysis of drifter data with an application to a warm core ring in the Gulf of Mexico. J. Geophys. Res. 89(C3): 3425-3438.

Kirwan, A.D., Jr., J.K. Lewis, A.W. Indest, P. Reinersman and I. Quintero. 1987. Observed and simulated kinematic properties of Loop Current rings. J. Geophys. Res. (In press).

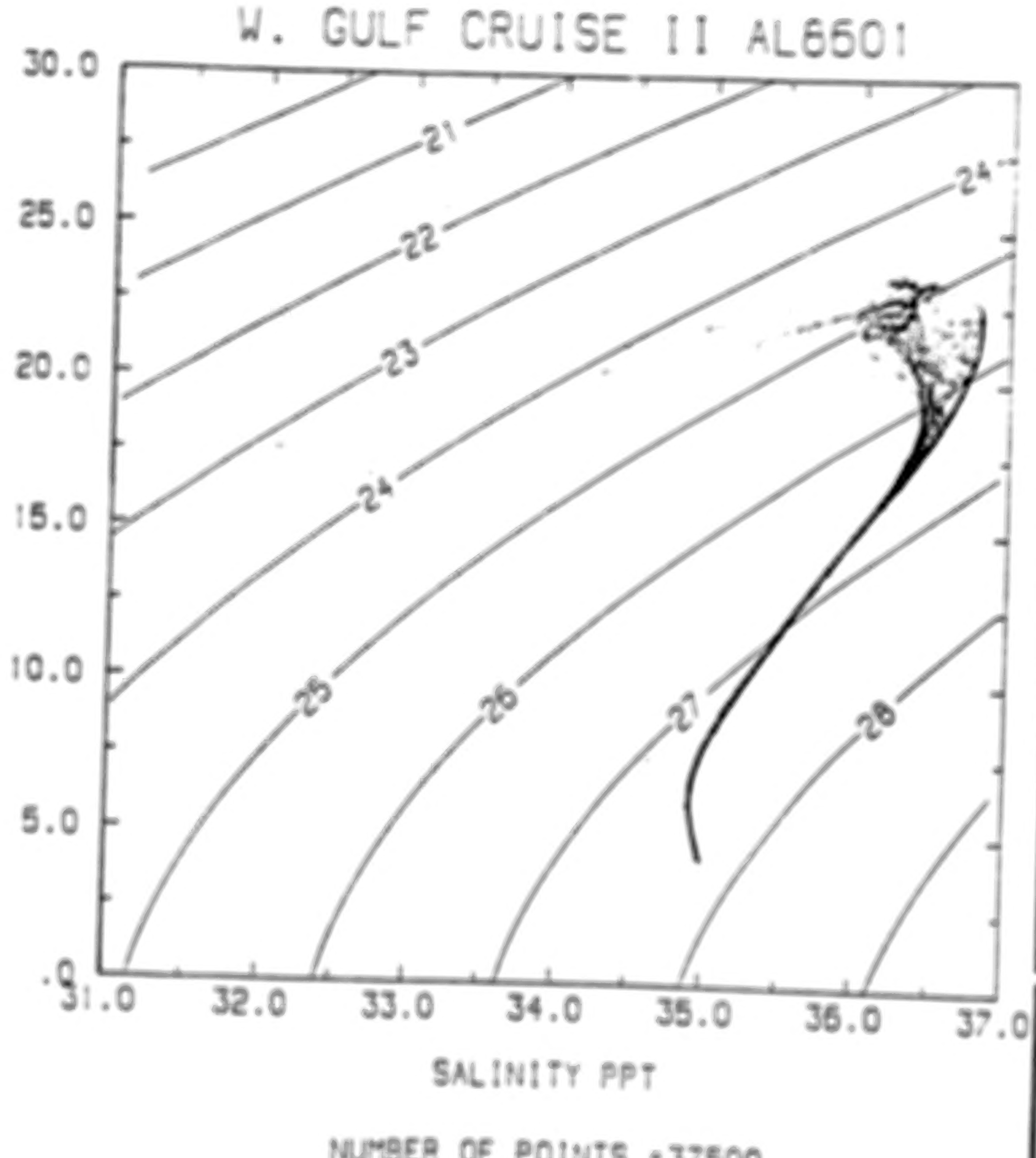

Figure 3.3-3. Composite T-S plot of all CTD data collected during the January 1986 R/V ALTAIR cruise.

EDDY CENTER

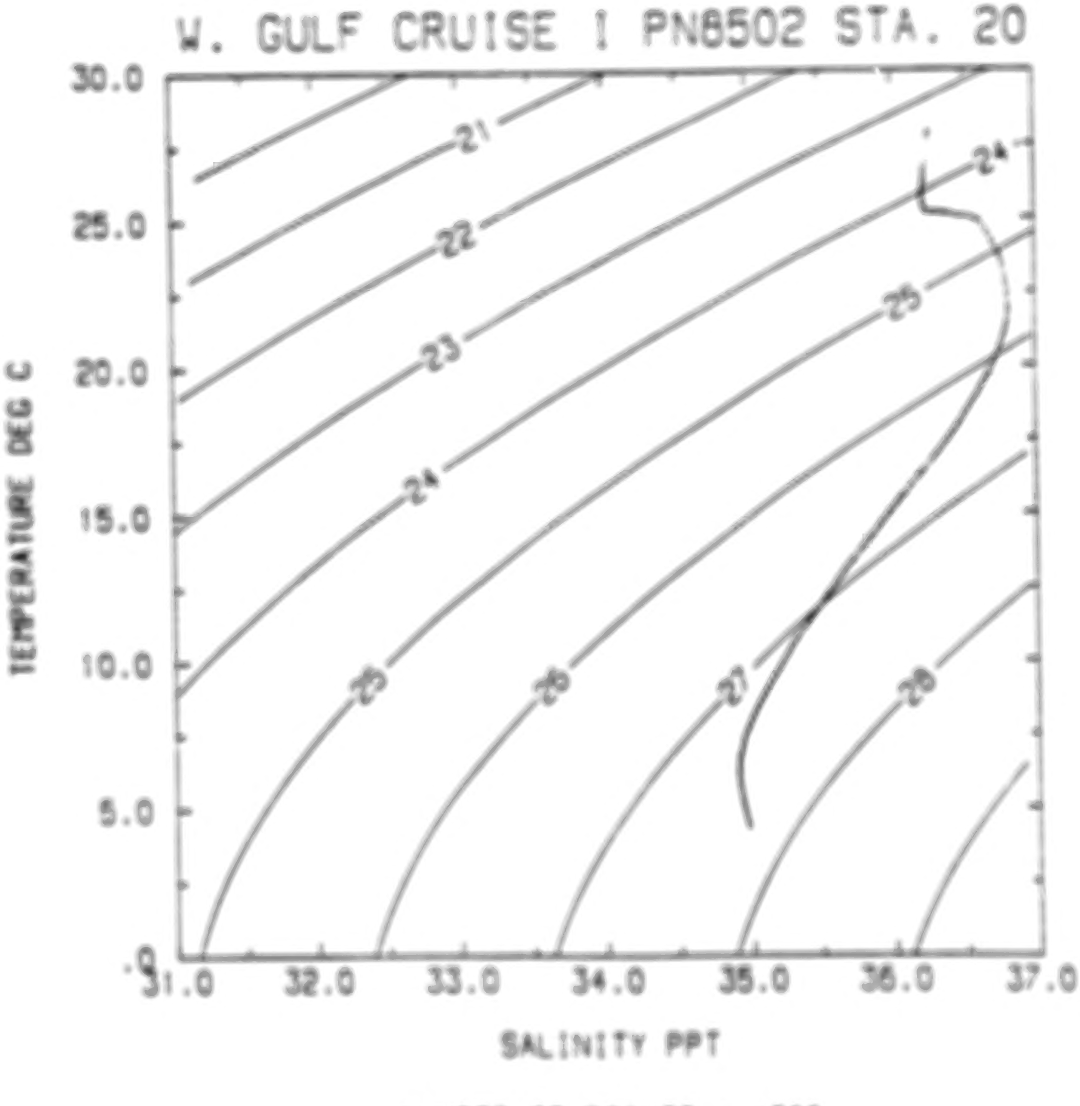

Figure 3.3-4. T-S diagram of Station 20 in the center of Eddy B from October 1986.

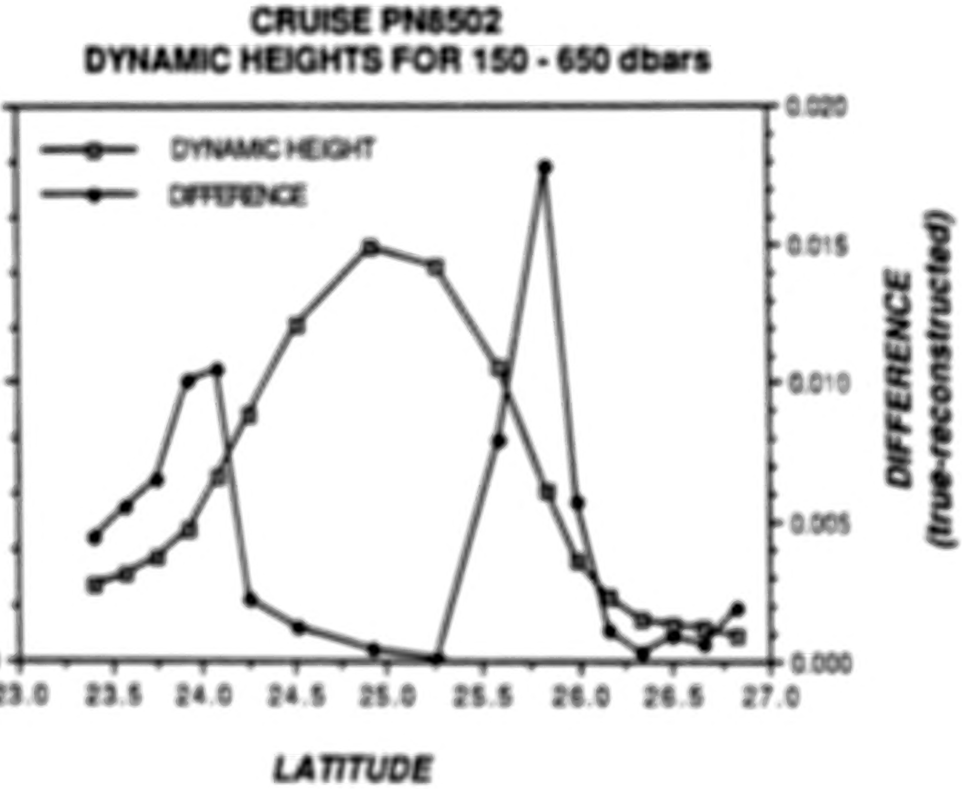

Figure 3.3-5. Plot of the dynamic heights and the difference between true and synthetic dynamic heights derived from XBT data for 150-650 decibars for the R/V PELICAN cruise in October 1985.

Science Applications International Corporation. 1986. Gulf of Mexico physical oceanography program, final report, years 1 and 2. Volume II: technical report. MMS Contract No. 14-12-0001-29158, SAIC Report No. SAIC-86/1023. 378 pp.

IV. TECHNICAL DISCUSSION

4.1 Introduction

A discussion of processes associated with the westward migration of a Loop Current (LC) eddy (Eddy B) is presented in this chapter. The conditions inside the eddy and the conditions affecting it from the outside varied as it moved to the west. The chronological approach by which the material in this chapter is organized coincides with that migratory process. The key intervals and associated descriptions are as follows:

Section 4.2:	General Chronology.
Section 4.3:	Eddy Separation and Initial Movement.
Section 4.4:	Eddy-Slope Interaction and Cyclone Intensification in the Western Gulf.
Section 4.5:	Reflection and Dissipation.
Section 4.6:	Eddy-Eddy Interaction.

As discussed in Chapter II, an extensive and relevant data set was taken during this project, with a focus on documenting conditions in and immediately adjacent to the primary eddy. Some data were also collected in the extended neighborhood of the eddy. Analyses of the complete data set made it apparent that other features and organized circulation patterns had a direct influence on the primary characteristics of these features. Understanding the role of these other features was not always possible because they were not as well documented as the primary feature. Hence, it is necessary to extend some of the thinking to evaluate what these "environmental" influences may have been. It is also necessary to remember that this intermediate and far field becomes important primarily because of the excellent documentation of the changes and processes in the feature itself.

4.2 General Chronology

The data set described in Chapter II permits the most detailed analysis yet of Loop Current eddies and their relation to the mesoscale variability of the western Gulf. The field experiment began in June 1985 with the deployment of current meter moorings. With some degree of serendipity, a large, warm-core, anticyclonic (clockwise) rotating eddy (Eddy B) separated from the Loop Current in early July 1985. It was continuously observed by one or more of the techniques previously described until it finally coalesced with a newer (i.e., more recently shed) Loop Current eddy (Eddy C). The goal of this report is to describe the motion and evolution of Eddy B. The origin and evolution of associated, cold-core, cyclonic (counterclockwise) rotating features are an integral part of the description.

This section provides a general overview of the sequence of events that occurred during the study. The four principal phases in the life of Eddy B are identified, and other observed mesoscale features are identified and discussed. A more detailed analysis of each phase in the life of Eddy B begins with Section 4.3.

The observed depth of the 8°C temperature surface during each of the major surveys indicates the pattern of geostrophic flow and the evolution of the spatial structure of Eddy B. Regions where the temperature surface is deep correspond to anticyclonic (clockwise) circulation, and those regions where the temperature surface is shallow correspond to cyclonic (counterclockwise) circulation. Previous studies of the Gulf generally have used warmer (i.e., shallower) surfaces for this purpose. But surfaces warmer than about 14°C in the western Gulf are frequently relatively flat in cyclonic eddies and so do not always depict these features well. Nowlin's (1972) Section D of the vertical temperature structure from the HIDALGO 62-H-3 data set clearly illustrates this fact. Some 1-day, mean current vectors from the moored current meters and trajectories of satellite-tracked drifters are plotted on the maps of the 8°C surfaces to provide a qualitative comparison with the implied baroclinic flow. Between the times of the surveys, drifter trajectories are used to indicate the general behavior of Eddy B.

The first phase in the evolution of Eddy B began with separation from the LC in early July 1985 and covers its initial westward movement across the deep Gulf through October. The initial separation pattern is discussed in the Final Report for Program Year 4 (SAIC, 1987). ARGOS Drifter 3378 was placed in Eddy B on July 18. Figure 4.2-1 shows the trajectory of Drifter 3378 to September 18 and the positions of the five current-meter moorings deployed in June. The center of the eddy moved almost due west during this period, a distance of about 280 km (150 nautical miles), or about 4.6 km d^{-1} (Note: 1 km d^{-1} equals 1.16 cm sec^{-1}). The diameters of the orbits of the drifter were roughly 130 km during the first half of September when they were relatively circular. This value does not, however, indicate the size of the eddy as the radial position of the drifter moves in and out because of convergence and divergence in the surface layer. Figure 4.2-2 shows the trajectory of Drifter 3378 during the month of October 1985. The orbits of the drifter were about half the diameter of the earlier ones. The net rate of translation was about 3.7 km d^{-1} to the southwest, but since the eddy was almost stationary during the first 3 weeks of October, the rate was faster during the latter portions of this interval.

The hurricane-shortened hydrographic survey by the R/V PELICAN from October 21 through 29, 1985 (Section 2.3.2, p. 11), together with the XBT data collected by the R/O ALTAIR while servicing the current meter moorings from October 17 through 21, defined the structure of Eddy B three months after separation from the Loop Current. Figure 4.2-3 shows the depth of the 8°C isotherm based on both CTD and XBT stations and on the assumption of axial symmetry in regions with no data (dashed lines). (Note: the bold letters H and L signify deep and shallow isotherms in maps of the depth of an isotherm). The main transect, made from October 22 through 24, passed about 30 km east of the eddy's center as estimated from the trajectory of Drifter 3378 and the several additional XBT/CTD stations shown in Figure 4.2-3. The heavy curved line is the track of Drifter 3378 from October 22 through 27. The drifter's motion was fairly circular during the time of the main transect and then acquired a component of westward translation. Figure 4.2-4, a vertical temperature section using the CTD stations of the main transect, illustrates the size and symmetry of Eddy B. The radius of an eddy can be defined in several ways. Elliott (1979) used the position where the curvature of the 20°C isotherm changes sign. The curvature of the 20°C isotherm in Figure 4.2-4 does not change sign, but for deeper isotherms the change occurs near Stations 6 and 34, indicating a radius of at least 180 km. Elliott estimated a root mean

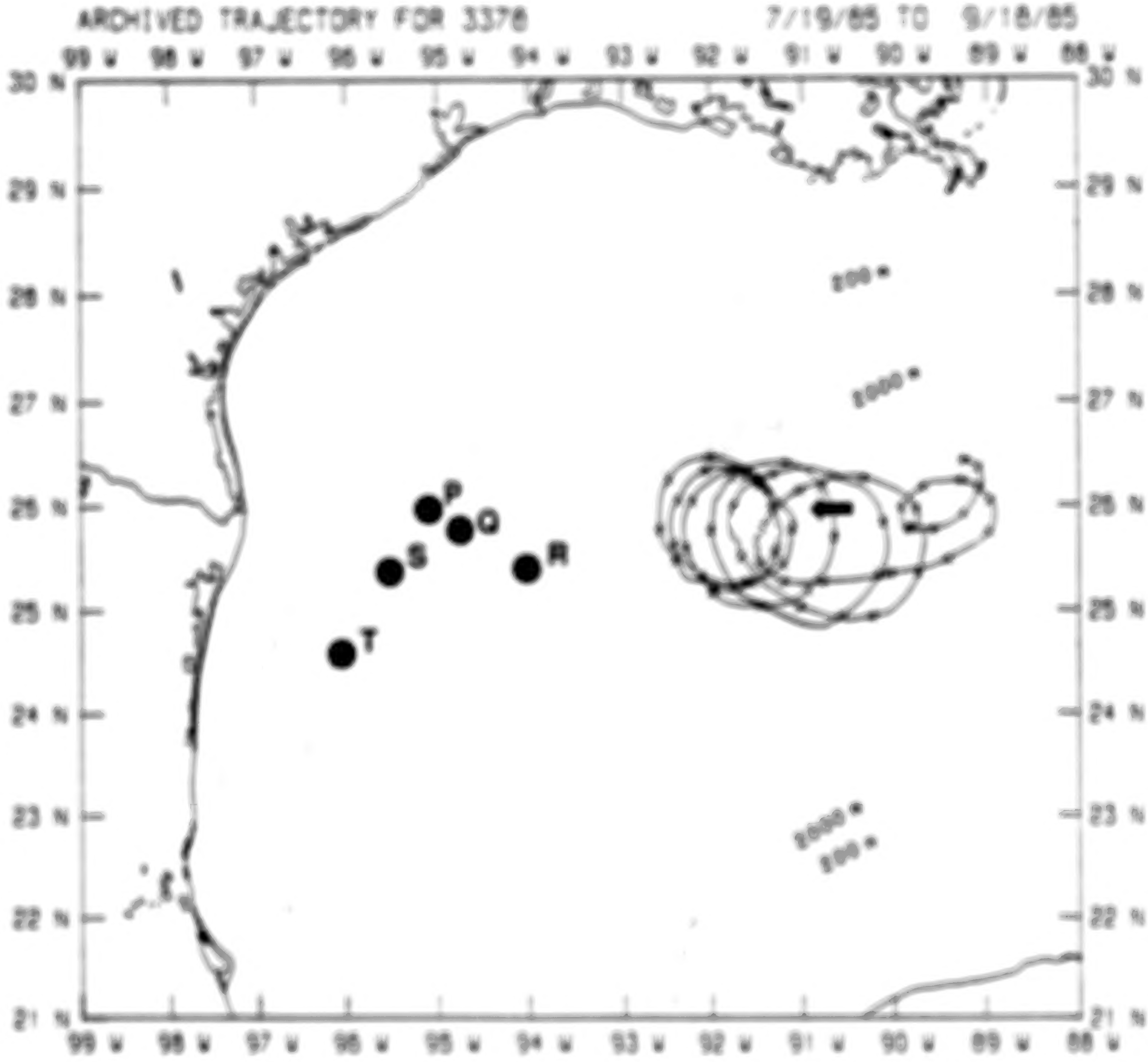

Figure 4.2-1. Partial trajectory for Drifter 3378 and the locations of the five current meter moorings (P, Q, R, S and T). Each X indicates a one-day interval.

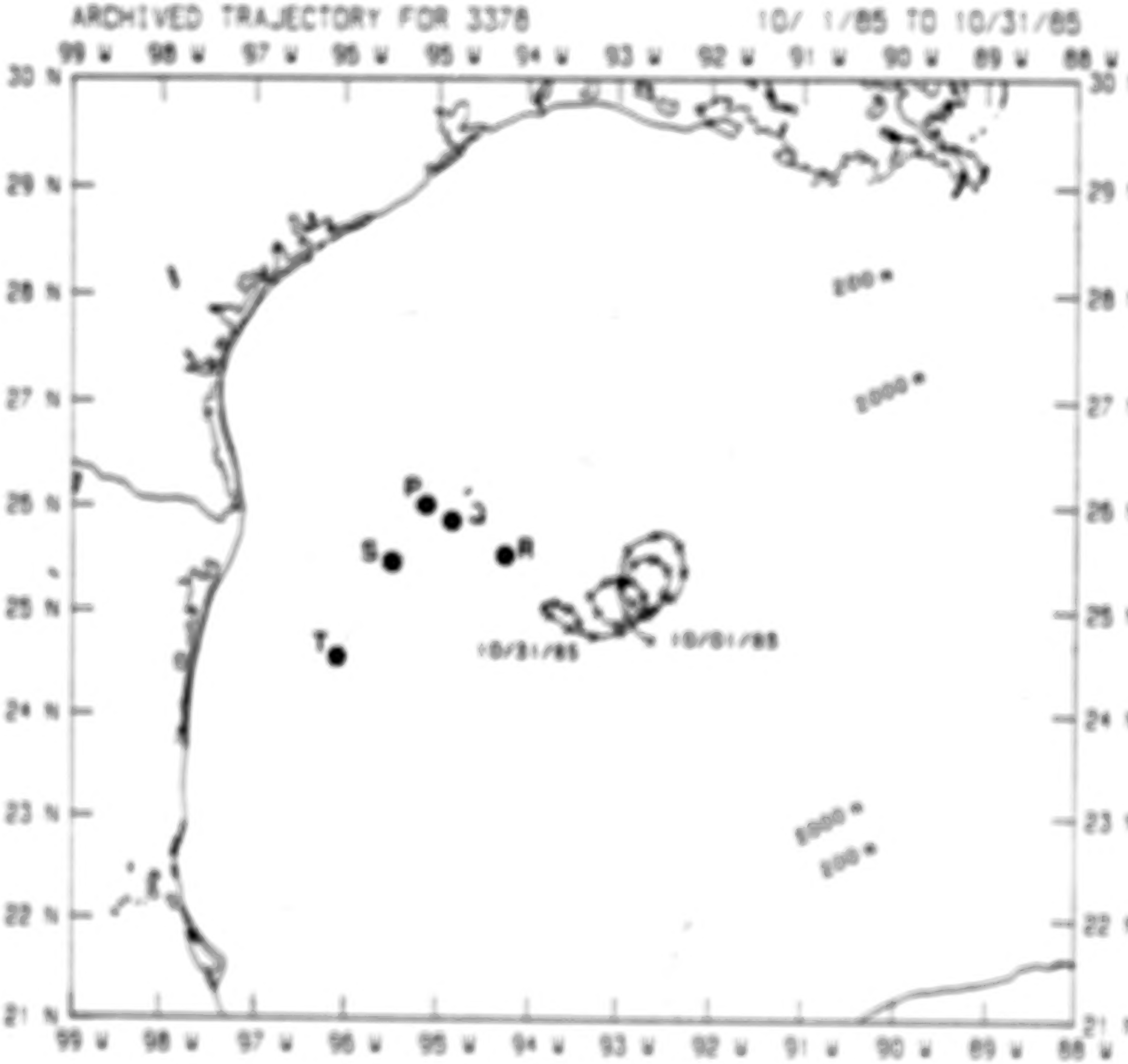

Figure 4.2-2. Trajectory of Drifter 3378 during the month of October 1985. Each X indicates a one-day interval.

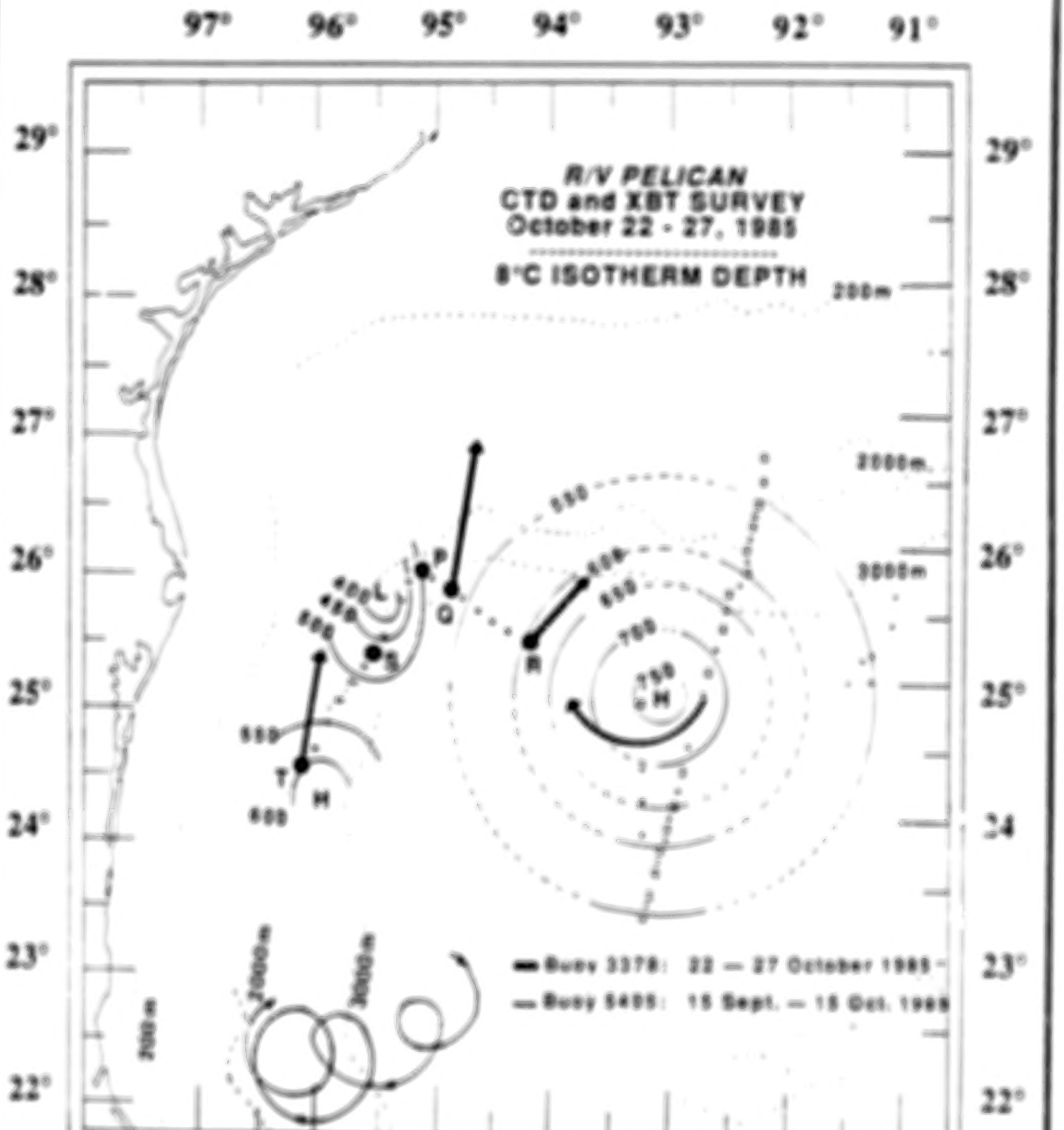

Figure 4.2-3. Topography of the 8°C temperature surface based on CTD and XBT data from the R/V PELICAN survey and XBT data from the B/O ALTAIR survey. Tracks of drifters and one-day averaged current vectors at moorings Q, R and T at 300m are also shown.

BLANK

PAGE

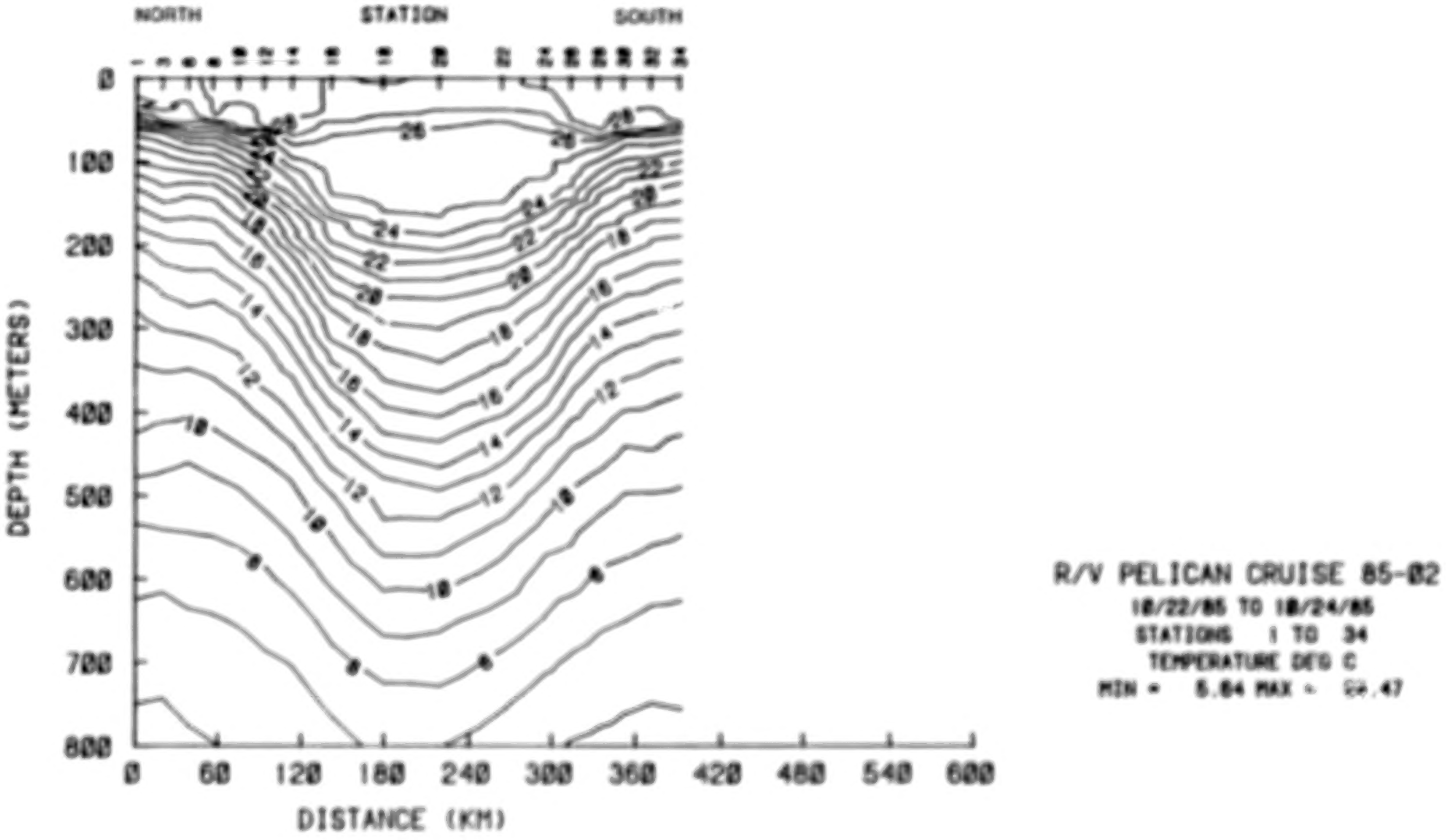

Figure 4.2-4. Vertical temperature section to 800m based on R/V PELICAN CTD data.

square (rms) radius of 183 km for relatively new eddies. Thus, Eddy B falls in the category of a typical Loop Current eddy; by comparison, warm-core eddies shed by the Gulf Stream north of Cape Hatteras average about half the area of Loop Current eddies (Auer, 1987).

Figure 4.2-3 also gives a slight indication that there were several mesoscale features over the western slope prior to the arrival of Eddy B. An anticyclone (Eddy A) centered near 22.5°N, 96.0°W is indicated by Drifter 5495, which had earlier been entrained in it near 24°N, 93°W in early August 1985. A small but intense cyclone and a partially resolved anticyclone are indicated to the west of Eddy B. Their origin is unknown, but they may be the source of a strong eddy signal detected at Mooring R in August 1985 (Section 4.3.5). The vectors in Figure 4.2-3 indicate the daily mean velocity at a depth of 300m at current Moorings Q and T on October 26 and at Mooring R on October 17. (See Figure 4.2-1, p. 51, for the identifying labels P, Q, R, S and T of the moorings).

The second phase covers the time of Eddy B's interaction with the western Gulf continental slope, roughly from November 1985 through early February 1986. After a period of rapid translation in the latter part of October, Eddy B became relatively stationary for much of November (Figure 4.2-5). A synoptic survey of the eddy's temperature structure was conducted from November 11 through 13, 1985 using AXBTs (Section 2.3.4, p. 22). The 8°C topography in Figure 4.2-6 reveals that the core and much of the southern and eastern portions of the eddy were still over the 3500m deep, flat Sigsbee Plain and continued to exhibit considerable axial symmetry. However, the western and northern sides of the eddy were by this time impinging on the 2000m isobath of the continental slope. Several small-scale cyclonic and anticyclonic features were located around the periphery of Eddy B.

To the northwest of the main anticyclone (Eddy B) were several less well resolved features. In particular, doming isotherms may represent the initial stage of development of a cyclone which is linked to the primary eddy and evolves and strengthens during subsequent stages of eddy-slope interaction. This intensification of the anticylone-cyclone pair (oppositely rotating vortices) has been observed in the past in the western Gulf (Merrell and Morrison, 1981; Brooks and Legeckis, 1982; Merrell and Vazquez, 1983; Brooks, 1984). Some possible explanations are discussed in Section 4.4.5 (p. 182).

During December 1985 and January 1986 the core of Eddy B moved to a position against the continental slope; its shape became quite elliptical, according to the trajectory data of Drifter 3378 shown in Figure 4.2-7. A detailed hydrographic survey was conducted aboard the R/O ALTAIR from January 23 through February 5, 1986, as described in Section 2.3.2 (p. 11). Figure 4.2-8 shows the depth of the 8°C temperature surface based on both CTD and XBT data from this cruise. Although the survey was conducted from northeast to southwest, the superposed trajectory of Drifter 3378 indicates that Eddy B moved little during the 2 weeks. Therefore, the two-to-one ratio of the major to minor axis is probably real. Mean current velocity on January 28 recorded at 300m depth on Moorings Q and T is consistent with the flow implied by the temperature distribution.

The cyclone located due north of the Eddy B core appears to have intensified considerably. Continuing clockwise around the periphery of Eddy B, hydrographic data suggest that other less well resolved features may have occurred. A lack of substantial documentation does not allow identification

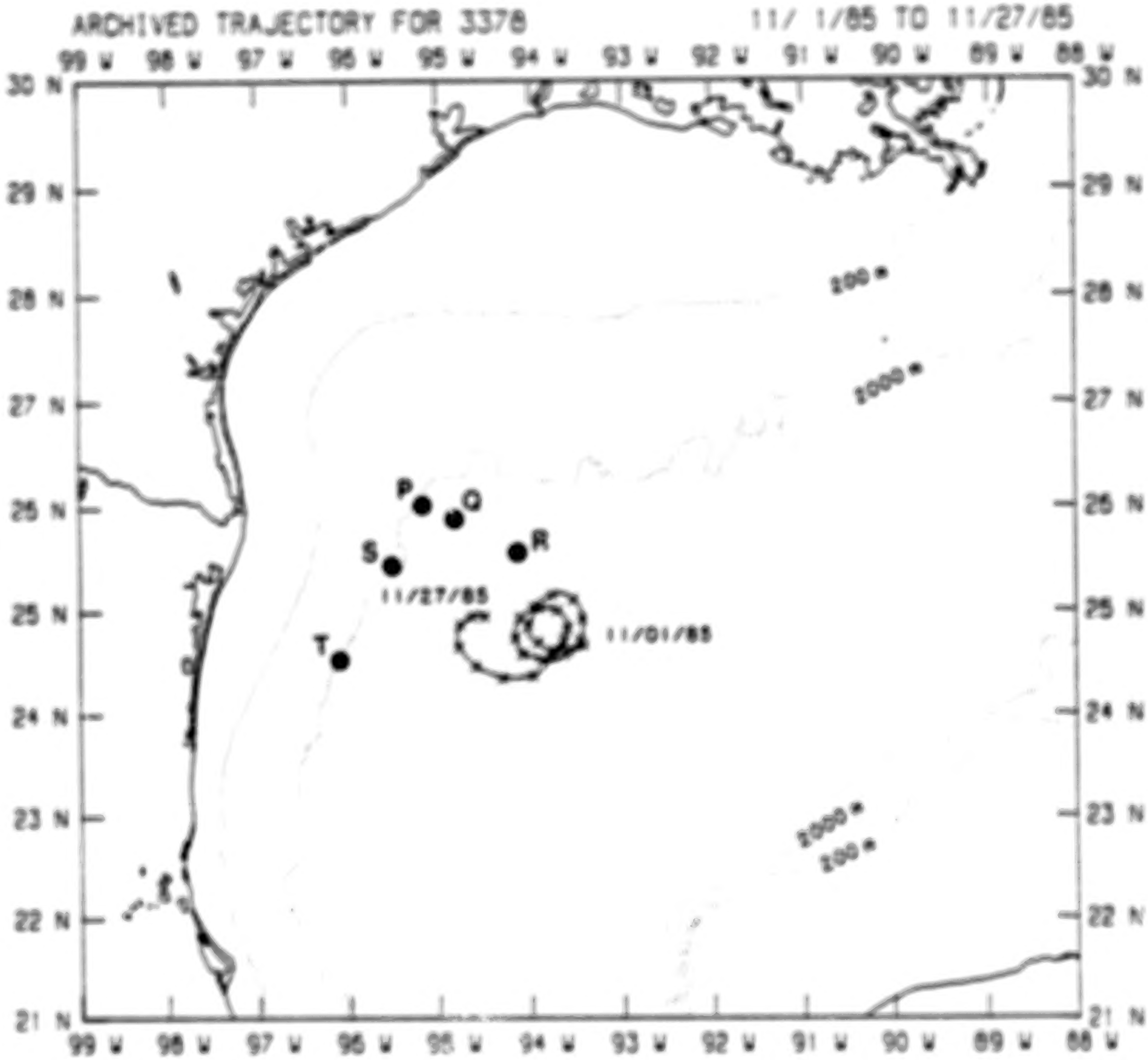

Figure 4.2-5. Trajectory of Drifter 3378 during the month of November 1985. Each X indicates a one-day interval.

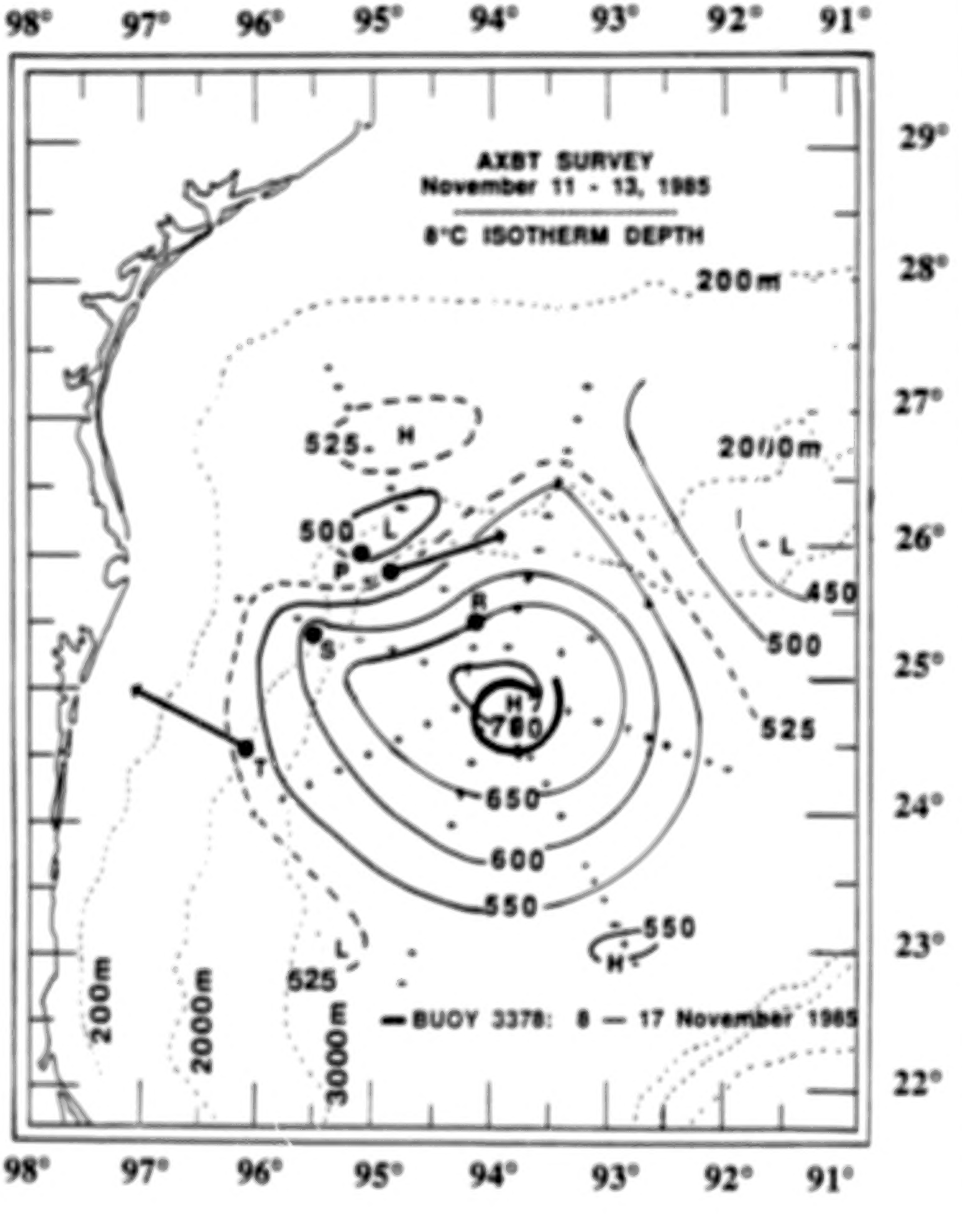

Figure 4.2-6. Topography of the 8°C temperature surface based on the AXBT survey. Data shown are in the same format as Figure 4.2-3.

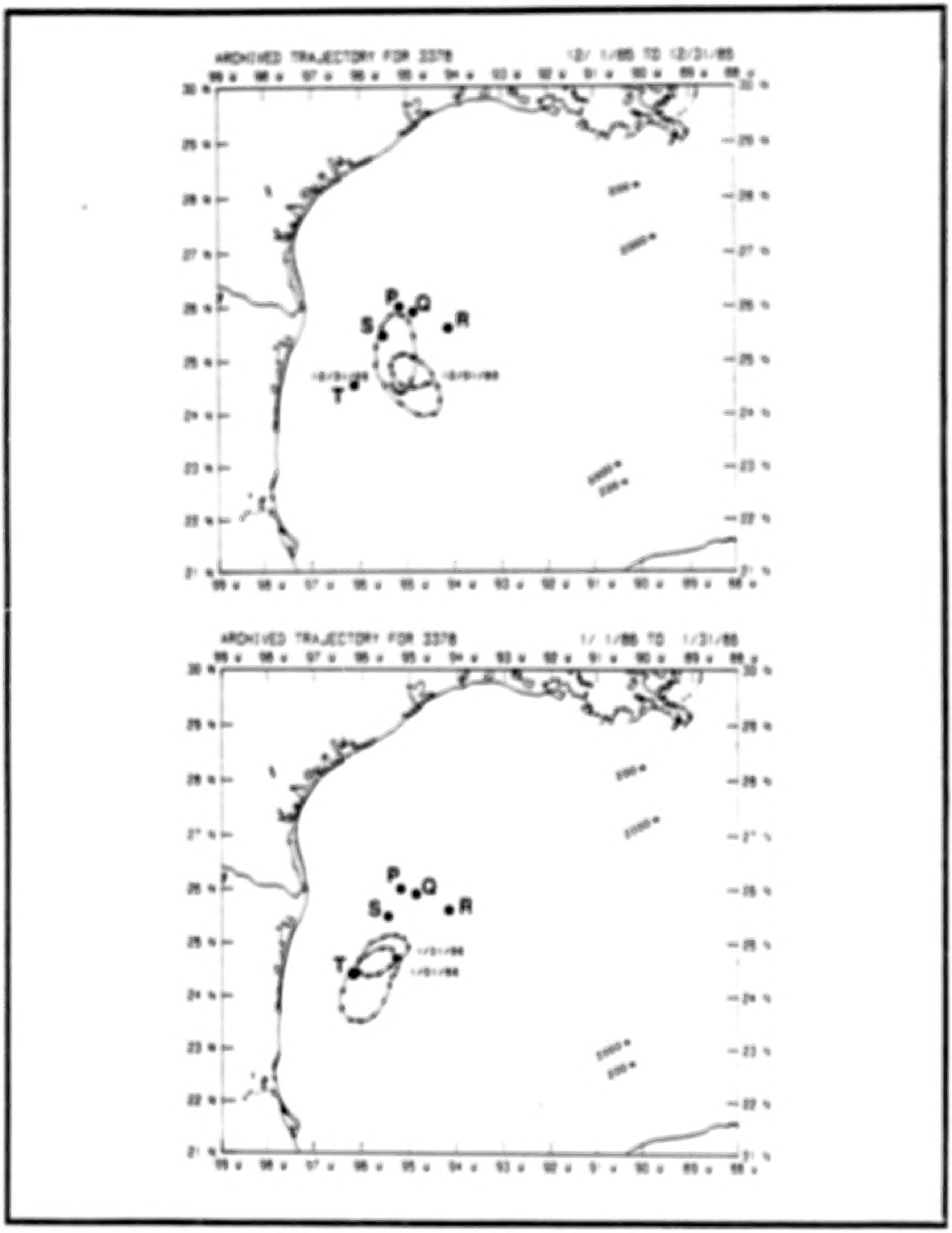

Figure 4.2-7. Trajectory of Drifter 3378 during the months of December 1985 and January 1986. Each X indicates a one-day interval.

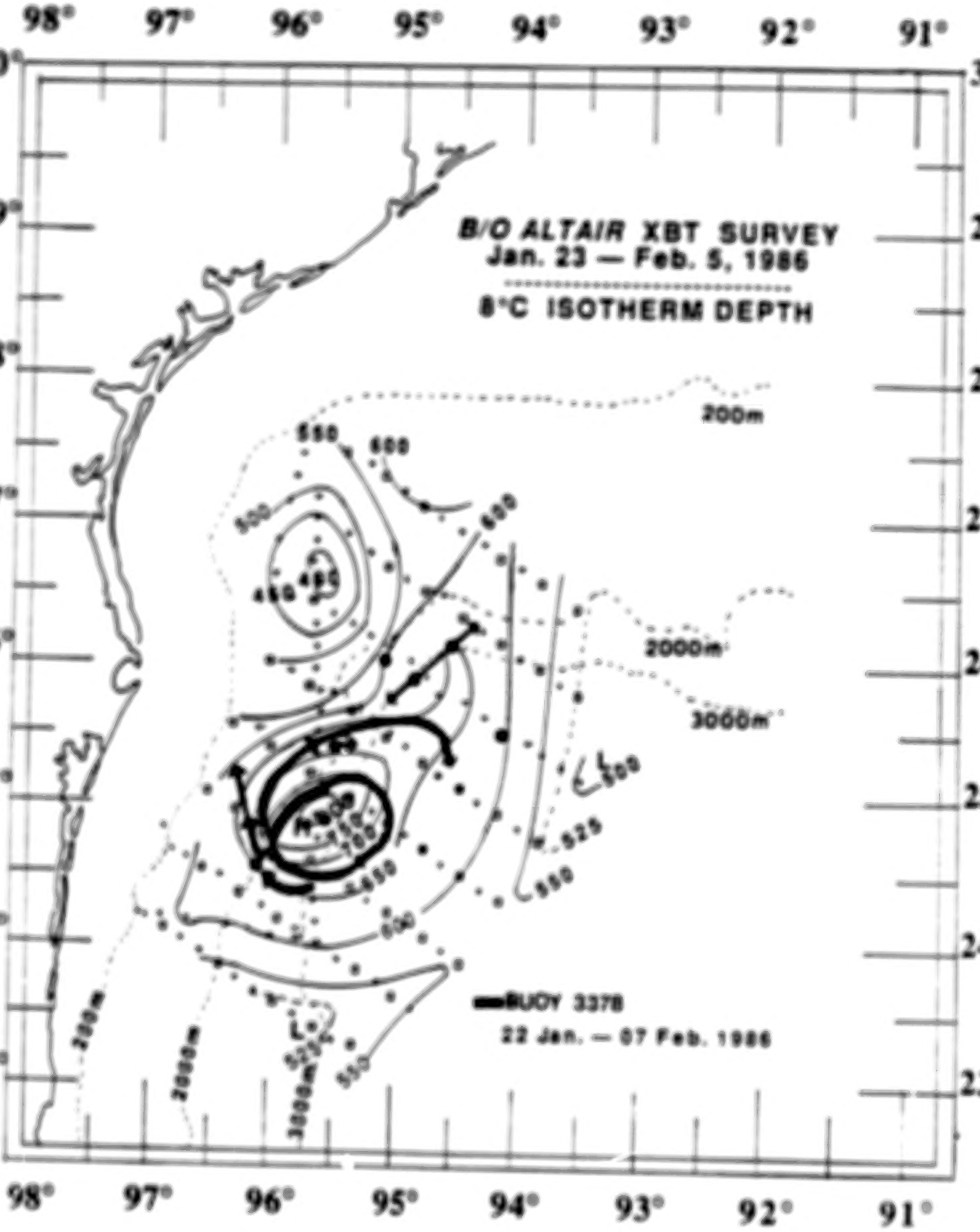

Figure 4.2-8. Topography of the 8°C temperature surface based on CTD and XBT data from the B/O ALTAIR survey. Data shown are in the same format as Figure 4.2-3.

or a better understanding of their relationship to the primary anticyclone-cyclone pair. A major result of this study is the observed intensification of the cyclonic circulation to the northwest of Eddy B as it moved to a position over the continental slope. These observations suggest that topographic interactions may have a basic role in the oft-observed intensifying cyclonic partners of Loop Current eddies in the western Gulf, but the details of the processes of such a transfer of energy to the cyclone, and presumably from the anticyclone, are not yet understood.

The third phase in the evolution of Eddy B occurred from February through May 1986. Eddy B moved to the southeast, that is, away from the topography into deeper water, and later returned to a position next to the continental slope about 1° of latitude south of its position in January. Figure 4.2-9 showing Drifter 3378's trajectory demonstrates this movement during February and March 1986. During April the movement of Eddy B was not well observed because Drifter 3378 was apparently "ejected" from the core of the eddy (Figure 4.2-10). However, XBT data collected from April 27 to May 14 clearly located the position of Eddy B and its companion cyclone (Figure 4.2-11). The diameters of the 500m contour for the cyclone and the 650m contour for the anticyclone indicate that both features had become smaller in horizontal size since the late January measurement (Figure 4.2-8). The maximum depth in the center of the anticyclone decreased from more than 800m to slightly over 750m, suggesting a decrease in strength, but the minimum depth in the cyclone remained the same. More importantly, the decrease in distance between the two centers from 185 km to 120 km indicates accelerated eastward flow in the region between them. Indeed, the current meter at 300m on Mooring T recorded a mean velocity of 40 cm sec^{-1} on April 27. Another partially resolved cyclonic feature is also seen to the northeast. The direction of mean current recorded on April 27 at 300m on Mooring Q is consistent with the flow implied by the topography of the 8°C surface in this region.

The final phase of Eddy B covers its interaction with a new anticyclone, Eddy C, which separated from the Loop Current in February 1986. Drifter 3379 was placed in Eddy C on March 7, 1986. Figure 4.2-12 shows its trajectory during March and April. Unlike Eddy B, which followed a westerly path, Eddy C took a southwesterly path. Figure 4.2-13 shows Drifter 3379's trajectory during May and June 1986. During May the orbit became increasingly elongated in the east-west direction along 24°N, and in June the drifter appeared to leave Eddy C to make an orbit around the last known position of Eddy B at 23.75°N, 95.5°W. During July and August (Figure 4.2-14), Drifter 3379 made large anticyclonic orbits on the order of 330 km in diameter. The trajectory of Drifter 3379 from May through August suggests that Eddies B and C may have coalesced. From August 16 through 22, 1986 an XBT survey was conducted aboard the HO-2 of the Mexican Navy; Figure 4.2-15 shows the topography of the 8°C surface. The data partially resolve a large, elongated anticyclonic feature that is believed to be Eddy C joined with Eddy B. A cyclonic feature is also indicated, but its relation to the earlier-noted structure is not clear.

4.3 Eddy Separation and Initial Movement

4.3.1 Introduction

During 1985 and 1986, a warm core eddy (Eddy B) shed by the Loop Current was observed as it migrated towards the western Gulf of Mexico. This movement was well documented by observations that included drifter data within and outside the eddy, sea surface temperature at weekly intervals, XBT surveys at various

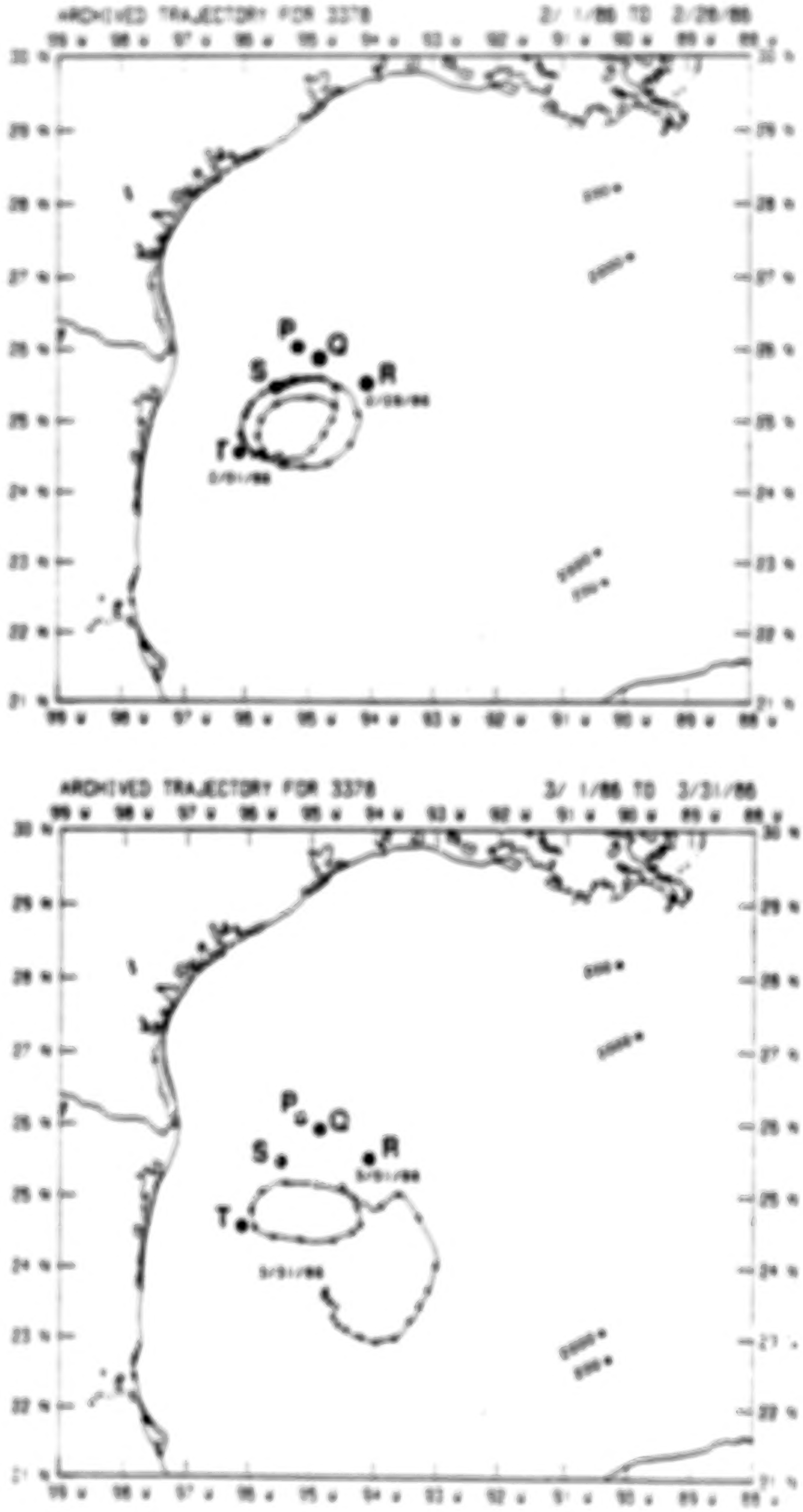

Figure 4.2-9. Trajectory of Drifter 3378 during the months of February and March 1986. Each X indicates a one-day interval.

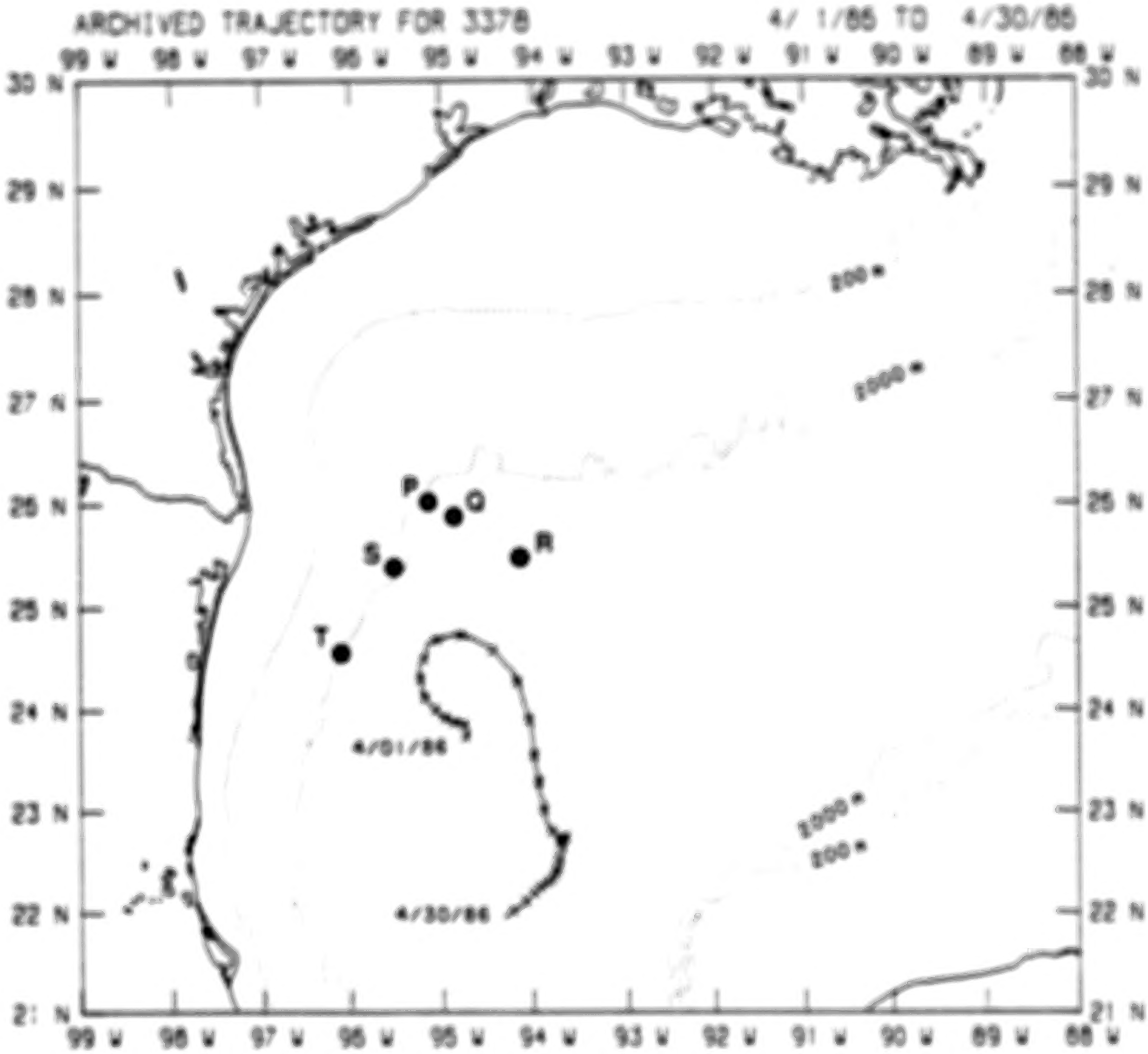

Figure 4.2-10. Trajectory of Drifter 3378 during the month of April 1986. Each X indicates a one-day interval.

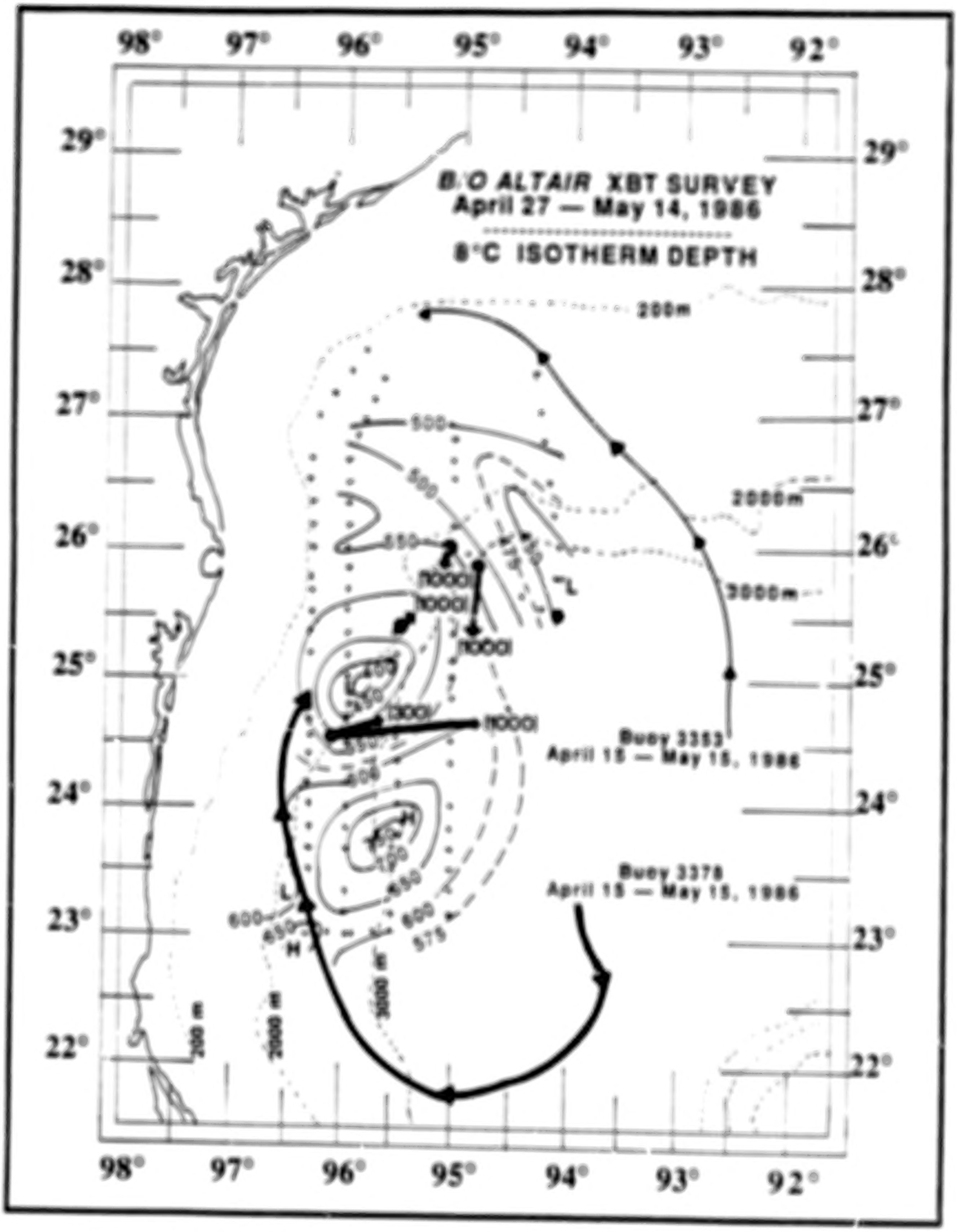

Figure 4.2-11. Topography of the 8°C temperature surface based on all SOOP XBT data collected by the B/O ALTAIR during the period from April 27 to May 14, 1986. Data shown are in the same format as Figure 4.2-3, except that numbers in brackets specify whether 1-day averaged current vectors are at 300m or 1000m.

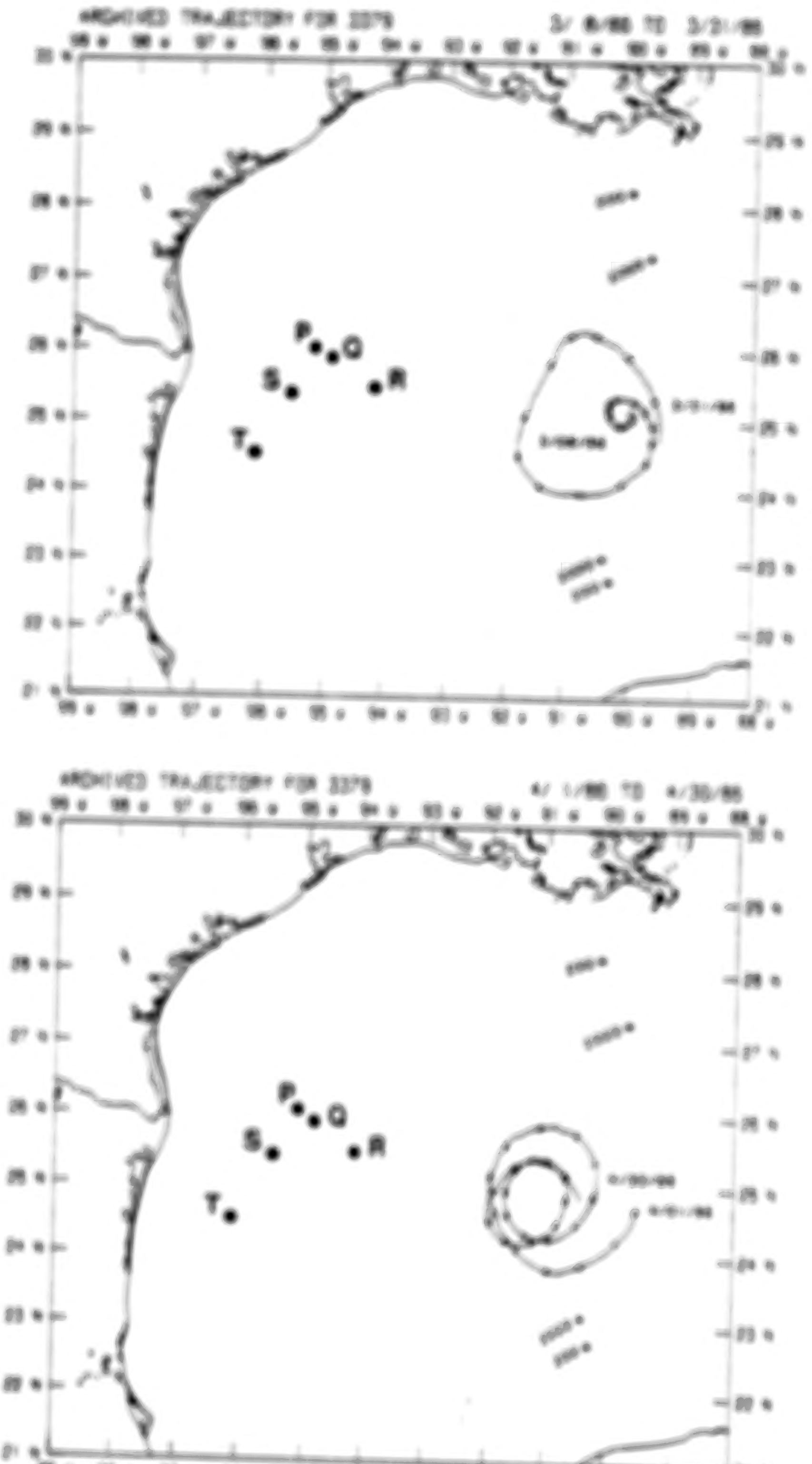

Figure 4.2-12. Trajectory of Drifter 3379 during the months of March and April 1986. Each X indicates a one-day interval.

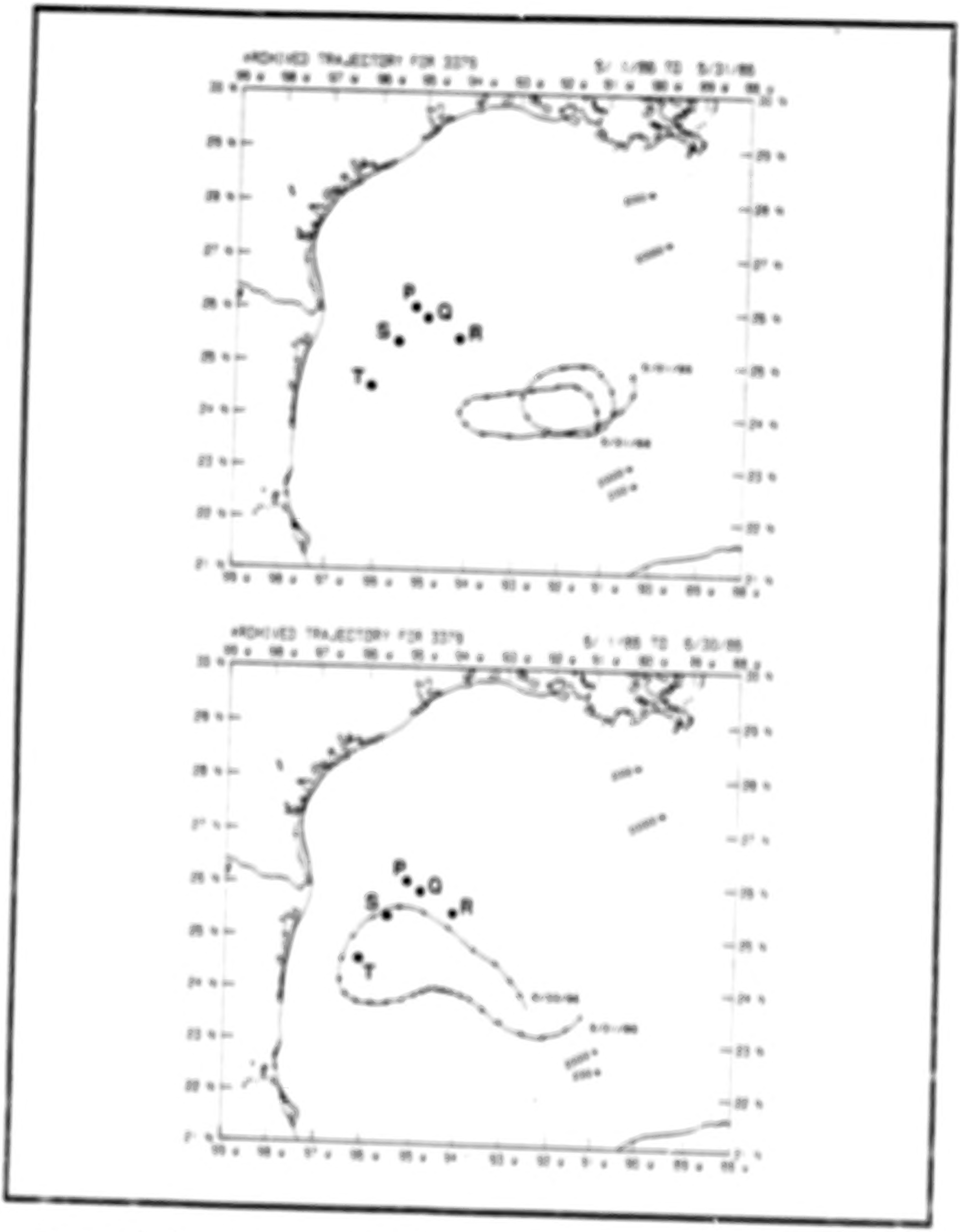

Figure 4.2-13. Trajectory of Drifter 3379 during the months of May and June 1986. Each X indicates a one-day interval.

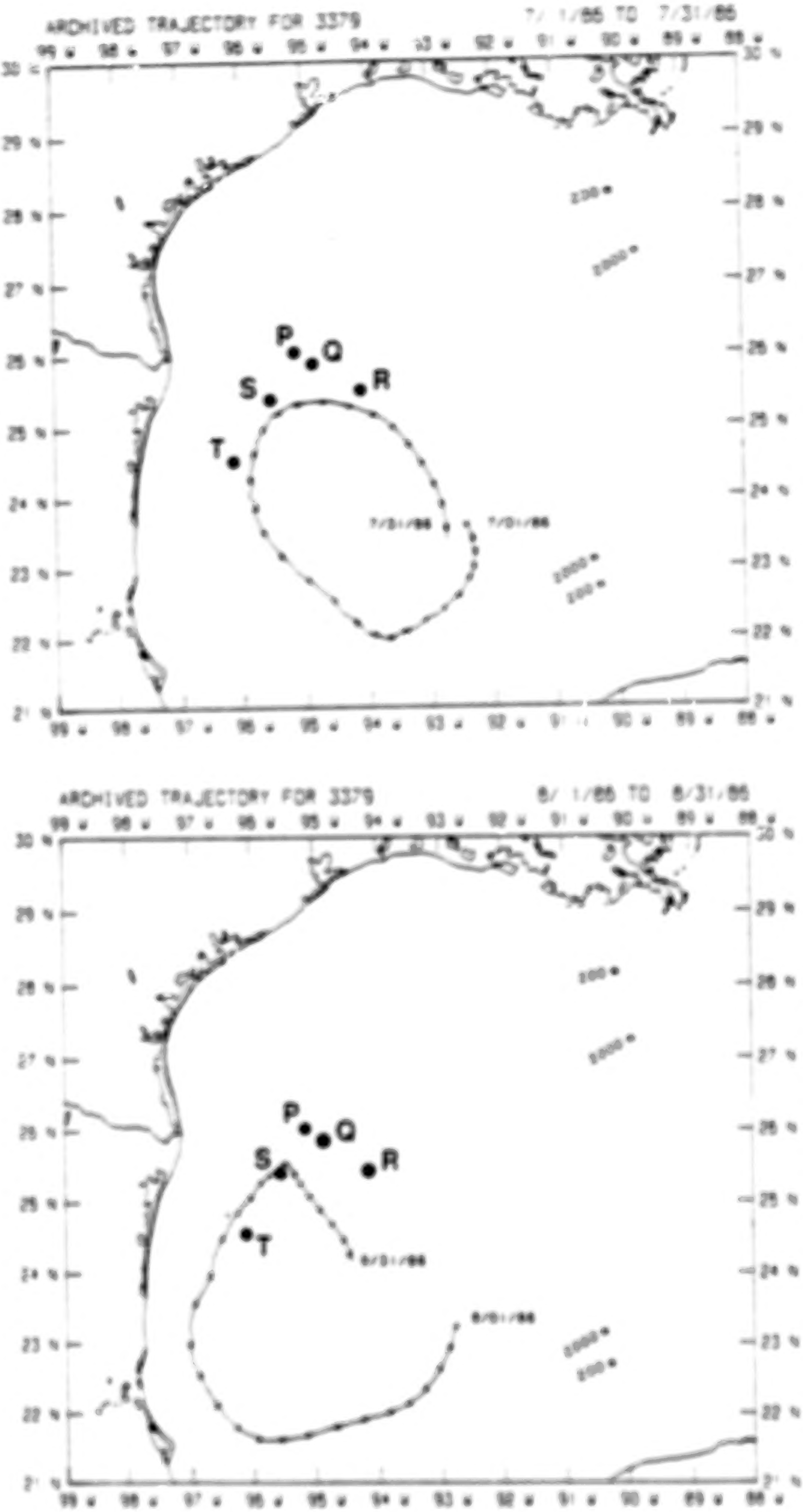

Figure 4.2-14. Trajectory of Drifter 3379 during the months of July and August 1986. Each X indicates a one-day interval.

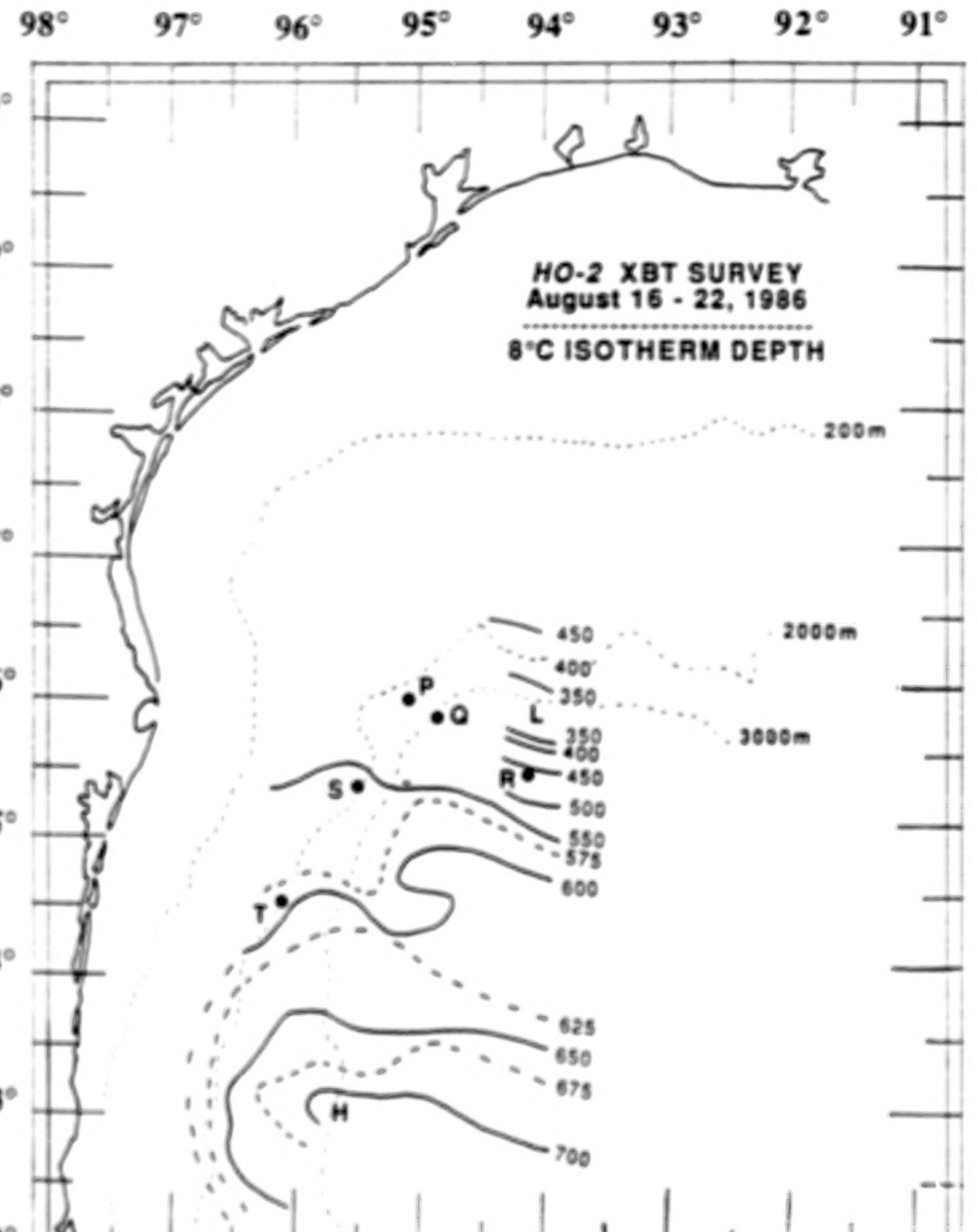

Figure 4.2-15. Topography of the 8°C temperature surface based on SOOP XBT data collected by the HO-2 during the period from August 17-22, 1986.

times, one major hydrographic cruise when the eddy was in the northwestern Gulf and currents from moorings over which the eddy passed. The drifter data were used to infer the movement of the eddy center as well as the eccentricity and orientation of the major axes. Data from the drifters bridge the gaps between detailed surveys to the extent that a daily history of the position and shape of the eddy can be constructed. Synthesis of these diverse but complementary data sources provides a detailed description of how the eddy interacted with the bathymetry of the northern Gulf of Mexico as well as with previously and subsequently shed eddies.

4.3.2 Separation of Eddy B

4.3.2.1 SST and Path Data

This section discusses eddy-related processes just prior to, during and directly after the breakoff of Eddy B. Cruise tracks for the period May 26 through 31, 1985 are shown in Figure 4.3-1a. The resulting XBT data are shown in Figures 4.3-1b through d. These data were collected before Eddy B was shed, and the edges of the Loop Current (maximum horizontal temperature gradients indicated by the XBT data) are shown by arrows in Figure 4.3-1a (smaller slopes of the isotherms were taken as an indication that the transects were crossing the Loop Current edge at an angle, and some of the edges were thus drawn at a 45° angle to the cruise track). It appears that the Loop Current was flowing northward on the east side of the Yucatan Straits, curved westward and around the region where Eddy B would be spawned, and then turned northeastward then southward before exiting the Gulf of Mexico.

Drifter 3354 was deployed in the northward extension of the Loop Current during mid-June 1985. The trajectory of this drifter from June 18 to 24, 1985 is plotted on the corresponding SST chart in Figure 4.3-2. As indicated by the trajectory (and to some degree by the SST data), Eddy B had not separated from the Loop Current during this period. The return flow from the area of northward extension appears to be mostly southeastward, toward the northern coast of Cuba.

Three XBT data sets were collected during June 26 through July 2, 1985 (Figure 4.3-3a), and the vertical temperature profiles are shown in Figures 4.3-3b through d. The extent of Eddy B is distinct in Figures 4.3-3b and d, while the Loop Current can be seen to extend to 25.0°N in Figure 4.3-3c. These data would seem to imply that Eddy B is still connected to the Loop Current. The SST data for June 29 through July 5, 1985, along with the associated trajectory of Drifter 3354, are shown in Figure 4.3-4. Some of the rotational characteristics within the Loop Current can be visualized from the path of the drifter. The rotation near the Cuban coast continued into mid-July.

During July 16 through 19, 1985, two XBT data sets were collected (Figures 4.3-5a through d) which show distinctly that Eddy B had separated from the Loop Current. The SST contours for the period are shown in Figure 4.3-6. There is no surface signature of Eddy B, although its rotation is well delineated by the trajectory of Drifter 3378. As for the Loop Current, Figure 4.3-6 shows that the rotational feature within it had reached the northern edge of the Loop Current at about 25.0°N.

Both the Loop Current and Eddy B drifters continued to rotate anticyclonically through August 1985. An XBT data set collected from August 16

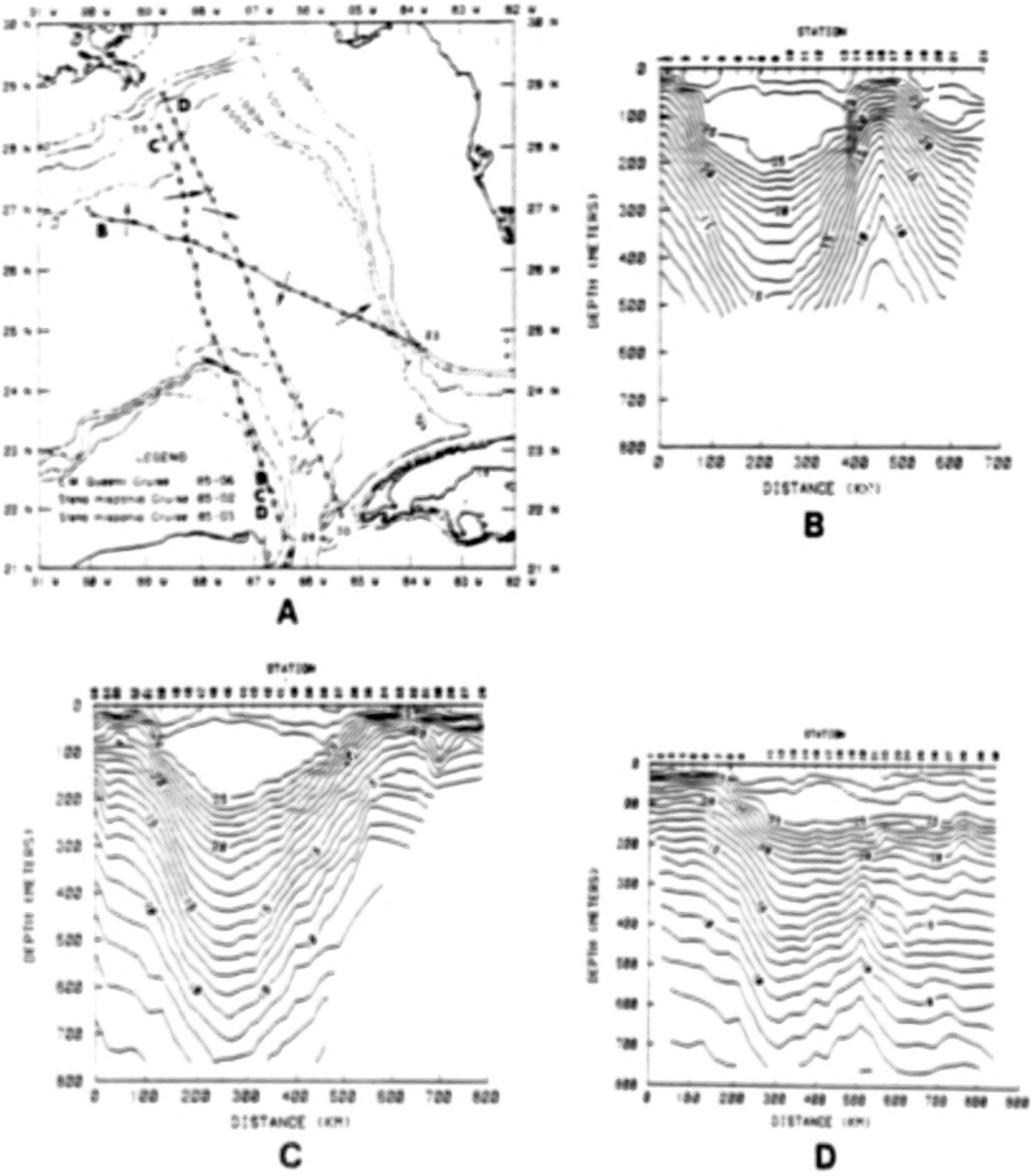

Figure 4.3-1. (a) Cruise tracks for SOOP XBT data collected during May 26-31, 1985. The arrows denote the flow at the edges of the Loop Current based on the vertical temperature structure shown in temperature data from three cruises: (b) the E.M. QUEENY cruise, May 26-27, 1985; (c) the STENA HISPANIA cruise, May 27-28, 1985 and (d) the STENA HISPANIA cruise, May 30-31, 1985.

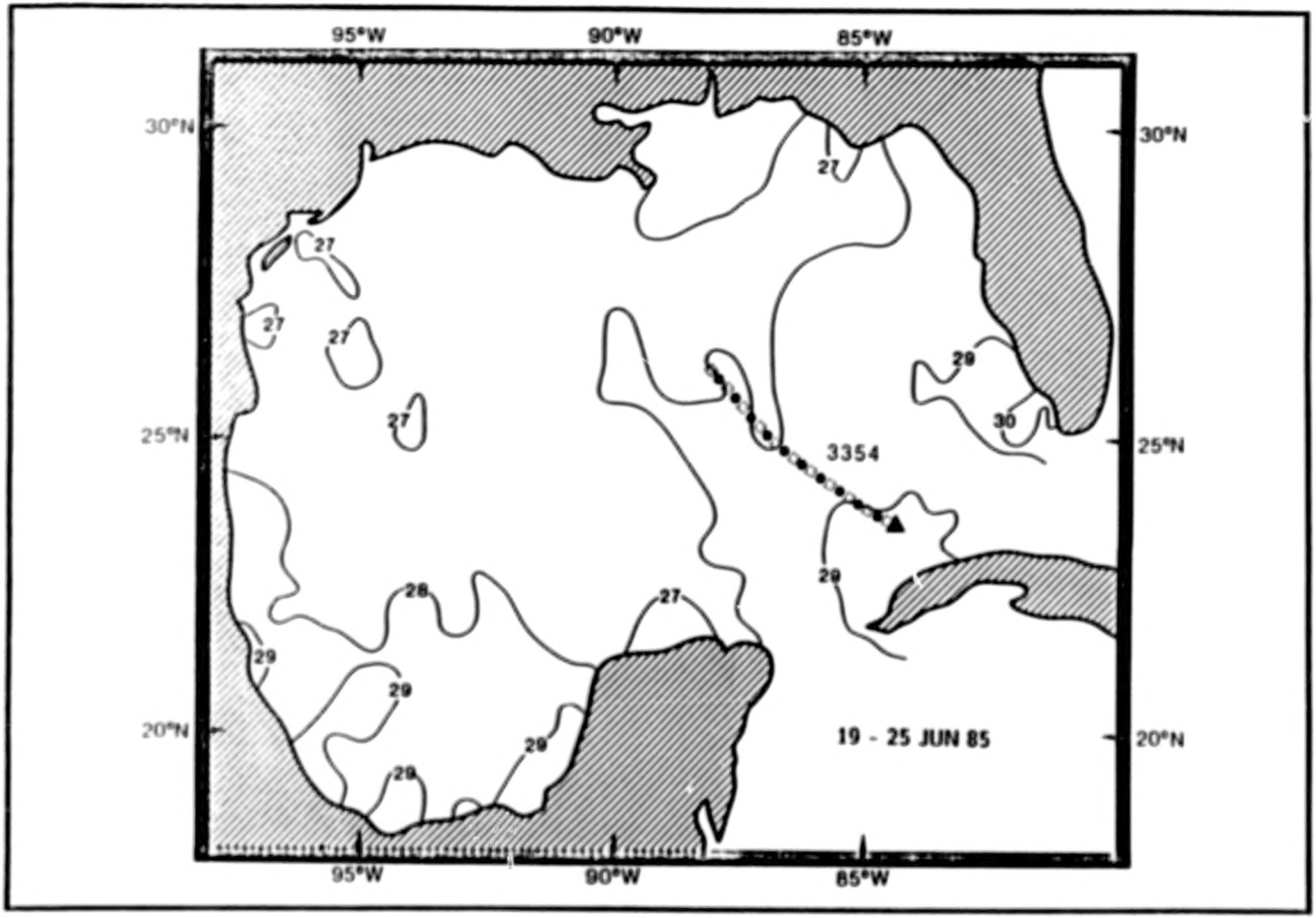

Figure 4.3-2. SST data (°C) for June 18-24, 1985. The drifter trajectories, shown by arrows, are identified in Table 2.2-1.

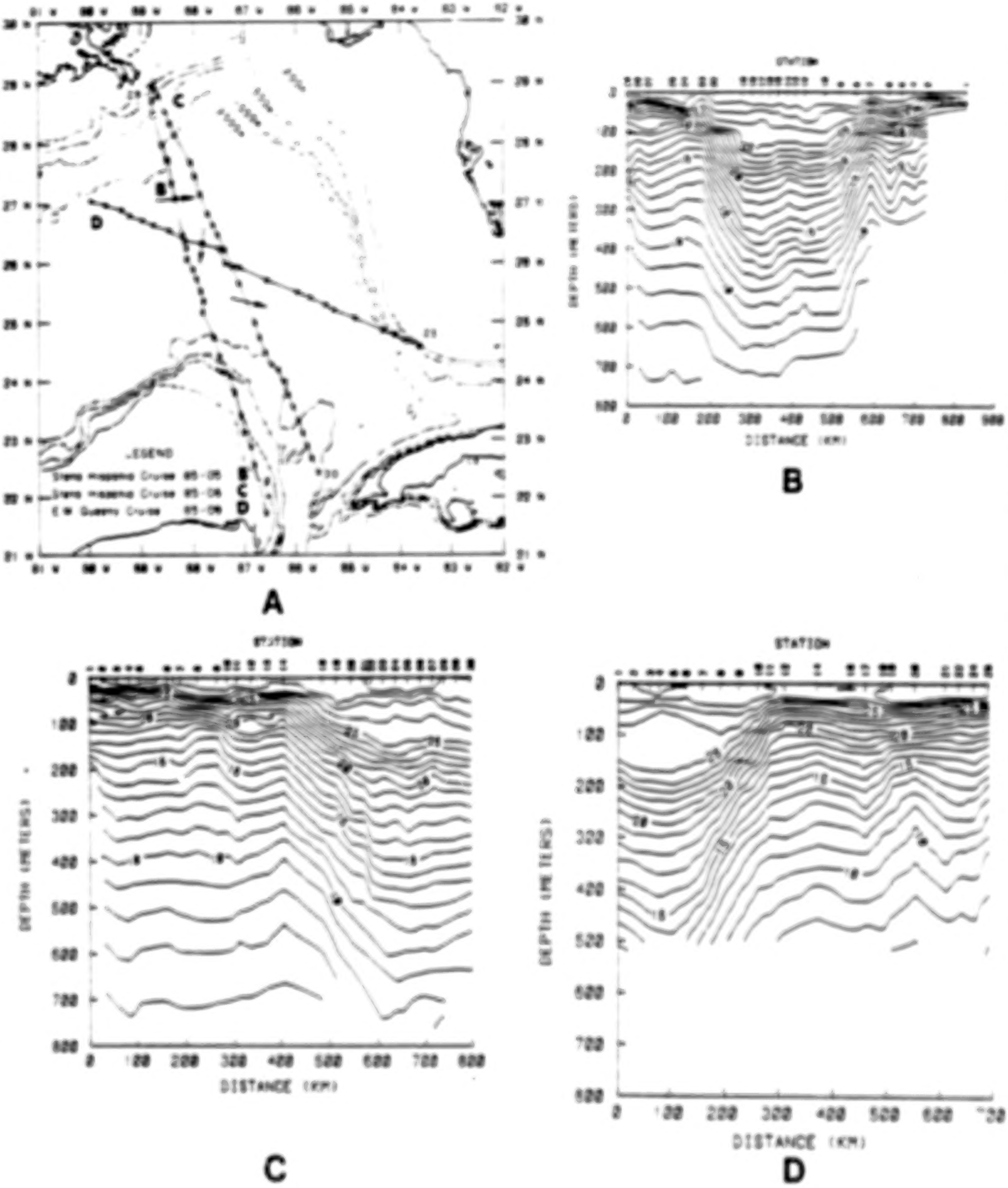

Figure 4.3-3. (a) Cruise tracks for SOOP XBT data collected during June 26 through July 2, 1985. The arrows denote the flow at the edges of the Loop Current based on the vertical temperature structure shown in temperature data from three cruises: (b) the STENA HISPANIA cruise, June 26-28, 1985; (c) the STENA HISPANIA cruise, June 29-30, 1985 and (d) the E.M. QUEENY cruise, July 1-2, 1985.

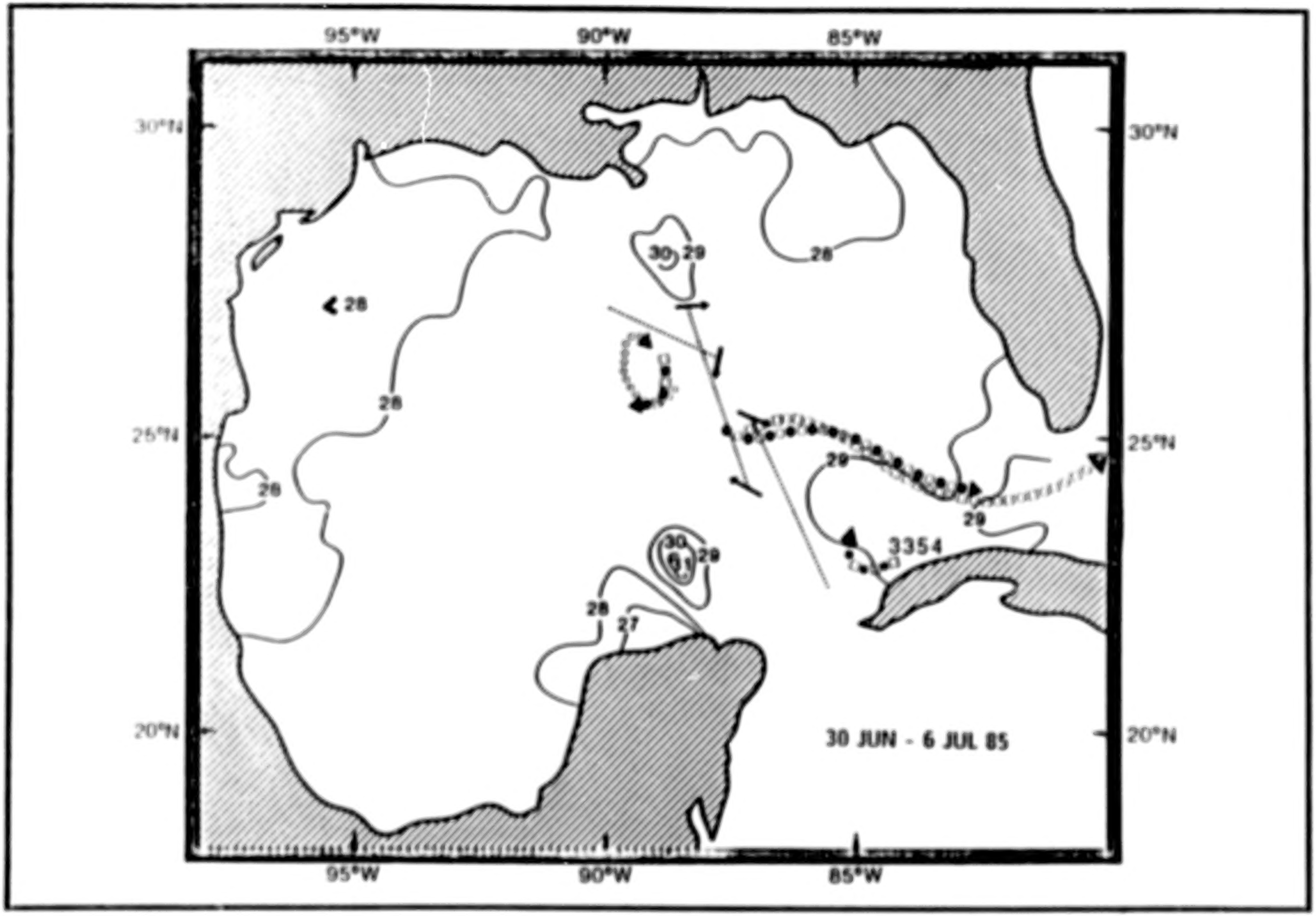

Figure 4.3-4. SST data (°C) for June 29 through July 5, 1985. Shorter arrows denote the flow at the edges of the Loop Current while dotted lines indicate the locations of Loop Current waters (based on XBT data). The drifter trajectories, shown by arrows, are identified in Table 2.2-1, except for three extraneous drifters (alternating open and closed circles, alternating open and closed squares, and alternating open circles and

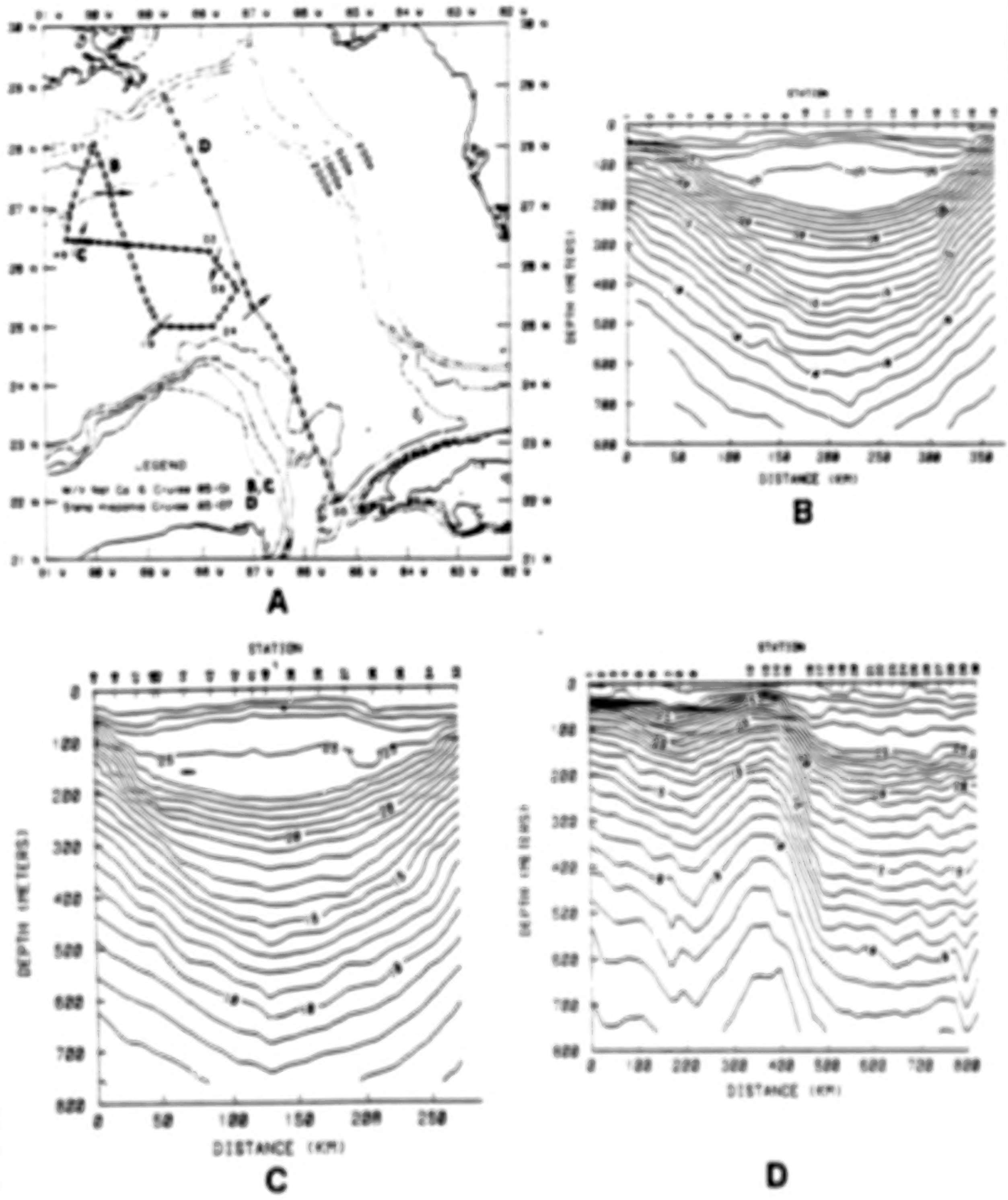

Figure 4.3-5. (a) Cruise tracks for SOOP XBT data collected during July 16-19, 1985. The arrows denote the flow at the edges of the Loop Current and eddy based on the vertical temperature structure shown in temperature data from three cruises: (b) the M/V NAT CO 6 cruise, July 16-19, 1985; (c) the M/V NAT CO 6 cruise, July 16-19, 1985 and (d) the STENA HISPANIA cruise, July 16-17, 1985.

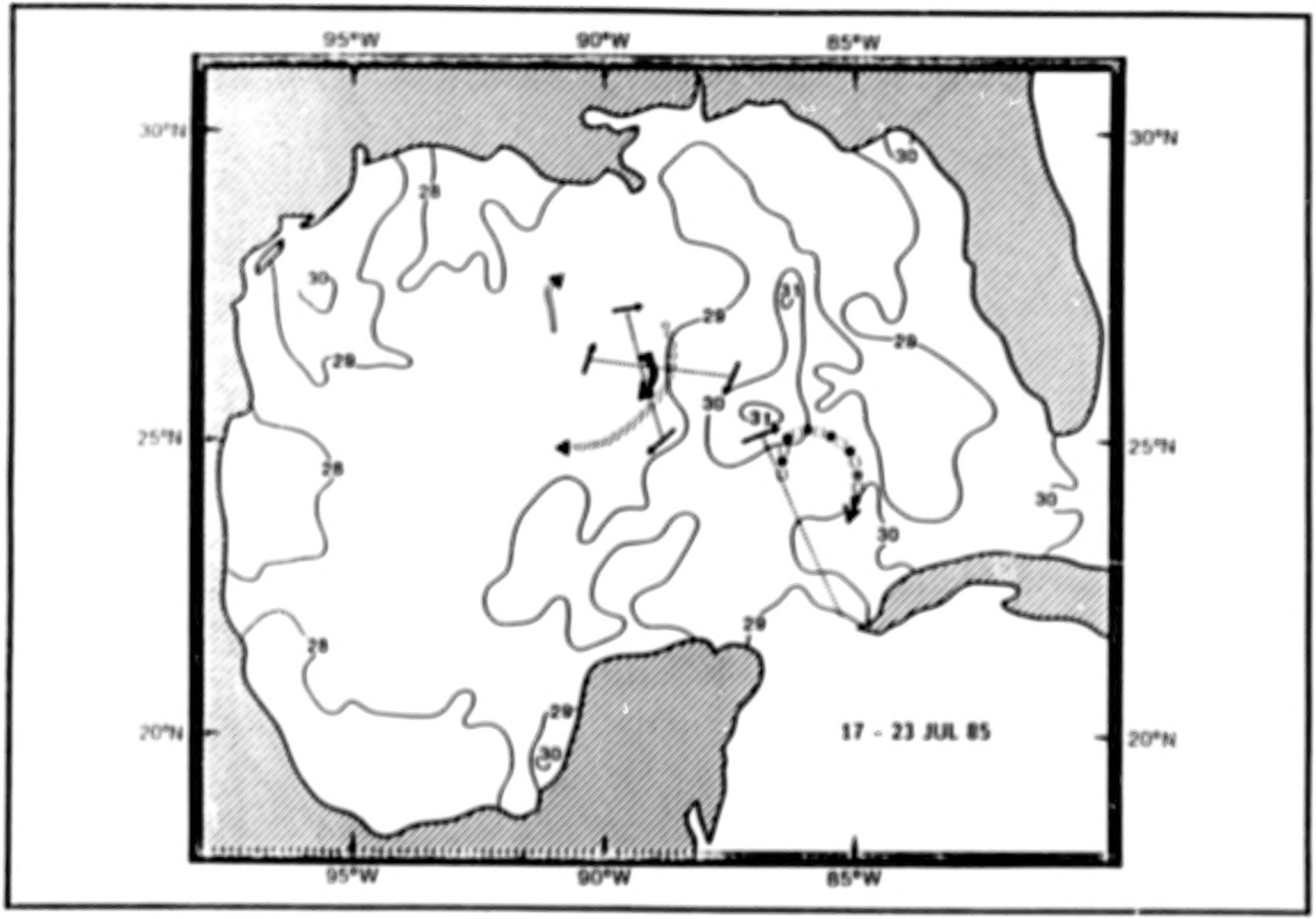

Figure 4.3-6. SST data (°C) for July 16-23, 1985. Shorter arrows denote the flow at the edges of the Loop Current or Eddy B while dotted lines indicate the locations of Loop Current-like waters (based on XBT data). The drifter trajectories, shown by arrows, are identified in Table 2.2-1.

through 18, 1985 (Figure 4.3-7) indicates that the Loop Current had extended northward to 26.6°N. The SST map for August 13, 1985 showed that Eddy B and the Loop Current were rotating at about the same latitude: 25.5°N (Figure 4.3-8a). By mid-September, the sea surface had cooled sufficiently in the eastern Gulf so that the northern extension of the Loop Current was readily defined (Figure 4.3-8b). The trajectories for this period show Eddy B strongly rotating but Drifter 3354 leaving the rotational feature of the Loop Current along the eastern side of a 28°C tongue of water. The following week's SST chart (Figure 4.3-8c) shows the 28°C tongue reaching up to 27.5°N while Drifter 3354 moved toward the Florida Straits along the northern coast of Cuba. Eddy B was still rotating with a center at about 25.5°N, 92.0°W.

4.3.2.2 Loop Current vs. Eddy Kinematics

Drifters 3354 and 3378 were both in the Gulf during Julian Days 199 through 264 (July 18 through September 21, 1985). However, the initial variations of the kinematic parameters of Eddy B (Figures 4.3-9 through 4.3-10) indicate an adjustment period from Days 199 through 220 during which the drifter (with its 200m weighted line) "found" an appropriate orbit within the ring. Thus, eddy and Loop Current kinematics are compared (Figures 4.3-11 through 4.3-12) from Day 225 to Day 264. At the beginning of this time period, the Loop Current, as reflected by Drifter 3354, was rotating with a period of about 10.5 days while Eddy B had a period of approximately 8.2 days. The orientations of the ellipses of rotation (Figures 4.3-10c and 4.3-12b) were quite similar (generally east/west), but the Loop Current was slightly more elliptical ($e = 1.5$) than Eddy B ($e = 1.25$).

The swirl speeds and the radii of revolution for the drifters in both anticyclones (80 cm sec^{-1} for the swirl speeds and approximately 90 km for the radii relative to the eddy center) were quite similar for Days 225 through 264. Interestingly, both anticyclones experienced longer periods of rotation for smaller distances from the center of rotation.

4.3.2.3 Kinematics Before and After an Eddy Detachment

The kinematics of the Loop Current at its most northerly extension (Julian Days 230 through 264) and of Eddy B soon after it broke free from the Loop Current (Julian Days 225 through 235) are briefly discussed below. Keeping in mind that these data represent two different anticyclonic phenomena, the following question arises: How typical are they of Gulf eddies before and after break off from the Loop Current?

Similarities between the two sets of kinematics are considerable. First, magnitudes of the swirl speeds and of the radii are practically identical. Second, their elliptical orientations are both northwest/southeast. The Loop Current was slightly more elliptical than Eddy B, but one might expect such a difference in ellipticity since an anticyclone attached to the Loop Current is a "captured" phenomenon while a detached eddy is an isolated vortex. The similarities of the anticyclones plus their close periods of rotation suggest that some basic kinematic characteristics of Gulf rings might be estimated from the Loop Current as it extends northwestward from the shore of Cuba (SAIC, 1987).

BLANK

PAGE

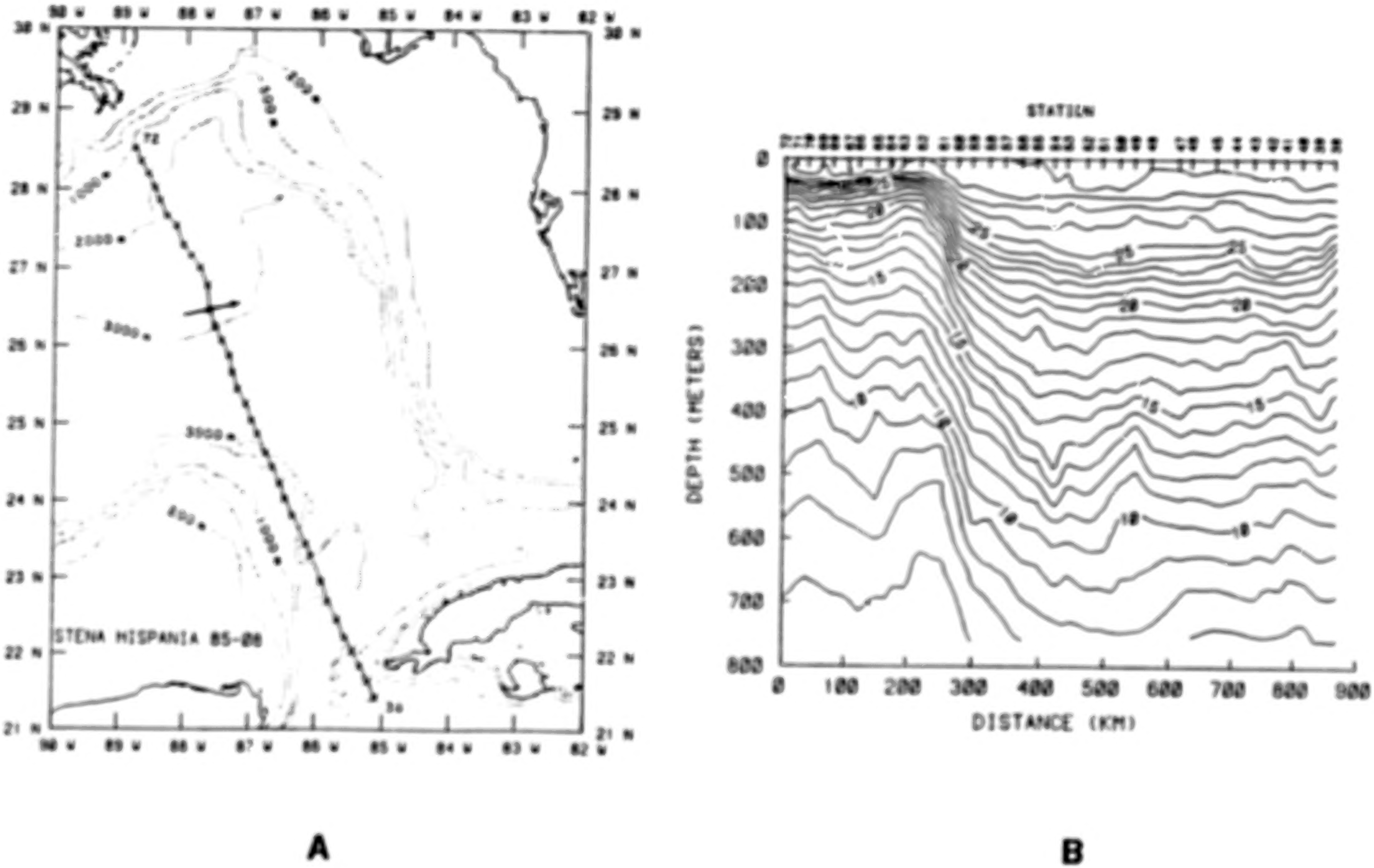

Figure 4.3-7. (a) Cruise track for SOOP XBT data collected by the STENA HISPANIA August 16-18, 1985. The arrow denotes the flow at the edge of the Loop Current based on: (b) the vertical temperature structure.

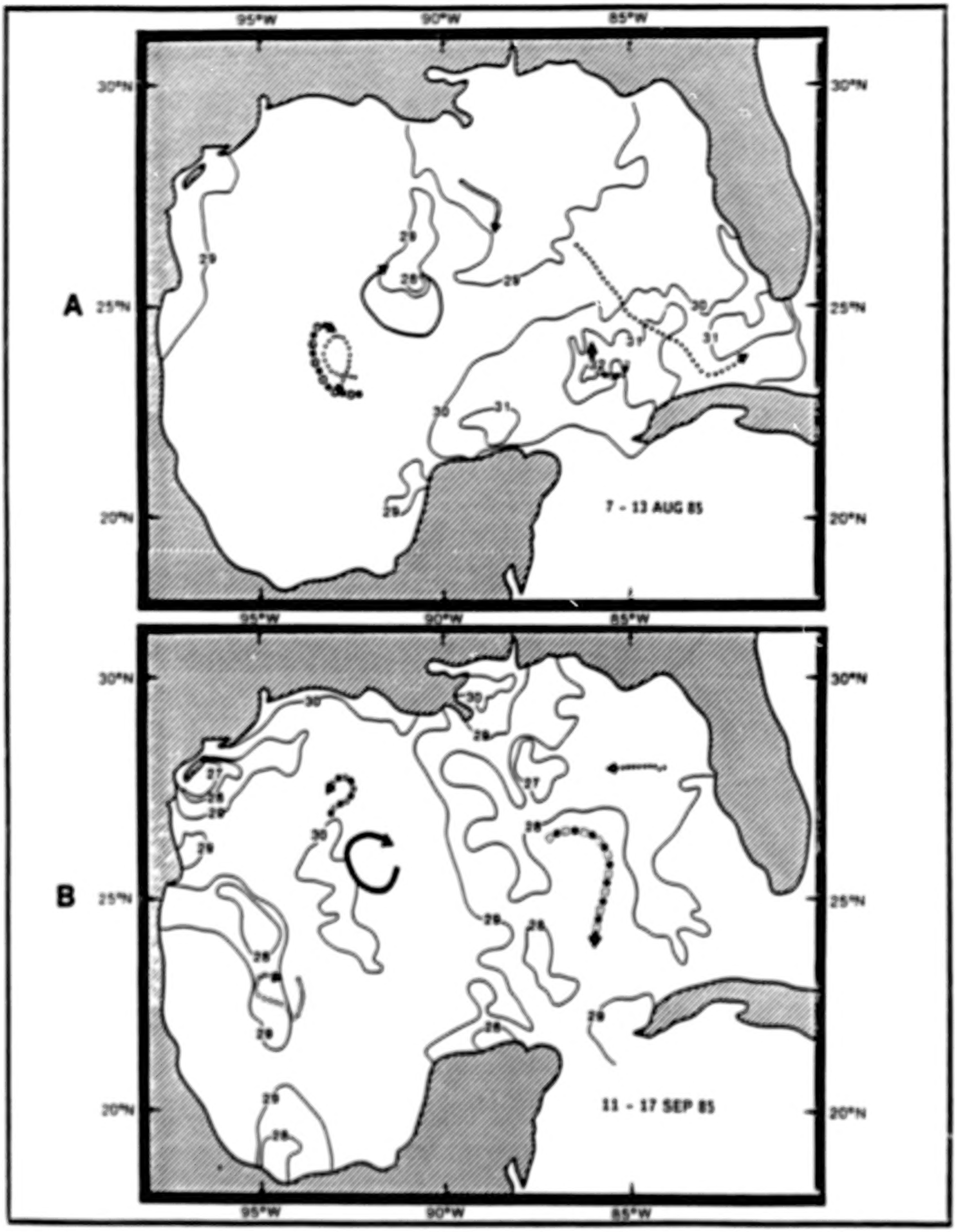

Figure 4.3-8a-b. SST data (°C) for: (a) August 7-13, 1985 and (b) September 10-17, 1985. The drifter trajectories, shown by arrows, are identified in Table 2.2-1.

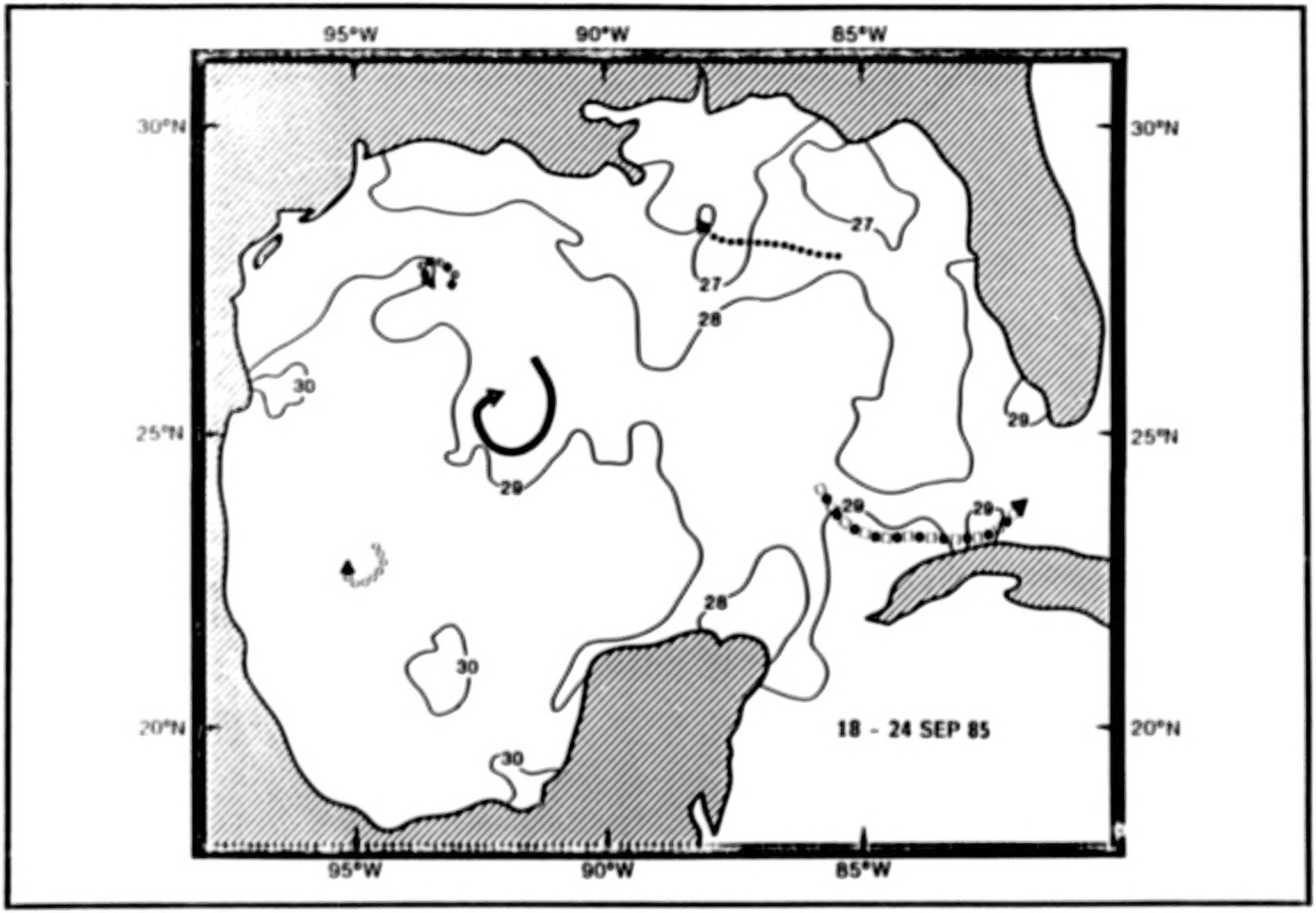

Figure 4.3-8c. SST data (°C) for September 17-24, 1985. The drifter trajectories, shown by arrows, are identified in Table 2.2-1.

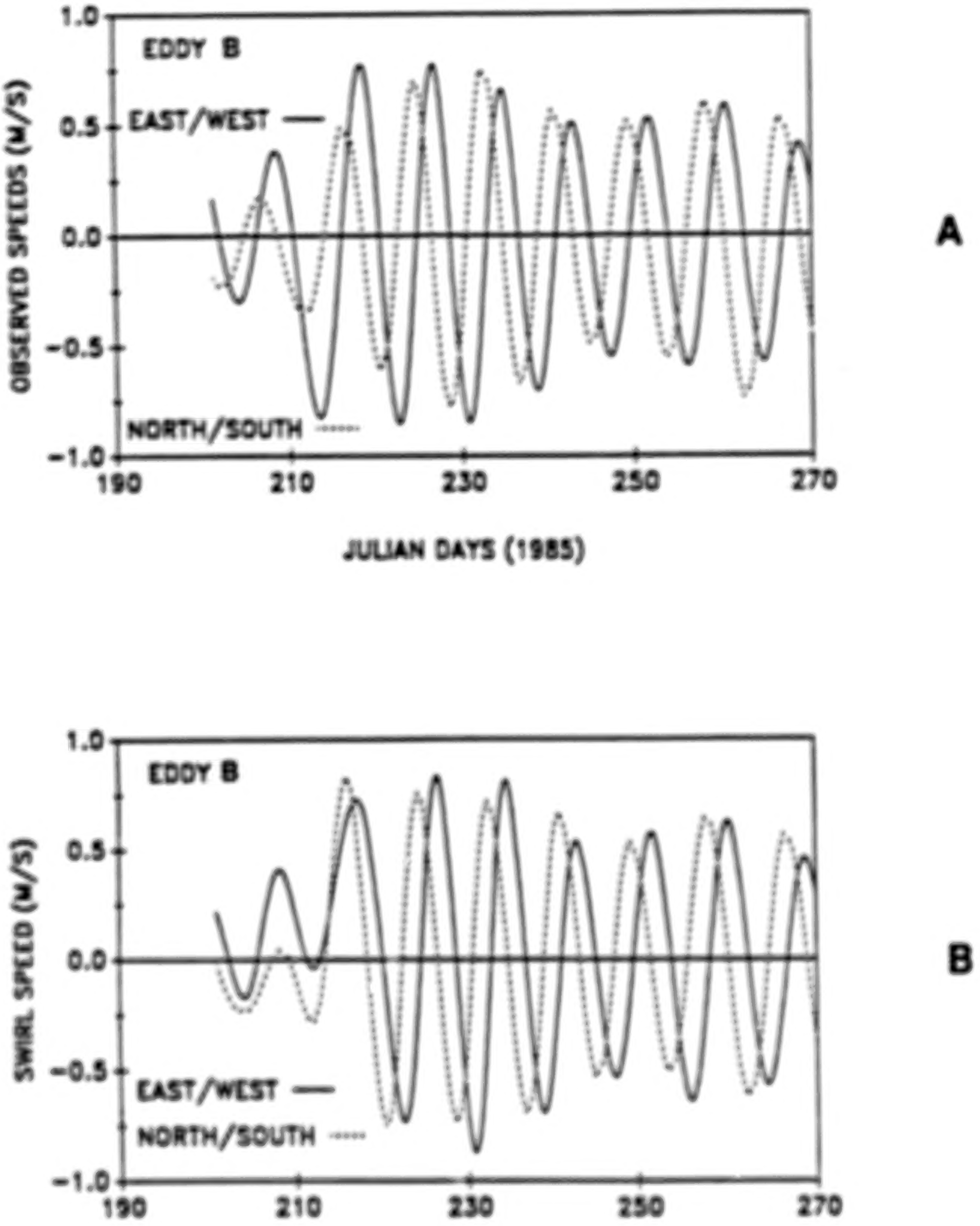

Figure 4.3-9. Time histories of: (a) filtered observed speed components for Eddy B and (b) swirl speed components about the center of rotation for Eddy B. Solid line is the east/west speed and dashed line is the north/south speed.

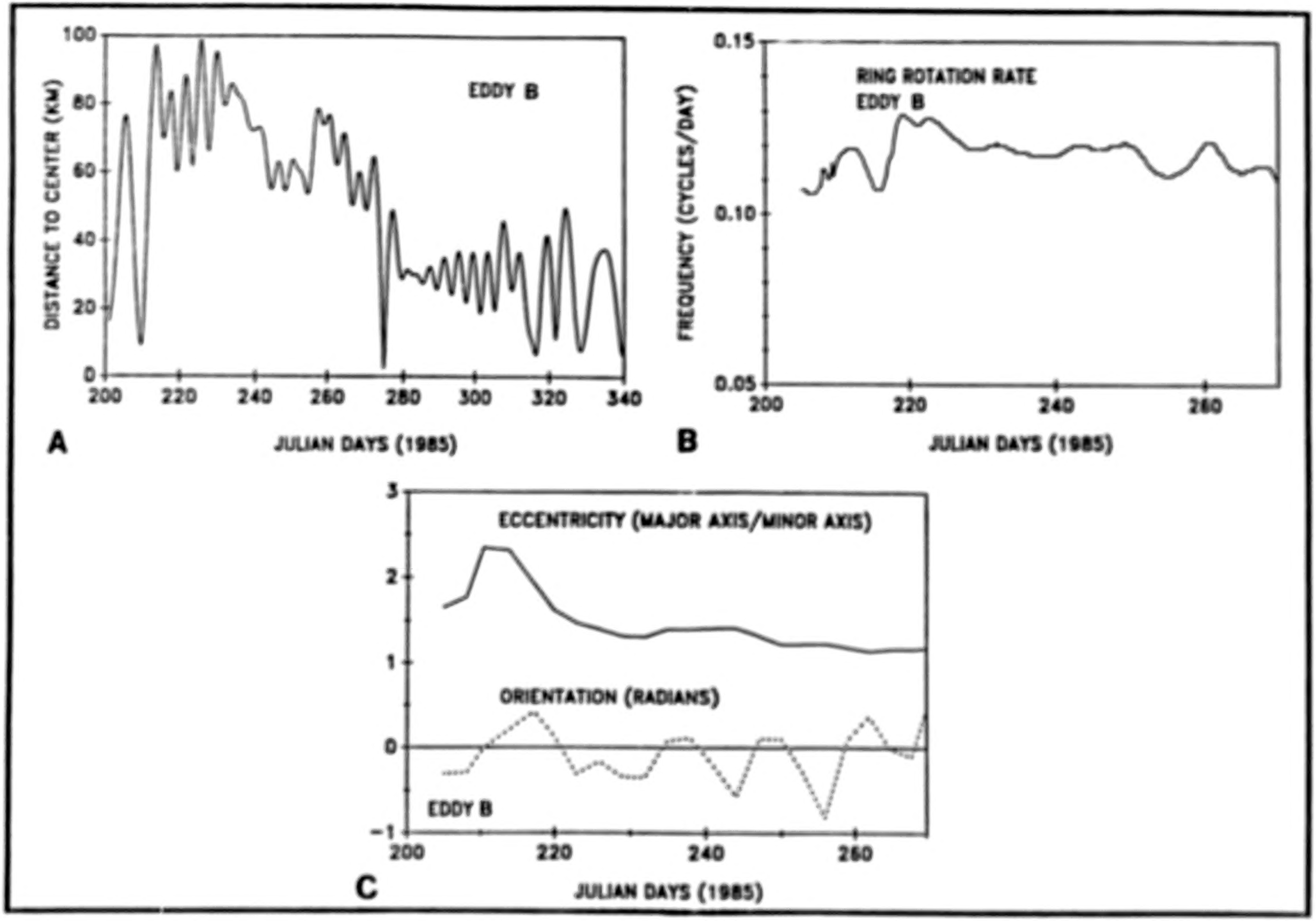

Figure 4.3-10. Time history of: (a) distance to the center of rotation of Eddy B as seen by Drifter 3378, (b) rotational frequency of Eddy B and (c) eccentricity (solid line) and major axis orientation (dashed line) for Eddy B. Flow field orientation is with respect to east/west.

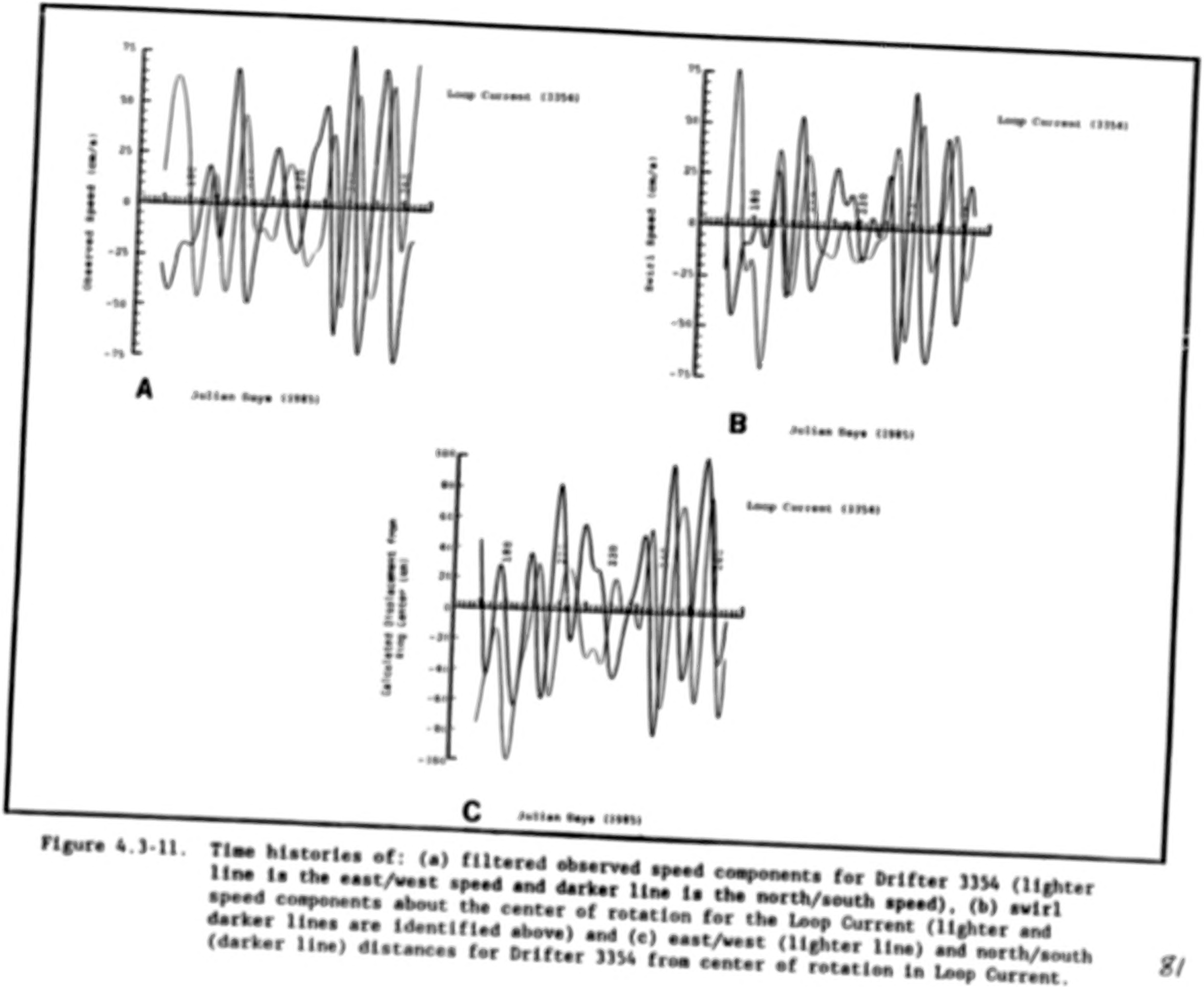

Figure 4.3-11. Time histories of: (a) filtered observed speed components for Drifter 3354 (lighter line is the east/west speed and darker line is the north/south speed), (b) swirl speed components about the center of rotation for the Loop Current (lighter and darker lines are identified above) and (c) east/west (lighter line) and north/south (darker line) distances for Drifter 3354 from center of rotation in Loop Current.

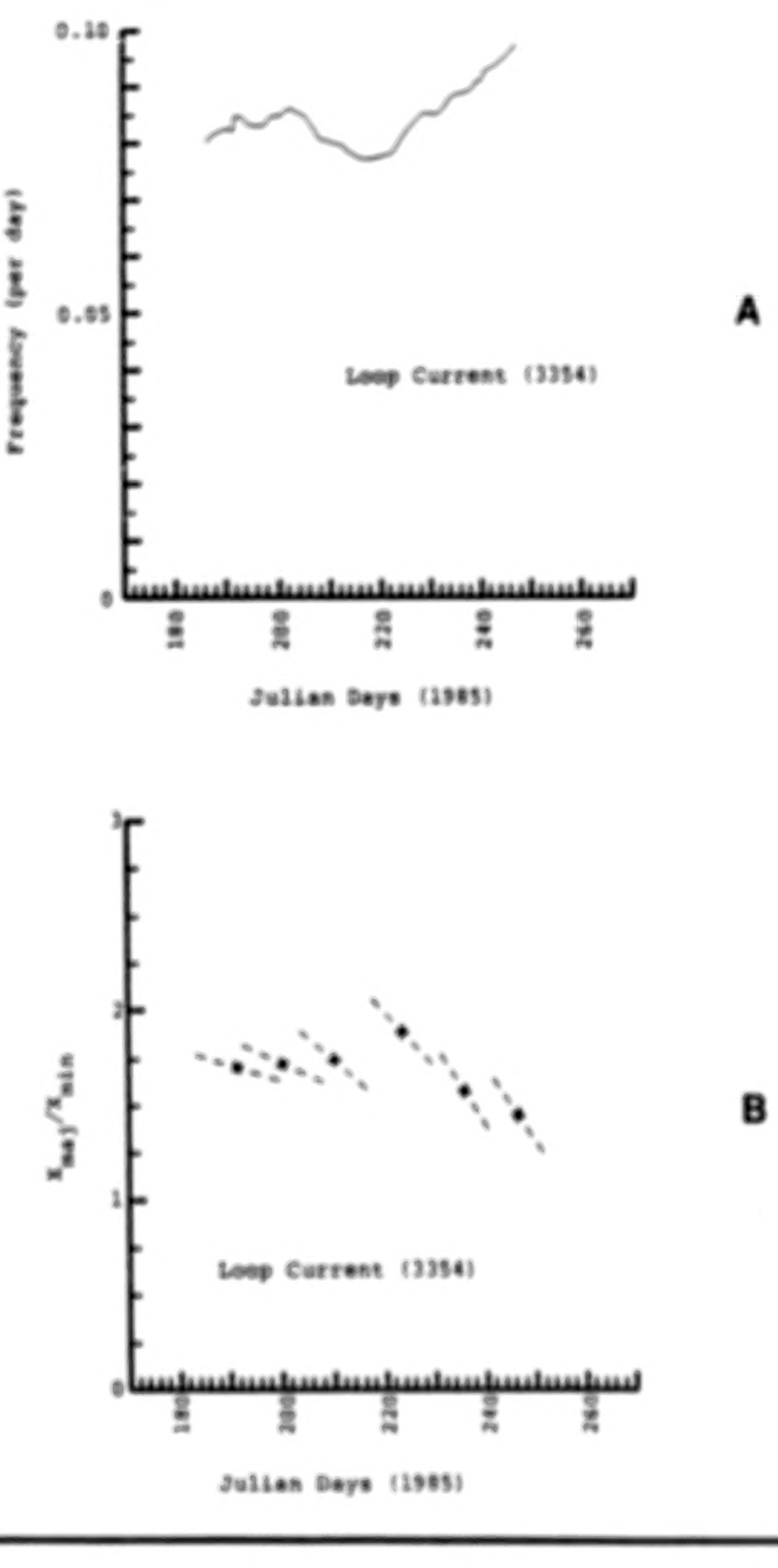

Figure 4.3-12. Time history of: (a) the rotational frequency within the Loop Current and (b) the Loop Current eccentricity (asterisk) and the orientation of the major axis (dashed line). For the flow field orientation, north is in the positive eccentricity direction and east is in the positive time direction.

4.3.3 Initial Eddy Configuration

4.3.3.1 Temperature and Salinity

The initial configuration of Eddy B was relatively circular after it moved past 88°W (Figure 4.3-13). The main transect completed by the R/V PELICAN (in October 1985) indicates that Eddy B was a typical Loop Current eddy in terms of both size and property distributions. The vertical temperature section from the M/V NAT CO 6 (Figures 4.3-5b and c, p. 73) taken during July 16 through 19, 1985 shortly after Eddy B had separated from the Loop Current can be compared with that from the R/V PELICAN taken during October 22 through 24, 1985 (Figure 4.2-4, p. 54). There was very little change in the eddy's vertical temperature structure during the three intervening months.

Figure 4.3-14 shows a vertical section of salinity corresponding to the vertical temperature section in Figure 4.2-4. The prominent feature is the subsurface salinity maximum, that is, values greater than 36.6 ppt, centered near 200m. This Subtropical Underwater (SUW) originates in the tropical North Atlantic (Nowlin, 1972) and is the hallmark of Loop Current eddies. The T-S diagram for this transect is given in Figure 4.3-15. In addition to the salinity maximum, the diagram shows the salinity minimum, that is, values slightly less than 34.9 ppt, associated with a remnant of Subantarctic Intermediate Water (Nowlin, 1972). Figure 4.3-16 shows a vertical section of sigma-t to 1500m. The concave, downward form of the isopycnals, which identifies the baroclinic core of the eddy, is clearly evident to at least 1100m. Below this, however, the density contrast is too weak to be contoured using a 0.2 contour interval.

4.3.3.2 Nutrients

Figure 4.3-17 contains vertical sections for dissolved oxygen, silicate and phosphate, respectively. Oxygen values are greatest in the near surface water directly over the core of the eddy where they exceed 5 ml l^{-1}. The values decrease to a minimum of less than 3 ml l^{-1} between 400m and 600m, or more specifically, along the 27.1 contour of sigma-t. The oxygen values in this minimum layer are slightly elevated at Stations 16, 26 and 28. These are near the radius of maximum velocity in the eddy where there is slightly more vertical mixing. Silicate values increase monotonically from minimum values near the surface to maximum values of about 25 ug-at l^{-1} between 1000m and 1200m or near the 27.7 contour of sigma-t. Phosphate values also increase downward from the near surface to a maximum near 600-800m. The associated sigma-t contour is 27.4. These nutrient distributions are consistent with those observed by Morrison et al. (1983).

4.3.3.3 Velocity

There are three sources of velocity data for Eddy B at the time of the R/V PELICAN cruise. The first, surface drifter velocity, was discussed in Section 4.3.2.2 (p. 76). Typical swirl speeds (i.e., the speed of flow around the eddy) were 60-80 cm sec^{-1}. Another estimate comes from geostrophic velocities computed from the CTD stations. Since the main transect did not pass directly through the center of Eddy B, the stations were moved to a line which did, by assuming axial symmetry. Figure 4.3-18 shows the resulting vertical section of geostrophic velocities relative to a level of no motion at 950m. On the north side, the maximum of about 97 cm sec^{-1} occurs between Stations 14 and 16

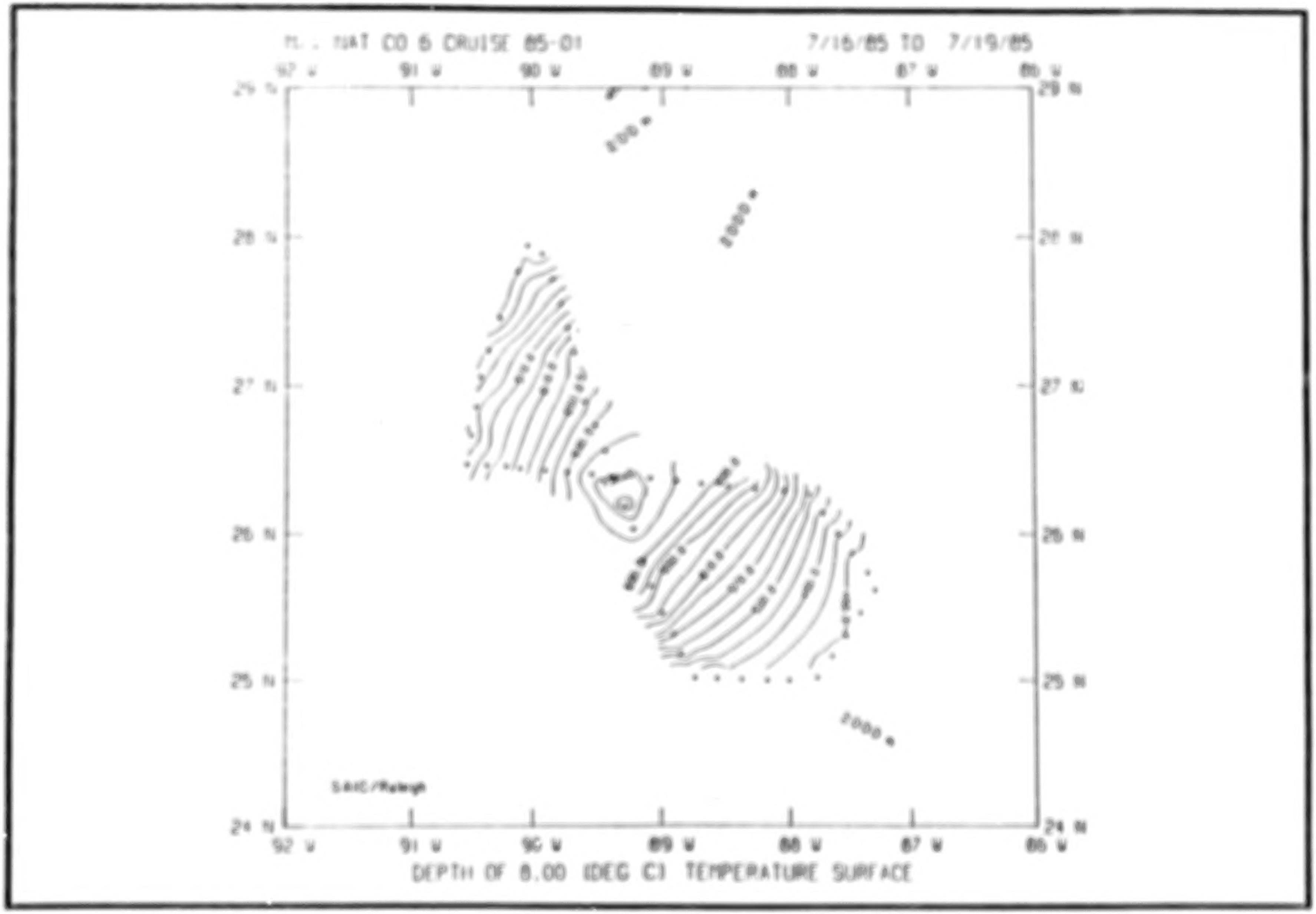

Figure 4.3-13. Topography of the 8°C temperature surface based on all XBT data collected by the M/V NAT CO 6 during the period from July 16-19, 1985.

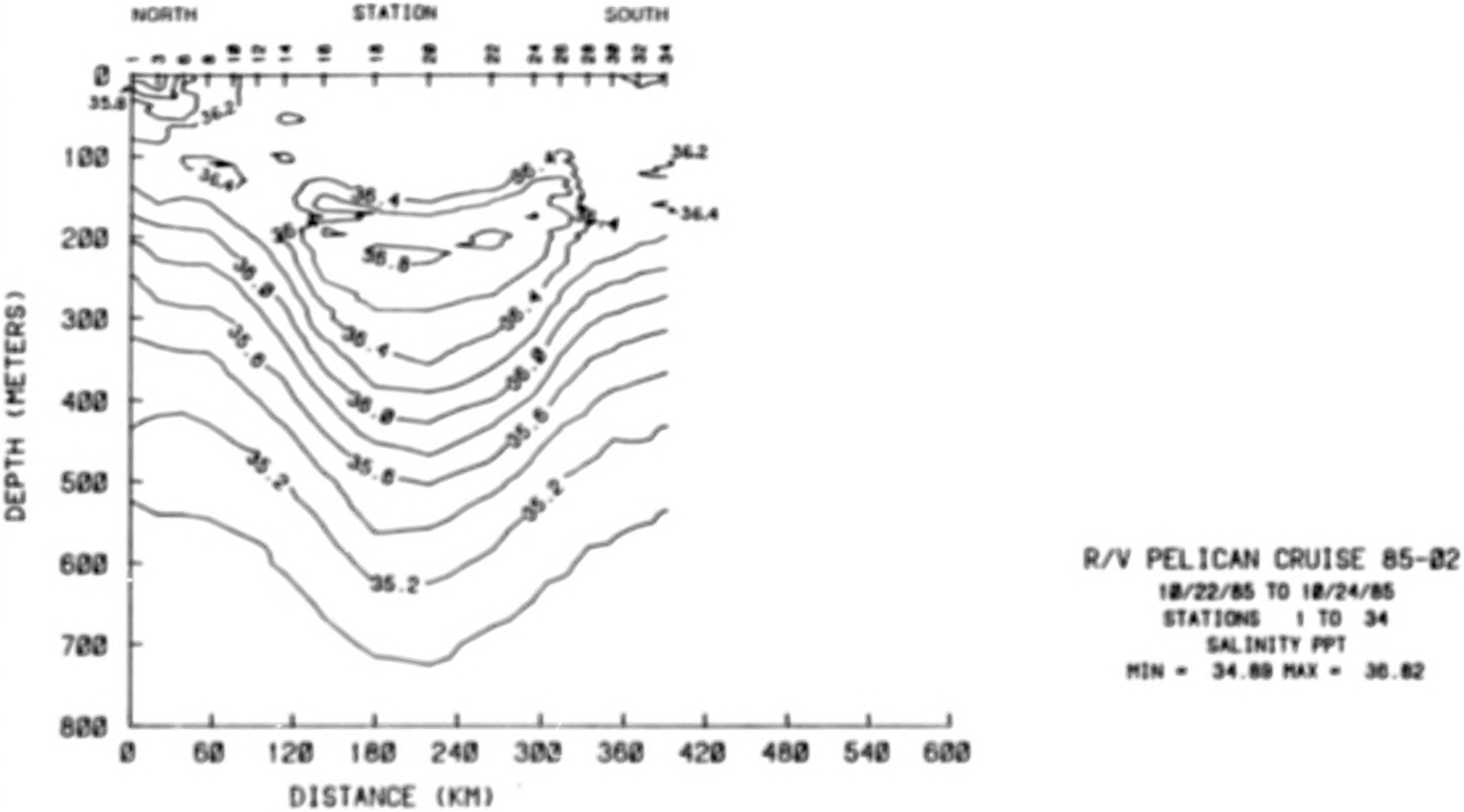

Figure 4.3-14. Vertical section of salinity along the R/V PELICAN CTD transect through Eddy B.

85

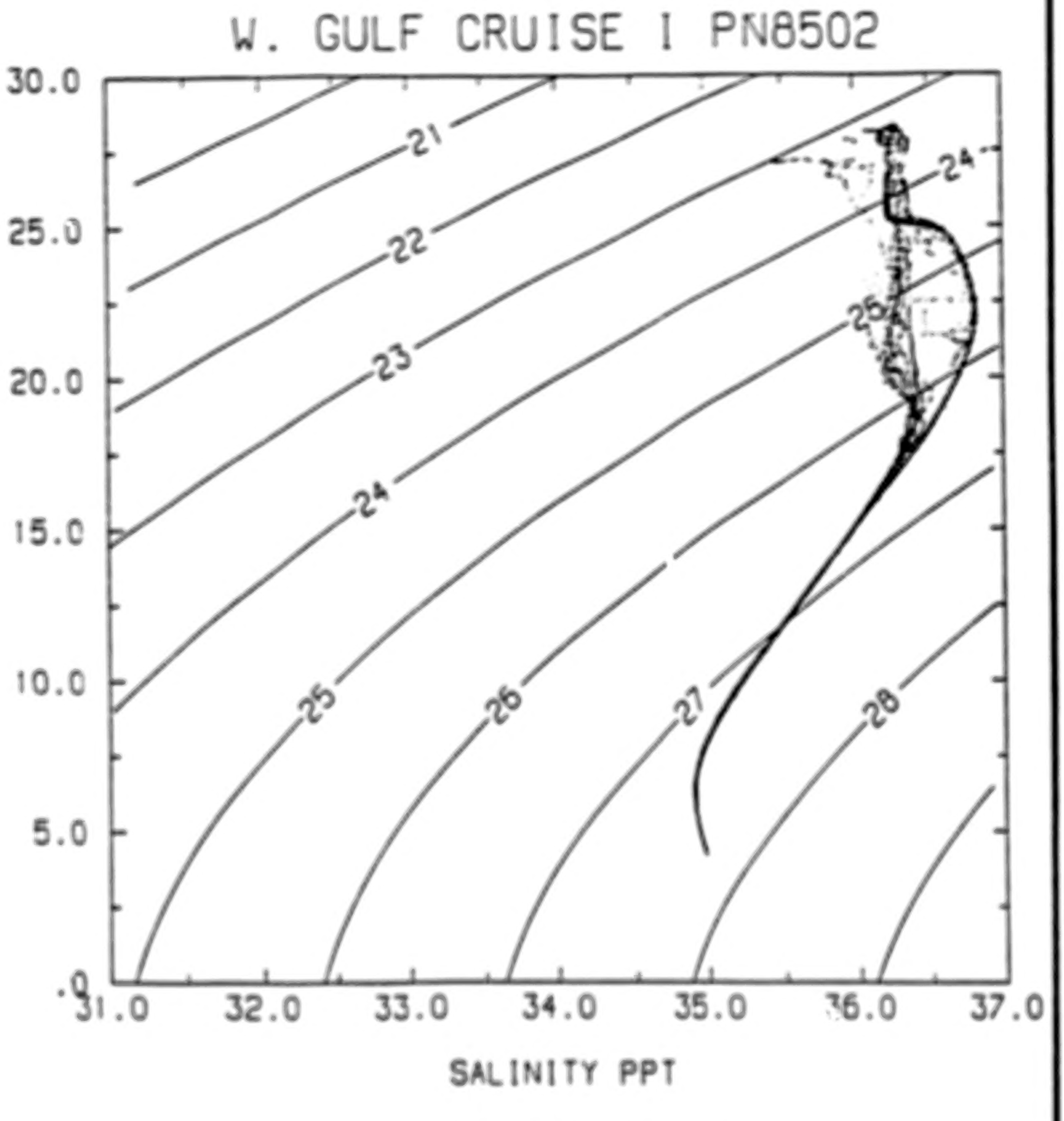

Figure 4.3-15. Composite T-S plot of all CTD data collected during the October 1985 R/V PELICAN cruise.

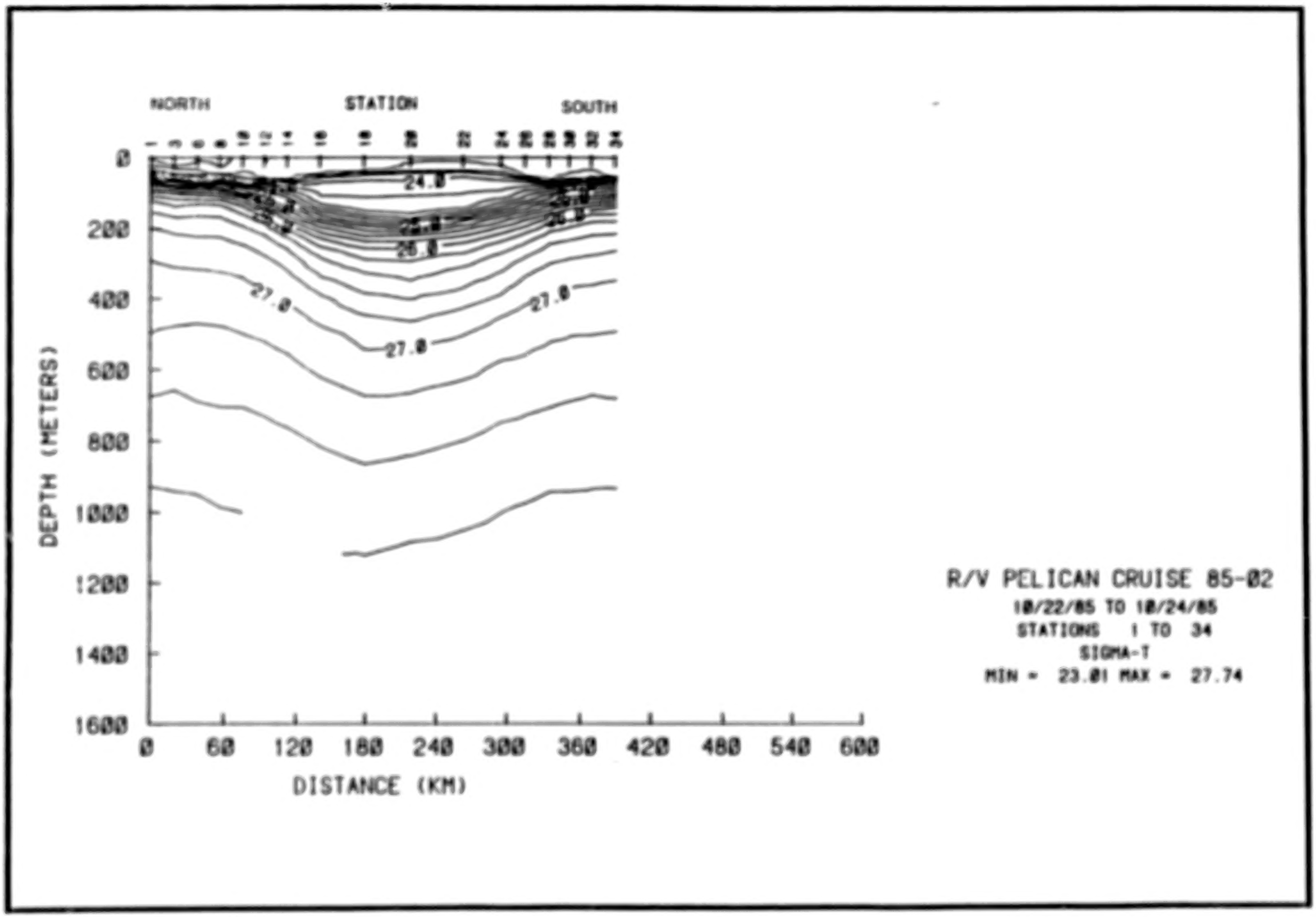

R/V PELICAN CRUISE 85-02
10/22/85 TO 10/24/85
STATIONS 1 TO 34
SIGMA-T
MIN = 23.01 MAX = 27.74

Figure 4.3-16. Vertical section of sigma-t to 1500m along the R/V PELICAN CTD transect through Eddy B.

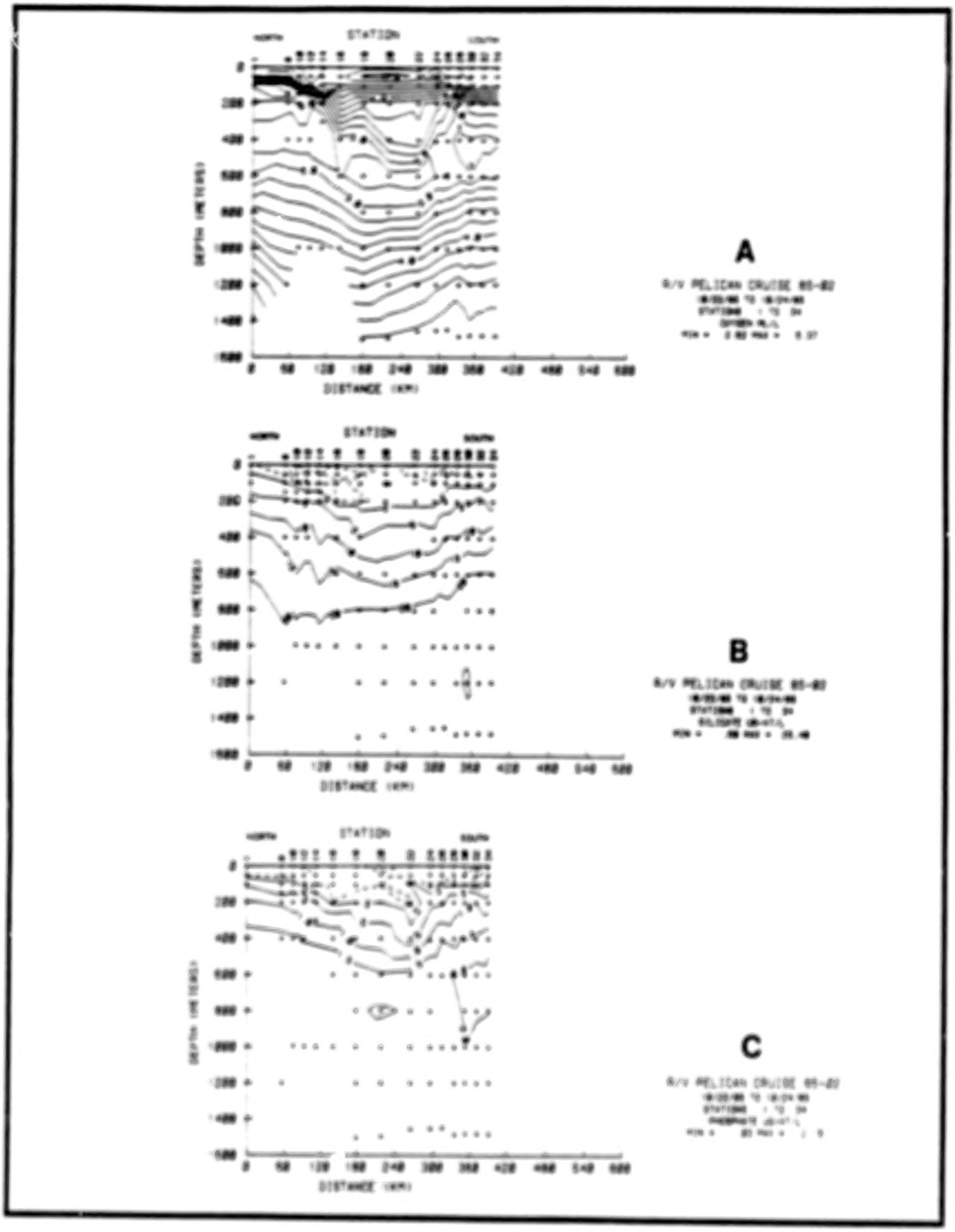

Figure 4.3-17. Vertical section of (a) dissolved oxygen, (b) silicate and (c) phosphate to 1500m along the R/V PELICAN CTD transect through Eddy B.

BEST COPY AVAILABLE

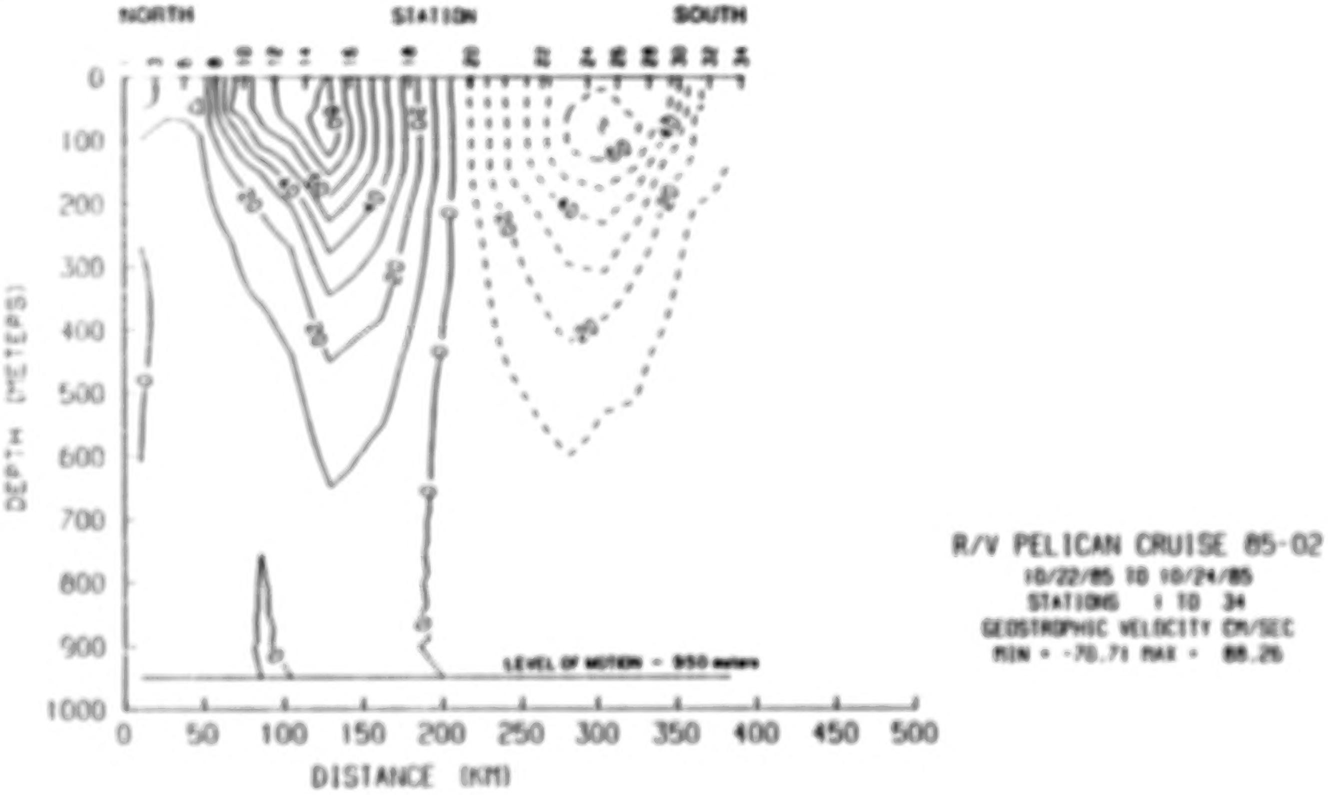

Figure 4.3-18. Vertical section of geostrophic velocities relative to 950m for the PELICAN CTD transect.

at a depth of 100m. On the south side, the maximum lies between Stations 24 and 26, again at 100m, with a value of about 78 cm sec^{-1}.

The currents measured on Mooring R in latter October can be compared with the above geostrophic velocities. Figure 4.2-3 (p. 53) shows the position of Mooring R in Eddy B at this time. Assuming axial symmetry, it corresponds to a position between Stations 12 and 14 on the north side and between Stations 26 and 28 on the south side. Figure 4.3-19 is a plot of 40-hour, low-pass-filtered velocity vectors for all currents recorded at Mooring R. Eddy B begins to influence currents at Mooring R on approximately October 1, 1985 (Julian Day 275 in Figure 4.3-19). At 100m the observed speed is 40 cm sec^{-1}, and the geostrophic speeds are 70 cm sec^{-1} on the north side and 65 cm sec^{-1} on the south. At 300m the observed speed is 20 cm sec^{-1} and the geostrophic speeds are about 30-35 cm sec^{-1}. Figure 4.3-19 is probably the first presentation of directly measured currents from near surface to near bottom in the deep part of the western Gulf. An important feature is the magnitude of the almost purely barotropic signal below 1000m. Also note that on October 17 (Julian Day 292) the currents below 1000m were directed almost opposite to the shallower currents in the baroclinic eddy.

4.3.4 Westward Translation after Separation (Northern Route)

4.3.4.1 SST and Path Data

Eddy B became stalled along the northern continental slope until mid-September 1985. During this time, Drifter 3378 exhibited slightly weaker velocities (50-70 cm sec^{-1}) at radii from 50-80 km from the eddy center. The eddy then made a rather rapid southern movement, and the resulting conditions are shown in Figure 4.3-20. There are two important occurrences illustrated in this figure. The first is that Eddy A (whose origin date is unknown) was well southwest of Eddy B at this time (late September). Apparently, Eddy A continued its southwestward migration, the preferred path of most Gulf eddies (Vukovich and Crissman, 1986; Lewis and Kirwan, 1985). The second interesting factor is the location of Drifter 5683. This drifter had been near the Florida Straits (Figure 4.3-8a, p. 78), but moved northward and then westward to a position off the Mississippi delta. As will be seen, this drifter eventually became entrained in the flow field of Eddy B.

During October 1985, Drifter 3378 moved to tighter orbits (~40 km radius) in Eddy B. Conditions for October 23 through 29 are shown in Figure 4.3-21. Eddy B had moved west-southwest into deeper water, and Eddy A had reached the Mexican coast at ~22.5°N. Drifter 5678 is seen to have some anticyclonic motion to the north of Eddy B, and Drifter 5683 appears to be following Drifter 5678.

4.3.4.2 Eddy-Related Processes

Eddy B is the first reported Gulf eddy tracked by a drifter that followed a northerly route westward across the Gulf (Lewis and Kirwan, 1985). Three previously tracked eddies had all moved westward along a more southerly route. It is logical to consider what factors caused Eddy B to take the more northern path.

Eddy B not only moved on a more northerly path, but also stalled for a time on the 3000m isobath (Figure 2.2-1a, p. 6). This is an important occurrence for a number of reasons. First, the vertical extent of Loop Current eddies can be

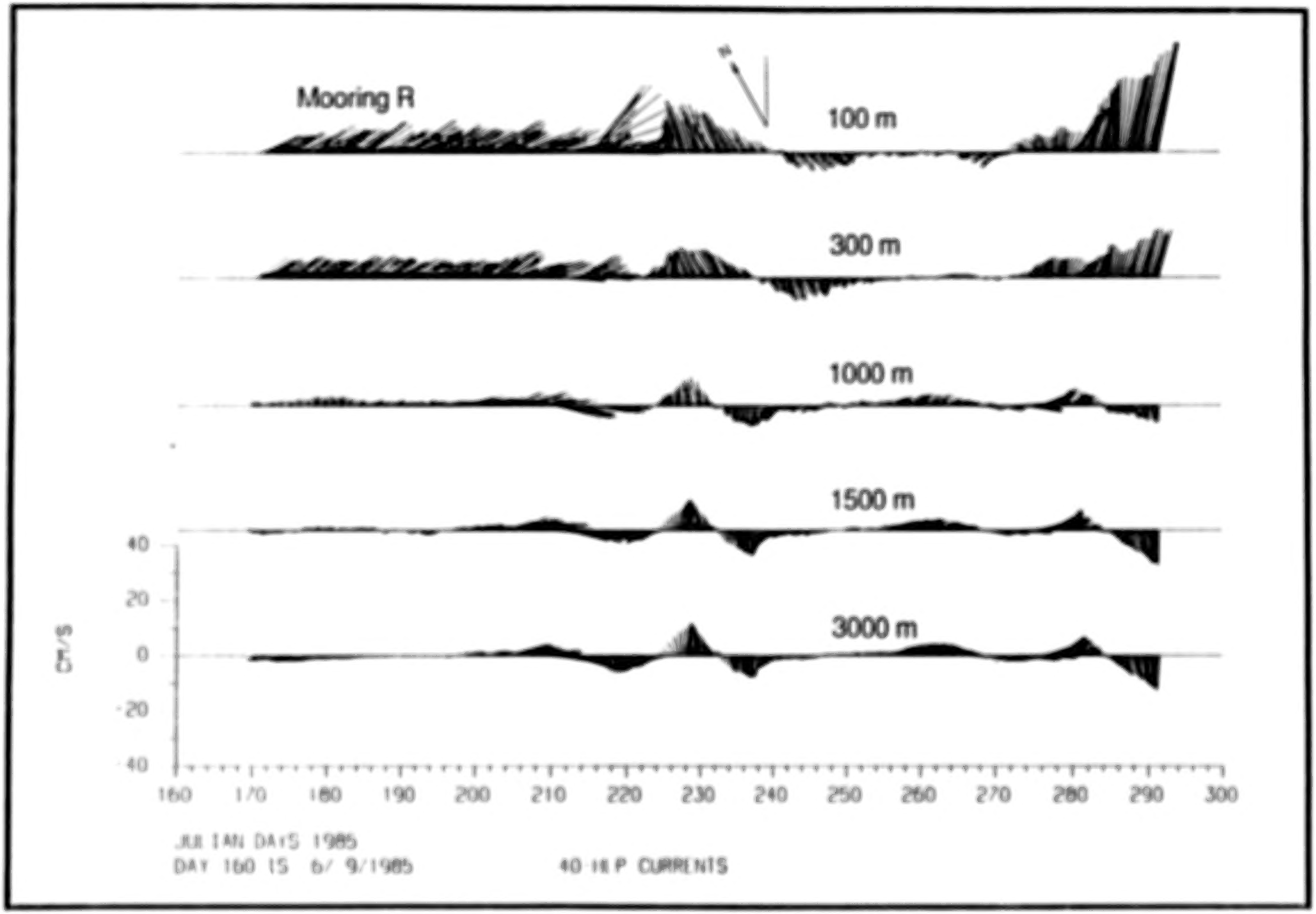

Figure 4.3-19. Velocity vector time series of 40-hour, low-passed currents recorded at Mooring R.

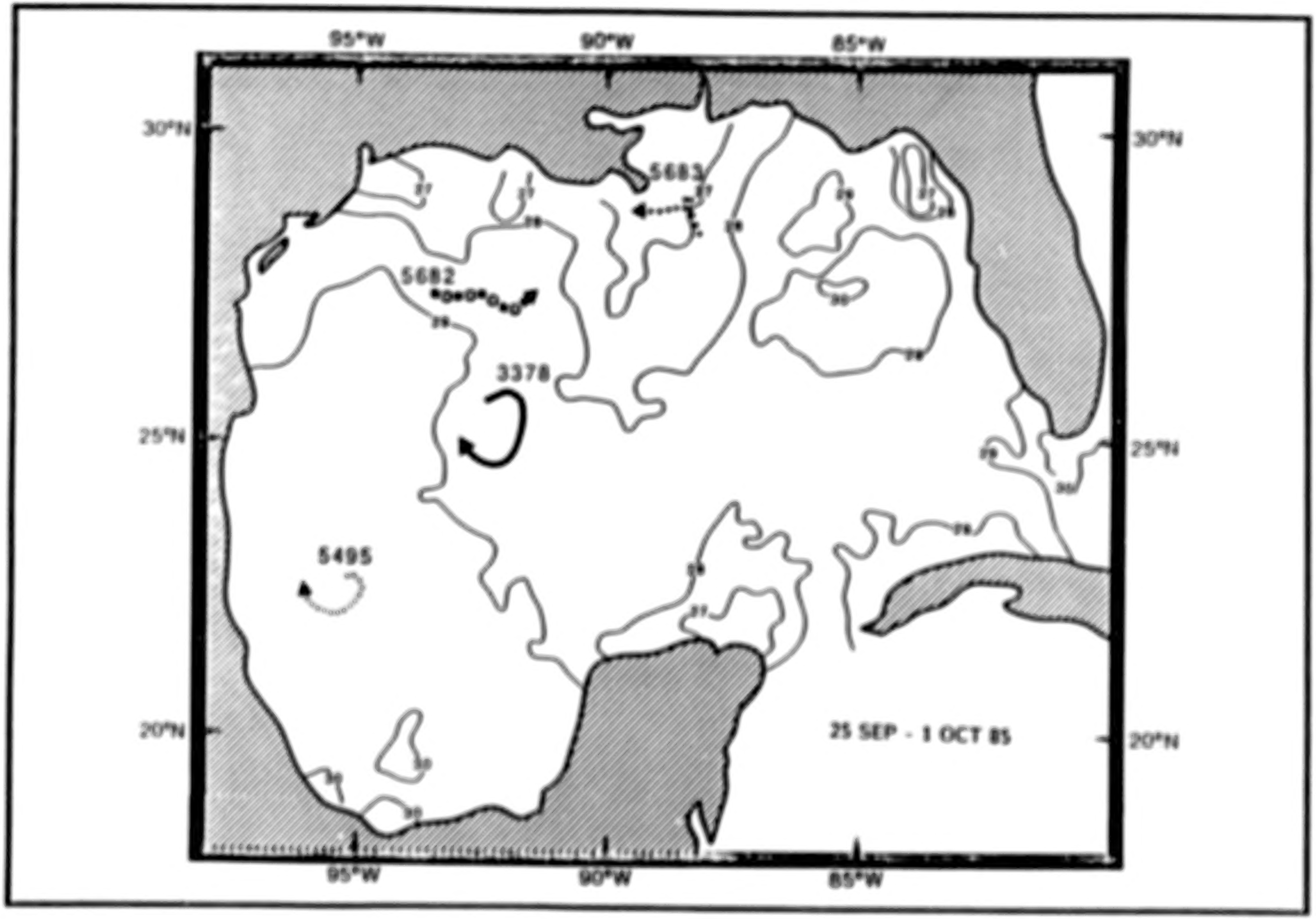

Figure 4.3-20. SST data (°C) for September 25 through October 1, 1985. The drifter trajectories, shown by arrows, are identified in Table 2.2-1.

BLANK

PAGE

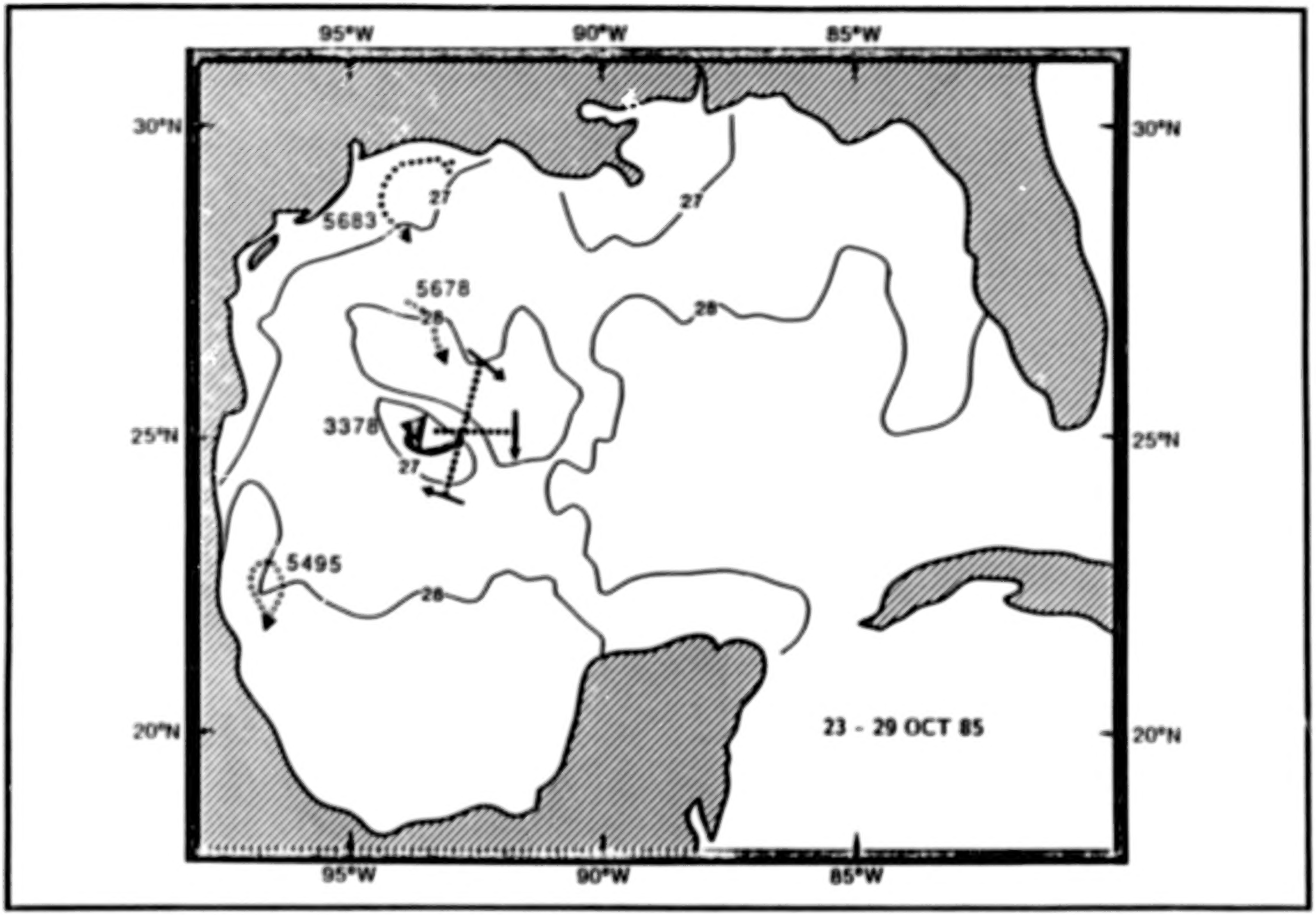

Figure 4.3-21. SST data (°C) for October 23-29, 1985. Shorter arrows denote the flow at the edges of Eddy B while dotted lines indicate the locations of eddy waters (based on XBT data). The drifter trajectories, shown by arrows, are identified in Table 2.2-1.

substantial. An objective analysis of hydrographic observations by Hofmann and Worley (1986) showed that an eddy flow field could reach as deep as 3000m or more. Current meter data for Eddy B, as it later reached the western Gulf of Mexico, showed that this was true here as well. Considering the spatial extent of the eddy when it detached from the Loop Current (Figure 4.3-22), movement onto the 3000m isobath would mean that the northern edge of flow would reach into water depths at least as shallow as 1200m. This seems contrary to the concept of the conservation of potential vorticity in which a flow field of constant total vorticity moves along a constant depth contour. In addition, the distance of Drifter 3378 from the center of the eddy (Figure 4.3-10a, p. 80) decreased while moving into shallower water (Julian Days 235 through 255), which is opposite of what would be expected from conservation of potential vorticity.

Finally, Eddy B made a relatively abrupt southward move off the 3000m isobath into deeper water during Julian Days 255 through 275. This was accompanied by a further decrease in the distance from the center of the eddy to Drifter 3378 (Figure 4.3-10a).

If the conservation of potential vorticity is assumed to hold within the eddy, then the movement into shallow water must result from an external flow field. In Figure 4.3-8a (p. 77) Eddy A was quite close to Eddy B prior to its movement onto the 3000m isobath. However, the interaction of the flow fields of two anticyclones results in the rotation of the pair in an anticyclonic sense (Hooker, 1987; Cresswell, 1982). Such an interaction would result in Eddy B moving southeastward and not onto the continental slope. Moreover, two interacting vortices tend to coalesce, being drawn together as their flow fields merge (Chang, 1983; Nof and Simon, 1987). There is, however, no indication of such a coalescence at this time. These considerations support an assumption that an external flow field may have interacted with Eddy B and caused it to move into shallower water to the north.

The stalling of Eddy B on the 3000m isobath may be a common event for eddies traveling along the northern slope of the Gulf. Westward propagation can be explained by the beta effect on individual water parcels within the eddy (Smith and O'Brien, 1983). But when the eddy feels the effect of bathymetry to the north, non-linear accelerations can become important (Smith, 1986). The narrower and shallower region along the northern edge of the eddy causes an acceleration and an increase in momentum. As a result, the eastward flowing water north of the eddy center exceeds the westward flow to the south. This counteracts the beta effect. The stalling of Eddy B may result from a balance between the westward-tending beta effect and the eastward-tending non-linear acceleration.

Still to be accounted for, however, is why the orbits of Drifter 3378 became smaller as Eddy B moved over and stalled on the northern continental slope. One clue to what may have occurred is found in the XBT data. Table 4.3-1 shows the maximum depths of the 8°C isotherms for various surveys. Also shown are the volumes between the 15°C and 8°C isothermal surfaces. The M/V NAT CO 6 and R/V PELICAN cruises demonstrate that the maximum depth of the 8°C isotherm decreased by 5m but the volume between the 8°C and 15°C surfaces increased by 60%. The net result is a substantial growth of Eddy B from the period between when it was spawned and after it moved southward off the 3000m isobath. This suggests that Eddy B may have entrained a substantial amount of water. Such a process is consistent with the paths of Drifters 5683 (Figures 4.3-23a through c) and 5678 (Figures 4.3-23a through e). These

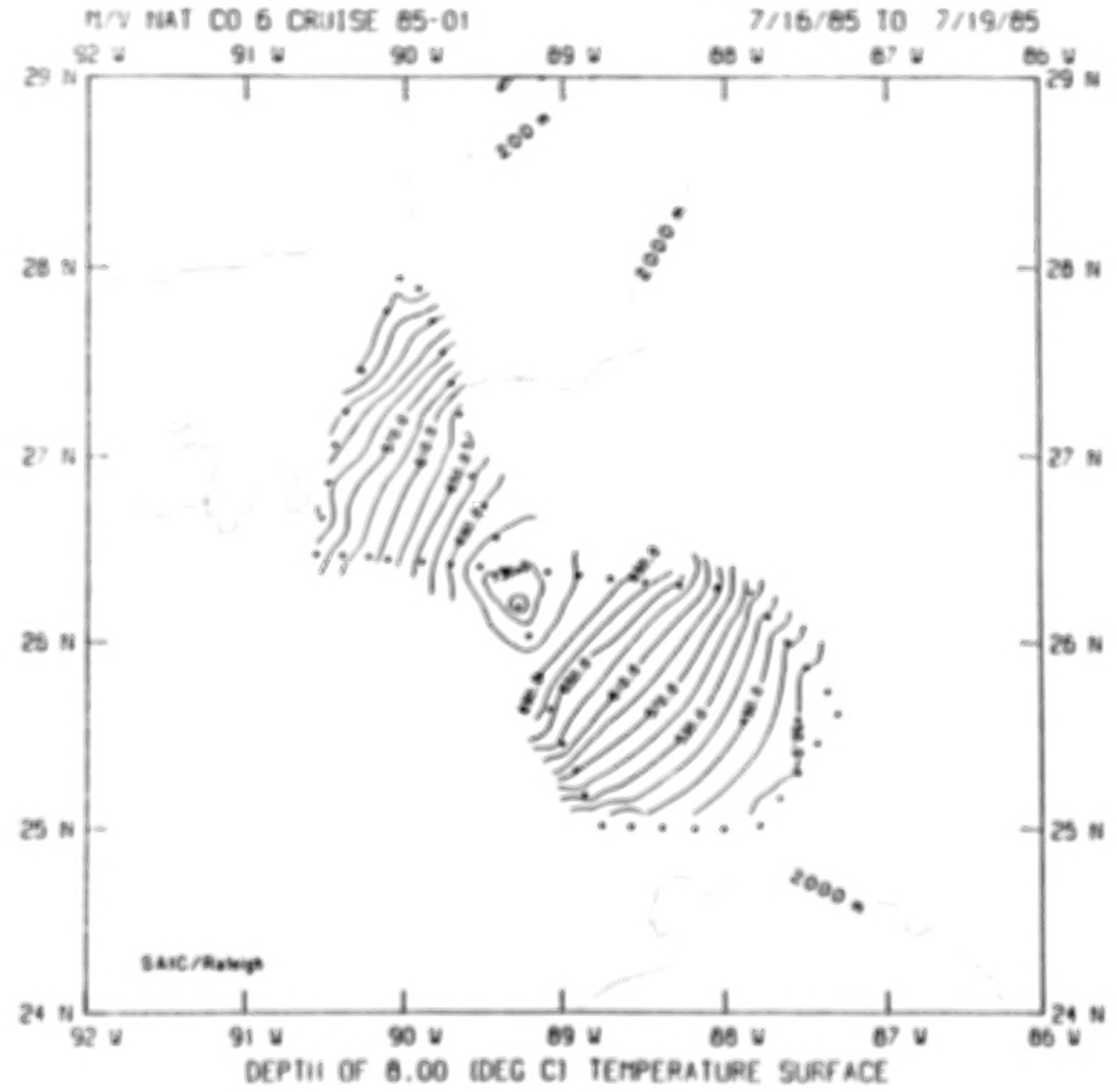

Figure 4.3-22. Topography of the 8°C temperature surface based on all XBT data collected by the M/V NAT CO 6 during the period from July 16-19, 1985.

Survey Source and Date	Maximum Depth of the 8° Isotherm (m)	Estimated Mass Between 15° and 8°C at 550m ($\times 10^{13} m^3$)
M/V NAT CO 6, July, 1985	760	1.67
R/V PELICAN, Oct, 1985	755	2.67
AXBT Survey, Nov, 1985	710	2.82
B/O ALTAIR, Feb, 1986	810	2.46
B/O ALTAIR, Apr, 1986	720	1.37
HO-2, Aug, 1986	700+	3.92

Table 4.3-1. Estimates for Eddy B of the vertical extent of the 8°C isotherm and of the volume of water between the 8°C and 15°C isothermal surfaces. These are used as indicators of the changes in the size of the ring between various cruises.

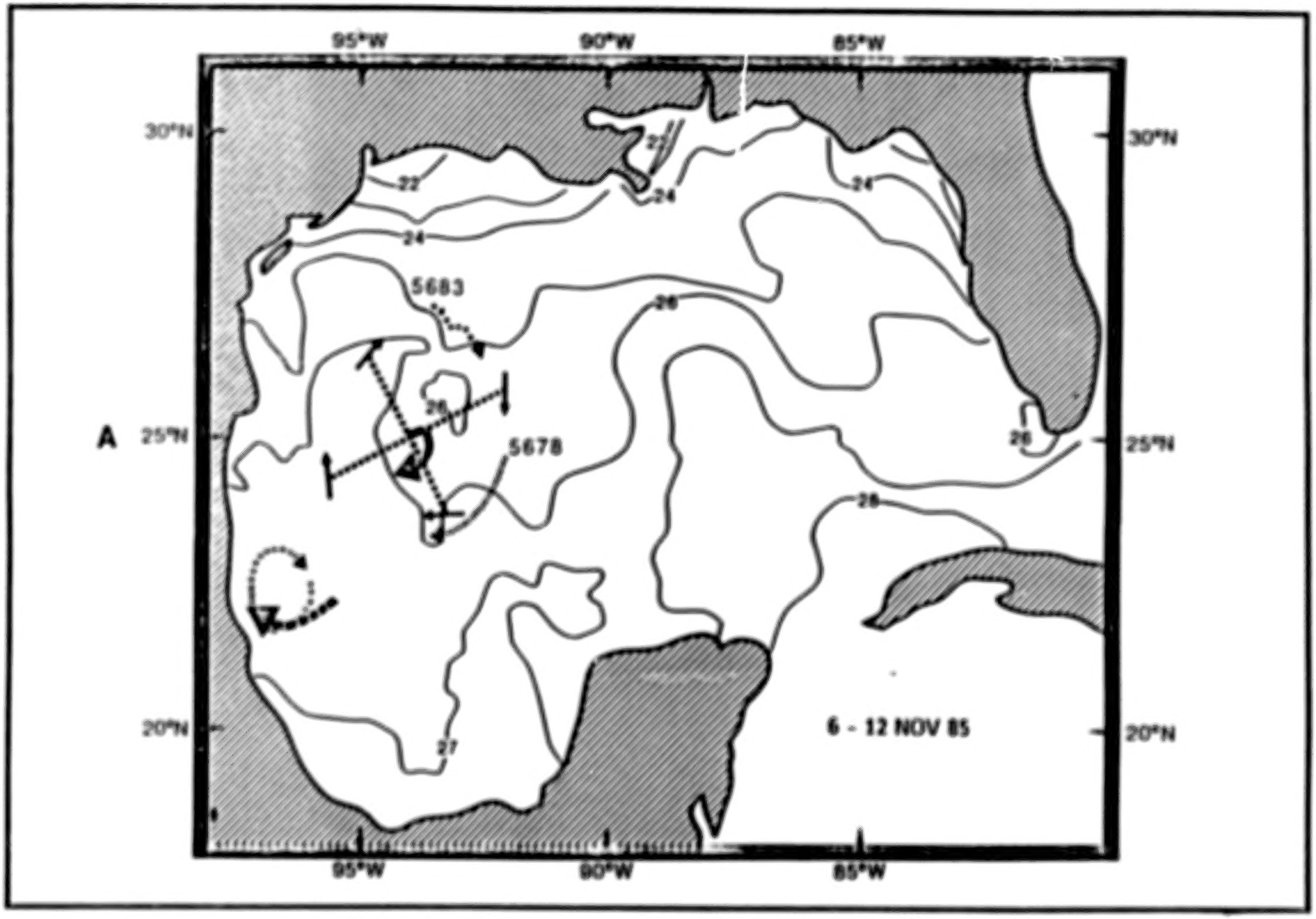

Figure 4.3-23a. SST data (°C) for November 6-12, 1985. Shorter arrows denote the flow at the edges of Eddy B while dotted lines indicate the locations of eddy waters (based on XBT data). The drifter trajectories, shown by arrows, are identified in Table 2.2-1.

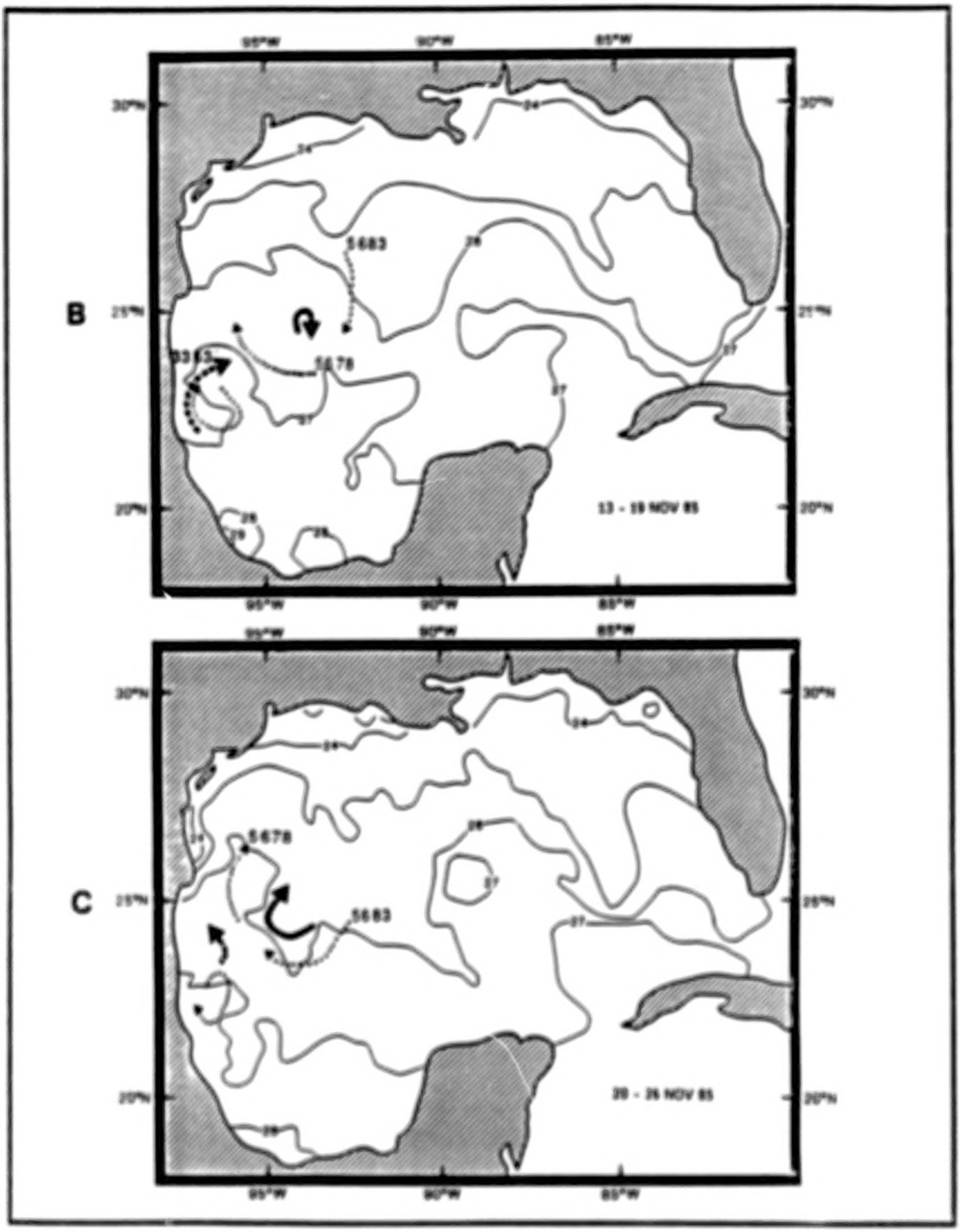

Figure 4.3-23b-c. SST data (°C) for: (b) November 13-19, 1985 and (c) November 20-26, 1985. Shorter arrows denote the flow at the edges of Eddy B while dotted lines indicate the locations of eddy waters (based on XBT data). The drifter trajectories, shown by arrows, are identified in Table 2.2-1.

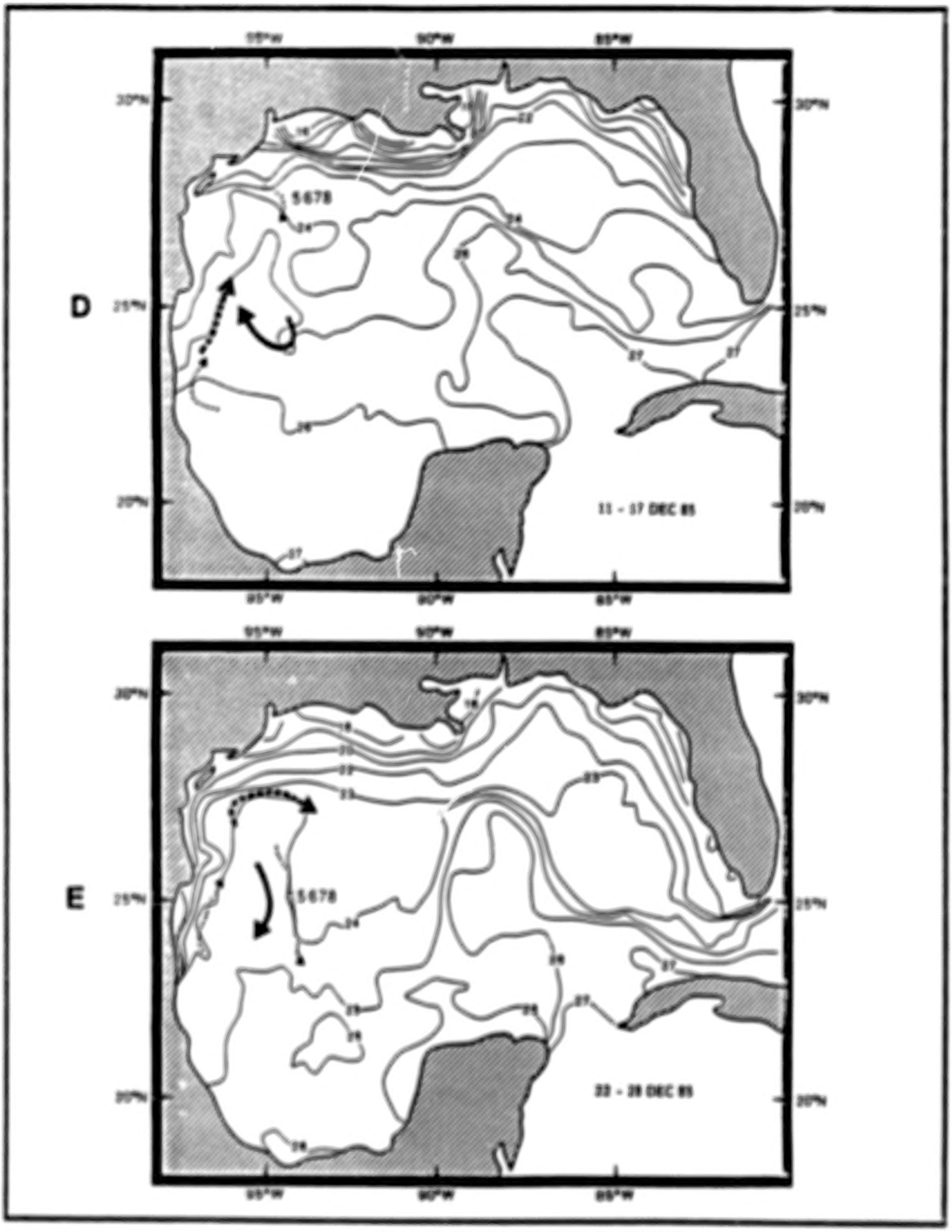

Figure 4.3-23d-e. SST data (°C) for: (d) December 11-17, 1985 and (e) December 22-28, 1985. Shorter arrows denote the flow at the edges of Eddy B while dotted lines indicate the locations of eddy waters (based on XBT data). The drifter trajectories, shown by arrows, are identified in Table 2.2-1.

drifter data would seem to suggest that the source of the water was the warm shelf waters of the northern Gulf. Clearly, these implications are dependent on the volume calculations giving an accurate estimate.

The entrainment process could explain both the decrease in the radius seen by Drifter 3378 and the abrupt offshore movement of the eddy. First, the entrainment of shallow, warm shelf water would produce a convergence in the top layer of Eddy B. Convergence would then produce smaller drifter orbits, and upper layer entrainment would have to be compensated by divergence in the lower layers of Eddy B. Some portion of the decrease in eddy radius after moving off the 3000m isobath could be the result of vortex stretching as the eddy goes into deeper water. Assuming the eddy extends to the bottom at all depths in the Gulf, vortex stretching can only account for a third of the decrease in eddy radius. The remainder may be attributed to mass entrainment in Eddy B. Overall, the net decrease in the eddy radius indicates a volume increase of 50%, quite consistent with the 60% estimate obtained using the 8°C and 15°C isotherm data.

An entrainment process would also help account for why Eddy B moved southward into deeper water. To see this, consider the conservation of mass and potential vorticity:

$$dH/dt + H\,D = Q$$

$$d(z + f)/dt + D\,(z + f) = 0$$

where H is the average depth, t is time, D is the horizontal convergence, Q is some source of mass (the mass entrainment process), z is the vertical component of vorticity and f is the Coriolis parameter. Solving the top expression for D and substituting into the second expression gives

$$d[\ \ln(z + f)/H\ ]/dt = -Q/H.$$

Since Q is positive for entrainment, the above implies that (z + f)/H must decrease. This can be accomplished by increasing H and/or decreasing f. Either possibility is consistent with the southward movement of Eddy B off the northern continental slope.

4.3.5 Receiving Field

The most extensive set of direct current measurements yet obtained in the western Gulf of Mexico is available to characterize the conditions prior to the arrival of Eddy B, but there is little in the way of supporting information such as XBT, CTD, satellite or drifter data that would indicate the spatial extent and paths of mesoscale features. The "receiving field" for Eddy B was not quiescent. The current meter data indicate considerable mesoscale activity, which is not surprising since the present conceptual model of the western Gulf is that it is filled with both warm-core and cold-core eddies of various sizes and in various stages of generation and decay. Although the lack of other information makes it difficult to relate events and fluctuations in the records to the influence of specific mesoscale features, the data provide a benchmark characterization of the temporal, statistical and spectral properties of the western Gulf that can be used in interpreting the data of the second deployment period.

The XBT data collected during the current meter rotation cruise in October 1985 show that at least two mesoscale features existed in the vicinity of the moorings near the end of the first deployment period. They were located over the continental slope due west of incoming Eddy B (Figure 4.2-3, p. 53). A vertical temperature section along the line joining Moorings P, S and T is shown with the R/V ALTAIR cruise track in Figure 4.3-24. A cold-core eddy is evident in the doming isotherms centered at Station 13. The existence of a warm-core eddy is inferred from the combination of the downward slope of the isotherms towards Station 3 and the observed currents at Mooring T. Since eddies move around, these cyclonic and anticyclonic features might be the source of the strong signal at Mooring R during August 1985 (Figure 4.3-19, p. 91). Eddy A, which was moving across the Gulf during the latter part of the first deployment period, probably passed too far south of the moorings to have a direct influence.

4.3.5.1 Time Domain Description

Data from Mooring R were introduced in Figure 4.3-19 in the discussion of velocity in Eddy B at the time of the R/V PELICAN cruise. In this figure the vertically up direction is toward 30°T, and horizontally right is toward 120°T. The rotation aligns the V component with the mean direction of the bathymetry of the continental slope in the study area. The direction of North is indicated by the bold arrow labeled "N". The 40-hour, low-pass filtered vectors are plotted to the same scale at all five levels for ease in visual comparison. Figures 4.3-25 through 4.3-28 show the currents from Moorings Q, P, S and T, respectively, in the same format.

Mooring R was located on the flat, abyssal plain (3500m), away from the influence of the continental slope. In Figure 4.3-19, there is an obvious difference in the appearance of the plots at and above 300m compared with those at and below 1000m. At any given time, vectors at 300m are generally similar to those at 100m in direction but smaller in magnitude. Maximum speeds are about 40 cm sec^{-1} at 100m and 20 cm sec^{-1} at 300m. From 1000-3000m the vectors are very similar in both magnitude and direction at any given time. Maximum speeds (40-hour, low-passed) from 1000m down are about 15 cm sec^{-1}. There are two periods when the currents at all levels are relatively strong. The first, about Julian Day 229 (Aug.), may be attributable to mesoscale features discussed in the previous section. The second begins in October and is due to the arrival of the western edge of Eddy B.

The form of the current velocities, particularly deep versus shallow, can be explained in terms of barotropic and baroclinic flow components. Barotropic flow is thought of as the flow due to a uniform tilt of the pressure surfaces in water where the density essentially depends only on pressure and the velocity is uniform with depth. Baroclinic flow is the part due to additional tilts of the pressure surfaces caused by density variations. Both flow components are geostrophic; that is, the Coriolis force balances the pressure gradient force. The baroclinic part may be obtained by the standard method for calculating geostrophic velocity shear from density versus depth, as was done, for example, in creating Figure 4.3-18 (p. 89). The barotropic part must be obtained by some other means such as directly measuring the absolute current and subtracting the baroclinic component.

At depths below 1400m in the Gulf, the range of potential temperature is 4.01°C to 4.15°C, and the range of salinity is 34.962 to 34.976 ppt (Nowlin, 1972). Below 2000m, the approximate sill depth of the Yucatan Strait, these

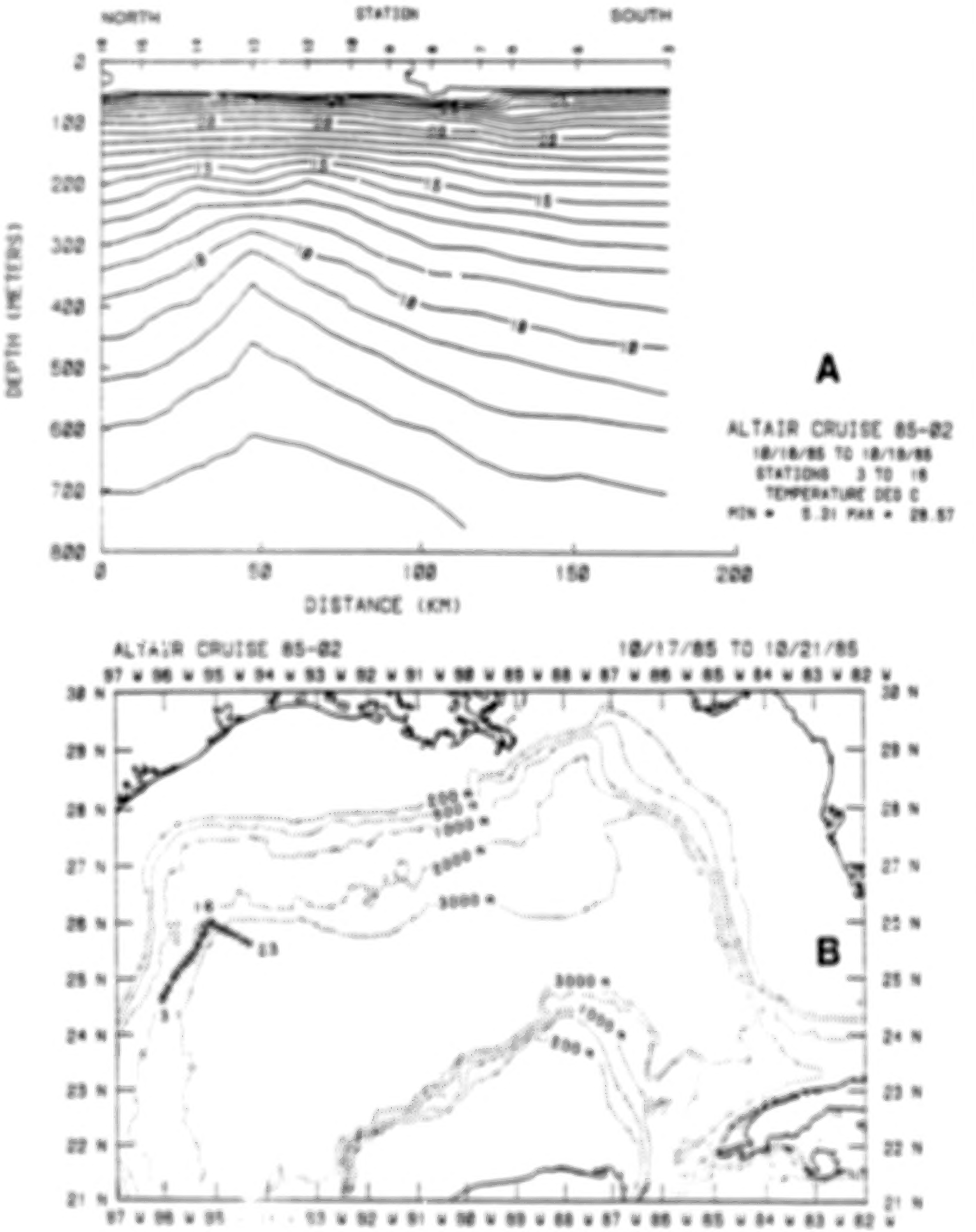

Figure 4.3-24. Vertical section of temperature along the line between Moorings T and P, based on XBT data collected by the R/V ALTAIR during the period from October 18-19, 1985.

BLANK

PAGE

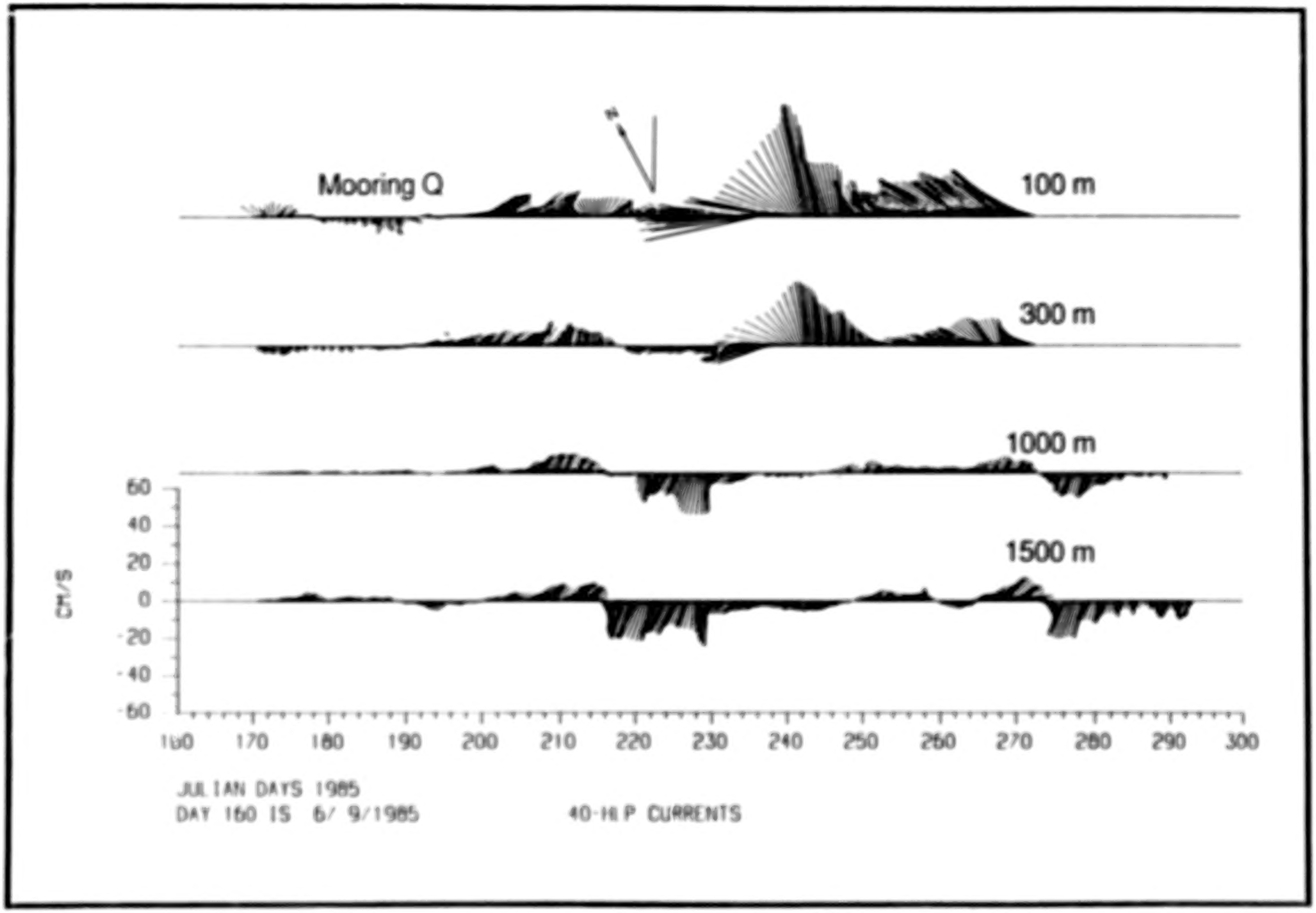

Figure 4.3-25. Stick plots of 40-hour, low-passed currents at Mooring Q for the first deployment period. Vertically up (+V) is towards 30°.

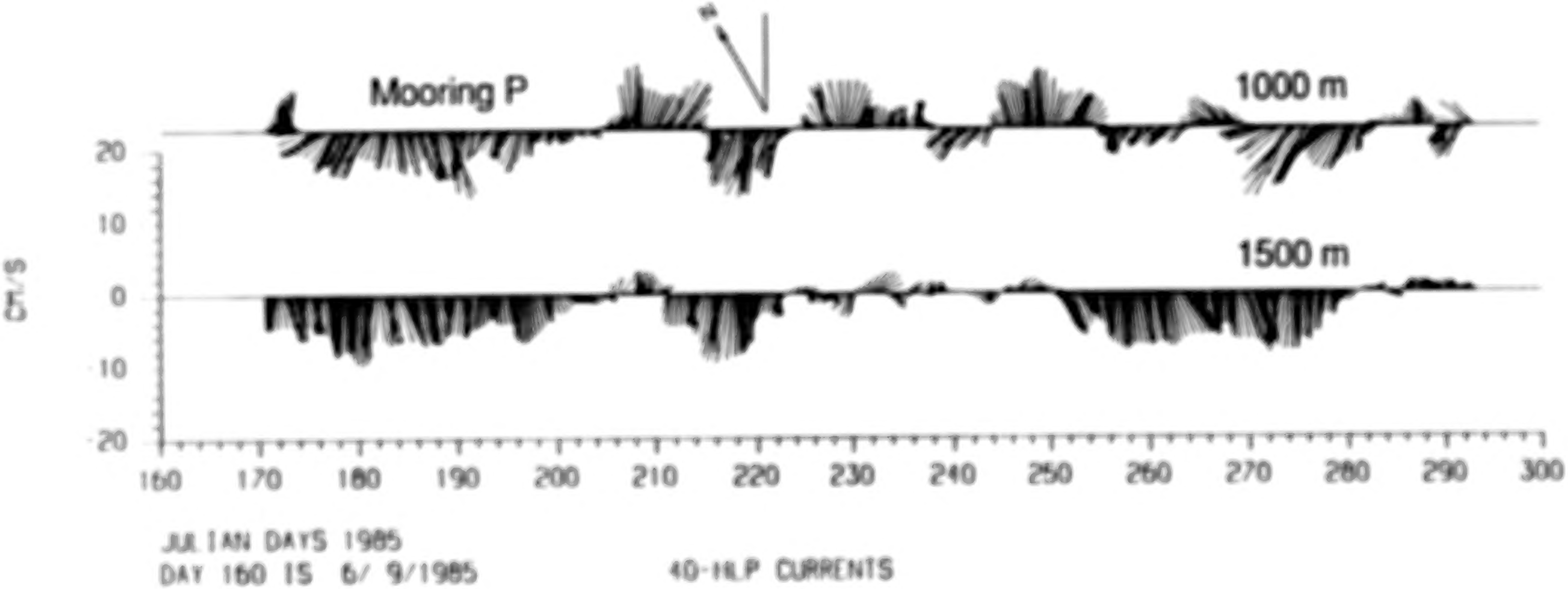

Figure 4.3-26. Stick plots of 40-hour, low-passed currents at Mooring P for the first deployment period. Vertically up (+V) is towards 30°.

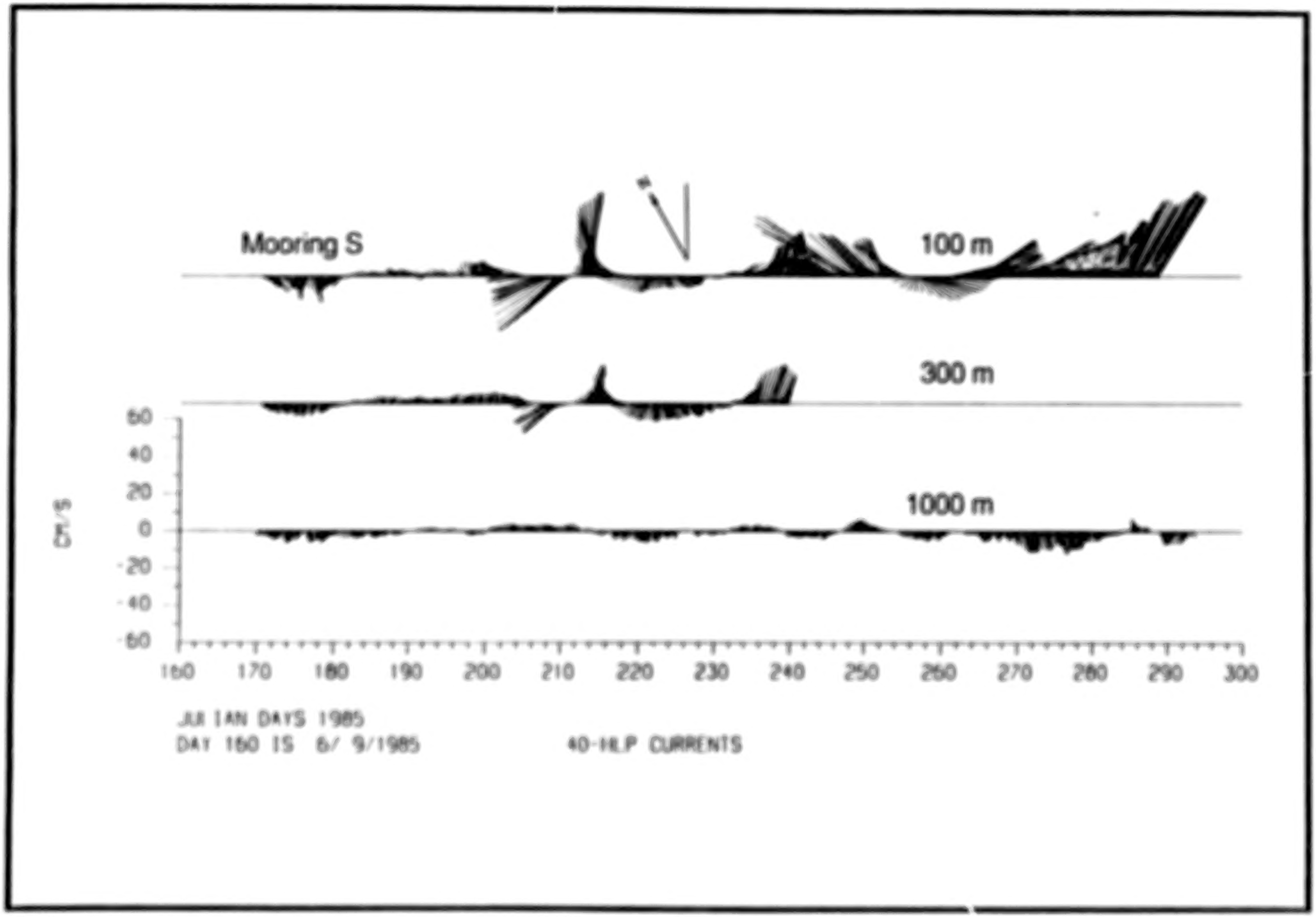

Figure 4.3-27. Stick plots of 40-hour, low-passed currents at Mooring S for the first deployment period. Vertically up (+V) is towards 30°.

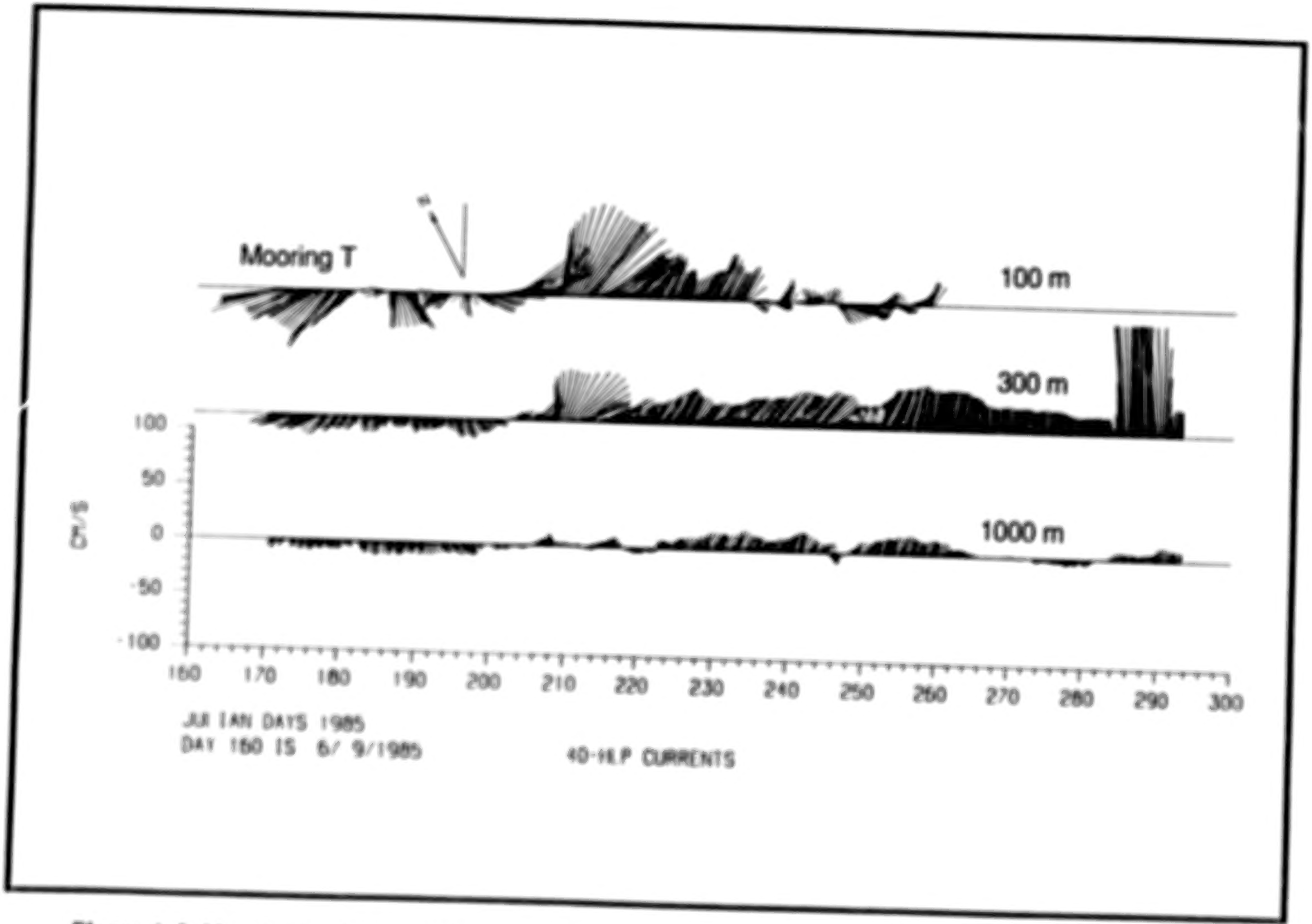

Figure 4.3-28. Stick plots of 40-hour, low-passed currents at Mooring T for the first deployment period. Vertically up (+V) is towards 30°.

parameters are even more uniform. This explains the vertical uniformity of the currents below 1400m in Figure 4.3-19 (p. 91); the indicated velocities are essentially the barotropic component. Since the barotropic velocity must be uniform with depth, it extends all the way to the surface. Therefore, it is a component of velocities at 100 and 300m, as can be illustrated by considering the velocity vector at 300m on Mooring R at the end of the record (Figure 4.3-19). This vector is plotted on the map of the topography of the 8°C temperature surface (Figure 4.2-3, p. 53). The vector is not tangent to the circumference of the eddy, and its magnitude is only about 20 cm sec^{-1}, but the topography of a temperature surface is related only to the baroclinic component of flow. The current meter velocity includes both components. Isolating the baroclinic part is possible by subtracting the velocity measured at 1500m (Figure 4.3-29). The result is a vector that is more closely tangent to the circumference of the eddy and has a greater magnitude. At the distance from the center of Eddy B at which Mooring R is located, Figure 4.3-18 (p. 89) indicates a geostrophic (baroclinic) speed at 300m relative to 950m of about 30 cm sec^{-1}.

Mooring Q was located in 3000m of water at the foot of the continental slope. Its composite record (Figure 4.3-25) shows the same type of division between upper and lower layer flow as that of Mooring R. Velocities at 100m at the end of August approach 65 cm sec^{-1} and are caused by a cold-core cyclonic eddy that will be described below. Velocities at 1000m and 1500m are quite similar; the differences are attributable to small baroclinic effects at 1000m. There are two major flow events in the lower layer. One occurs in early August and the other at the beginning of October. Maximum speeds at 1500m during the first event are about 25 cm sec^{-1}. Since it is barotropic, this value extends all the way to the near bottom. Revelation of the magnitude of the barotropic flow events in the deep portions of the western Gulf is a major result of this study. Such large speeds have significant implications for biological and geological processes in the Gulf's basin and for the distribution of both sediments and certain species of bottom life (Pequegnat, 1972).

At Mooring P, located on the continental slope in 2000m of water, velocities at 1000m and 1500m (Figure 4.3-26) are similar but not as much as at Moorings Q and R. Maximum speeds are about 10 cm sec^{-1} in both records at Mooring P (40-hour, low-pass filtered data only). The difference between the velocities at P and Q is striking because they are only about 25 km apart.

Mooring S was located in 1500m of water on a small ridge which causes the local 2000m isobath to deviate from the regional trend. The velocity at 1000m (Figure 4.3-27) is weaker than that at Mooring P much of the time, and maximum values are only about 10 cm sec^{-1}. The reason for the small amplitudes of the low frequency fluctuations at 500m above the bottom at Moorings P and Q is not understood. In the upper layer, at 100m, maximum values exceed 60 cm sec^{-1}. The direction of the vectors slowly goes through several partial and full rotations. The pattern of velocity vectors suggests that an eddy may have moved by the mooring as described below.

The strongest velocities of all were recorded at Mooring T (Figure 4.3-28), which was located in 2200m of water. Maximum speeds exceed 90 cm sec^{-1} at 100m. At 1000m, which is 1200m above the bottom, maximum speeds approach 20 cm sec^{-1}. Current velocities at all three depths are similar in direction but decrease in magnitude with depth. This type of vertical velocity shear

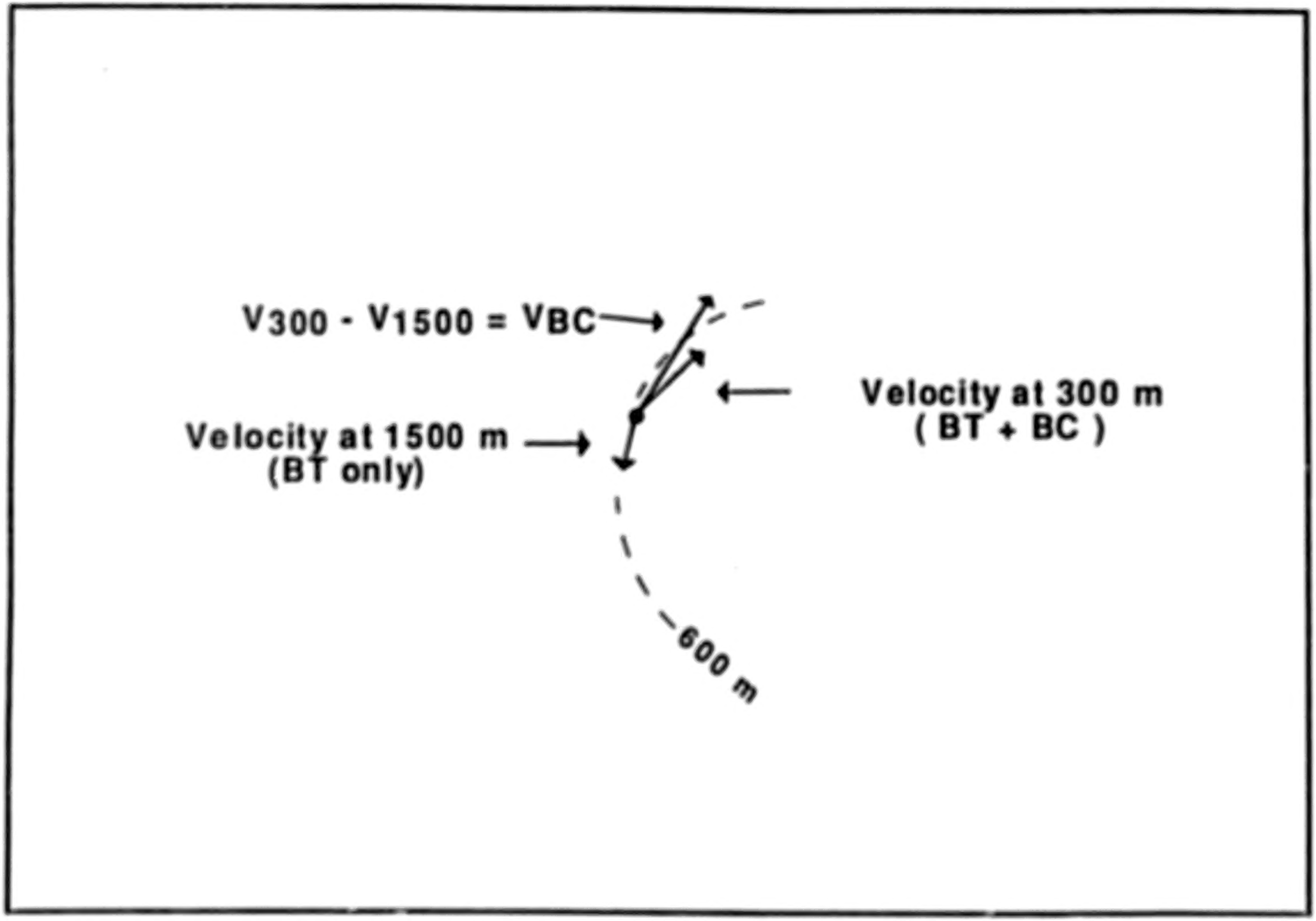

Figure 4.3-29. Illustration of the vector subtraction of observed velocity on October 17 at Mooring B at 1500m. This is assumed to be barotropic (BT) from the observed velocity at 300m, which contains both baroclinic (BC) and barotropic components. Result is a vector of just the baroclinic component, and it is more nearly tangent to the circumference of Eddy B as depicted by the partial 600m contour of the depth of the 8°C temperature surface taken from Figure 4.2-3. Magnitude of the resultant is about 30 cm sec^{-1}, which agrees with the geostrophically computed value.

suggests the presence of strong baroclinicity such as may be expected with an eddy.

Although in general it is difficult to infer unambiguously the nature of an eddy event with only four velocity vectors, it is possible to analyze the one that occurred in August because the center passed through the middle of the mooring array. The velocity vectors at 100m on August 15 are plotted in Figure 4.3-30, and a stream function pattern consistent with the vectors is subjectively drawn around them. The flow is obviously consistent with the presence of a strong cyclone. The temperature records from the current meters at Moorings S and Q (Figures 4.3-31 and 4.3-32) support this conclusion. For Mooring S at 100m, temperatures are cool at the beginning of August (Day 213). They rise slowly until Day 247 and then drop. At Mooring Q temperatures are warm initially but show a cool fluctuation between Days 234 and 250. The conclusion is that the cyclone moved northeastward across Mooring S to Mooring Q and then moved back towards Mooring S. It appears that this August event is the same cyclone identified in the October XBT data (Figures 4.2-3, p. 53, and 4.3-24, p. 102, and Section 4.3.5, p. 101). It would also appear, therefore, that the anticyclone south of this cyclone was the cause of the strong currents at Mooring T.

A characteristic feature of many of the time-series records of current velocity is the presence of energetic bursts of oscillations with a near-inertial period, near 24 hours at this latitude. Figure 4.3-33, from Mooring P at 1000m, shows an example. The light lines in the center panels are the 3-hour, low-pass filtered data. The oscillations have an amplitude of about 10 cm sec^{-1}, which is the same order of magnitude as the amplitude of the low-frequency component. Rotary spectra (Section 4.3.5.3.2, p. 119) demonstrate that the oscillations have a clockwise sense of rotation and, therefore, appear to be inertial. Their cause, that is to say, what "triggers" or initiates these currents, is unknown.

4.3.5.2 Statistical Characteristics of the Velocity Field

The basic statistics for all of the time series data of the first deployment period are listed in Table 4.3-3. They quantify some of the features already discussed and provide additional insight into the location and persistence of a pair of features (an anticyclone and cyclone). To show the mean values, the currents are plotted in vector form in Figure 4.3-34. Consider an imaginary line running from a point between Moorings S and T to a point between Moorings Q and R. At 100m, the pattern of the vectors suggests anticyclonic mean flow south of the line and cyclonic mean flow north of it. The mean-flow pattern together with the analysis of the currents in August (Figure 4.3-30) and the XBT data at the end of the deployment period support a conclusion that the anticyclone and cyclone pair were the principal forcing factors in the region of the mooring array during the first deployment period. Since there were strong frontal zones between this pair and around its periphery, small changes in position caused abrupt changes in current velocity when such fronts were near the locations of moorings. However, the mean positions were apparently fairly stable.

The mean vectors in the lower layer are also shown in Figure 4.3-34. Even at the 1000m level, the vectors at Moorings T and R suggest the clockwise influence of the north side of an anticyclone. At Moorings P, Q and S, however, the means are weaker and allow no facile interpretation. The vectors

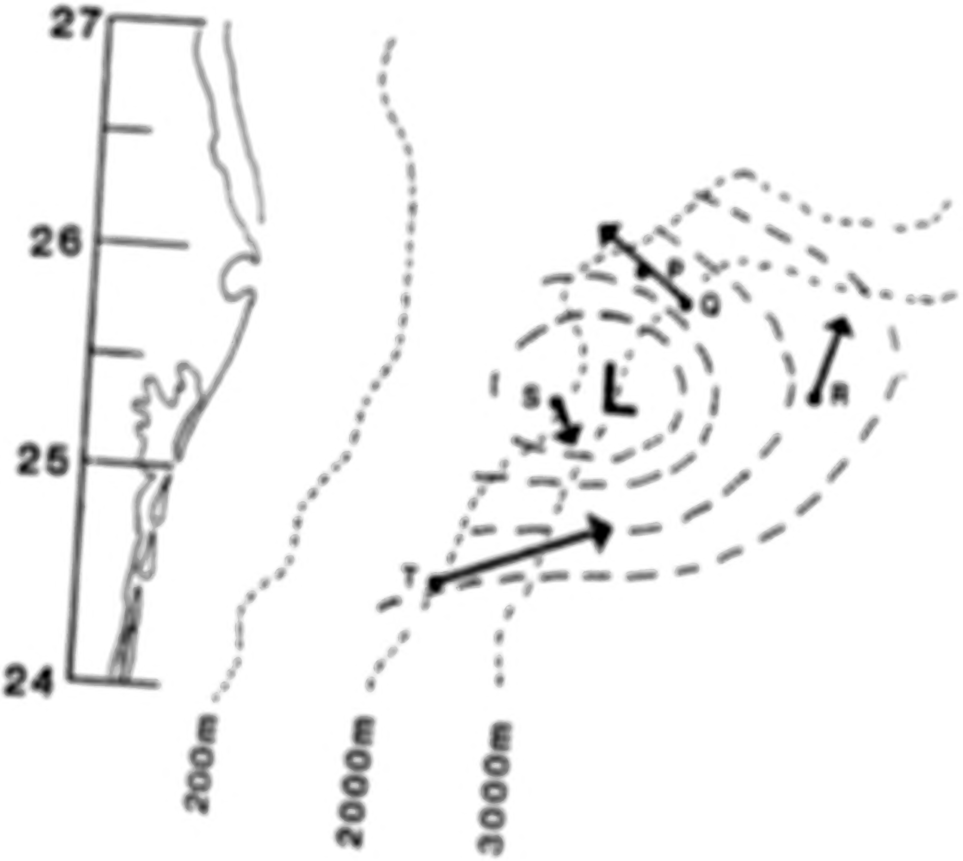

Figure 4.3-30. A subjectively drawn stream function field that is consistent with the pattern of observed currents at 100m on August 15, 1985.

BLANK

PAGE

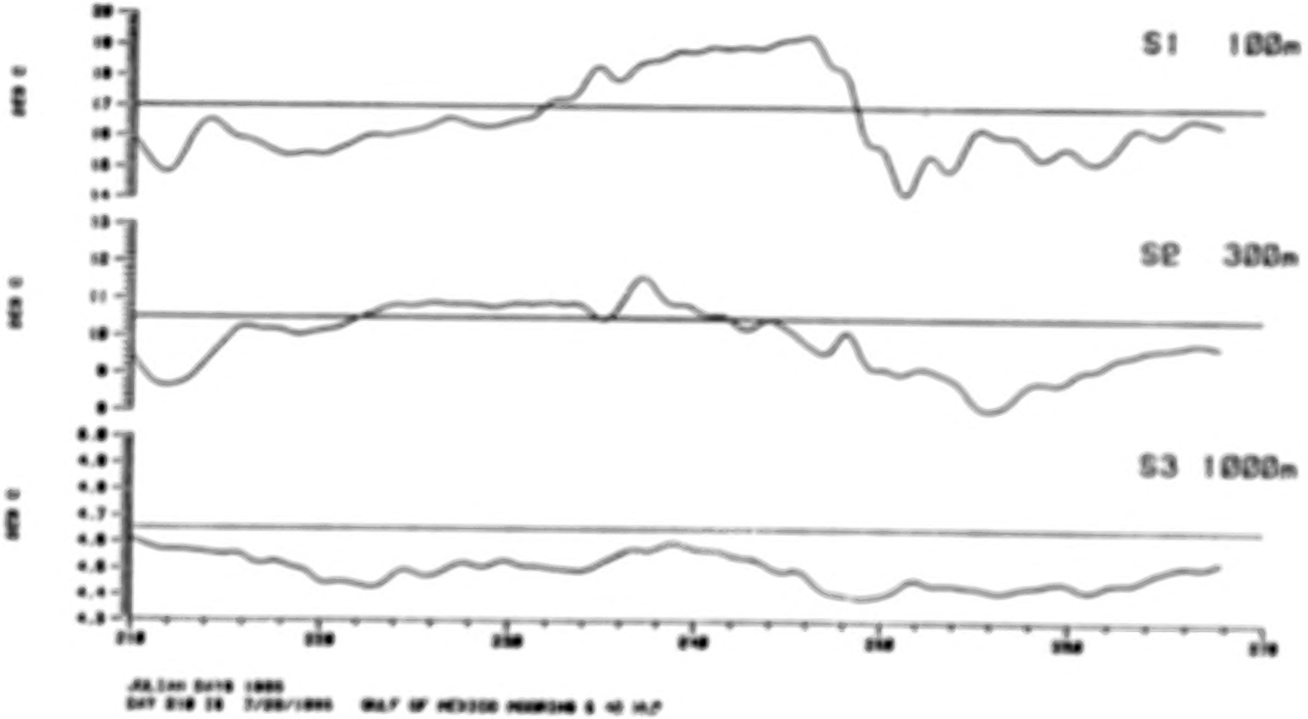

Figure 4.3-31. Forty-hour, low-passed temperature series at Mooring S from July 28 through September 27, 1985 (Days 210-270).

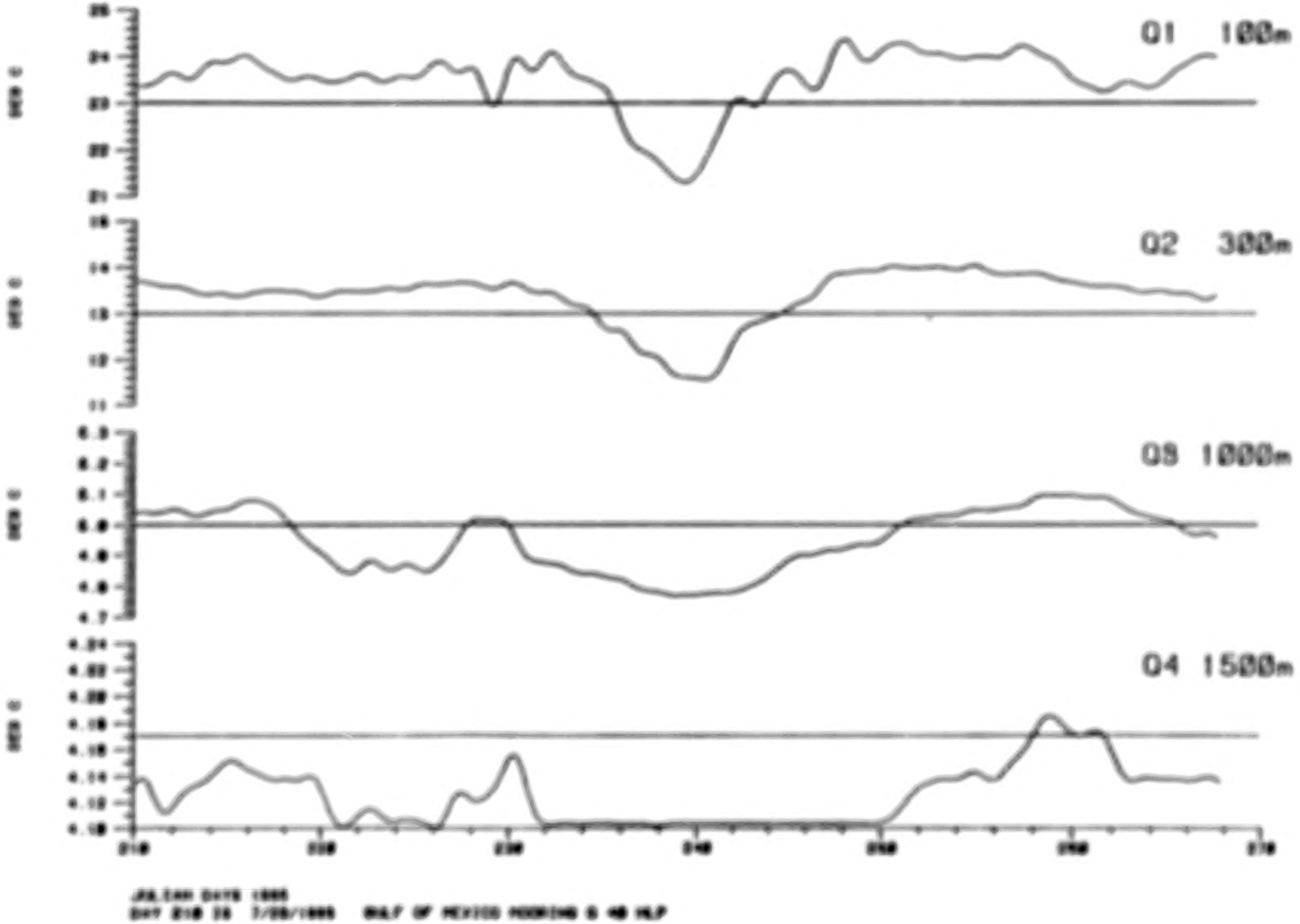

Figure 4.3-32. Forty-hour, low-passed temperature series at Mooring Q from July 28 through September 27, 1985 (Days 210-270).

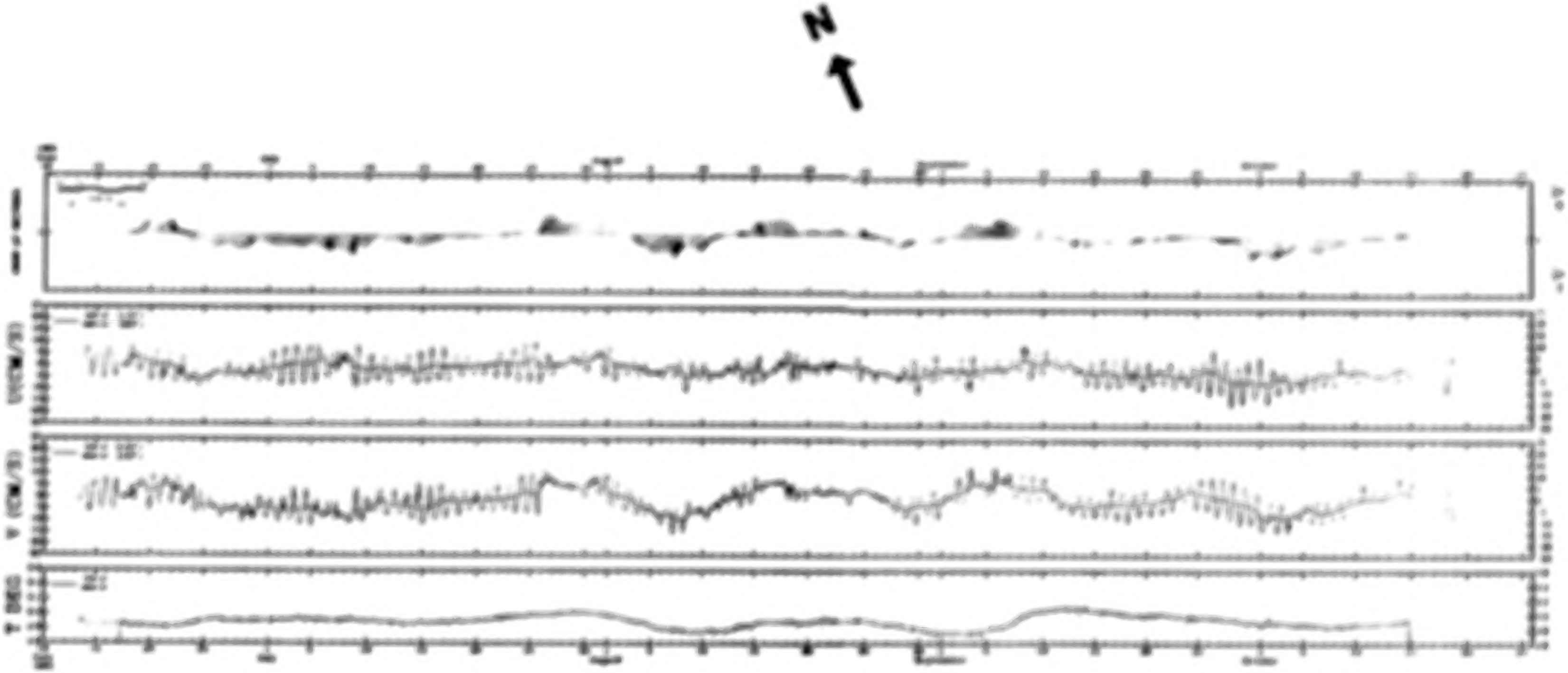

Figure 4.3-33. Time-series plots of 40-hour, low-passed stick vectors, and 3-hour (light line) and 40-hour (heavy line), low-passed U and V components and temperature for the first deployment period at Mooring P at 1000m. Vertically up (+V) is toward 30°.

METER ID	DEPTH(M) WATER DEPTH	DIRECTION OF V-COMPONENT	VARIABLE U,V (CM/S) T: (C),P:(DB)	MAXIMUM (3-HLP)	MINIMUM (3-HLP)	MEAN	VARIANCE <X'**2>(ETC) (3-HLP)	VARIANCE <X'**2>(ETC) (40-HLP)	RATIO 40-HLP 3-HLP (%)	ORIENTATION OF PRINCIPAL AXIS (DEGREES TRUE)
MOP2	300	30	U	15.2	-14.2	-.12	61.53	5.26	100	62.6
	2000		V	13.1	-20.6	-5.61	76.25	8.23		
			T	15.94	14.51	14.998	.027	.003		
MOP3	1000	30	U	10.2	-16.2	-.84	17.68	4.84	478	42.8
			V	13.8	-15.7	-.54	27.86	16.55		
			T	5.10	4.70	4.910	.027	.007		
MOP4	1500	30	U	6.4	-5.8	.61	3.84	1.90	795	32.8
			V	6.6	-10.6	-3.46	11.57	10.19		
			T	4.30	4.14	4.165	.000	.000		
MOQ1	150	30	U	32.5	-63.0	-0.47	467.45	451.48	945	127.8
	2000		V	64.1	-33.3	6.80	154.83	136.84		
			T	24.64	23.86	23.245	.518	.472		
MOQ2	300	30	U	17.8	-44.2	-3.94	126.61	113.73	884	107.5
			V	27.5	-15.1	4.26	74.62	63.22		
			T	14.36	11.22	13.549	.307	.285		
MOQ3	1000	30	U	8.2	-12.6	.29	16.18	15.19	937	54.6
			V	16.8	-24.6	.16	38.21	34.66		
			T	5.12	4.79	4.926	.008	.007		
MOQ4	1500	30	U	16.2	-18.0	-1.38	27.68	27.25	1.000	62.2
			V	15.0	-16.8	-1.48	58.84	59.33		
			T	4.31	4.09	4.125	.000	.000		
MOR1	150	30	U	38.6	-19.8	4.84	103.67	95.33	835	105.4
	2500		V	30.5	-12.2	4.00	44.97	33.83		
			T	18.76	15.75	17.778	.383	.179		
MOR2	300	30	U	22.6	-11.5	5.22	53.77	47.09	819	100.7
			V	18.1	-10.5	3.28	27.45	19.37		
			T	12.46	10.42	11.393	.142	.117		
MOR3	1000	30	U	22.4	-9.8	3.15	45.45	35.88	847	118.8
			V	11.9	-10.1	.77	11.74	8.53		
			T	4.96	4.46	4.609	.016	.016		
MOR4	1500	30	U	20.5	-9.8	3.28	50.22	46.62	935	115.8
			V	12.6	-10.7	.07	16.72	10.46		
			T	4.33	4.14	4.253	.000	.000		
MOR5	2000	30	U	21.8	-11.1	1.67	53.45	48.85	930	114.0
			V	14.6	-9.7	.26	16.58	16.73		
			T	4.32	4.21	4.219	.000	.000		
MOS1	150	30	U	46.0	-62.0	-.84	362.80	325.07	899	117.5
	1563		V	48.7	-33.1	5.03	161.81	147.59		
			T	19.89	14.08	17.456	2.485	2.465		
*MOS2	300	30	U	16.1	-36.8	-.82	45.34	38.54	850	63.5
			V	28.3	-31.6	1.26	63.22	53.76		
			T	12.44	7.96	10.636	1.273	1.251		
MOS3	1000	30	U	8.4	-10.0	-.76	6.75	2.88	587	33.3
	1538		V	10.3	-16.6	-1.27	14.05	9.35		
			T	4.77	4.16	4.549	.027	.027		
*MOT1	150	30	U	82.4	-96.5	12.93	1050.66	928.12	842	78.4
	2200		V	65.5	-61.6	8.64	911.67	725.75		
			T	30.28	13.71	26.499	3.983	1.774		
MOT2	300	30	U	53.6	38.8	10.77	109.38	886.00	926	64.8
			V	70.1	-51.6	16.28	342.23	330.84		
			T	18.80	12.83	16.587	.897	.856		
MOT3	1000	30	U	19.8	-17.8	4.08	32.48	18.40	771	48.2
			V	26.8	-17.6	1.26	79.21	49.85		
			T	5.58	4.74	5.097	.058	.048		

* - SHORT RECORD

Table 4.3-2. Basic statistics of the U and V components of current and temperature over the available record lengths at Moorings P, Q, R, S and T for the first deployment period: June 17, 1985 through October 20, 1985.

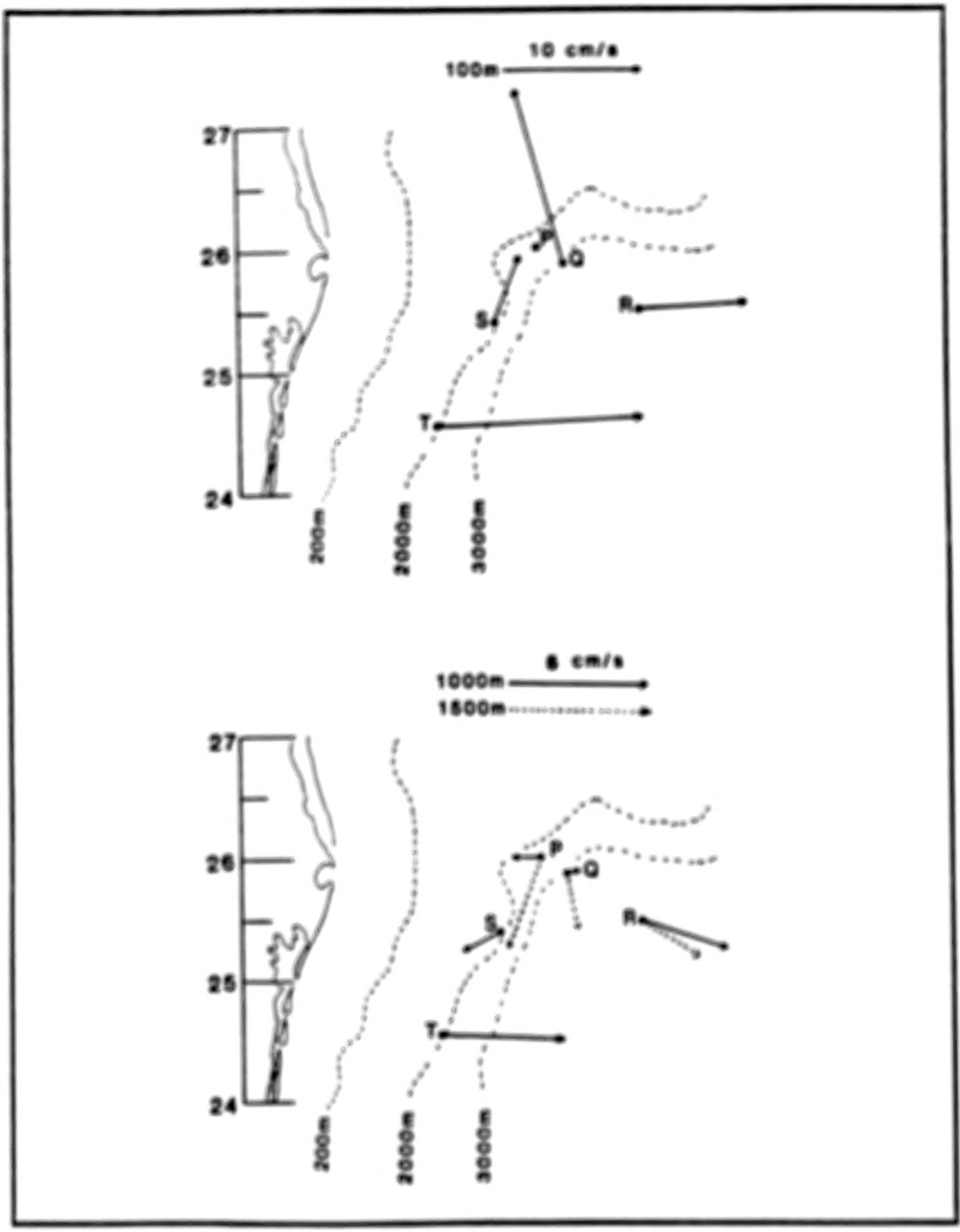

Figure 4.3-34. Mean values, over the record length, of velocity presented in vector form for the first deployment period: June 17 through October 20, 1985.

at 1500m at Moorings P and Q are actually larger than their counterparts at 1000m, and their direction suggests topographic steering.

In the lower layer, the relative variances of the U and V components as well as the orientation of the principal axes at Moorings P, Q, S and T also demonstrate topographic steering. The variances of the along-isobath components (V) are uniformly at least double those of the U components. At Mooring P it is more like five times. (The greater the difference, the more rectilinear the flow fluctuations). The reverse is true at Mooring R at all depths and at all the other moorings in the upper layer. Thus, these flow fluctuations are oriented more perpendicularly to the adjacent isobaths. As the principal axes indicate, the upper flow fluctuations are more perpendicular at Moorings Q and S than at Mooring T. Also note that the variance is greatest at Mooring T. As with the component means, the variances imply that, on the average, Moorings Q and T lay to the north and south, respectively, of the center of a cyclone, and Mooring T lay in the northwest part of an anticyclone.

The ratio of 40-hour, low-pass to 3-hour, low-pass kinetic energy showed a minimum near 1000m. At Moorings P and S at 1000m it is about 0.5. Spectral analyses (Section 4.3.5.3, p. 110) show that at periods shorter than 40 hours, inertial oscillations account for most of the energy.

The variance of temperature is quite small except at Moorings S and T at 100m. The mean temperature at 100m at Mooring T is 28.5°C, which indicates the instrument was just above the top of the thermocline, that is, in the base of the mixed layer. At Mooring S the mean temperature at 100m is 17.4°C, which places the instrument in the main thermocline. At these two instrument locations, the temperature variance is relatively large due primarily to horizontal fluctuations in the position of the frontal zone between the two eddies.

4.3.5.3 Frequency Domain Description

The moored array of this experiment was designed to form an "antenna" that would detect the structure and nature of the flow field in an eddy encountering topography and that might detect the wave energy dispersing from it. The preceding sections related the position and movement of the eddies to events in the time-series records and to the basic statistics of the flow field. The present section examines more quantitatively the fluctuating nature of the current and temperature fields.

The principal mechanisms that are expected to influence spectral characteristics of the current/temperature data are due directly to eddies or are triggered by them. An eddy begins to lose its shape and high current speeds by dispersion of planetary Rossby waves (beta effect), by frictional dissipation and under certain conditions by inertial, baroclinic or barotropic instability mechanisms. The dispersive process is enhanced when an eddy encounters shoaling topography and when an eddy becomes weak and small. The process is retarded by non-linearity, such as occurs when an eddy is large and strong or when it is tightly coupled to an oppositely signed eddy in a vortex pair. Eddy dispersion produces smaller wave "packets," which themselves may resemble smaller eddies of alternating rotation sense. The rich eddy structure evident in this study shows that the western Gulf is an area of active eddy dispersion. It is difficult to estimate the time and space scales of current fluctuations associated with eddy dispersion over the continental slope, but linear calculations suggest 10-20 days and 100 km as typical values for Loop Current eddies.

Over topography, eddies can excite topographic Rossby waves. These Rossby waves do not depend on gravity for their existence, so their most visible manifestations are horizontal current patterns. Their characteristic time and length scales can be from a few days to weeks and hundreds to thousands of kilometers. Because of their long wavelengths and the distributed effects of forcing, topographic Rossby waves often have a "signature" that includes selective responses in certain frequency bands, but with inconclusive or confusing evidence of phase propagation.

The response to abrupt forcing by movement of frontal zones will also include waves of near-inertial frequency which in the northwestern Gulf have periods of about one day. Inertial wave energy will propagate vertically and horizontally away from the forcing region, spreading the current response over a wide area.

Unusually intense storms can have an influence on the currents in the slope region. The most obvious instance is the response to a hurricane (Brooks, 1983). However, only one such vigorous surface forcing occurred, and that was during the beginning of the second deployment period. Hurricane Juan was small and passed well to the east of Mooring Q, the easternmost mooring of the second period. Strong cold fronts passing over the Gulf ("blue northers") can also produce significant currents by direct forcing and by breaking down density stratification. As noted above, the winter of 1985-1986 was relatively mild, and hydrographic data for the upper layer indicate that during this study the net effect of wind stirring was relatively weak. Tidal currents are primarily diurnal and weak (<5 cm sec^{-1}) in the western Gulf. Wind and tide forcing are not considered in the subsequent analyses.

Major events in the observed currents are due to the movement of eddies. The events take place over weeks and are aperiodic and thus appear in the frequency domain as very low frequency and very broad-banded energy. Therefore, energy spectra exhibit generally "red" backgrounds in which the energy level increases with decreasing frequency. The more periodic waves of planetary and topographic dispersion and possible instability processes are superposed on this background variance.

4.3.5.3.1 Autospectra

The present material examines characteristics of the Eulerian current field prior to the arrival of the primary eddy. Mesoscale features which may be in or close to the instrument mooring array have been discussed in previous sections of this report. Because spectral analysis looks for regular and periodic signals, current patterns dominated by moving, evolving and rotating circulation patterns do not always lend themselves to spectral decomposition. In the presentation below, key or major features of spectra are enumerated with causative explanations where they are apparent.

In the upper layer at Mooring R, the spectral variance (and therefore the kinetic energy) of the U and V components (Figure 4.3-35a, b) drops by three orders of magnitude between the longest resolvable period and a period of 2 days (0.5 cycles per day). Near the local inertial period, which is nearly diurnal in the study area, the variance rises two orders of magnitude above the background level. Between periods of 2 and 10 days there are relative

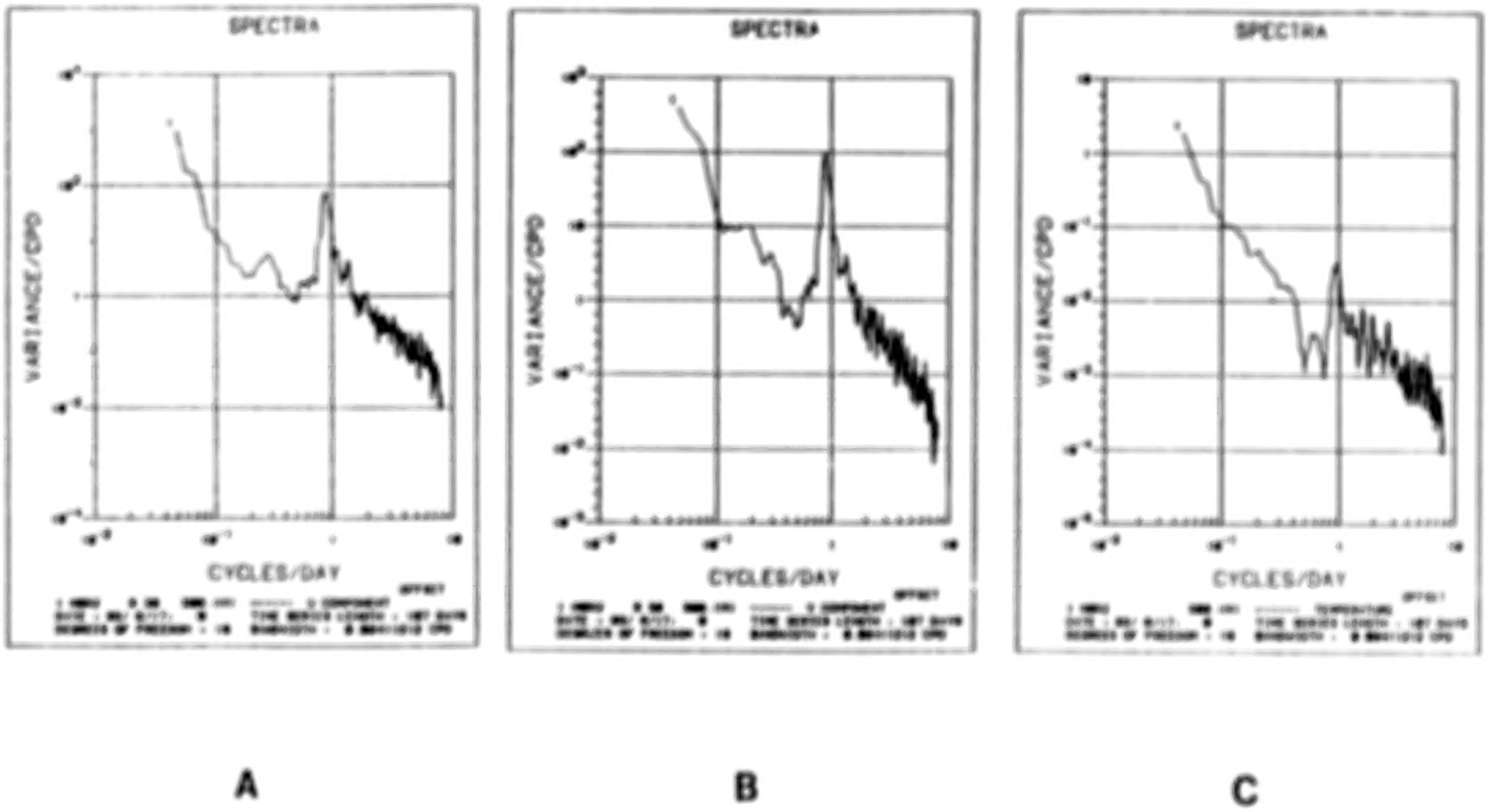

Figure 4.3-35. Spectra for Mooring R at 300m: (a) U velocity component, (b) V velocity component and (c) temperature for the 107-day period beginning June 17, 1985.

maxima and plateaus, the most prominent being near 3 days (0.33 cycles per day), that are one order of magnitude weaker than the inertial maximum. Temperature variance (Figure 4.3-35c) has a similar pattern, but with less synoptic-period structure and a less pronounced inertial maximum.

The spectral characteristics of the lower layer currents (1500m) at Mooring R (Figures 4.3-36a and b) are similar to those in the upper layer, but are weaker by an order of magnitude. The 3-day peak (0.33 cycles per day) is prominent for the U component, and inertial energy is relatively high for both components but not as markedly as in the upper layer. Temperature variance (Figure 4.3-36c) is lower by two orders but has the same form and also a peak at 3 days.

At 100m on Mooring Q (in the bottom of the mixed layer), variance of all three parameters (Figure 4.3-37a-c) decreases almost linearly by three orders of magnitude, and there is little structure in the synoptic band of 2-10 days which indicates little wind forcing. At 1000m, the spectra of the U and V components (Figures 4.3-38a and b) show a minor peak at 3 days. The components and the temperature spectra (Figure 4.3-38c) have a "red" background variance and high inertial energy.

The autospectra of the U and V components of current and temperature at Moorings P, S and T are similar in form and magnitude to those at Moorings Q and R at a given depth. Therefore, figures showing these autospectra are omitted, but their characteristics are described briefly.

At 1000m at Mooring P, the inertial peak of the U component exceeds the variance at the long period end of the spectrum; for the V component, the inertial peak is equally pronounced. The temperature spectrum is basically "red" with an identifiable but not strong inertial peak.

The U and V components at Mooring S have three principal features: a "red" low frequency end, strong inertial energy and a small peak between 2.5 and 3 days. Energy at the lower level is generally an order of magnitude smaller than the upper level but as much as two orders of magnitude at periods longer than 10 days for the U component. Temperature spectra for the two levels have identical form but differ by two orders of magnitude.

The autospectrum for the U component at Mooring T has a significant peak near a period of 5 days (0.2 cycles per day), superposed on a "red" background. The peak is not evident at 1000m or in the V components. The temperature spectrum for 100m has a large inertial peak that extends two decades above the background. At all three levels there are several peaks in temperature variance between 5 days and the diurnal period.

In summary, the pattern of the autospectra of the velocity components and temperature at all depths in the receiving field is a "red" spectrum that decreases by three orders of magnitude from the longest period to a period of about 2 days and then rises by one to two orders of magnitude approaching the inertial (diurnal) period. In the synoptic band, 3-10 days, low energy peaks are superposed on the "red" background, the one at 3-5 days being most prevalent. The high energy of the currents near the diurnal period has a clockwise sense of rotation that is characteristic of inertial oscillations.

BLANK

PAGE

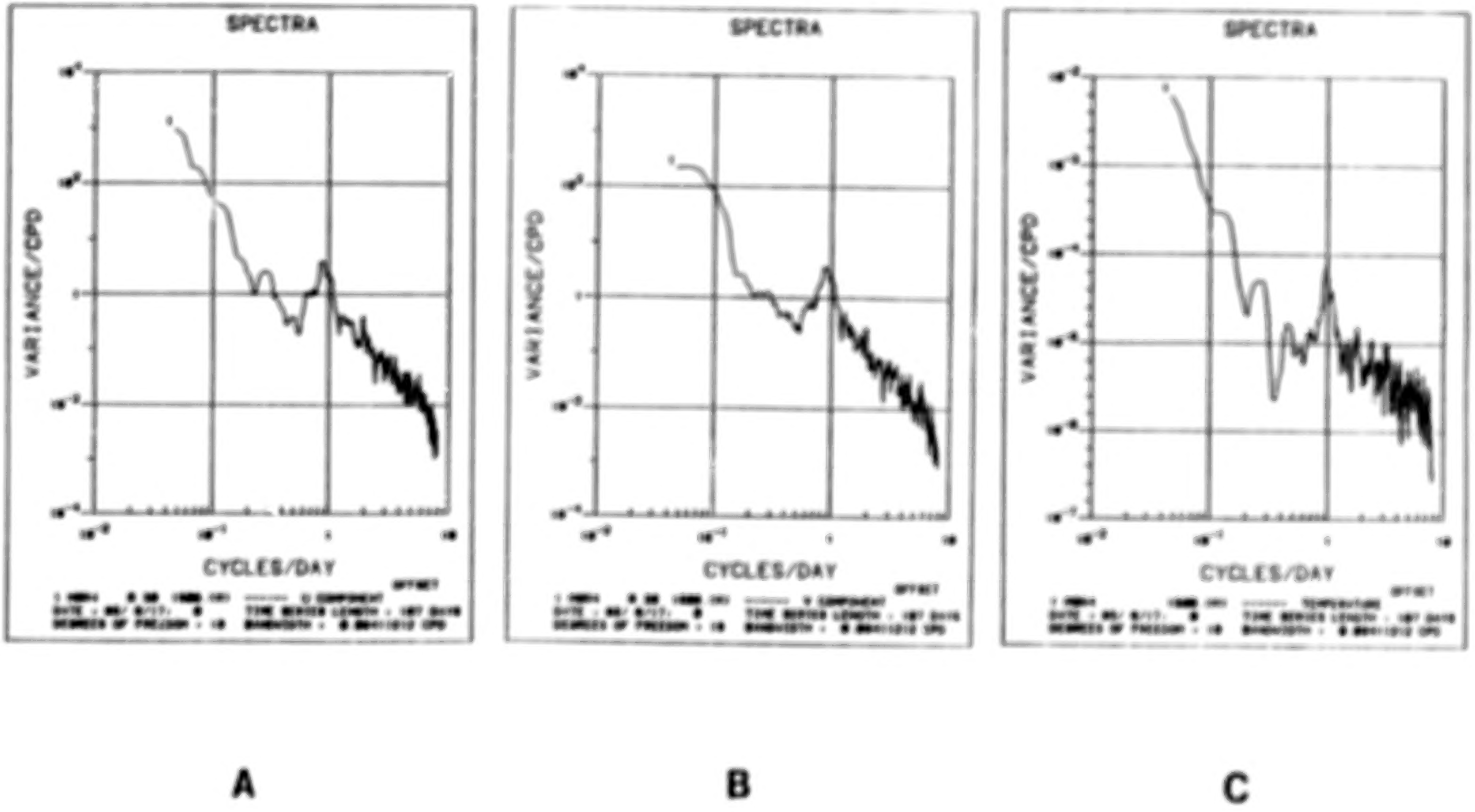

Figure 4.3-36. Spectra for Mooring R at 1500m: (a) U velocity component, (b) V velocity component and (c) temperature for the 107-day period beginning June 17, 1985.

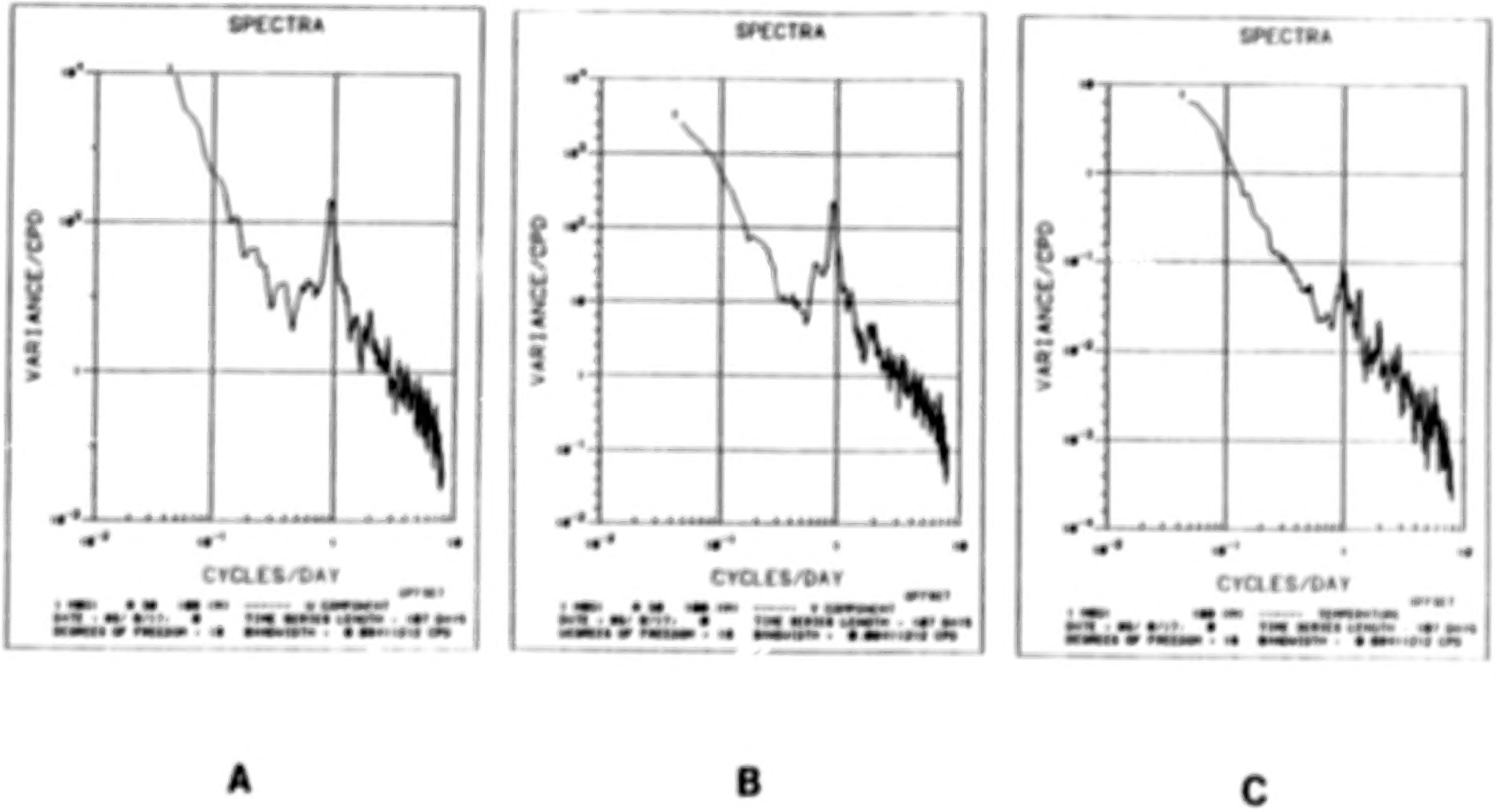

Figure 4.3-37. Spectra for Mooring Q at 100m: (a) U velocity component, (b) V velocity component and (c) temperature for the 107-day period beginning June 17, 1985.

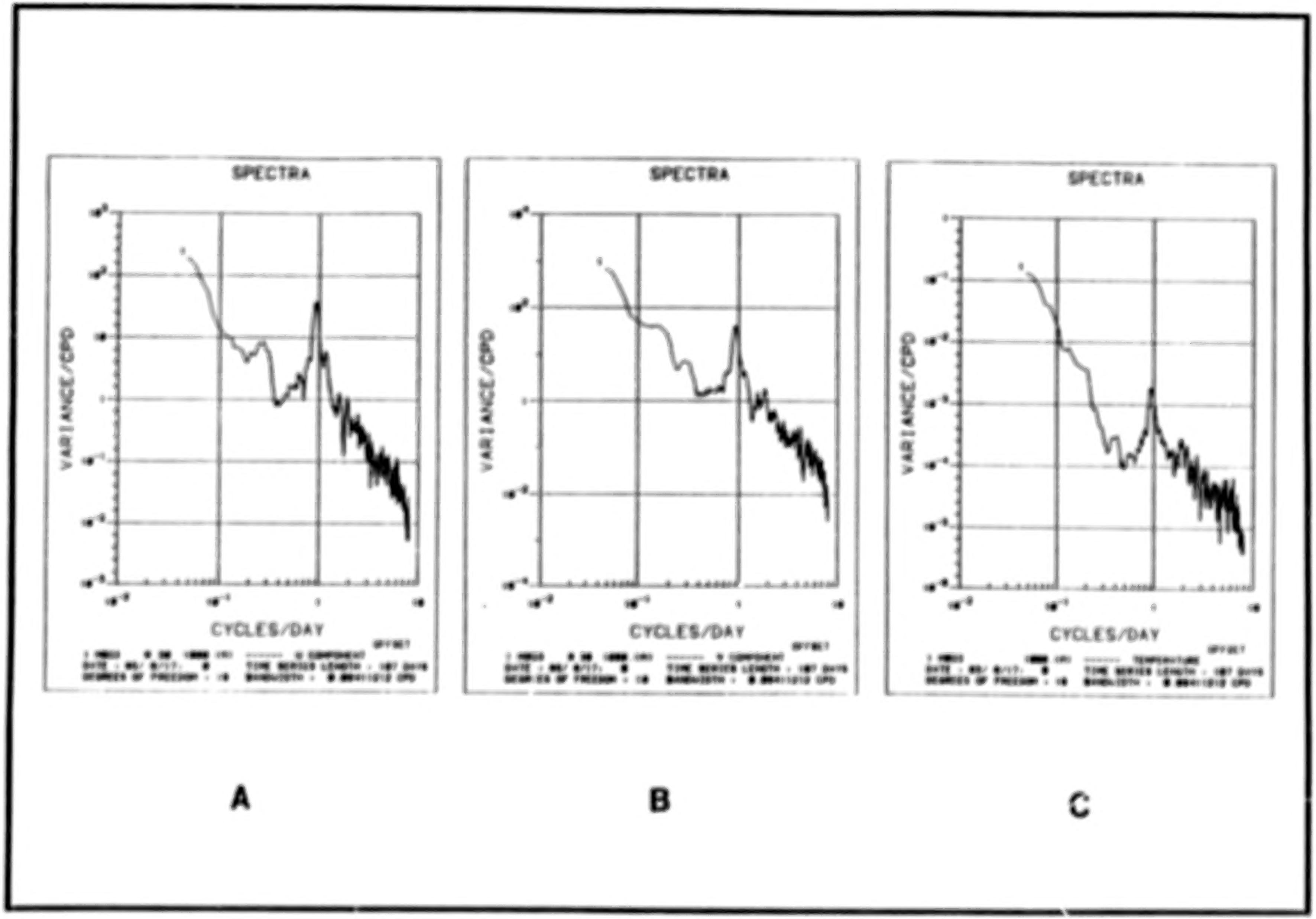

Figure 4.3-38. Spectra for Mooring Q at 1000m: (a) U velocity component, (b) V velocity component and (c) temperature for the 107-day period beginning June 17, 1985.

4.3.5.3.2 Rotary Spectra

The rotary analysis technique decomposes the vector currents into components that rotate counterclockwise (CCW, solid or heavy line) and those components that rotate clockwise (CW, light or dashed line). The relative intensity of the two spectrum components indicates the polarization of the current fluctuations as a function of frequency. For example, circularly-polarized currents would exhibit all their energy in either the CCW or CW component, whereas linearly-polarized currents would have equal energy in the CCW and CW components. Intermediate cases indicate elliptic polarization. A purely inertial motion would exhibit circular polarization (CW in the Northern Hemisphere).

Figure 4.3-39 shows the rotary spectra for current velocity at Mooring P at 1000m, of which the U and V components show very high variance near the inertial period. The rotary spectra demonstrate that all the near-diurnal energy is CW and thus inertial. Also note that at periods longer than 5 days (0.2 cycles per day), rectilinear motion is indicated by the equality of the CW and CCW rotary components.

Figure 4.3-40 shows the rotary spectra for Moorings S and T at 1000m for periods longer than 2 days (0.5 cycles per day). For Mooring S the motion is elliptical, CCW at periods longer than 10 days (0.1 cycles per day) and CW at shorter periods. For Mooring T this division occurs at 40 days (0.025 cycles per day). At periods shorter than this, CW flow dominates except near 10 days and 4 days where the CCW spectrum has distinct peaks.

4.3.5.3.3 Vertical and Horizontal Coherence

Phase and coherence squared (hereafter referred to simply as coherence) were computed for a large number of pairs of parameters for the longest common period, 99 days, beginning June 21, 1985. Vertical coherence was examined within the upper and lower layers and between layers, and horizontal coherence was examined between moorings within each layer. Selected plots of the results are presented. The term "upper layer" refers to the water column from about mid-thermocline down to a depth of about 1000m where density contrasts become small (Figure 4.3-16, p. 87). "Lower layer" refers to the portion of the water column from 1000m to the bottom. In the upper layer, only Moorings Q and R have data common to the 99-day period which can be used to compute coherence within the layer and between the moorings. There are no upper layer data at Mooring P, and the records from 300m at Mooring S and from 100m at Mooring T are too short. In addition, the data from 100m at Moorings S and T are probably too shallow to be considered part of the upper layer as defined above. In Section 4.3.5.2 (p. 110), it was concluded on the basis of the variance of temperature that the instruments at 100m on Moorings S and T were located in the bottom of the mixed layer or the top of the thermocline. In the lower layer, vertical coherence is examined within the layer at Moorings P, Q and R, and horizontal coherence is examined in the along- and cross-isobath directions between all moorings. The vertical coherence of temperature fluctuations is not examined in the lower layer because the fluctuations are small at 1500m and below.

The results for the various vertical pairs of parameters generally indicate that vertical coherence is high within each layer but low between them. The plots for Mooring Q (Figures 4.3-41 and 4.3-42) illustrate these conclusions. In the upper layer, between 100m and 300m, the V component is very coherent at

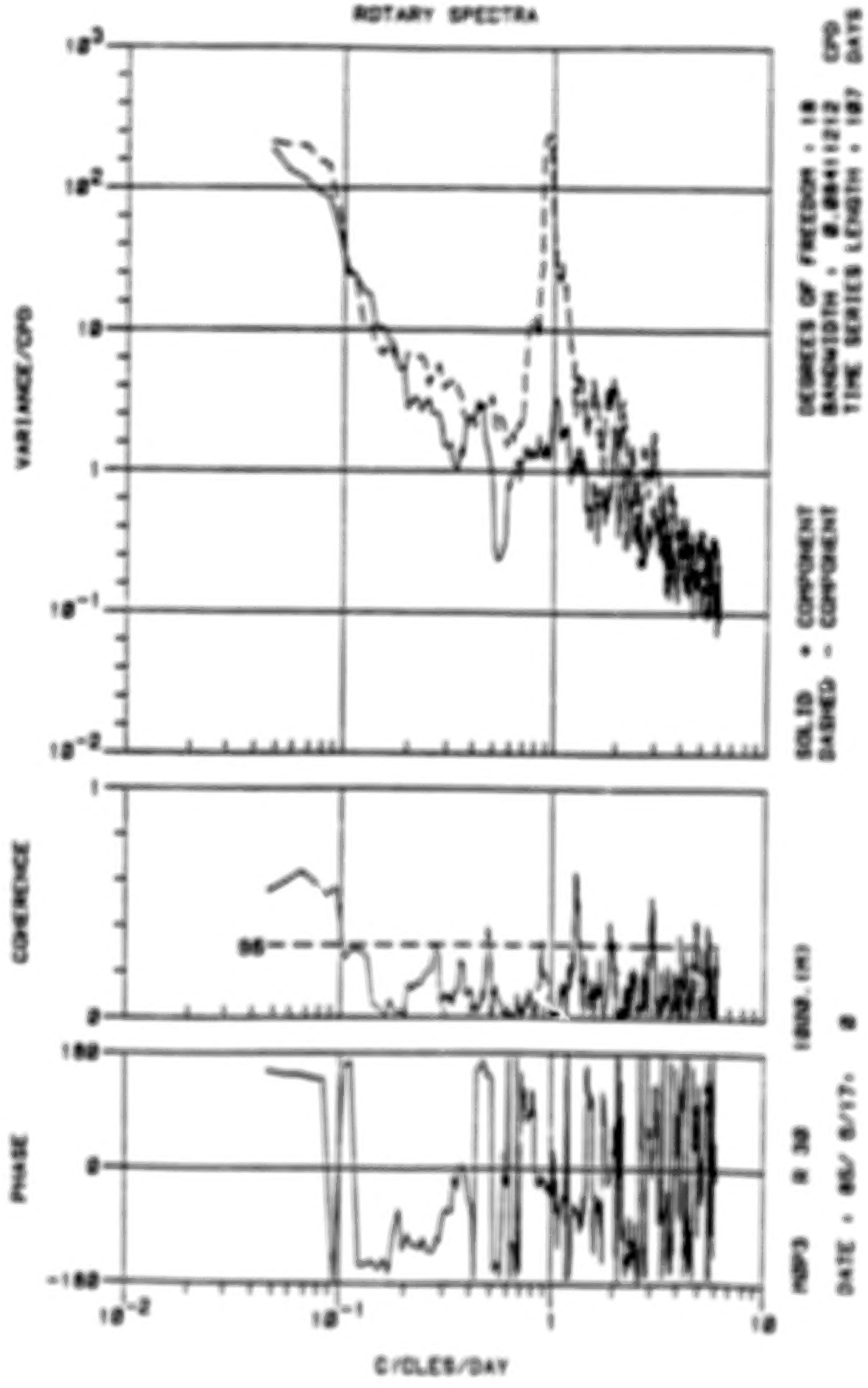

Figure 4.3-39. Rotary spectra for Mooring P at 1000m for the 107-day period beginning June 17, 1985. Dashed line is clockwise component.

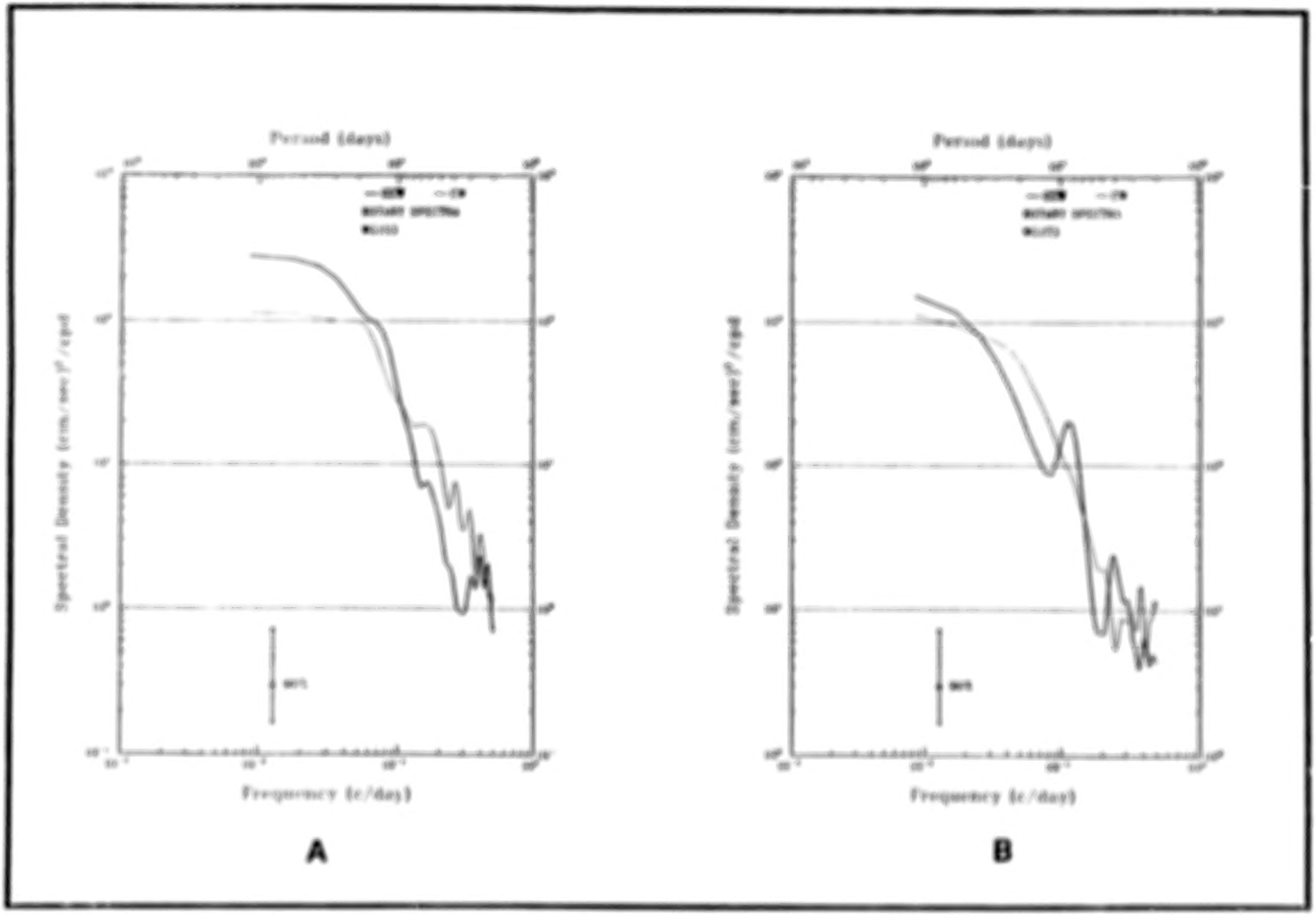

Figure 4.3-40. Rotary spectra at 1000m for the first deployment period beginning June 18, 1985 for (a) Mooring S and (b) Mooring T.

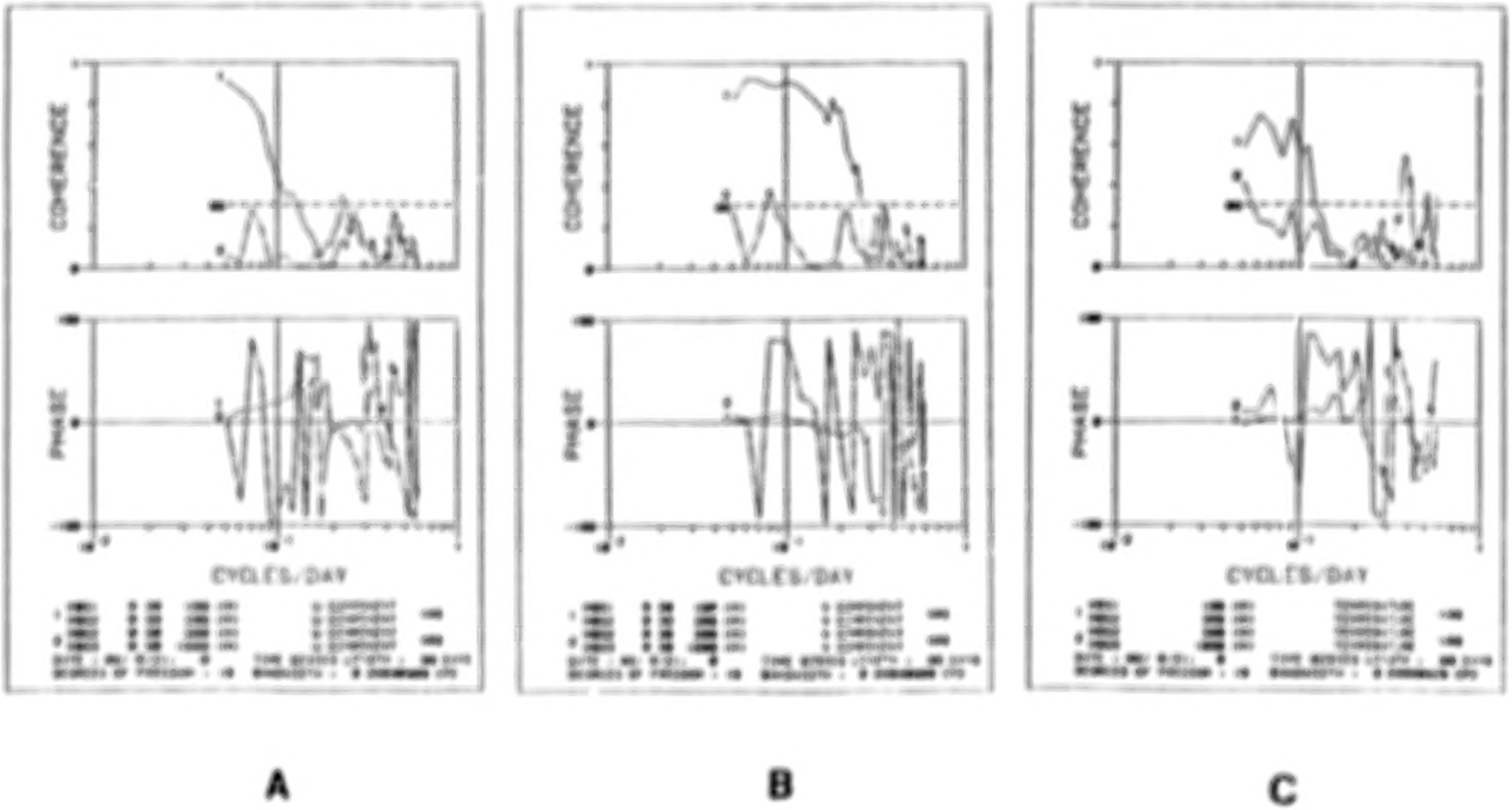

Figure 4.3-41. Vertical, cross-spectral coherence and phase at Mooring Q between 100m and 300m (solid line), and between 300m and 1000m (dashed line): (a) U components of velocity, (b) V components of velocity and (c) temperature for the 99-day period beginning June 21, 1985.

BLANK

PAGE

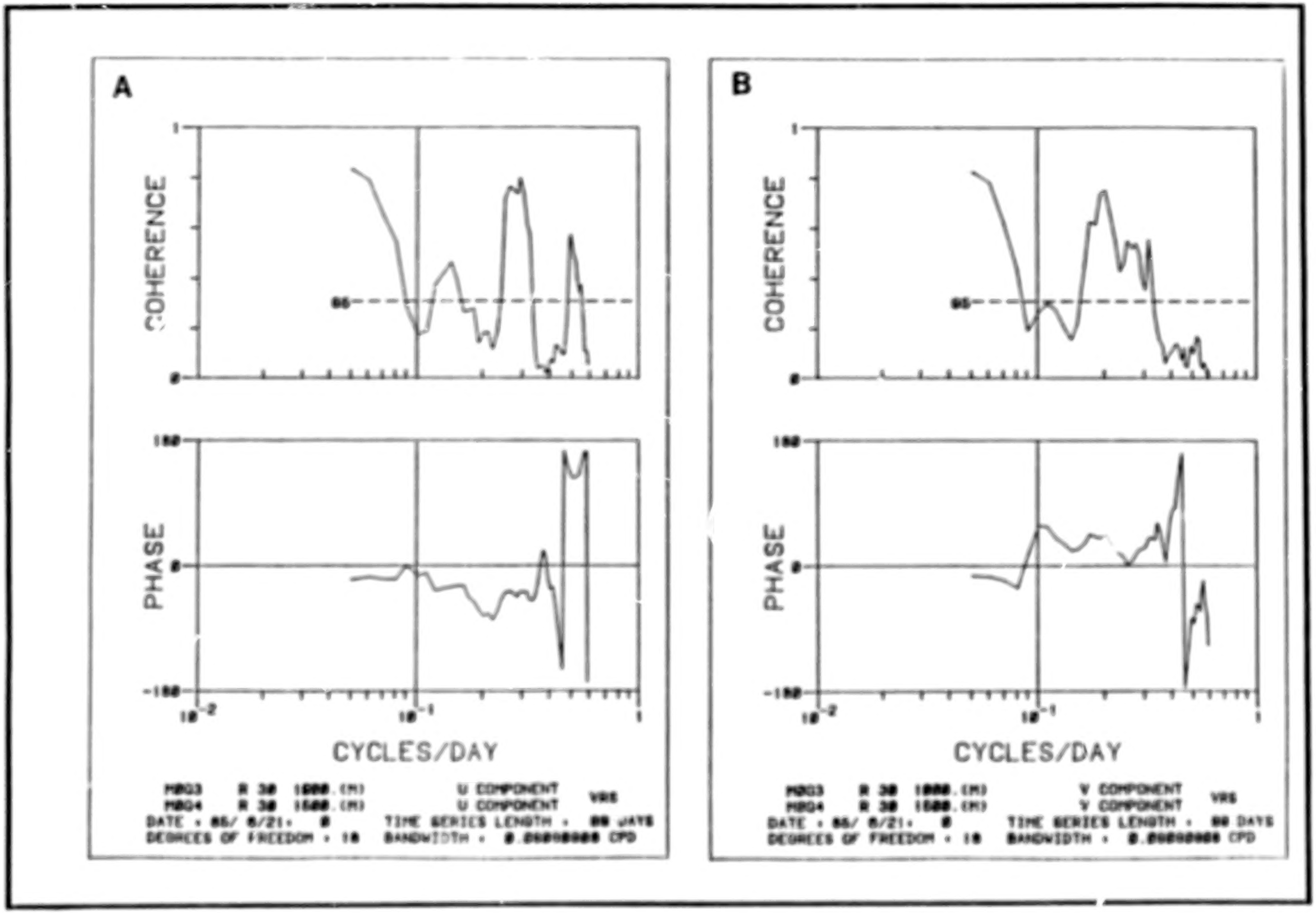

Figure 4.3-42. Vertical, cross-spectral coherence and phase at Mooring Q between 1000m and 1500m: (a) U components of velocity and (b) V components of velocity for the 99-day period beginning June 21, 1985.

periods longer than 3 days (Figure 4.3-41b, solid line), and both the U component and the temperature are coherent at periods longer than 10 days (Figures 4.3-41a and c, solid lines). For the upper layer at Mooring R, the results are similar, except that for temperature the coherence is strong only at periods longer than 12 days.

Between layers (300m to 1000m) all three parameters are incoherent at all periods at Mooring Q (Figure 4.3-41, dashed lines). The results are similar at the other moorings except for the V component at Mooring R, which is weakly coherent at periods near 10 days and longer than 12 days, and for Mooring T where the V component is coherent at periods of 6 to 8 days and temperature is coherent at periods longer than 7 days.

In the lower layer at Mooring Q (Figure 4.3-42), both components of current are strongly coherent between 1000m and 1500m at various periods between 2 and 9 days and at periods longer than 12 days. Vertical coherence of currents is similar at Mooring R between 1000m and 1500m and even stronger between 1500m and 3000m. At Mooring P, the V component is coherent between 1000m and 1500m at periods near 2 and 6 days and at greater than 12 days, while the U component is weakly coherent at periods longer that 12 days and incoherent elsewhere.

Next, horizontal coherence is summarized, starting with the cross-isobath moorings. Again, only selected plots are shown. Between Moorings Q and R at 300m, the velocity components are weakly coherent at periods longer than 12 days and temperature is incoherent. In the lower layer, at 1000m, the V component is strongly coherent between Moorings Q and R throughout the period range of 8 to 20 days, with a phase relation close to 180°, and the U component is coherent at periods longer than 12 days (Figure 4.3-43). Between Moorings P and Q at 1000m, currents are coherent only at periods of 3 to 5 days, and temperature is incoherent. This low level of coherence is surprising because Moorings P and Q are only 29 km apart. At the deeper level of 1500m, however, currents are again coherent in the 8- to 20-day range of periods (Figure 4.3-44).

In the along-isobath direction at 1000m, the U component is incoherent between Moorings P and S, but the V component is strongly coherent at periods longer than 10 days, with a small positive phase value (Figure 4.3-45). However, between Moorings S and T at 1000m, neither component is coherent. Given the strong coherence between the V components at Moorings P and Q, it was suspected that changes in the trend of the direction of the topography between Moorings Q and T, in relation to the chosen orthogonal decomposition for the U and V components, were affecting the coherence estimates. Therefore, the coherence between currents at Moorings S and T at 1000m was also investigated by the rotary cross-spectral technique for pairs of vector time-series. The results of this method (Figure 4.3-46) indicate that currents are coherent between Moorings S and T at 1000m, particularly at periods of 11 to 14 days.

Mooers (1973) described in detail this technique, which uses the rotary decomposition of horizontal velocity vectors discussed in Section 4.3.5.3.2 (p. 119). Its advantage is that coherence is invariant under a coordinate rotation. In the Cartesian representation used in the preceding analysis, the orientation of the V component was chosen to be parallel to the mean, large-scale trend of the isobaths in the study area--that is, 30° clockwise from north--and basically it was rectilinear motion that was investigated with the U-U and V-V coherences. The two other pieces of information, the U-V and V-U

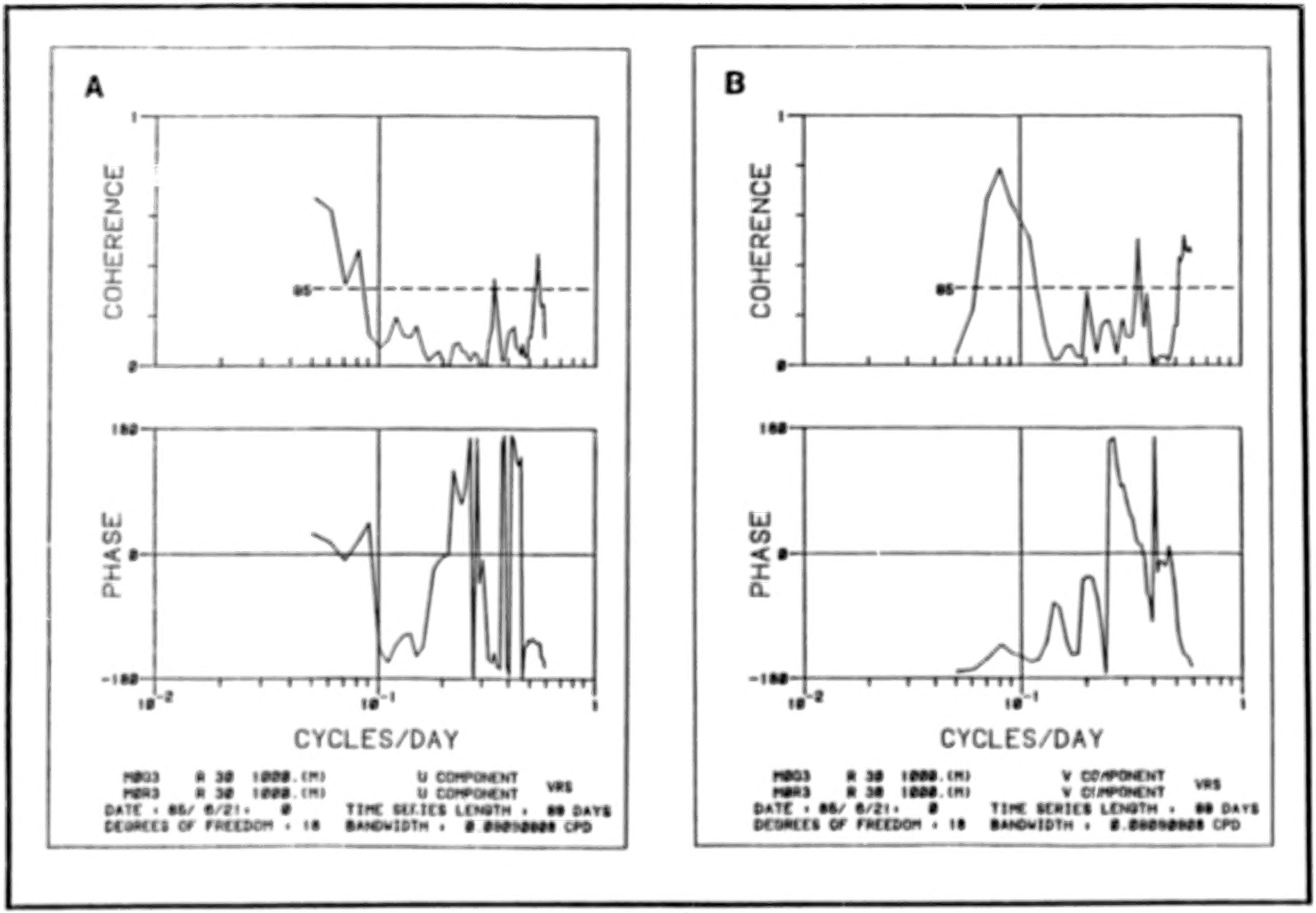

Figure 4.3-43. Horizontal, cross-spectral coherence and phase at 1000m between Moorings Q and R: (a) U component of velocity and (b) V component of velocity for the 99-day period beginning June 21, 1985.

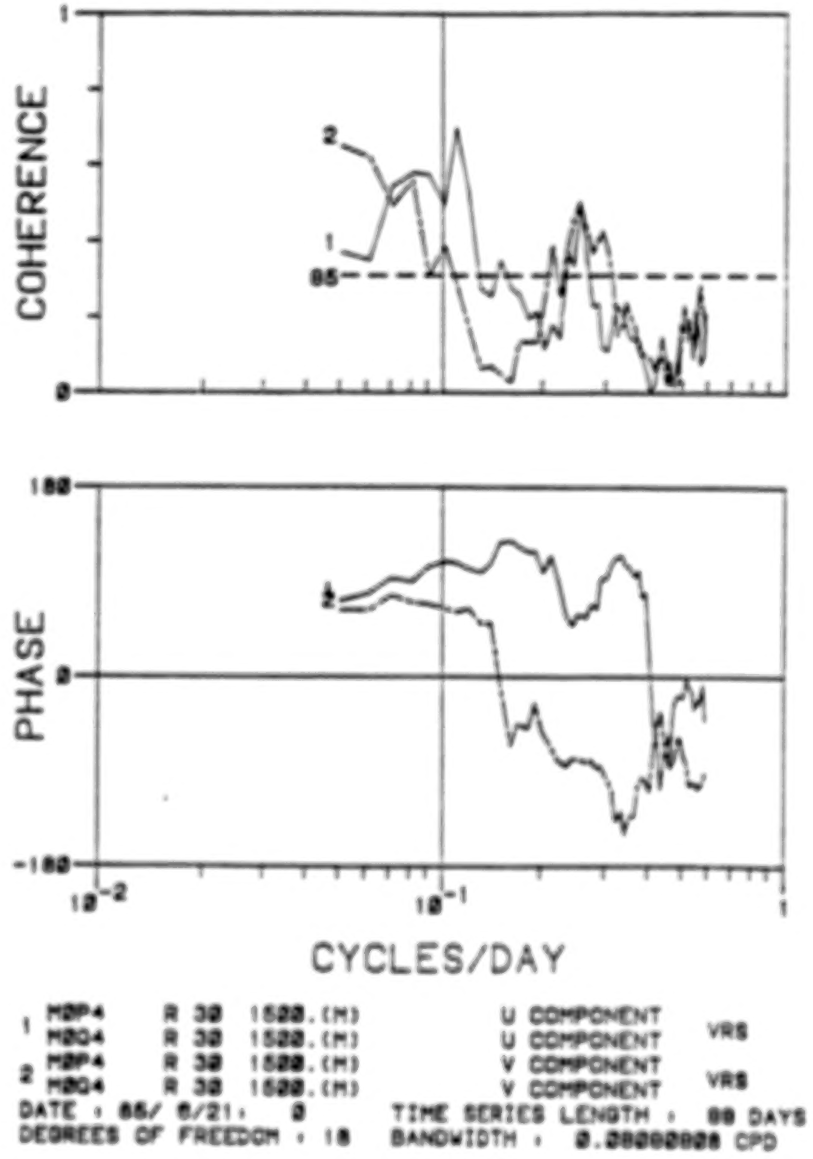

Figure 4.3-44. Horizontal, cross-spectral coherence and phase at 1500m between Moorings P and Q for U component of velocity (solid line) and V component of velocity (dashed line) for the 99-day period beginning June 21, 1985.

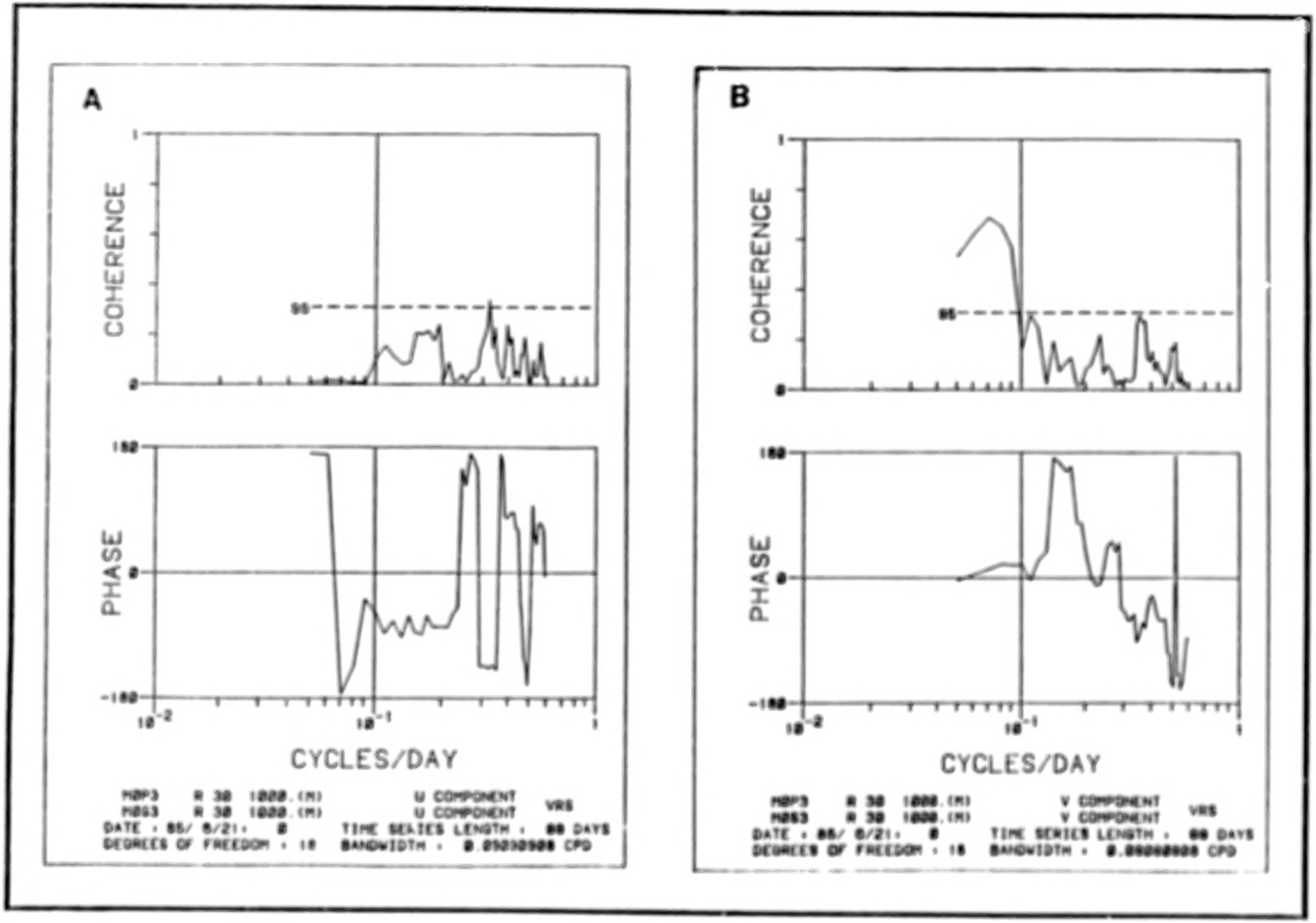

Figure 4.3-45. Horizontal, cross-spectral coherence and phase at 1000m between Moorings P and S: (a) U component of velocity and (b) V component of velocity for the 99-day period beginning June 21, 1985.

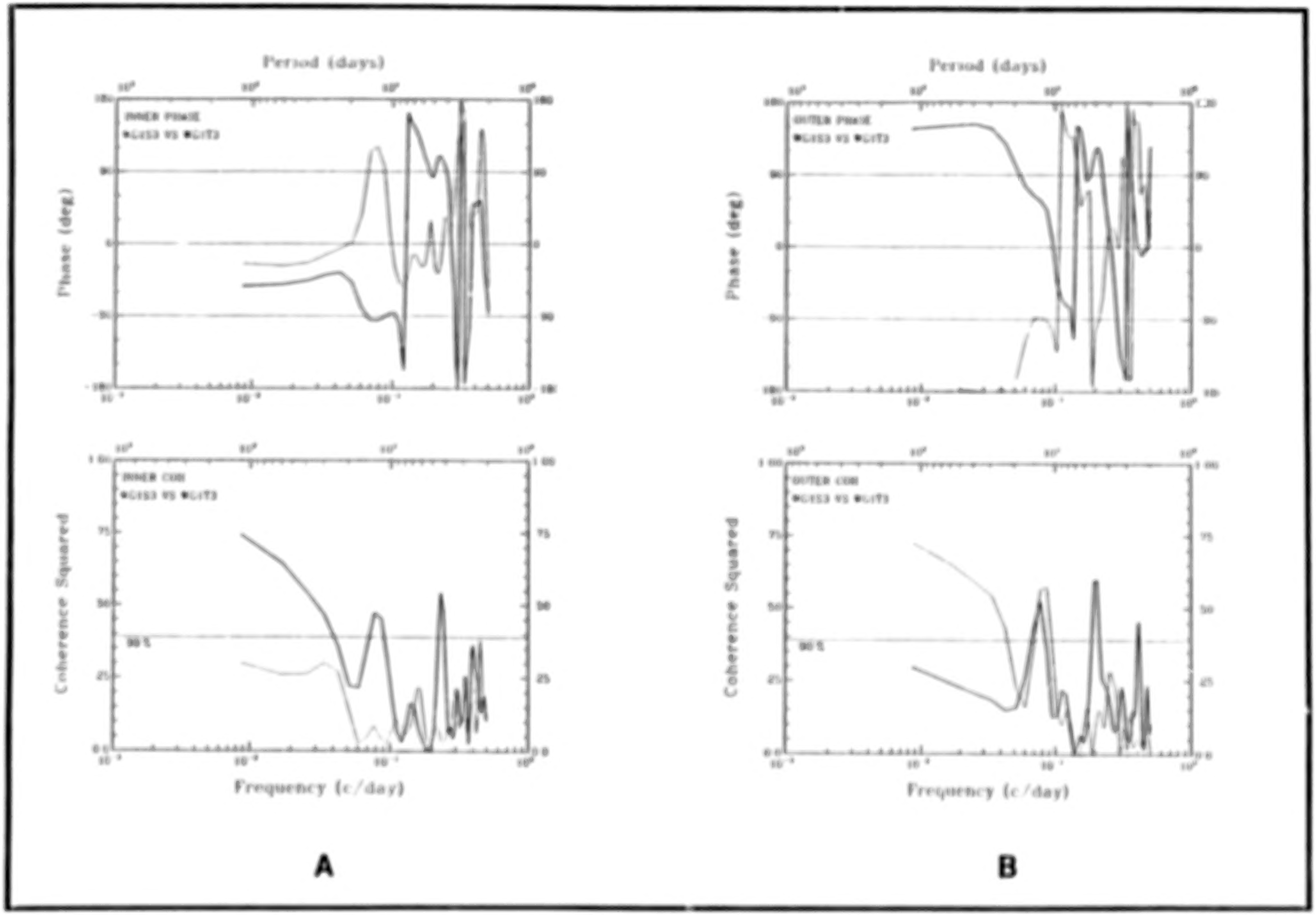

Figure 4.3-46. Rotary cross-spectral coherence and phase at 1000m between Moorings S and T: (a) inner coherence and phase and (b) outer coherence and phase. See text for explanation of rotary method.

coherences, were not discussed. The cross-rotary spectral analysis also yields four coherences: the inner coherence (actually, coherence squared) relates the co-rotating pairs--that is, clockwise with clockwise (light lines) and counterclockwise with counterclockwise (heavy lines). The outer coherence relates the counter-rotating pairs--that is, counterclockwise of the first with clockwise of the second (light lines) and vice-versa (heavy lines). (Positive phase means the first series leads the second series).

The rotary results indicate there is inner coherence (Figure 4.3-46a), at the 90% significance level between the CCW components (heavy line) in three bands of period: 3-5 days, 11-14 days and longer than 25 days. The phases are +90°, -90° and -50°, respectively. Figure 4.3-46b indicates coherence between CCW at Mooring S and CW at Mooring T (light line) at periods of 11-14 days and longer than 25 days (phases of -90° and -180°, respectively), and between CW at Mooring S and CCW at Mooring T (heavy line) at periods of 3-5 days and 11-14 days (phases of +60° and -120°, respectively).

In summary, coherence is low between layers but high at lower frequencies within them, particularly the lower layer. The pattern of horizontal coherence is confusing. Horizontal coherence, when it exists, generally occurs at periods of 3-5 days, 10-20 days or at the longest periods of the spectrum. Coherence in the range of 10-20 days suggests topographic waves, but phase relations are complicated. Evidence of propagating topographic and planetary waves is inconclusive in the results of these analyses.

4.4 Eddy-Slope Interaction and Cyclone Intensification in the Western Gulf

4.4.1 Introduction

Sea-surface temperatures derived from analysis of satellite thermal imagery on November 19, 1985 (Figure 4.4-1) show that western portions of the Loop Current (LC)--that is, the north-south region having water temperatures greater than 26°C--had extended as far west as 90°W, and a warm ridge (W) with surface water temperatures greater than 25°C was centered around 25.5°N, 93.8°W. Analysis of the depth of the 21°C isotherm from AXBT data collected from November 11 through 13, 1985 (Figure 4.4-2b) indicates that Eddy B was a quasi-circular feature at this time and that the center of the eddy was at 24.8°N, 94.0°W, essentially in the center of the warm ridge detected in the satellite data. This is also corroborated by the position data for Drifter 3378 in November (Figure 4.4-3), showing for the most part a tight circular anticyclonic trajectory with a center of circulation around 24.8°N and 94.0°W. The analysis of the depth of the 21°C isotherm (Figure 4.4-2a) also shows an isolated region of shallow depths immediately north of Eddy B. This feature is believed to be a cyclonic eddy. In addition, other regions of shallow depth were noted in Figure 4.4-2a to the northeast, south and west of the warm eddy. The available hydrographic data, however, are not sufficient in themselves to support the notion that these features are all cyclonic perturbations.

The November 1985 sea-surface temperature analyses (Figure 4.4-1) west of 95°W revealed isotherms generally oriented northeast-southwest. The main feature was a tongue of cold water with surface temperatures less than 25°C centered at 26.0°N, 96.5°W. This region (west of 95°W) was markedly affected when Eddy B encountered the western continental slope. Previous satellite images and the drifter data suggested that an anticyclonic eddy (Eddy A) was located near 22.5°N in that region, though there was no indication of Eddy A in the

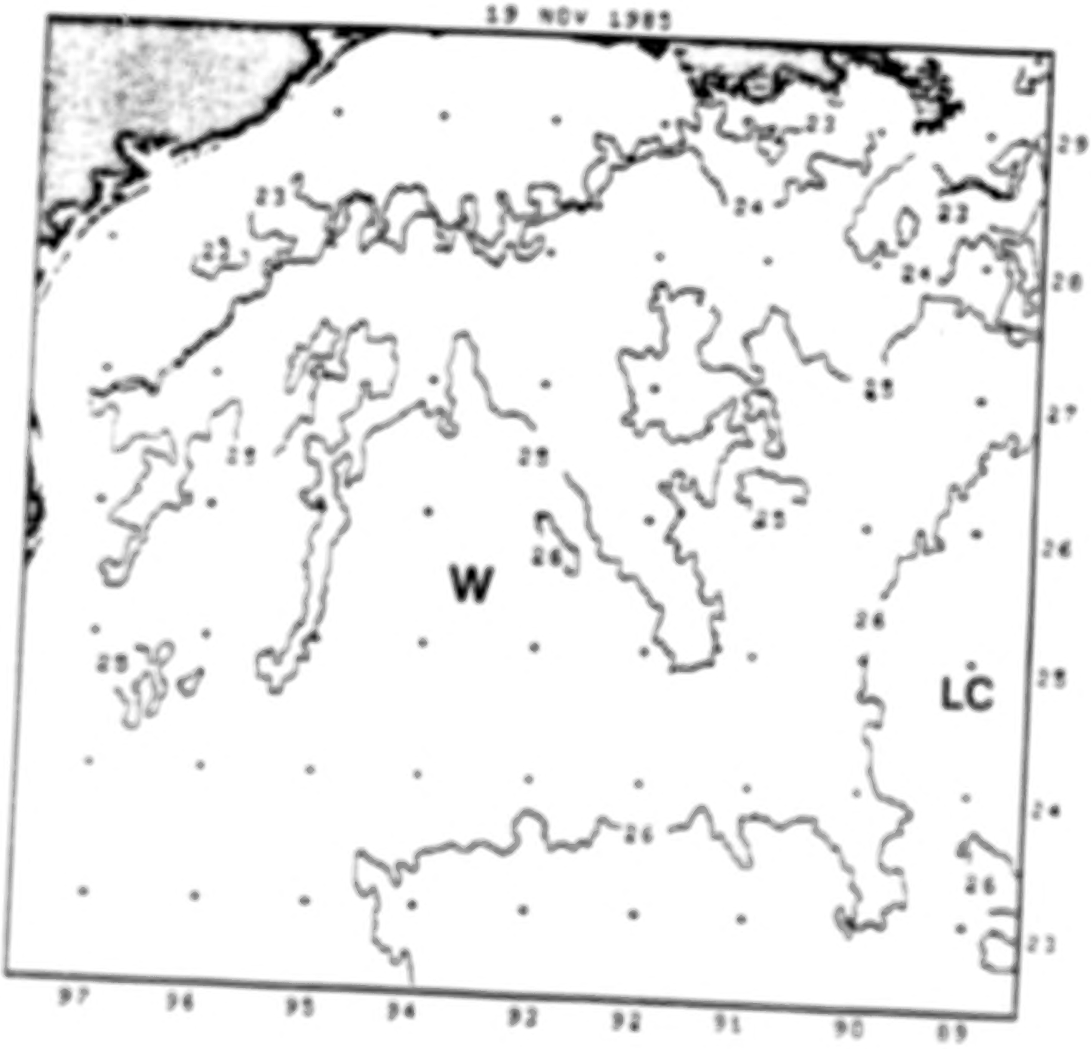

Figure 4.4-1. NOAA-9 SST (°C) analysis in the western Gulf of Mexico for November 19, 1985.

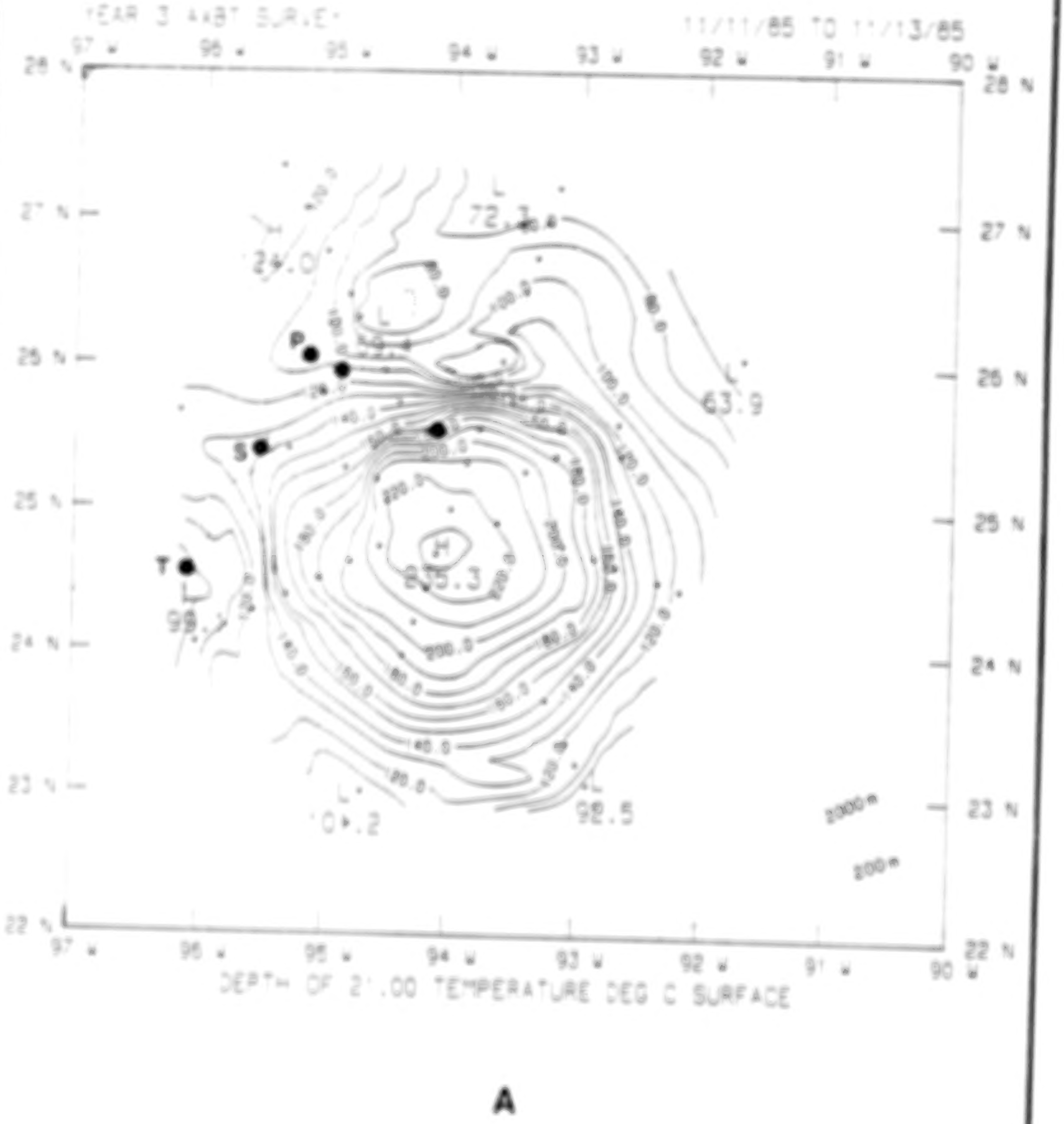

Figure 4.4-2a. Analysis of the topography (m) of the 21°C temperature surface from AXBT data collected for the period of November 11-13, 1985.

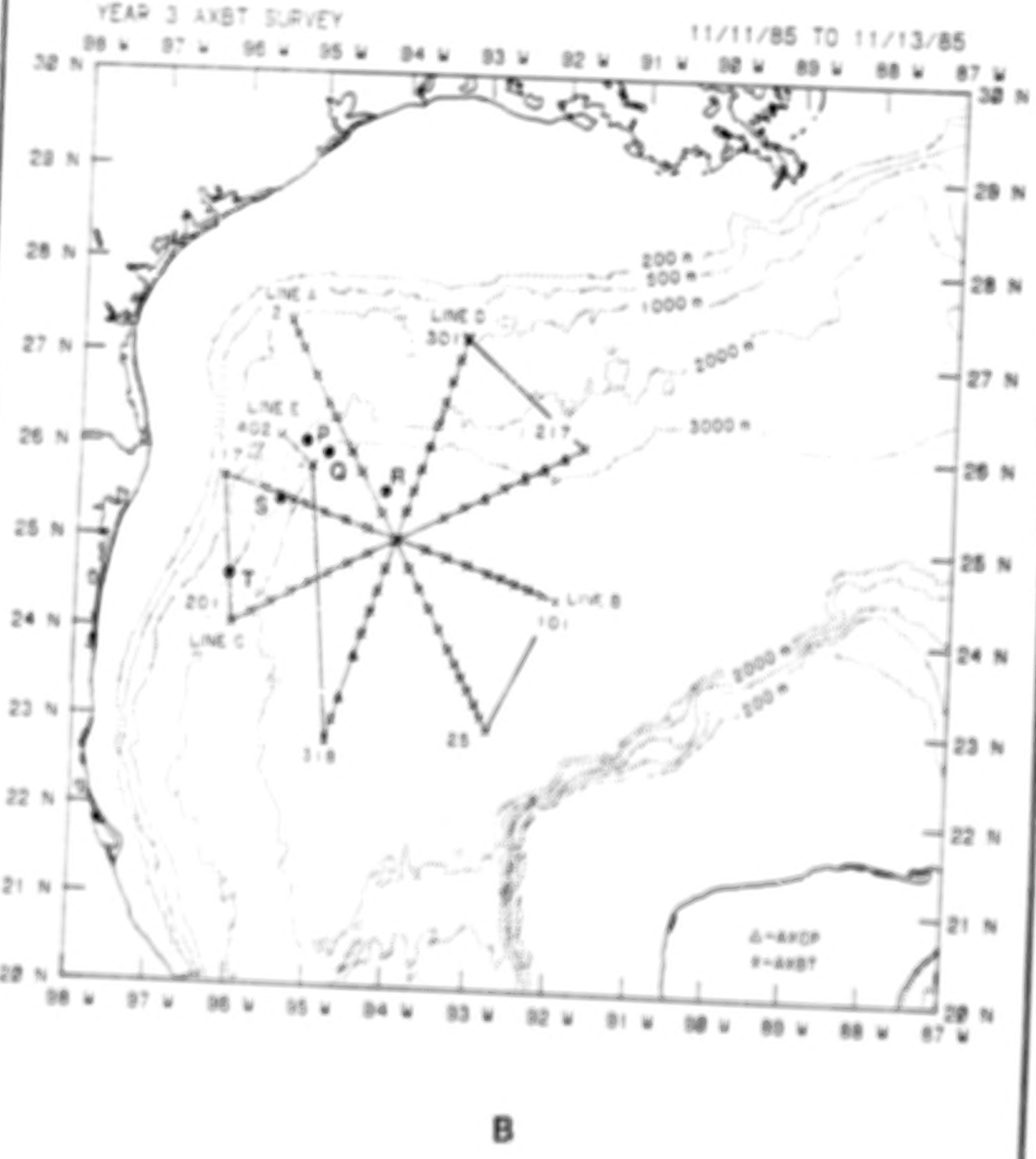

Figure 4.4-2b. Location of transect Lines A through E.

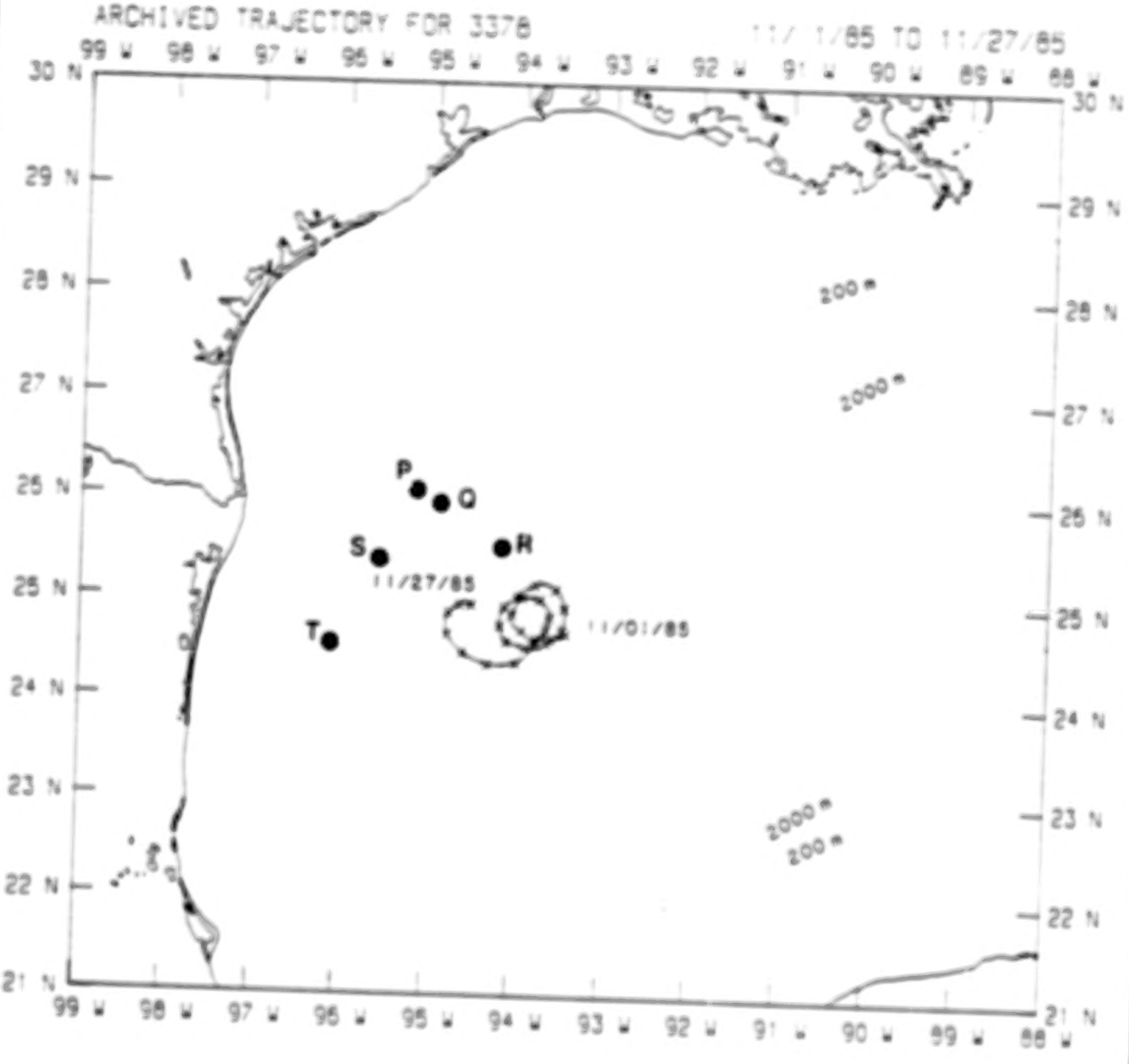

Figure 4.4-3. Path of ARGOS Drifter 3378 in the period of November 1-27, 1985.

sea-surface temperature analyses. In addition, a temperature section (Figure 4.4-4) along Line A of the November AXBT survey (Figure 4.4-2b) suggests that there may also have been an eddy in the northwestern corner of the Gulf (centered at Station 3) which was best defined at depths greater than 100m, although it was not seen in the satellite SST data.

4.4.2 Sea-Surface Temperature and Surface Processes

By the end of December 1985, significant seasonal cooling had occurred in the surface layer throughout the Gulf so that oceanic features were more easily detected. On December 25, 1985, the satellite SST distribution (Figure 4.4-5) showed significantly colder water on the shelf in the western Gulf of Mexico. Western portions of the Loop Current (SST greater than 25°C) were still evident to the east (LC). A westward extension of warm LC water was centered at around 26.5°N, 90.0°W, suggesting that a new eddy may have been separating.

The most significant feature in the western Gulf was the north-south oriented warm water (W) that was located immediately seaward of the western slope. The warm water extended from approximately 23.5°N to 28.0°N with the southern boundary defined by two cold features. One feature extended eastward from the shelf to the west, and the other extended westward from the broad zone of relatively cool water that separated the Loop Current from this warm SST. Located in the feature was an isolated lens of cold water (temperatures less than 23°C) that extended westward at approximately 23.8°N, 95.1°W. This lens may have been the surface manifestation of a cyclonic perturbation, but no further data could be found to support this thesis.

The December 25, 1985 imagery showed a cold perturbation (C) was located between the warm zone (W) and the shelf and was centered at 27.0°N, 96.2°W, and a warm filament was found shoreward of that perturbation. The configuration of this feature is reminiscent of the cyclonic cold perturbations detected through satellite data off the southeast coast of the United States (Rao et al., 1971; Brooks and Bane, 1978; Legeckis, 1979; Vukovich and Crissman, 1980; Bane et al., 1981).

By mid-January 1986, the satellite SST distribution (Figure 4.4-6) indicated that a new warm eddy (Eddy C) had separated from the Loop Current and extended as far westward as 91.0°W (at 25.0°N). The north-south oriented warm zone immediately east of the western slope wall was still apparent (W). Temperatures in the warm zone exceeded 23°C. The northern boundary of the warm zone was still at approximately 28°N; however, no southern boundary was apparent. The SST pattern gave no specific indication of the eddies (A or B) that were embedded within that warm zone.

In the January imagery, an isolated cold lens (C) having temperatures less than 22°C was located at approximately 26.5°N, 95.9°W. This lens may have been the surface manifestation of the cyclonic perturbation that was located north and west of that position in December 1985. The cold perturbation appeared to be moving to the south and east. The analysis also indicated that the surface manifestation of the perturbation had grown in size and intensity. The SST pattern associated with this feature suggests that the northern boundary of Eddy B was at around 26.3°N. It is also possibile that a cyclonic perturbation (C) was centered at 23.5°N, 94.5°W. The SST pattern at that location showed a quasi-isolated cold feature having temperatures less than 23°C.

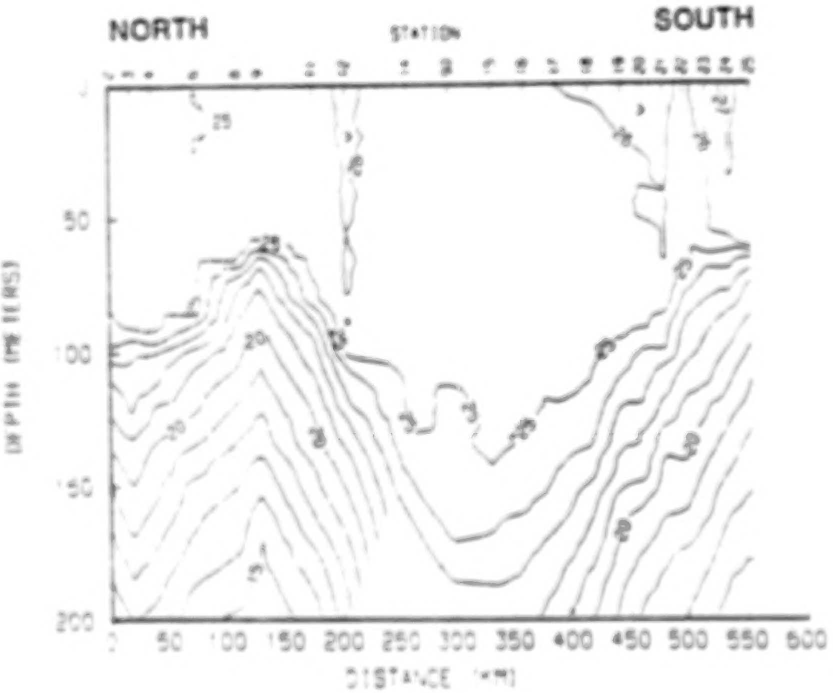

Figure 4.4-4. Vertical section of temperature (°C) along Line A from AXBT data collected for the period of November 11-13, 1985.

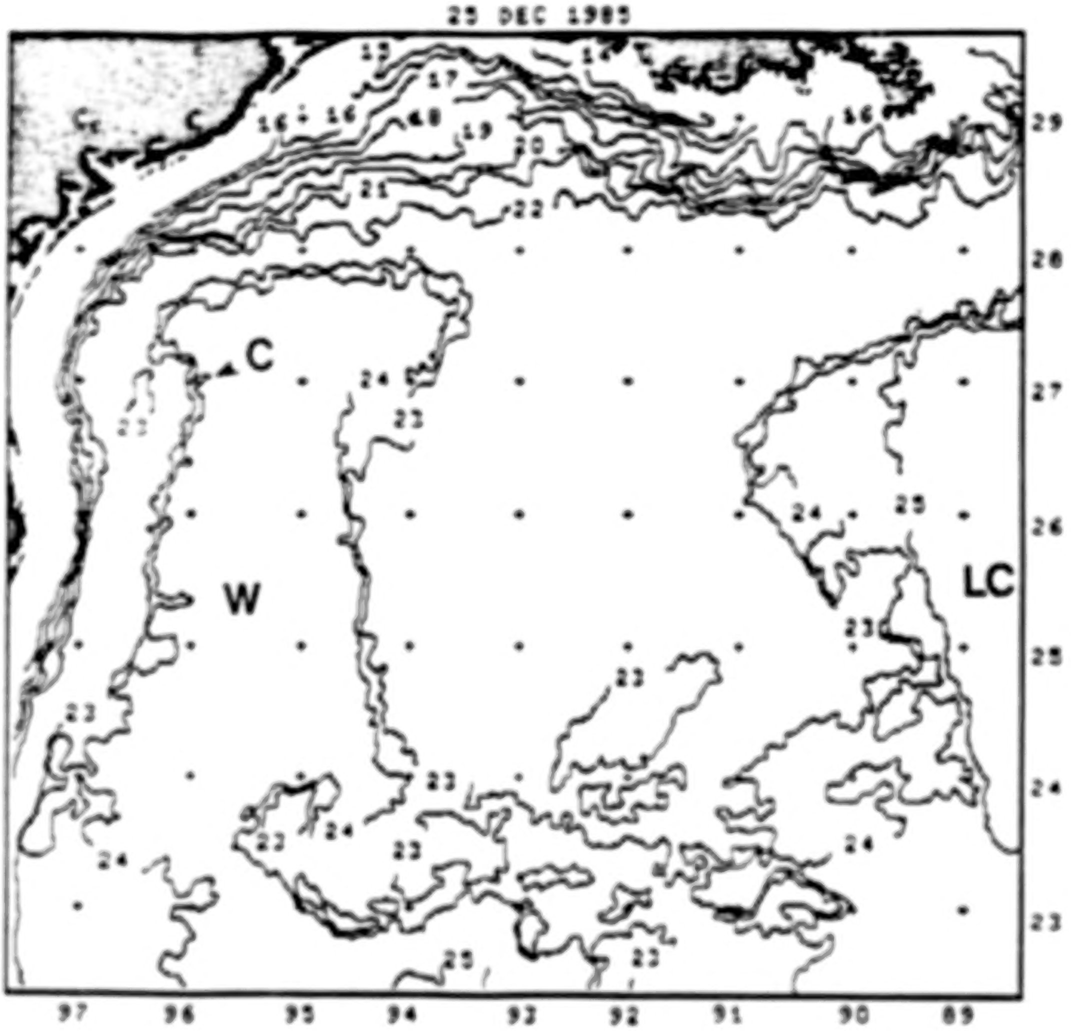

Figure 4.4-5. NOAA-9 SST (°C) analysis in the western Gulf of Mexico for December 25, 1985.

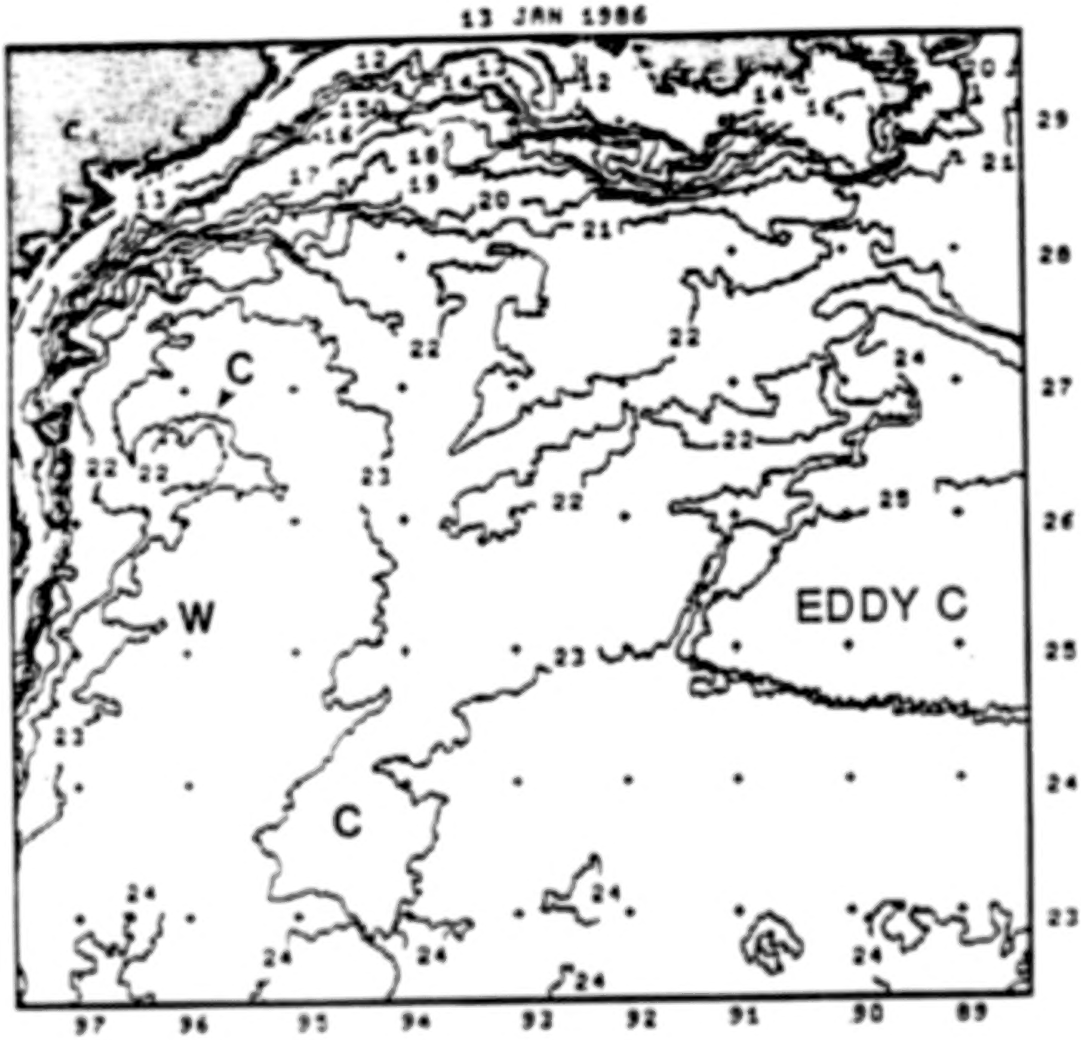

Figure 4.4-6. NOAA-9 SST (°C) analysis in the western Gulf of Mexico for January 13, 1986.

Hydrographic data were collected between January 23 and February 5, 1986 in the region immediately east of the western slope. These were used to develop the topography of the 21°C isotherm (Figure 4.4-7b) which showed a quasi-elliptical anticyclonic eddy (Eddy B) centered at 24.9°N, 95.4°W and whose major axis was oriented northeast-southwest. It was difficult from that analysis to determine the northern and southern boundaries of the eddy because of station spacing. The analysis also indicated the presence of a cyclonic cold perturbation that was centered around 26.3°N, 95.5°W. This location was south and east of the center of the perturbation noted in the mid-January SST analysis (Figure 4.4-6), suggesting that the perturbation continued to move southeastward.

During the January-February B/O ALTAIR cruise, hydrographic data were not collected as far south as 23.5°N, 94.5°W, so it was not possible to determine whether the cold lens detected using the satellite SST analyses (Figure 4.4-6) was in reality a cyclonic perturbation. The region of shallow isotherm depths noted in Figure 4.4-7b around 25°N, 94°W appears to be associated with the large cold zone that separated the warm zone, which was immediately east of the western slope, from the new warm eddy that had separated from the Loop Current (Figure 4.4-6).

To study characteristics of near-surface circulation in the eddy during this period, available drifting buoy data were combined. Position data from Drifters 3353 and 3378 and from offshore industry Drifter 5495 (Figure 4.4-8a) were used to develop a current field in the eddy between December 1985 and January 1986. Daily averaged position data are represented in Figure 4.4-8a and were used to obtain 24-hour vector displacements and velocity components. The velocities were screened to remove the effects of changes occurring near the eddy center within the 2-month period. The lines in Figure 4.4-8a represent position data that were used to develop the current field. The effects of non-stationarity on this procedure are acknowledged.

Figure 4.4-8b presents unit vectors showing estimates of the near-surface flow-field. Eddy B is characterized by a broad anticyclonic circulation near the surface which compares well with the SST pattern in that region (Figures 4.4-5 and 4.4-6) as well as with the analysis of the topography of the 21°C isotherm (Figure 4.4-7b). There is no indication of the cyclonic perturbations that were located at approximately 26.5°N, 95.9°W in the January 1986 SST analysis since drifters were not in that area (Figure 4.4-8a). However, a weak cyclonic circulation that was detected in the drifter data in the vicinity of 24°N, 97°W is maintained in the analysis. This feature was not documented by either the hydrographic data or the satellite data. Figure 4.4-8b also shows weak anticyclonic circulation at about 23.5°N, 96.6°W, which was detected in that region using data from Drifter 3353 (Figure 4.4-8a). The greatest surface speeds (Figure 4.4-8c) were found in the northwestern and eastern sectors of Eddy B. Smallest surface speeds were located in the southwestern sector and northern sectors.

Table 4.4-1 presents the near-surface area of Eddy B based on the analysis of the 21°C isotherm topography for November 1985 (B_1 in the Table) as given in Figure 4.4-2b, and three estimates of that area for the December 1985-January 1986 period. These three estimates were based on subsequent data explained in the figure. The area given by (B_2) is only slightly larger than (B_1), although they were derived from data that were collected 2-1/2 months apart. This similarity is because the analysis in Figure 4.4-7a does not present the entire northward and southward extent of the eddy. The estimated area (B_3)

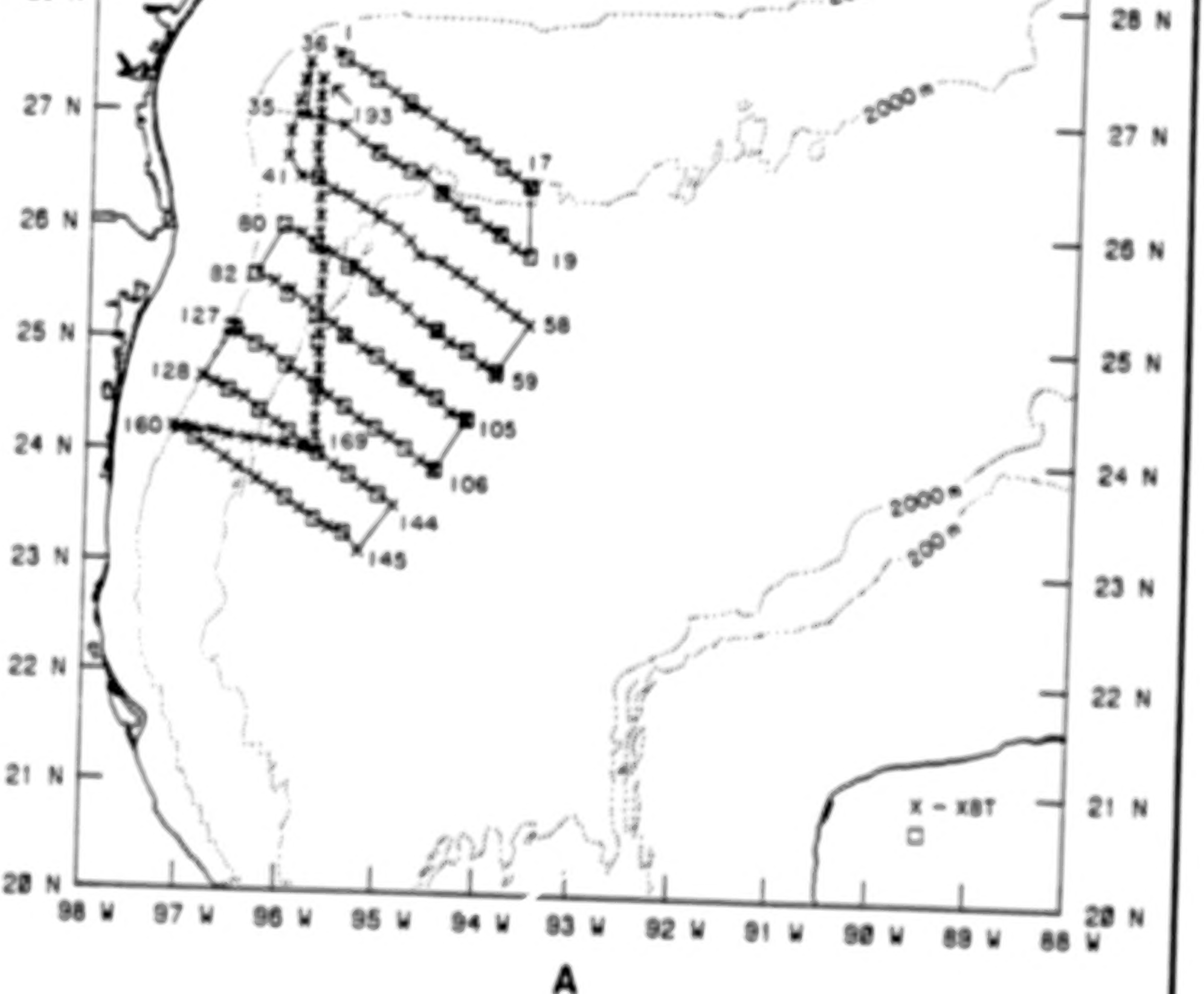

Figure 4.4-7a. Location of hydrographic and XBT stations.

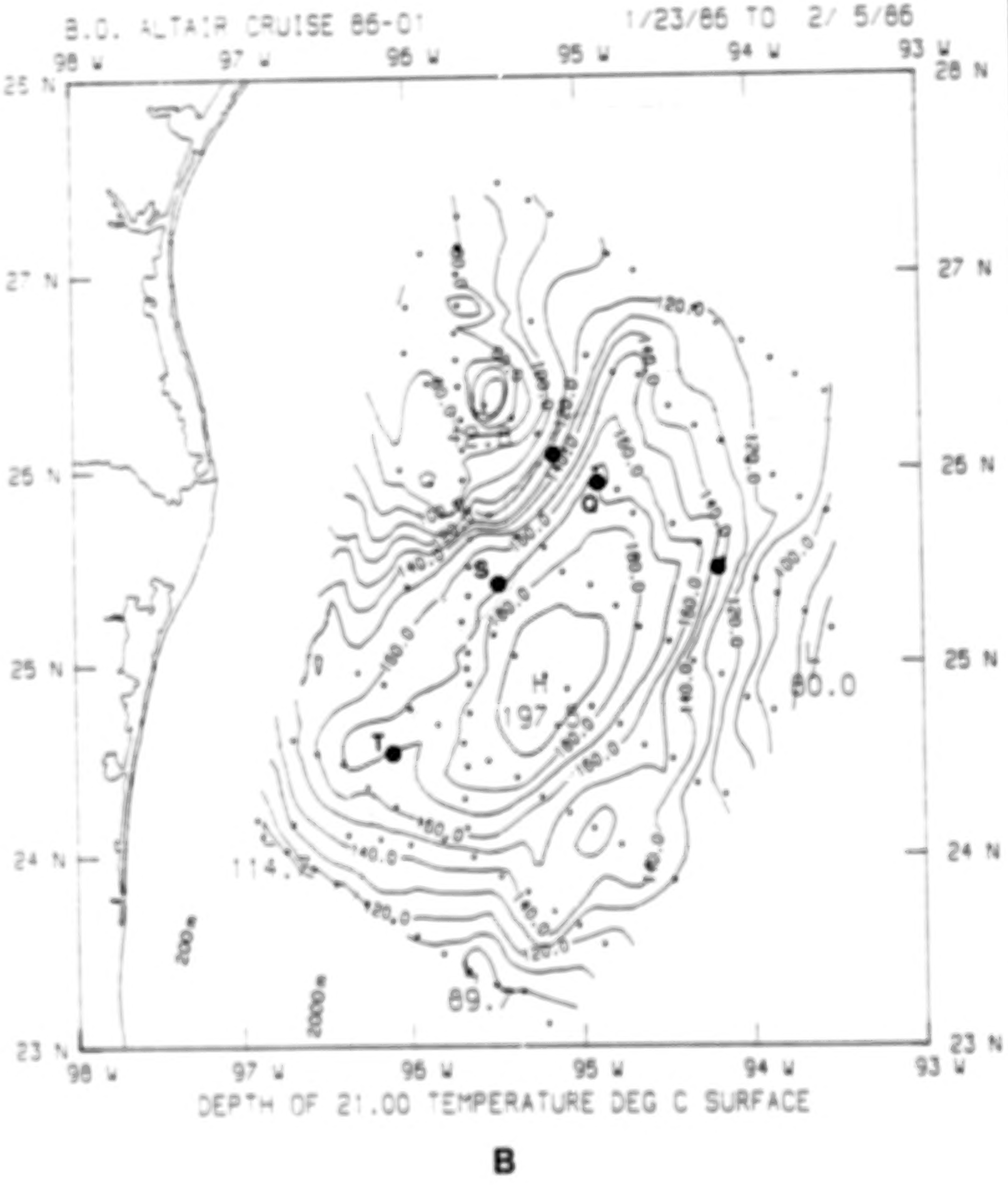

Figure 4.4-7b. Analysis of the topography (m) of the 21°C temperature surface from data collected in the period of January 23 through February 5, 1986.

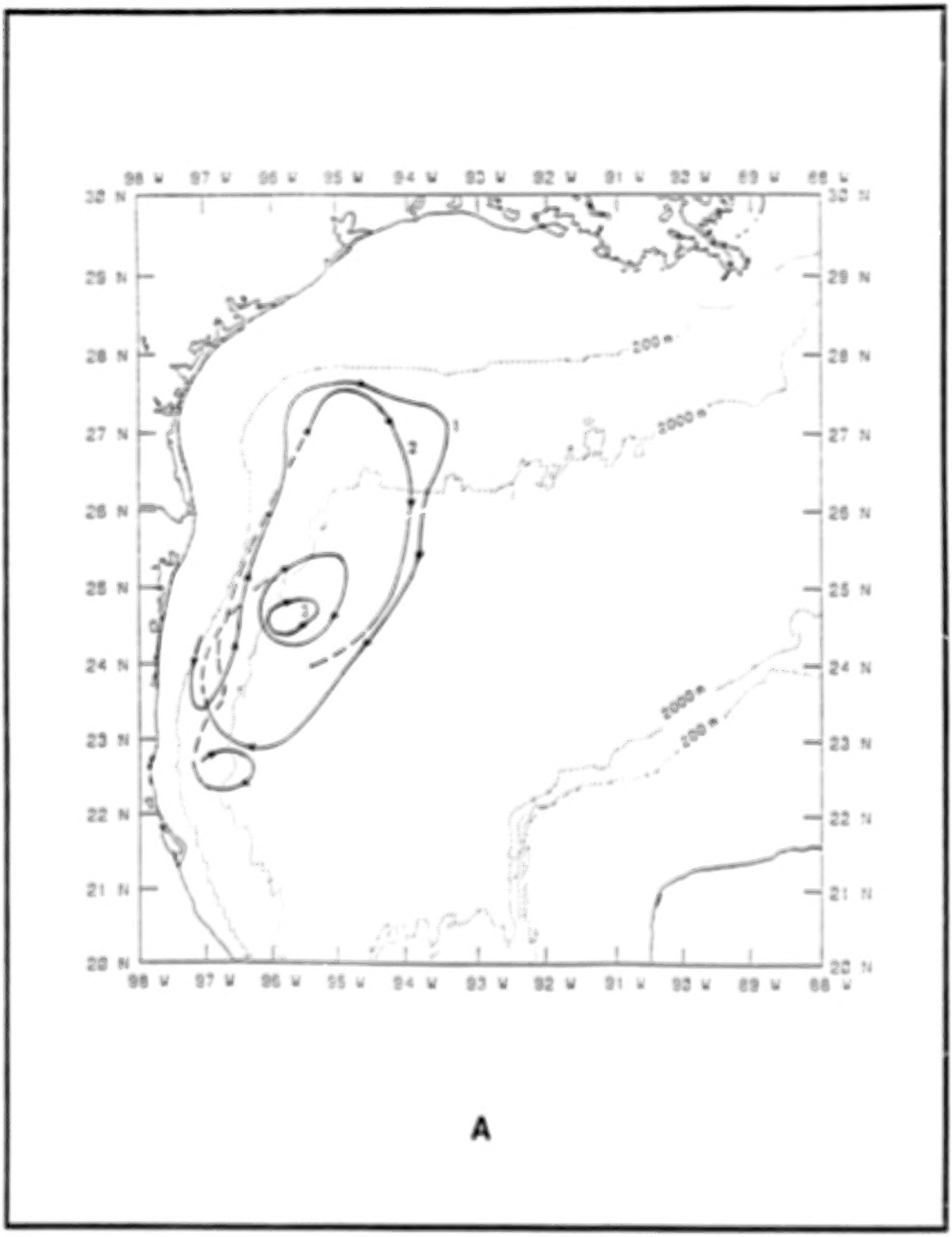

Figure 4.4-8a. Path of Drifters 3353 (1), 5495 (2) and 3378 (3) in the period of December 1985 through January 1986. Solid lines represent position data used to develop the current field; dashed lines represent omitted data. (See text for further explanation).

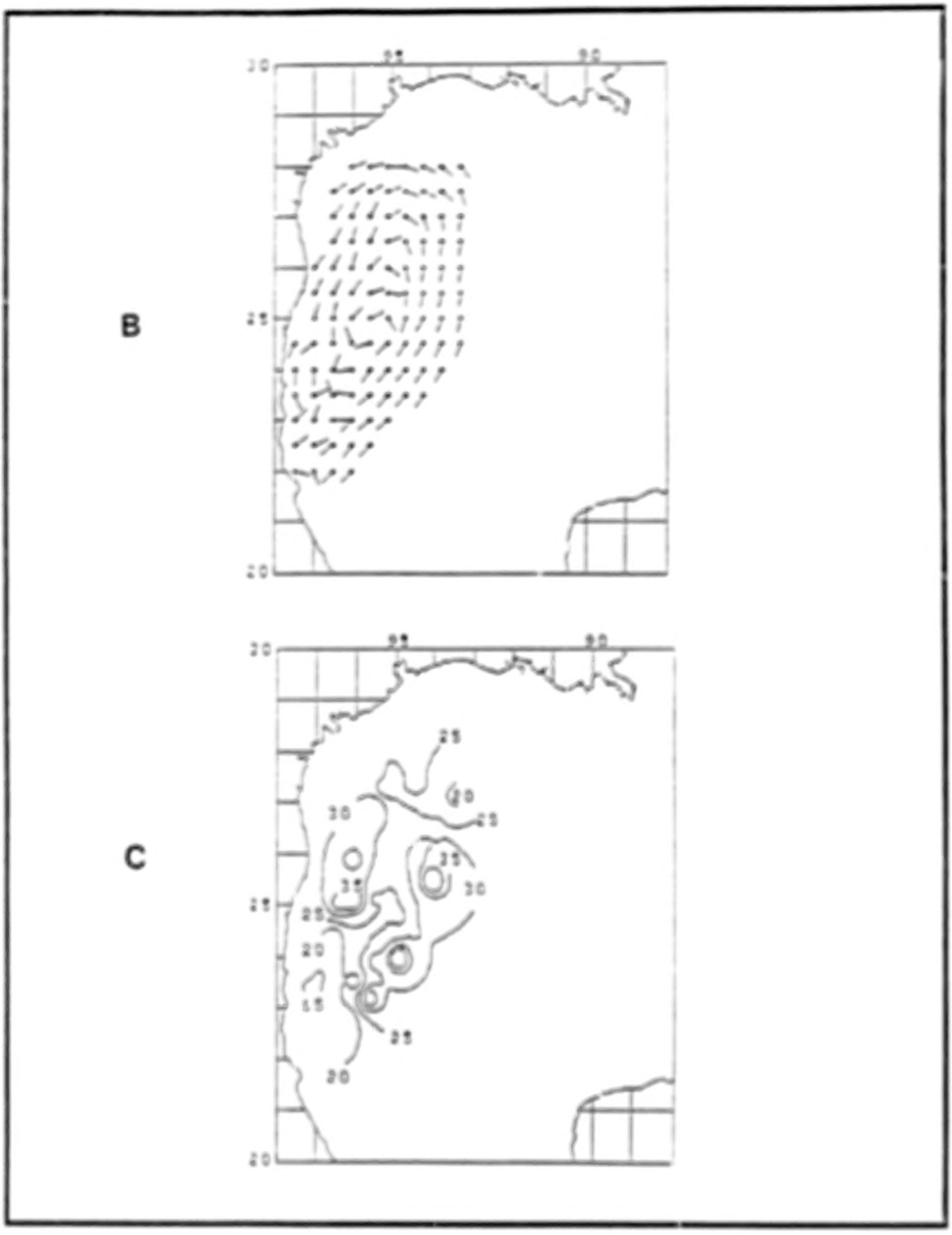

Figure 4.4-8b-c. (b) Unit vectors depicting the flow field near the surface derived from the drifter data in Figure 4.4-8a and (c) isotachs of surface current speed (cm sec^{-1}) derived from the drifter data in Figure 4.4-8a.

Eddy	Area (km^2)	Area Difference * (km^2)
(B_1)**	87,600	0
(B_2)**	90,700	3,100
(B_3)**	108,500	20,900
(B_4)**	122,300	34,700

* Area difference (km^2) = $B_i - B_1$

** (B_1) the analysis of the topography of the 21°C isotherm for November 1985 (Figure 4.4-2), (B_2) the analysis of the topography of this 21°C isotherm for January through February 1986 (Figure 4.4-7), (B_3) the drifters' paths in Figure 4.4-8a and (B_4) the circulation field depicted in 4.4-8b.

Table 4.4-1. Near-surface area estimates for Eddy B.

did not include the area defined by Eddy A to the south, whereas estimated area (B_4) did include that area. The latter two estimates suggest that after Eddy B encountered the western slope, the surface area of the eddy increased by 24 to 40%. Figures 4.4-2b and 4.4-7b reveal the depth of the 21°C isotherm at the eddy center as being 35m closer to the surface in late January 1986 than in November 1985. In that period, the area covered by the 190m contour line for the depth of the 21°C isotherm decreased by 46%. Since the 190m contour covered 37% of the eddy's area in November, this suggested that upwelling and horizontal divergence could have accounted for 40-70% of the increased surface area of the eddy. The increased surface area could also be accounted for by interaction with Eddy A to the south. Previously, such interactions have been noted by Wallcraft (1986) in numerical experiments in cases when the initial conditions were similar to those observed here (Figure 4.4-9).

The data presented in Figure 4.4-8 were used to calculate the near-surface distribution of the vertical component of the relative vorticity (ζ) and of the horizontal component of the divergence (D) in and around the eddy. The vorticity and divergence were calculated using the following expressions:

$$\zeta = \frac{\partial v}{\partial x} - \frac{\partial u}{\partial y} \ ; \text{ and}$$

$$D = \frac{\partial u}{\partial x} + \frac{\partial v}{\partial y}$$

Positive values of z reflect cyclonic vorticity, and negative values, anticyclonic vorticity. Positive values of D reflect divergence, and negative values, convergence. The results are presented in Figure 4.4-10.

The results of the calculations show a predominance of anticyclonic vorticity (Figure 4.4-10a) over the area that defined Eddy B with central values less than -4×10^{-6} sec^{-1}. The secondary center of anticyclonic vorticity to the south of the primary center with central values less than -2×10^{-6} sec^{-1} may be associated with Eddy A. The positive (cyclonic) vorticity to the west of the center of Eddy B with central values greater than 2×10^{-6} sec^{-1} indicates a cyclonic perturbation located in that region. The center of cyclonic vorticity east of the eddy center (central values greater than 2×10^{-6} sec^{-1}) cannot be associated with a particular feature and is may be due to interpolation noise. The divergence analysis (Figure 4.4-10b) shows alternating zones of divergence (positive values) and convergence (negative values) but with convergence characterizing most of the central area of Eddy B at that time. The path of Drifter 3353 (Path 2) in Figure 4.4-8a indicates that the buoy moved toward the center of Eddy B in mid- to late January 1986, supporting the notion that convergence characterized the central area of the eddy during this period.

The drifter data also reveal an aspect of the disturbed nature of Eddy B after it encountered the western slope wall. Figure 4.4-11 presents trajectories of Drifters 3353 and 3378 in the center of Eddy B during parts of December 1985 through January 1986. It can be seen that during that period the drifter paths described ellipses, a significant change from the circular path observed in November 1985 (Figure 4.4-3). Over the 2-month period, ellipse orientation changed rapidly. In the first half of December 1985, the

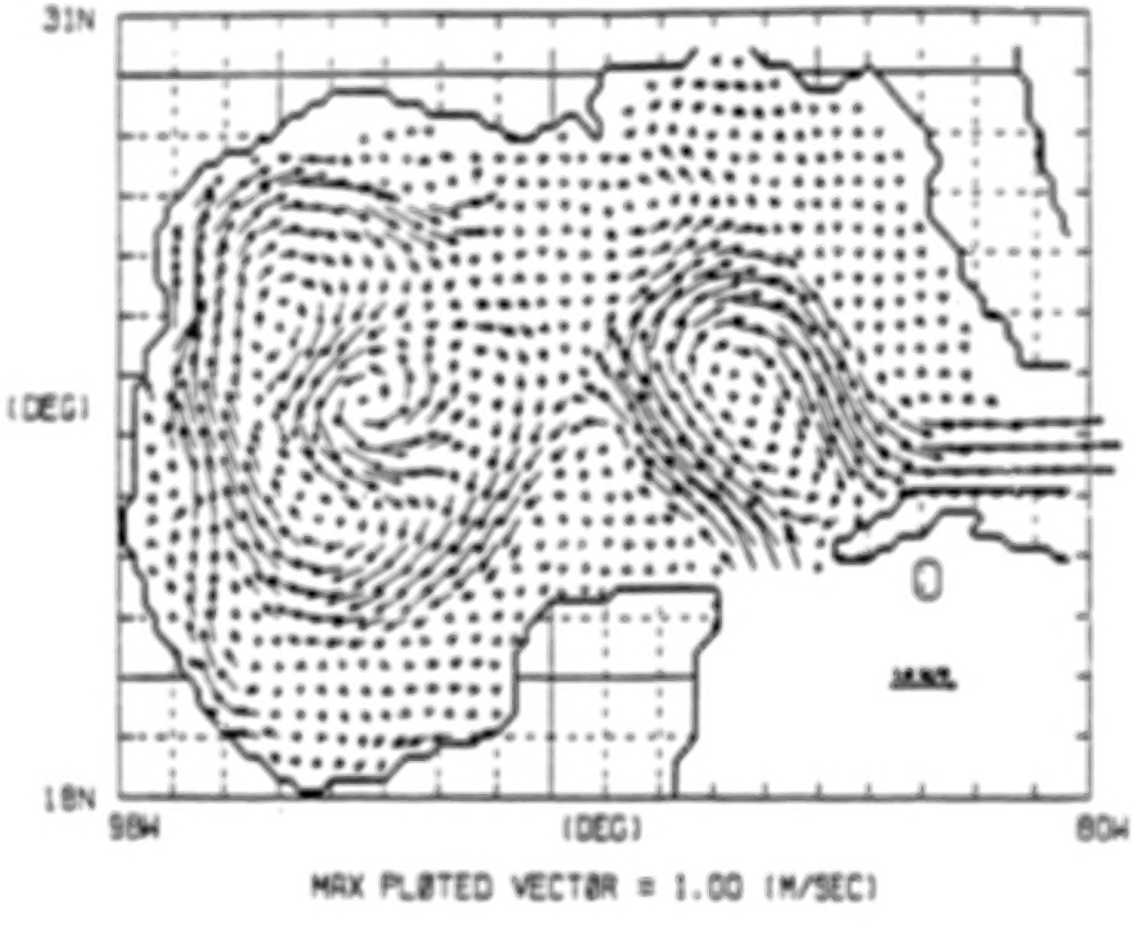

Figure 4.4-9. Simulated upper-layer flow field using a numerical model in the Gulf of Mexico for Experiment 68 (Wallcraft, 1986) in which an eddy encountered the western wall. The initial conditions in the western Gulf for the numerical simulation were identical to those for this study (i.e., a weak eddy in the northwest corner and a weak eddy south of 23°N).

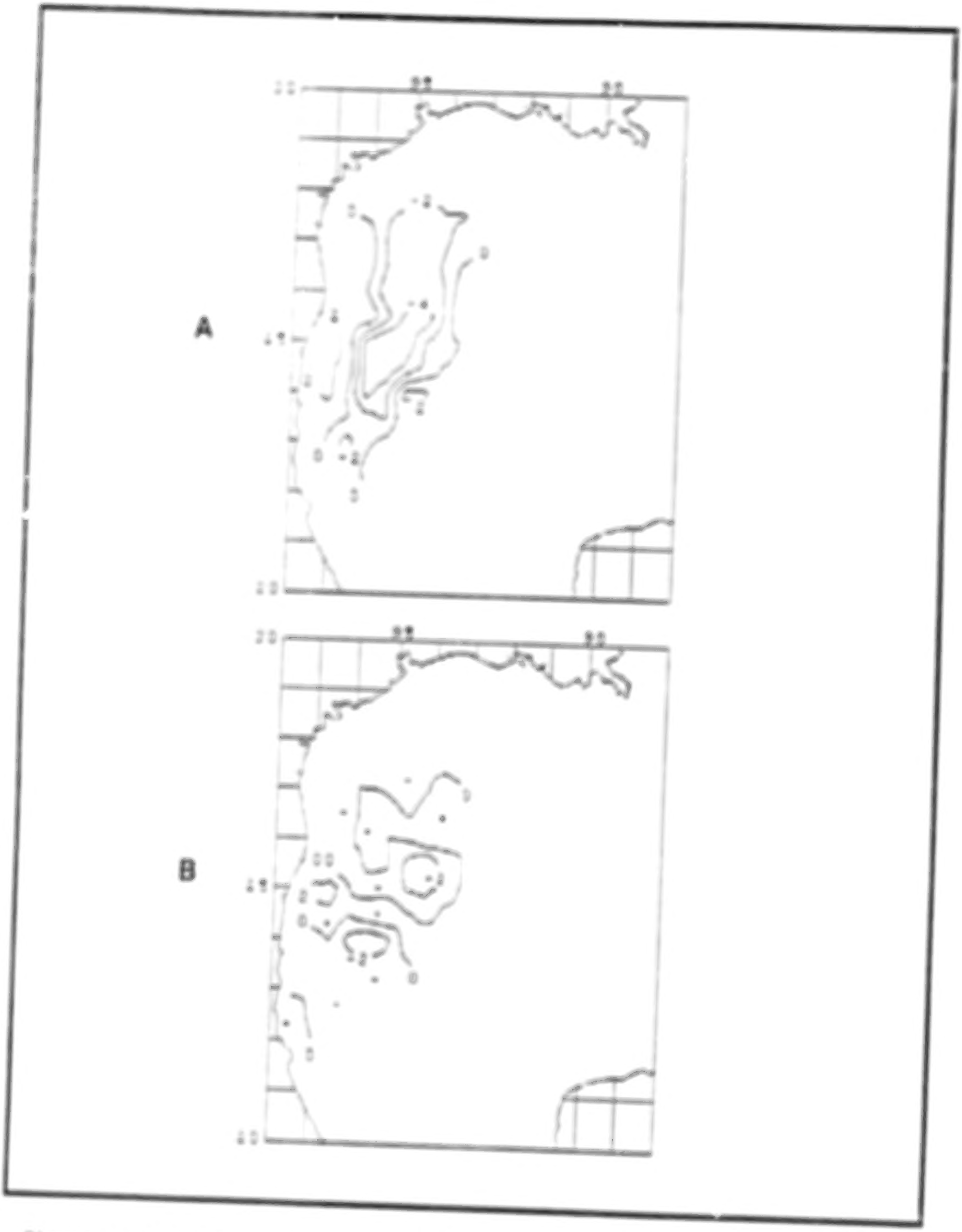

Figure 4.4-10. The analysis of: (a) the vertical component of the relative vorticity and (b) the horizontal component of the divergence. In both cases, the units are 10^{-6} sec^{-1}.

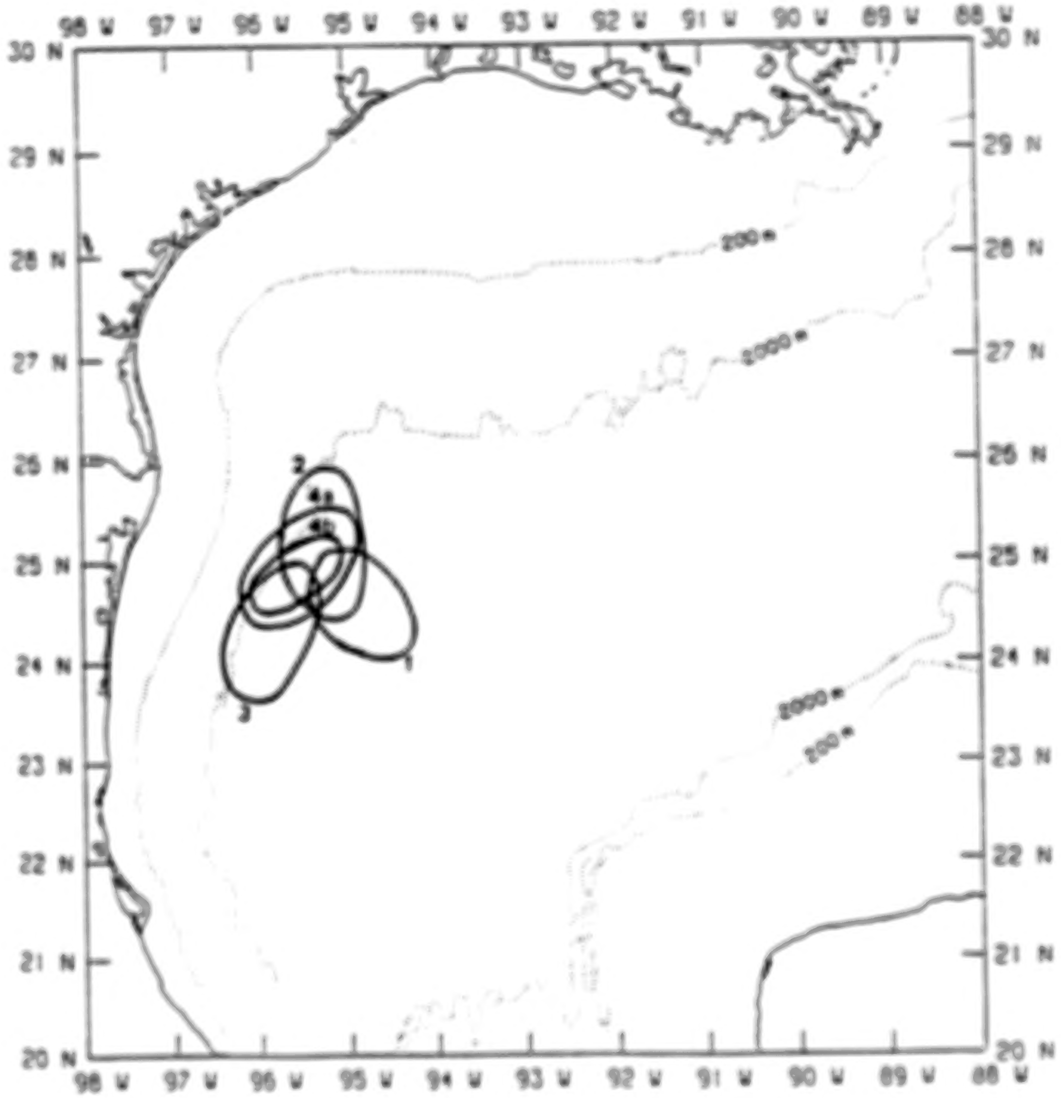

Figure 4.4-11. Stylized representation of the path of Drifters 3378 and 3353 for the December 1985 through January 1986 period. Path 1 occurred in the first half of December 1985, Path 2 in the last half of December 1985, Path 3 in the first half of January 1986 and Paths 4a and 4b in the last half of January 1986.

major axis was oriented southeast to northwest (Ellipse 1); in the last half of December, south to north (Ellipse 2); in the first half of January 1986, south-southwest to north-northeast (Ellipse 3); and in the last half of January, southwest to northeast (Ellipses 4a and 4b). Ellipses 4a and 4b were based on the paths of Drifters 3353 and 3378, respectively, which were in the center of the eddy at precisely the same time. The ellipses described by the drifters' paths in the last half of January are similar to that noted for the eddy from the analysis of the 21°C isotherm topography (Figure 4.4-7b). The data show that the orientation of the ellipse rotated in an anticyclonic manner and that the speed of rotation (the angular velocity) was larger in December than in January. The data also showed that the position of the eddy's center changed significantly over the period with displacements as large as 125 km in a 15-day period.

4.4.3 Surface Currents and Dynamics in the Western Gulf

4.4.3.1 SST and Path Data

After October 1985, Eddy B began to interact with the continental slope in the northwestern corner of the Gulf. Conditions for November 6 through 12, 1985 are shown in Figure 4.3-23a (p. 97). Two drifters were in Eddy A while three others were in Eddy B. The southern edge of the flow field of Eddy B was located at 23°N, the same latitude as the apparent northern edge of Eddy A. The northern edge of the influence of Eddy B is seen at ~27°N. These drifter data coincide well with the depth of the 8°C isothermal surface as determined from an AXBT survey for the period November 11 through 13, 1985 (Figure 4.4-12) and reveal that the eddy was being deformed along its northwestern edge. Finally, note the characteristic bulge of the Loop Current (26°C isotherm) in Figure 4.3-23a as it pushes northward into the Gulf. This was the beginning of a new eddy (Eddy C) which was shed from the Loop Current in January 1986.

An interesting sequence of events followed after mid-November. Over the next 2-1/2 months, Eddy B and Eddy A may have interacted significantly. The sequence begins with conditions from November 13 through 19, 1985 (Figure 4.3-23b, p. 98). Eddy B is seen to be quite large, with drifter motion implying a radius of at least 200 km. Eddy A is about half as large. In the following week's SST map (Figure 4.3-23c, p. 98), Eddy B is still seen to be quite circular, with the movement of Drifter 5678 being northward along a tongue of 26°C water. Also note that Drifter 3353 had left Eddy A to move northeastward along the same curvature as the southwestern section of Eddy B. Over the next 3 weeks, this drifter made a slow cyclonic loop near the Mexican coast at ~24°N. During the same period, Drifter 5678 continued moving north-northeast along the western edge of Eddy B and reached 28°N.

The conditions of December 11 through 17, 1985 (Figure 4.3-23d, p. 99) show a very energetic system. The Loop Current had extended far into the central Gulf. Both of the drifters that had been in Eddy A were moving northward along the west side of Eddy B. A tongue of 24°C water had extended well north of the center of Eddy B (by 320 km). Drifter 5678 abruptly turned southward along the northern edge of this 24°C water mass. By December 22 to 28, 1985 (Figure 4.3-23e, p. 99), the flow field became even better organized. A large tongue of 24°C water extended from Eddy A (22.5°N) to 27.5°N. The four drifters moved along or within this water mass in an anticyclonic manner.

By mid-January 1986, this large, highly elliptical anticyclone apparently began a process of consolidation. The SST map of January 7 through 13, 1986

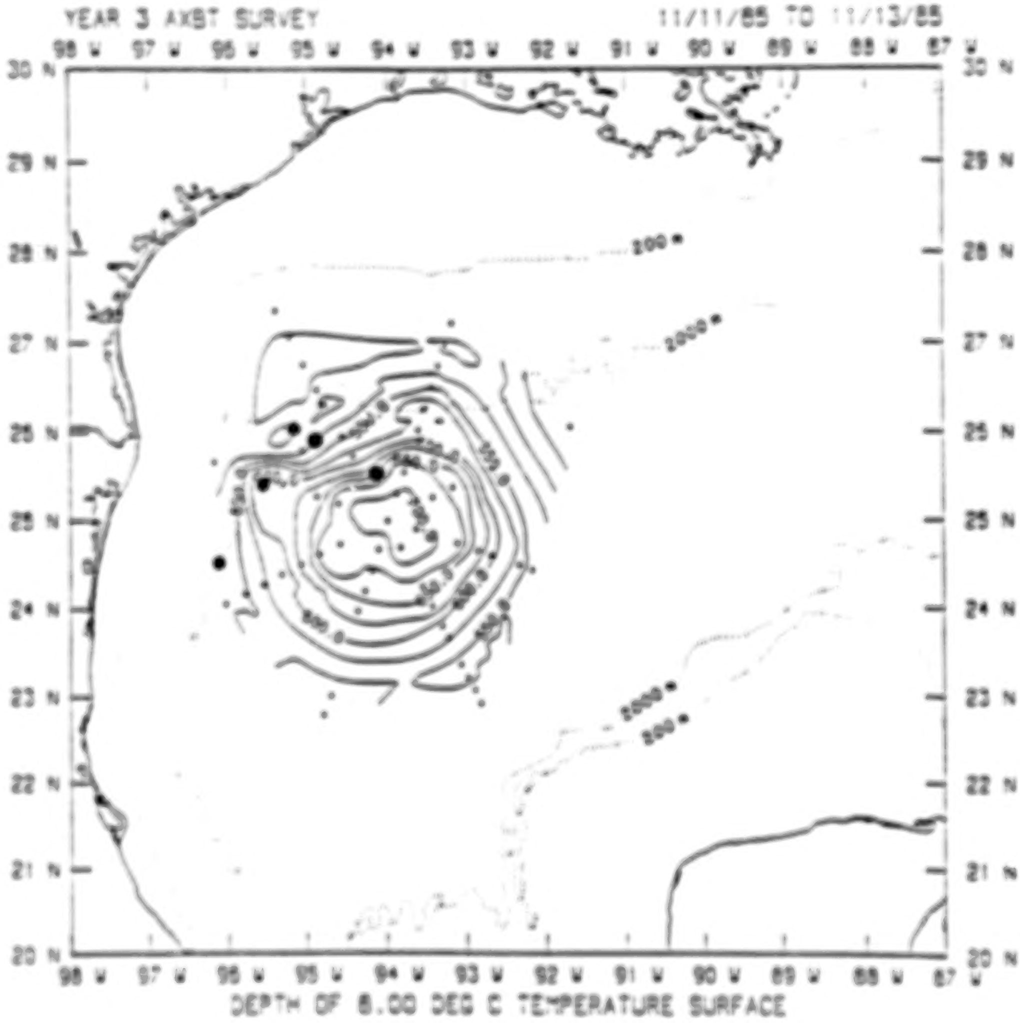

Figure 4.4-12. Topography of the 8°C temperature surface from the AXBT survey of November 11-13, 1985.

(Figure 4.4-13a) shows southern movement of the center of rotation and the beginning of a cyclonic feature. This cyclonic feature is seen as a small perturbation along the northwestern edge of a tongue of 23°C water extending from 22.5°N. In addition, the recently-shed Eddy C is easily discerned as a 24°C water mass in the central Gulf. From this, it would appear that Drifter 5678 had been affected by the flow field of this new eddy.

Within a week (Figure 4.4-13b), the center of rotation for Drifters 3378, 3353 and 5495 had moved to ~24°N with Eddy B's southern edge reaching at least to 22.5°N. The meander in the tongue of 23°C water had become quite extensive. By January 22 through 28, 1986 (Figure 4.4-13c), the flow field had become much less elliptical, and a cyclonic feature to the northwest of the anticyclone became apparent in the SST data. A hydrographic cruise was conducted during this period, from January 23 through February 5, 1986. The surface dynamic height field relative to 800m is shown in Figure 4.4-14. The cyclone-anticyclone pair is readily discerned, and the movements of the drifters are tightly coupled to this dynamic topography. However, there is no suggestion of any remnants of Eddy A.

4.4.3.2 Interaction with Eddy A

After moving into deeper water and crossing the Gulf, Eddy B began interacting with the Gulf western boundary. This interaction consisted of deformation caused by the bathymetry and interaction with Eddy A. On approaching the northwestern corner of the Gulf, Eddy B underwent considerable deformation (Figure 4.4-15a). As a result, the eddy became more elongated but with a variable orientation of the ellipse (Figure 4.4-15b). Swirl speeds as detected by Drifter 3378 were of the order of 25 cm sec^{-1}.

Figure 4.3-23c (p. 98) shows that Eddy B had begun to interact with Eddy A at least as early as November 22 to 26, 1985. At the beginning of this interaction, the elliptical orientation of Eddy B was northwest to southeast with an eccentricity varying between two and five (Figure 4.4-15b). This changed abruptly to a north to south orientation with an eccentricity as great as seven. This corresponds to the time that a tongue of warm water penetrated far north over the Texas continental slope and shelf (Figure 4.3-23e, p. 99). As the water mass became more consolidated (January 1986), the resulting anticyclone took on a northeast to southwest orientation and became more circular (Figure 4.4-15b).

The hydrographic and SST data indicate that Eddy B had coalesced completely with Eddy A. The coalescence process had many of the same features as those reported by Lewis and Kirwan (1985). Divergence associated with eddy coalescence is implied in the kinematic analysis of Drifter 5495 (Figure 4.4-16). The drifter and SST data indicate that Eddy B took approximately 1 to 1-1/2 months to extract and incorporate the waters of Eddy A.

The 8°C isotherm data for January 23 to February 5, 1986 (Table 4.3-1, p. 96) indicate the extent of the coalescence process. The maximum depth of this isotherm increased by 100m, and the volume of water between the 8°C and 15°C surfaces decreased slightly. The implication is that the coalescence process consisted substantially of the influx of warmer water from the south. These waters converged at the surface of Eddy B, resulting in the depression of isotherms.

A

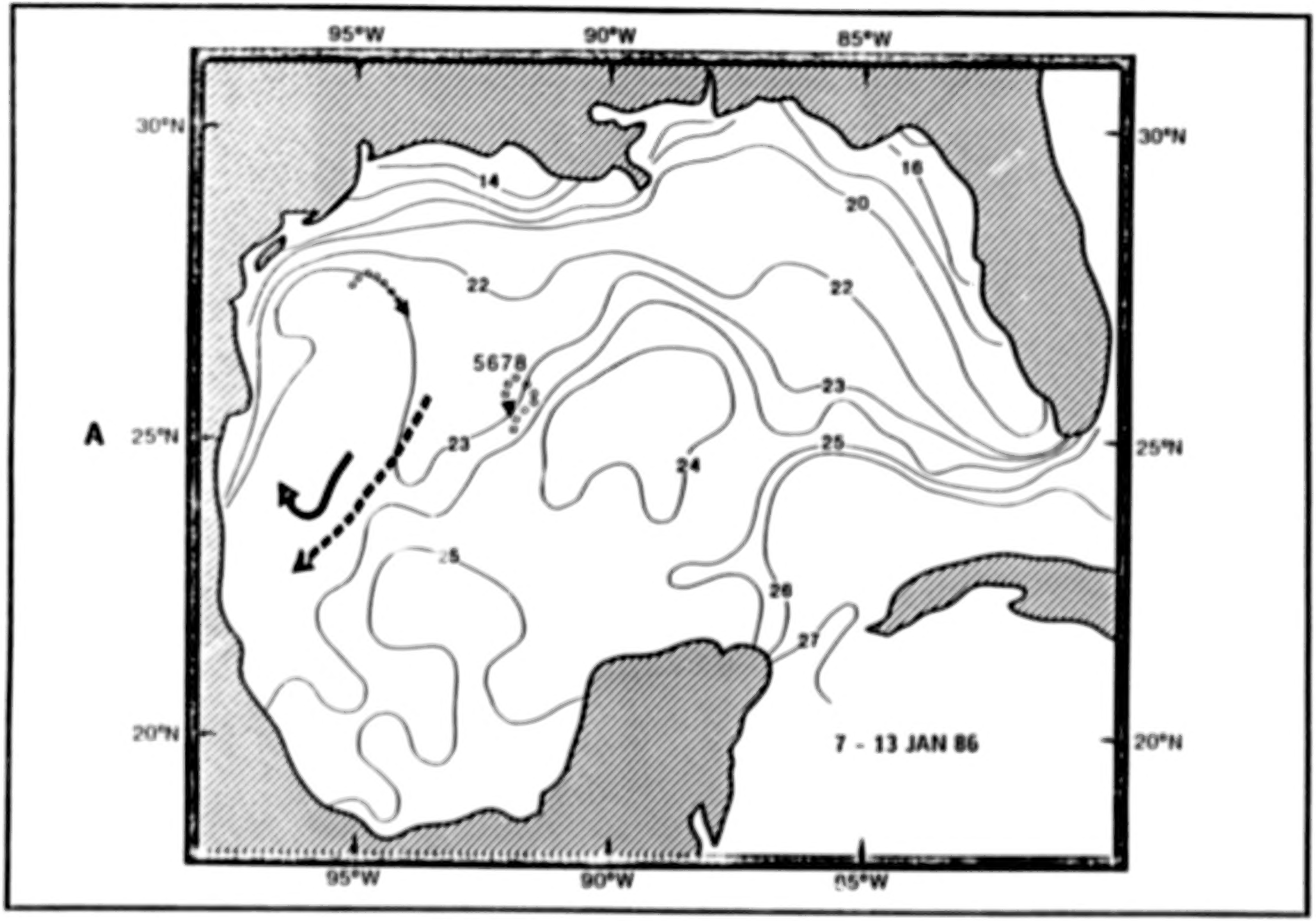

Figure 4.4-13a. SST data (°C) for 7-13 January 1986. Shorter arrows denote the flow at the edges of Eddy B while dotted lines indicate the locations of eddy waters (based on XBT data). The drifter trajectories, shown by arrows, are identified in Table 2.2-1.

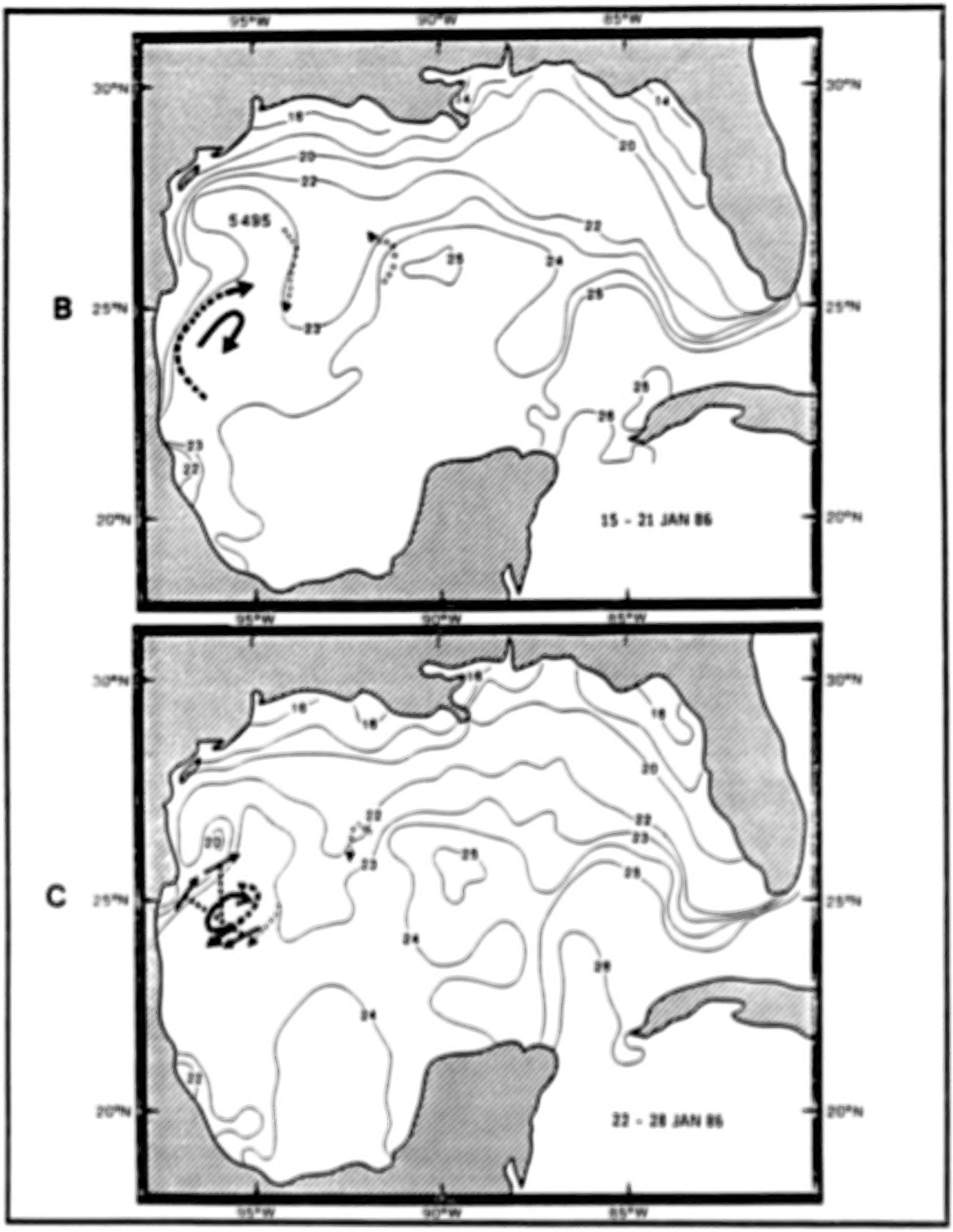

Figure 4.4-13b-c. SST data (°C) for: (b) January 13-21, 1986 and (c) January 22-28, 1986. Shorter arrows denote the flow at the edges of Eddy B while dotted lines indicate the locations of eddy waters (based on XBT data). The drifter trajectories, shown by arrows, are identified in Table 2.2-1.

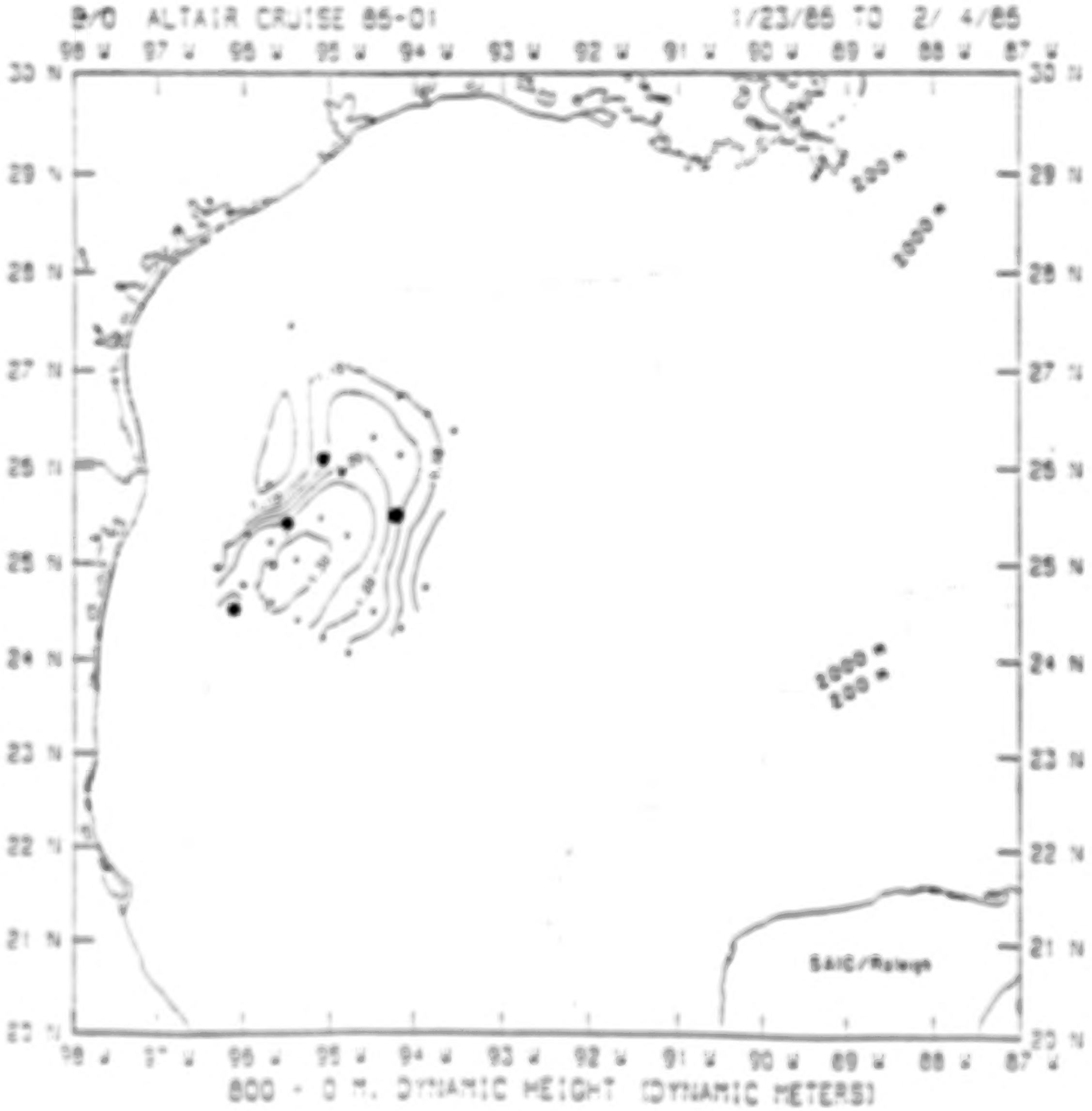

Figure 4.4-14. Surface dynamic topography (cm) with respect to 800m from the B/O ALTAIR survey of January 23 through February 5, 1986.

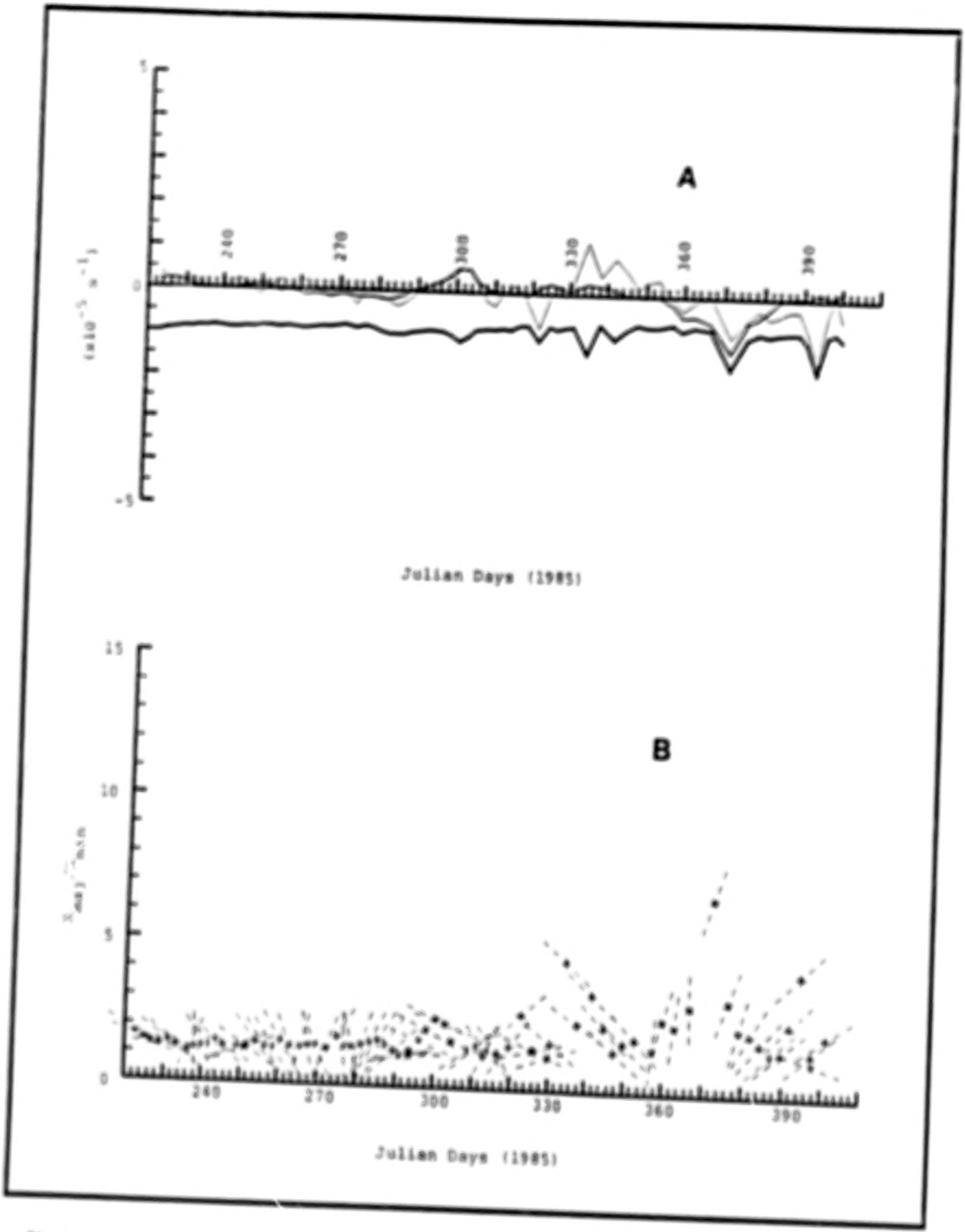

Figure 4.4-15. (a) Normal deformation rate (lightest line), shear deformation rate (darker line), and vorticity (darkest line) for Eddy B; (b) Time histories for the eccentricity (asterisk) and major axis orientation (dashed line) for Eddy B. For the flow field orientation, north is in the positive eccentricity direction and east is in the positive time direction.

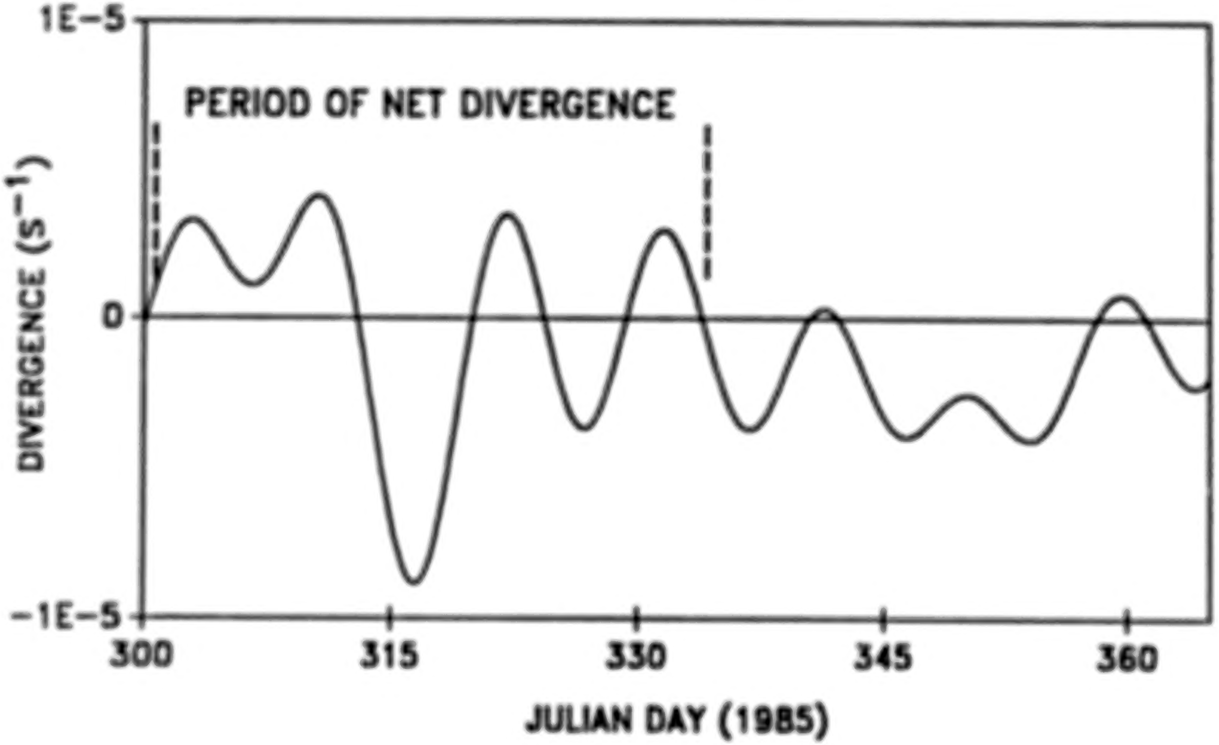

Figure 4.4-16. Divergence for Eddy A during the coalescing with Eddy B.

4.4.4 Hydrographic Characterizations

4.4.4.1 AXBT Survey (November 1985)

The AXBT flight sampled Eddy B rapidly with good spatial resolution just as the eddy began interacting with the topography in the northwestern corner of the Gulf of Mexico. Therefore, considerable weight may be given to the details of the structure of the observed temperature field. Figure 4.4-17 shows the 8°C, 15°C and 21°C temperature surfaces, contoured by computer. The southeastern part of Eddy B is relatively circular. The deviation from axial symmetry on the northern and western sides decreases upward, suggesting that the effects of topographic interaction on Eddy B take time to propagate upward through the thermocline. The perturbations are greatest along Line A which runs from northwest to southeast. A possible cyclone, which was identified in Section 4.2 (p. 51), is defined in the horizontal contour plots primarily by the data of the northwest portion of this line. Figure 4.4-18 is the vertical temperature section along Line A. A cyclone may be associated with the dome in the isotherms centered at Station 9. Although the distortion of the overall shape of Eddy B decreased upward (Figure 4.4-17), the dome in the isotherms of the much smaller scale feature (a possible cyclone) extends to the top of the thermocline and broadens above 12°C. Between 6°C and 12°C there is a trough in the isotherms centered at Station 6 that indicates an eddy.

Both the topography of 8°C (cf. Figures 4.2-3, p. 53, and 4.2-6, p. 57) and vertical temperature sections (cf. Figures 4.2-4, p. 54, and 4.4-18) suggest that the isotherms observed during the AXBT survey were systematically somewhat shallower than those in October by about 50m in the central part of Eddy B, but not in the outer parts. At the top of the thermocline the 25°C isotherm was also shallower in November than in October. Near the surface in the center of Eddy B the water was still slightly cooler than the outer parts but not as strongly so as in October.

A map of the dynamic height at 150m relative to 650m, computed using the AXBT data and the temperature-salinity relation derived from the CTD surveys (Section 3.3.2, p. 41), is plotted in Figure 4.4-19. The dynamic height map is smoother than the maps of individual isothermal surfaces because of the vertical integration involved in computing dynamic height, and thus it more clearly exhibits the principal features already noted: Eddy B is relatively circular to the southeast and distorted to the northwest, lobes protrude to the west and north, and related cyclones and anticyclones are weak but clearly visible. Note that the map of dynamic height is similar to the hand-contoured, and thus subjectively smoothed, map of the 8°C surface in Figure 4.2-6 (p. 57). Maximum horizontal gradients of the dynamic height field are typically about 0.09 dynamic meters per 27.5 km (1/4° of latitude). At 25.5°N this translates into a velocity of 52 cm sec^{-1} at 150m relative to 650m. For comparison, geostrophic velocities in Figure 4.3-18 (p. 89) use a reference level of 950m; at 150m maximum values are about 70 cm sec^{-1}, and at 650m they are about 10 cm sec^{-1}. The shallower reference level underestimates geostrophic speed, but Figure 4.4-19 still correctly indicates where flow is strong or weak.

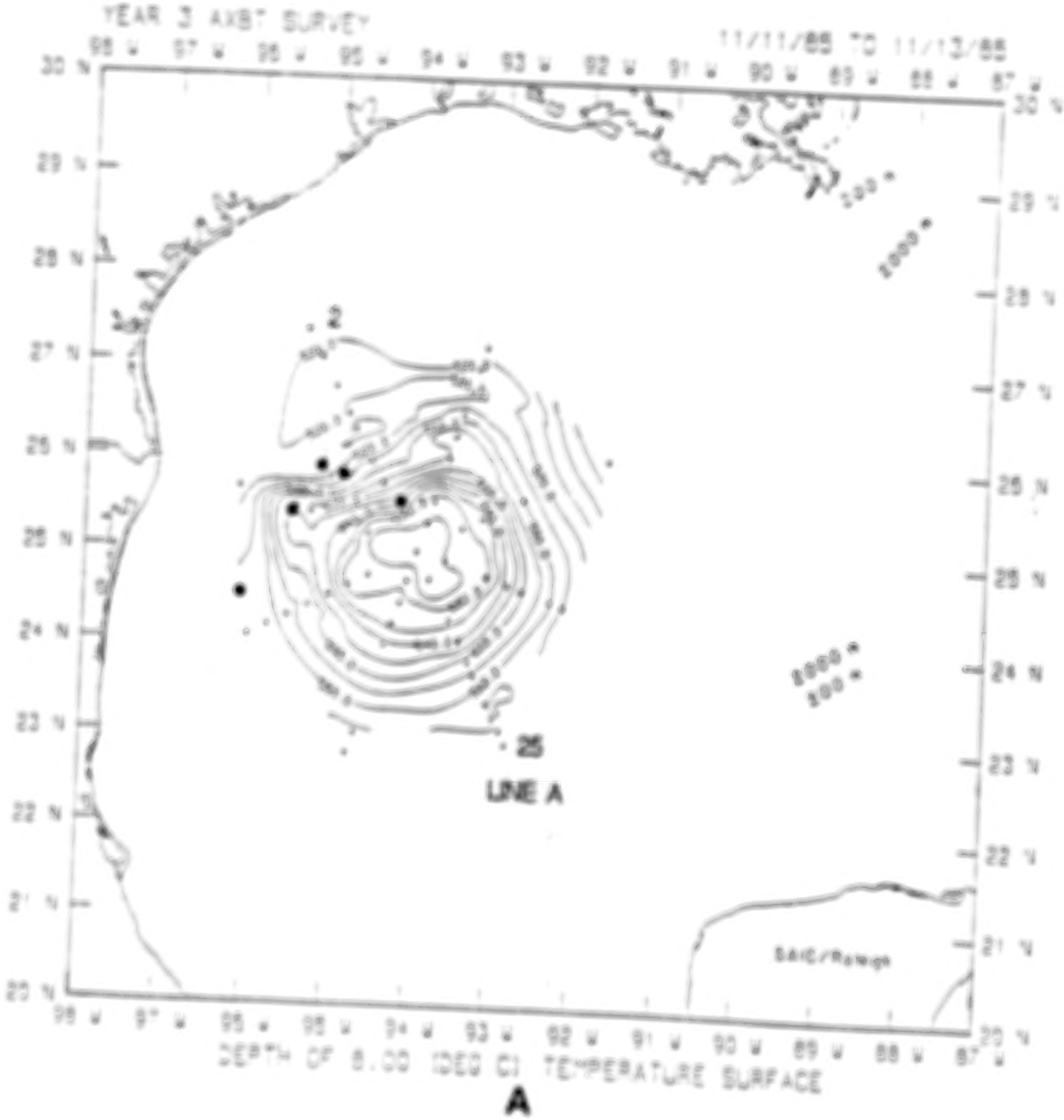

Figure 4.4-17a. Topography of the 8°C temperature surface based on the November 1985 AXBT survey.

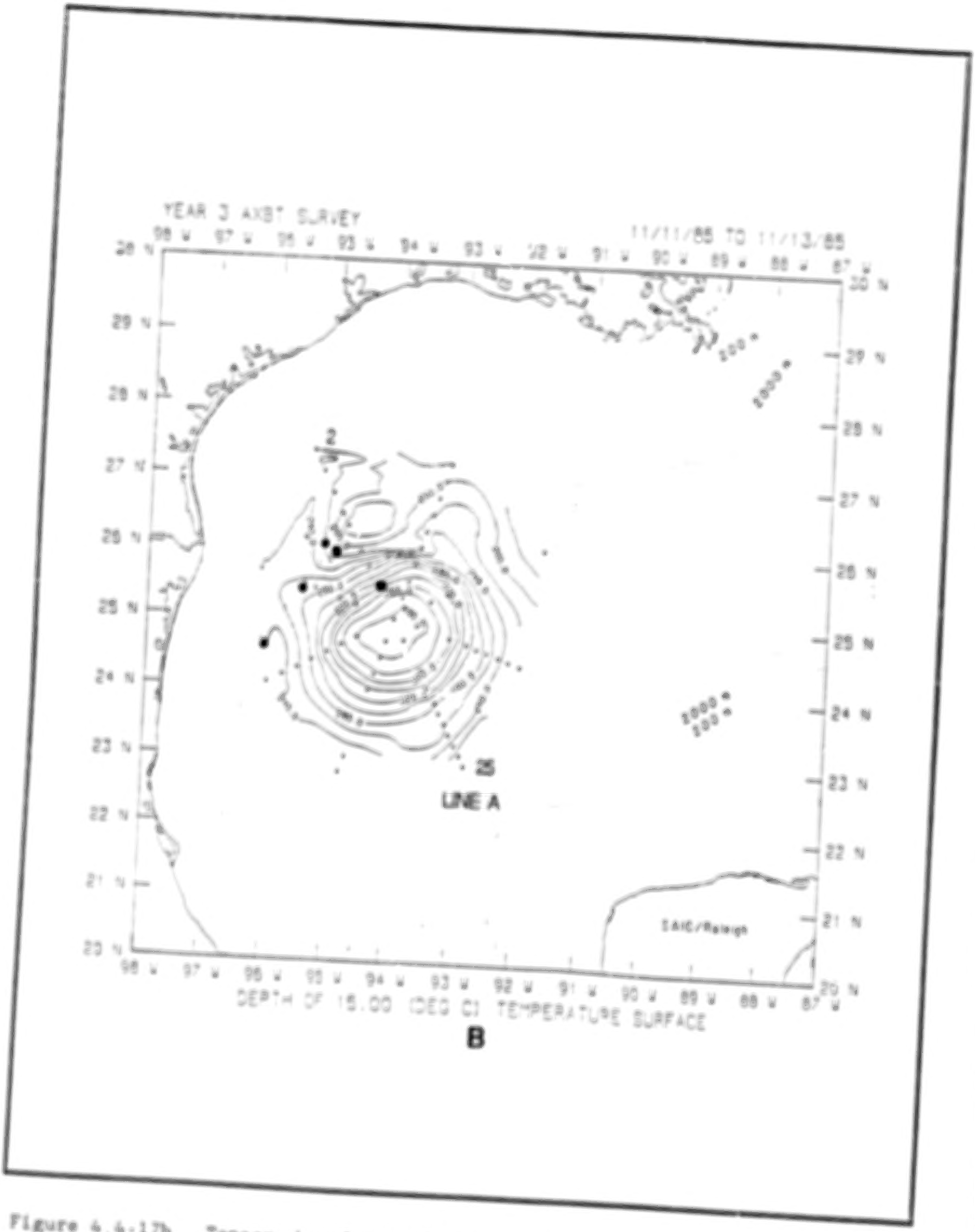

Figure 4.4-17b. Topography of the 15°C temperature surface based on the November 1985 AXBT survey.

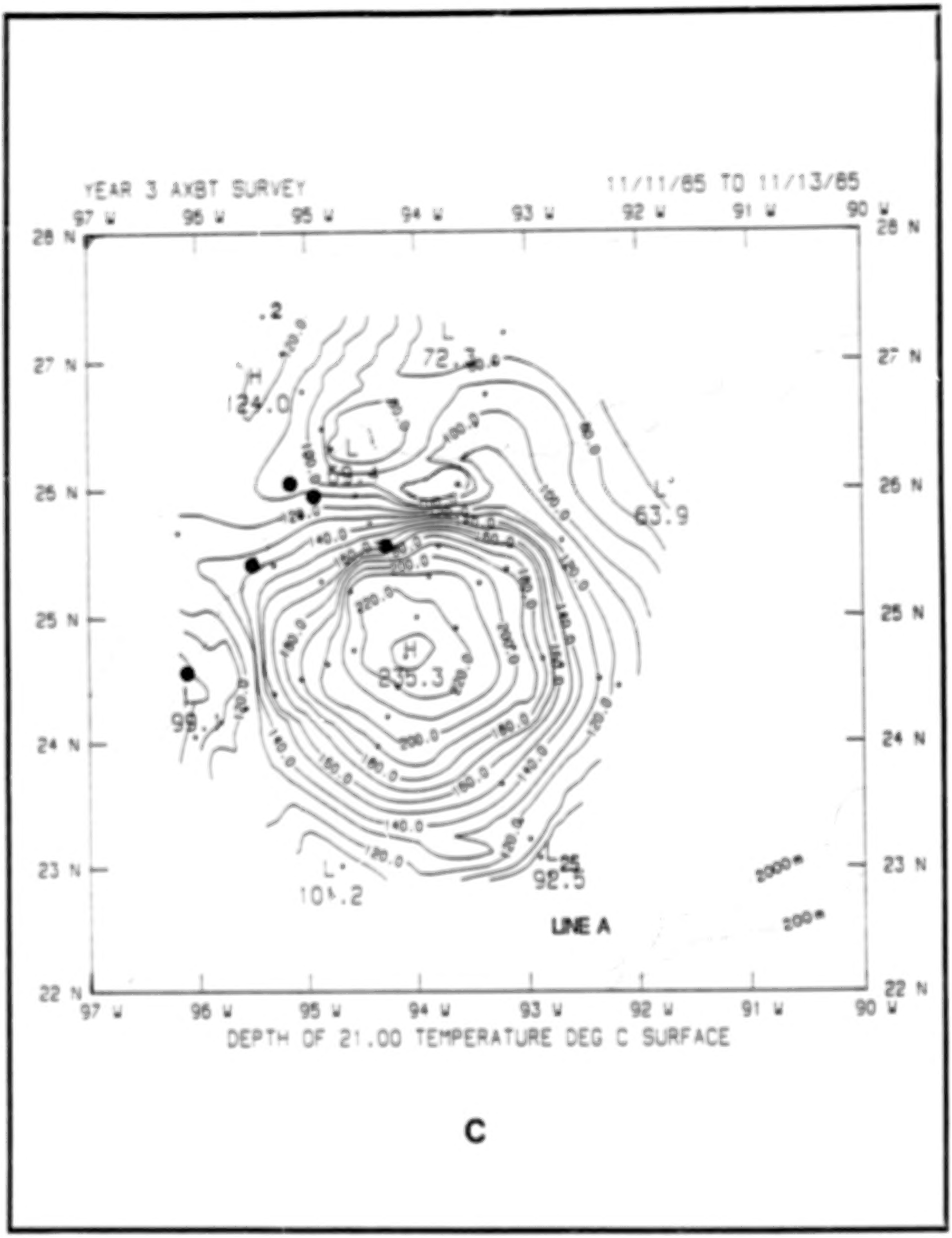

Figure 4.4-17c. Topography of the 21°C temperature surface based on the November 1985 AXBT survey.

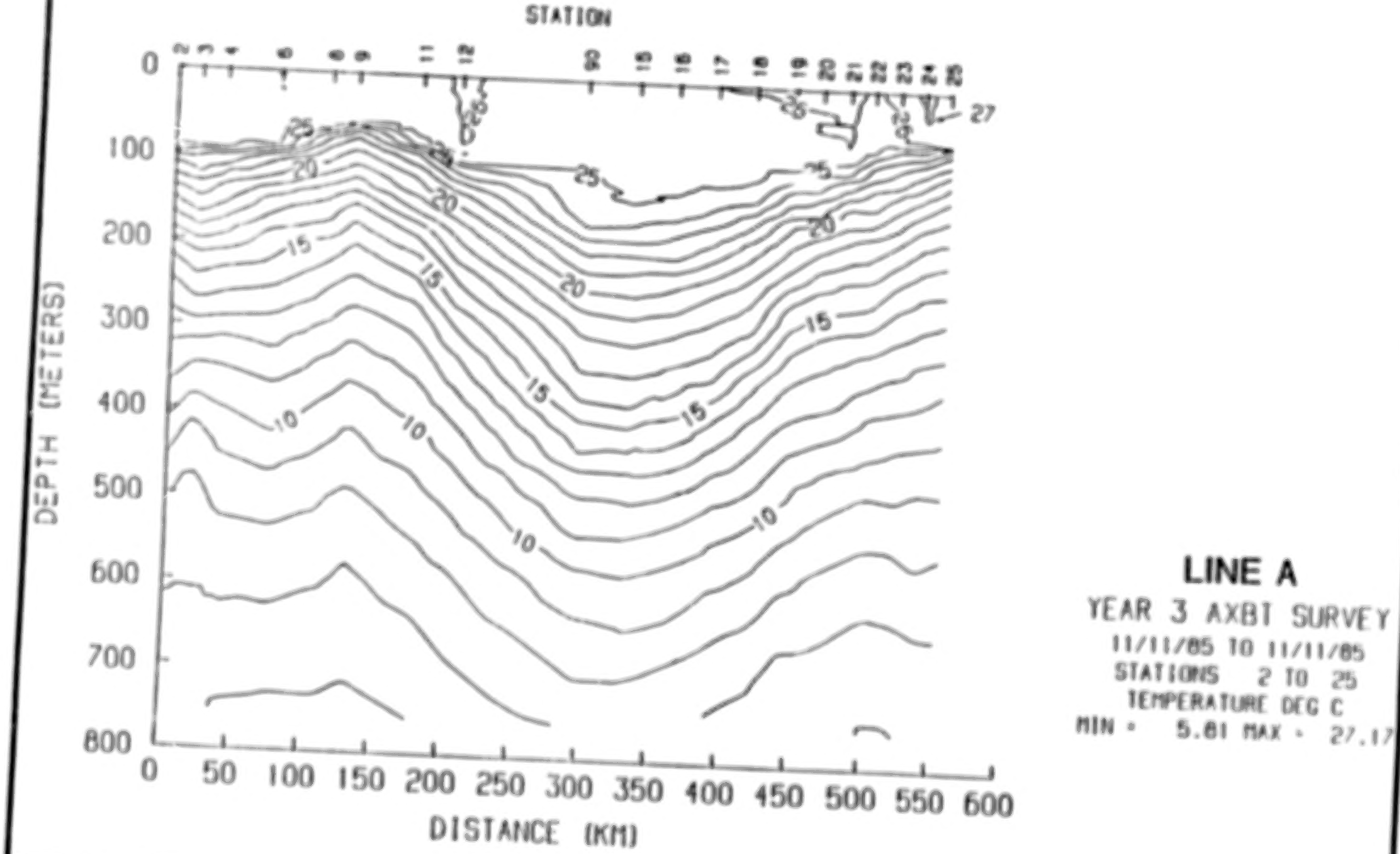

Figure 4.4-18. **Vertical section of temperature to 800m along Line A of the November 1985 AXBT survey. See Figure 2.3-5 for location of Line A.**

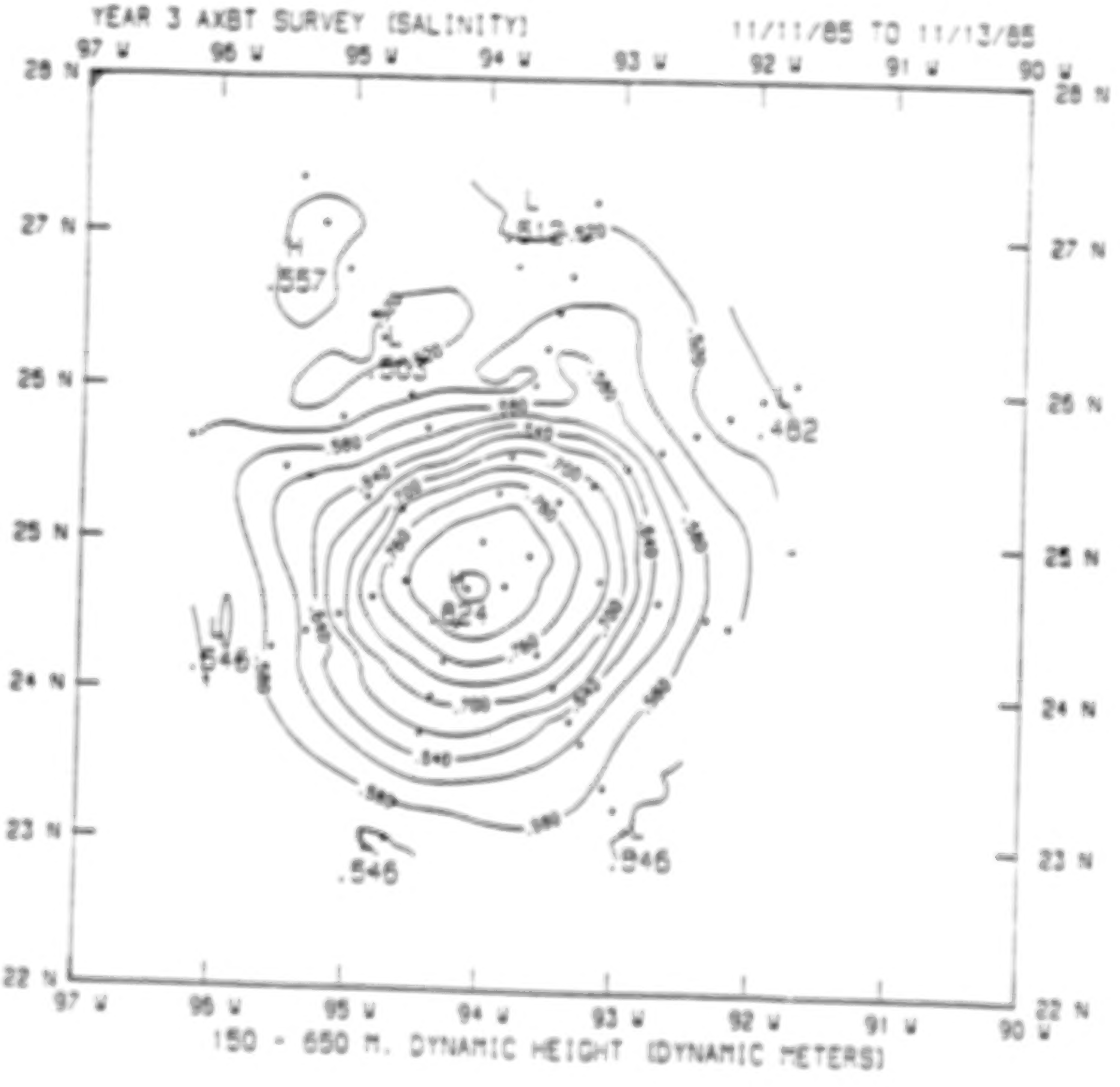

Figure 4.4-19. Map of "synthetic" dynamic height at 150m relative to 650m based on the November 1985 AXBT temperatures and the T-S relation.

4.4.4.2 B/O ALTAIR Hydrographic Cruise (January 23 to February 5, 1986)

4.4.4.2.1 Temperature

Figure 4.4-20 shows the 8°C, 15°C and 21°C temperature surfaces for the XBT data collected during the B/O ALTAIR hydrographic cruise. Eddy B is now very elliptical with an aspect ratio of about two. The major axis roughly parallels the 2000m isobath. At 8°C its core lies slightly east of the 2000m isobath, so all of the flow on the western side of Eddy B occurs over the continental slope between the 200m and 2000m isobaths. At 15°C and 21°C the core is located progressively farther offshore, which means that the vertical axis of the core tilts eastward. Despite the difference in shape, the core of Eddy B seems to be about the same size as in November, but its overall size in late January is smaller (cf. Figures 4.4-17 and 4.4-20).

In order to quantify the change in size, a digitizing planimeter was used to measure the areas of Eddy B inside the 550, 600, 650, 700 and 750m contours of the 8°C temperature surfaces for the October, November, January and April surveys of Eddy B (the measurements were made on hand-contoured Figures 4.2-3, p. 53; 4.2-6, p. 57; 4.2-8, p. 59 and 4.2-11, p. 63). The results, listed in Table 4.4-2, suggest the following conclusions. The deep core of Eddy B contained inside the 600m contour remained constant during the 3 months from October 1985 through January 1986. Outside this contour the structure of the eddy eroded so that by January contours shallower than 600m no longer closed around it. The areas of contours deeper than 600m pulsated, which suggests vertical motion in the core and horizontal convergence/divergence at other layers. After January the eddy decayed more rapidly so that by April 1986 the deep structure was about half its size in January.

Figure 4.4-21 shows a vertical temperature section along Line I, which passes through the centers of Eddy B and a paired cyclone (Eddy Z). One can see the decay in the strength of the upper part of Eddy B by comparing this figure with Figure 4.2-4 (p. 54) from the October 1985 survey. In January, isotherms above 12°C are shallower (e.g., 20°C) than in October. In fact, above 15°C they dome slightly, suggesting some lateral convergence at the base of the thermocline. This behavior is typical of decaying eddies.

Eddy Z, on the other hand, intensified greatly during the 2 and 1/2 months between the November and January surveys. The doming isotherms in Figure 4.4-21 show it to be a deep large feature with a diameter of about 200 km. The curvature of the isotherms is greatest below 10°C; above 15°C, they are flat. Figure 4.4-20 shows that Eddy Z lies entirely over the continental slope between the 200m and 2000m isobaths. The vertical axis of its core tilts southeastward from bottom to top.

4.4.4.2.2 Salinity

The strength and distribution of the subsurface salinity maximum of Subtropical Underwater observed in January demonstrates how little the central core of Eddy B was affected by mixing processes during the 7 months since being shed by the Loop Current. Figure 4.4-22 is a vertical transect of salinity using CTD stations along Line I. (See Section 2.3.4, p. 22, for the locations of the stations). Values greater than 36.6 ppt occur in a layer 80m thick just above 200m in the center of Eddy B and stretch from Station 88 to Station 138, a distance of more than 150 km. Vertical salinity transects along Lines D and F are shown in Figure 4.4-23. These lines run perpendicular to both the

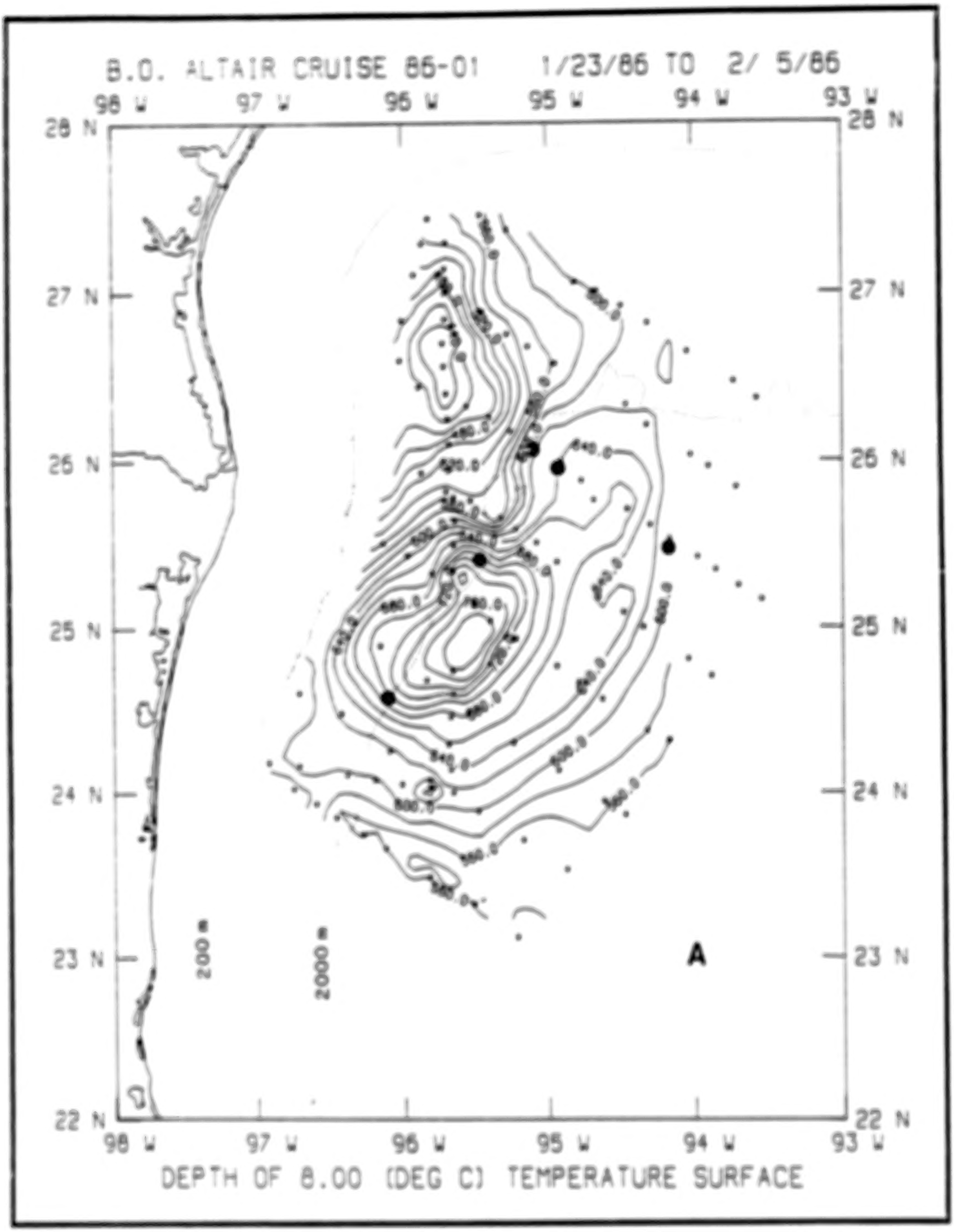
B.O. ALTAIR CRUISE 86-01 1/23/86 TO 2/ 5/86
98 W
97 W
96 W
95 W
94 W
93 W
28 N
27 N
26 N
25 N
24 N
23 N
22 N
200 m
2000 m
A
DEPTH OF 8.00 (DEG C) TEMPERATURE SURFACE

Figure 4.4-20a. Topography of the 8°C temperature surface based on XBT data collected during the January 1986 B/O ALTAIR cruise.

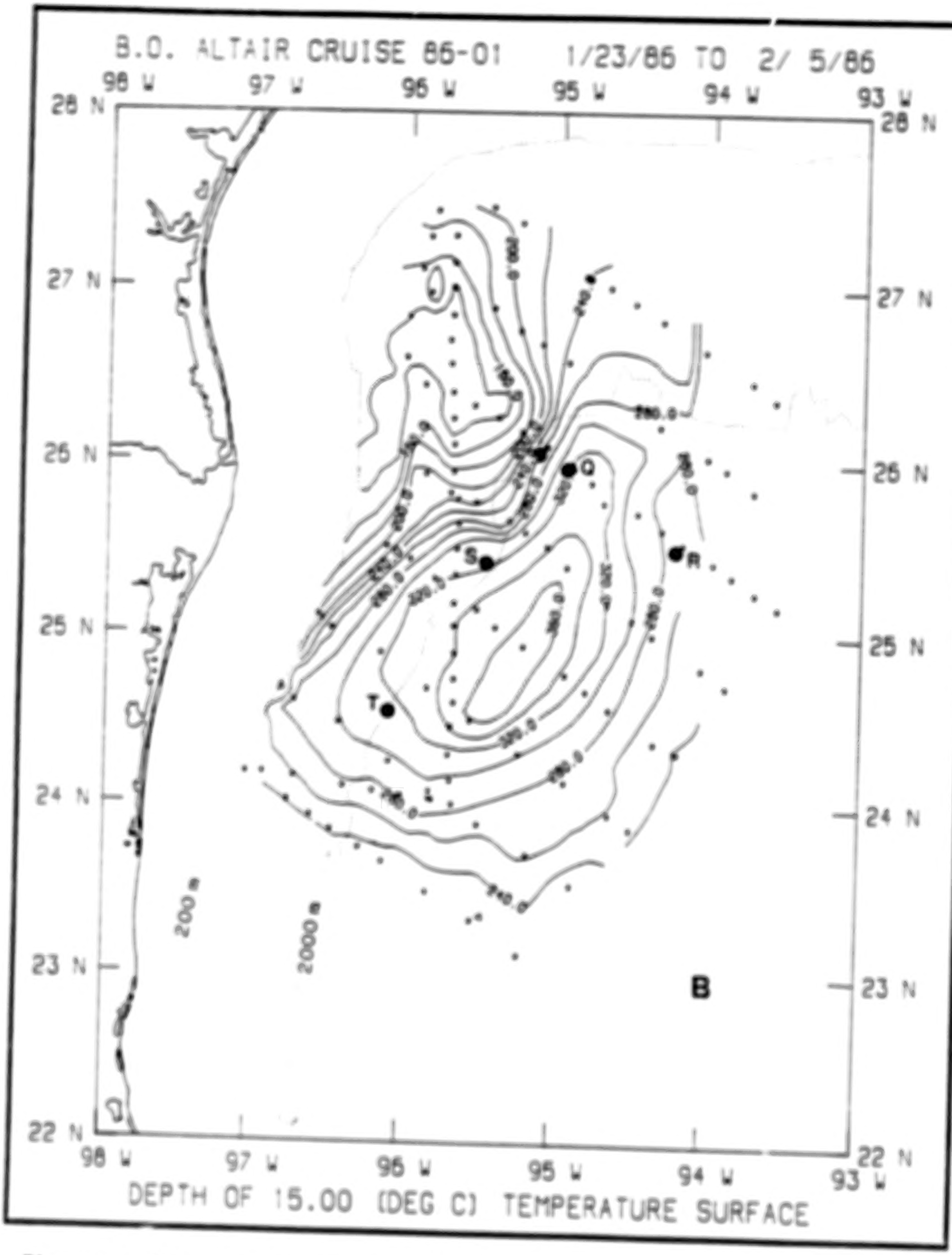

Figure 4.4-20b. Topography of the 15°C temperature surface based on XBT data collected during the January 1986 B/O ALTAIR cruise.

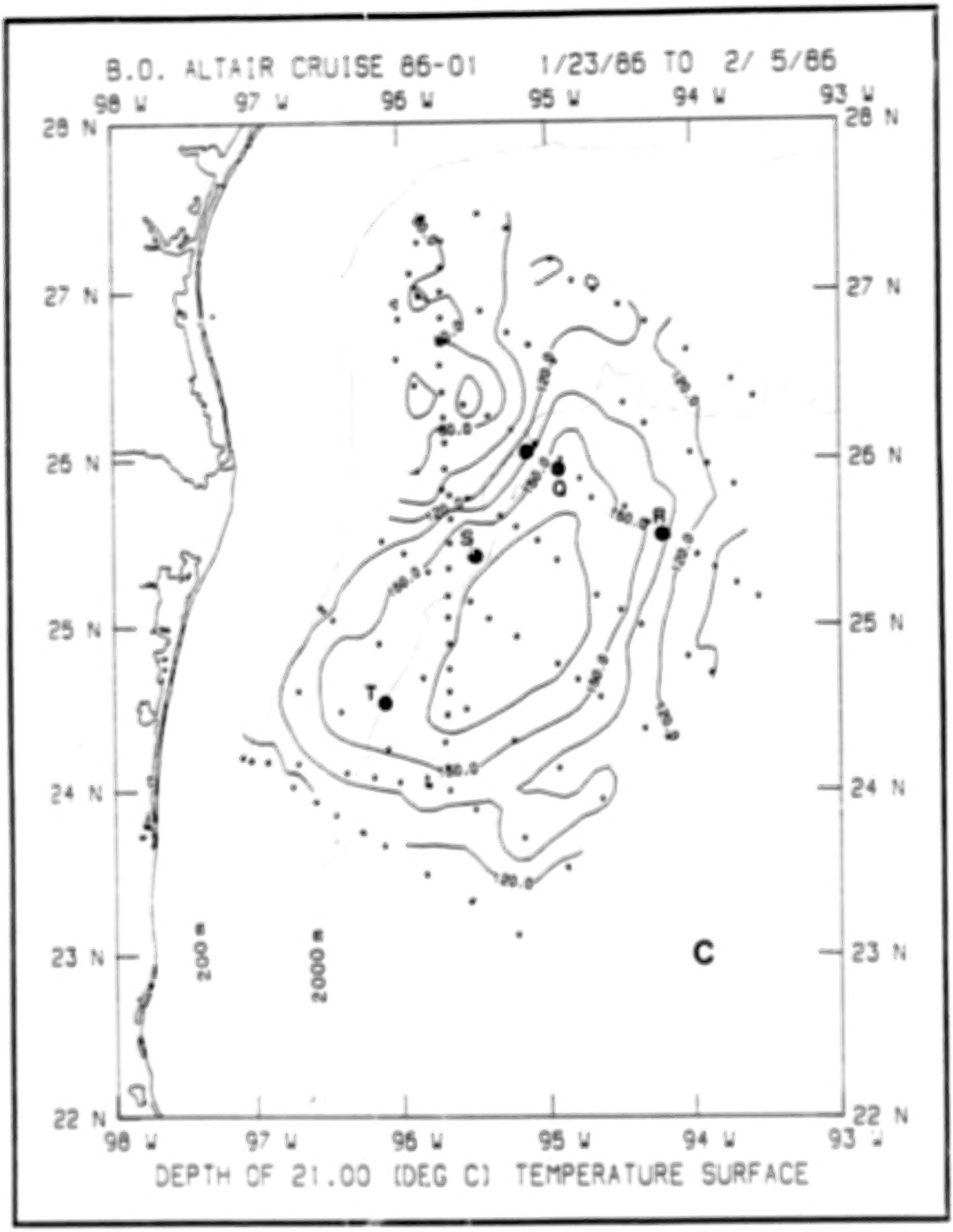
B.O. ALTAIR CRUISE 86-01 1/23/86 TO 2/ 5/86
98 W
97 W
96 W
95 W
94 W
93 W
28 N
27 N
26 N
25 N
24 N
23 N
22 N
120.0
150.0
180.0
Q
R
S
T
C
200 m
2000 m
DEPTH OF 21.00 (DEG C) TEMPERATURE SURFACE

Figure 4.4-20c. Topography of the 21°C temperature surface based on XBT data collected during the January 1986 B/O ALTAIR cruise.

Cruise	750m	700m	650m	600m	550m
October 1985	1.3	9.0	26.0	50.0	97.0
November 1985	0.0	2.7	26.0	48.0	85.0
January 1986	2.6	7.8	17.0	50.0	--
April 1986	0.3	2.4	8.1	24.0	--

Table 4.4-2. Areas (10^3 km^2) of Eddy B inside the given contours of the topography of the 8°C temperature surface.

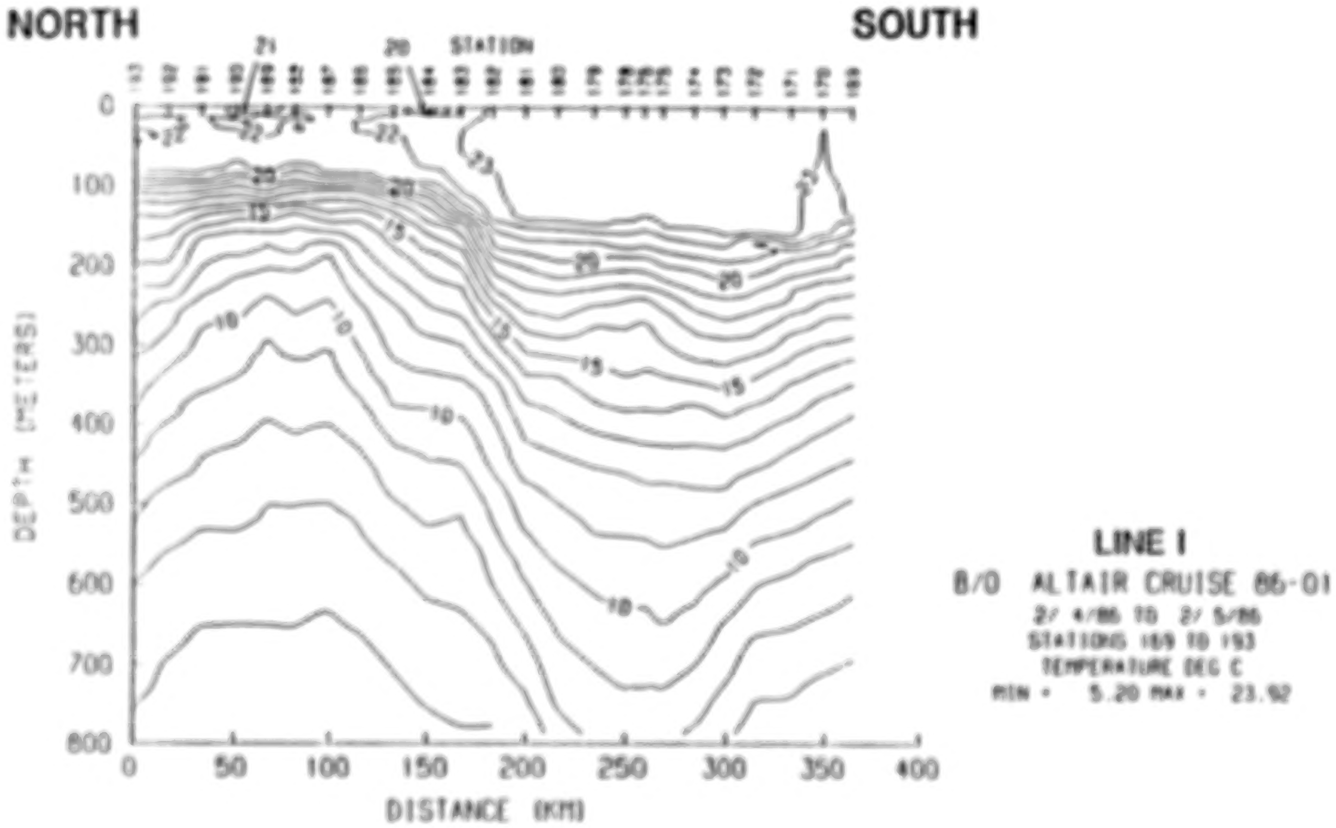

Figure 4.4-21. Vertical section of temperature to 800m along Line I of the January 1986 B/O ALTAIR cruise, passing through the centers of Eddy B and Eddy Z (based on XBT data).

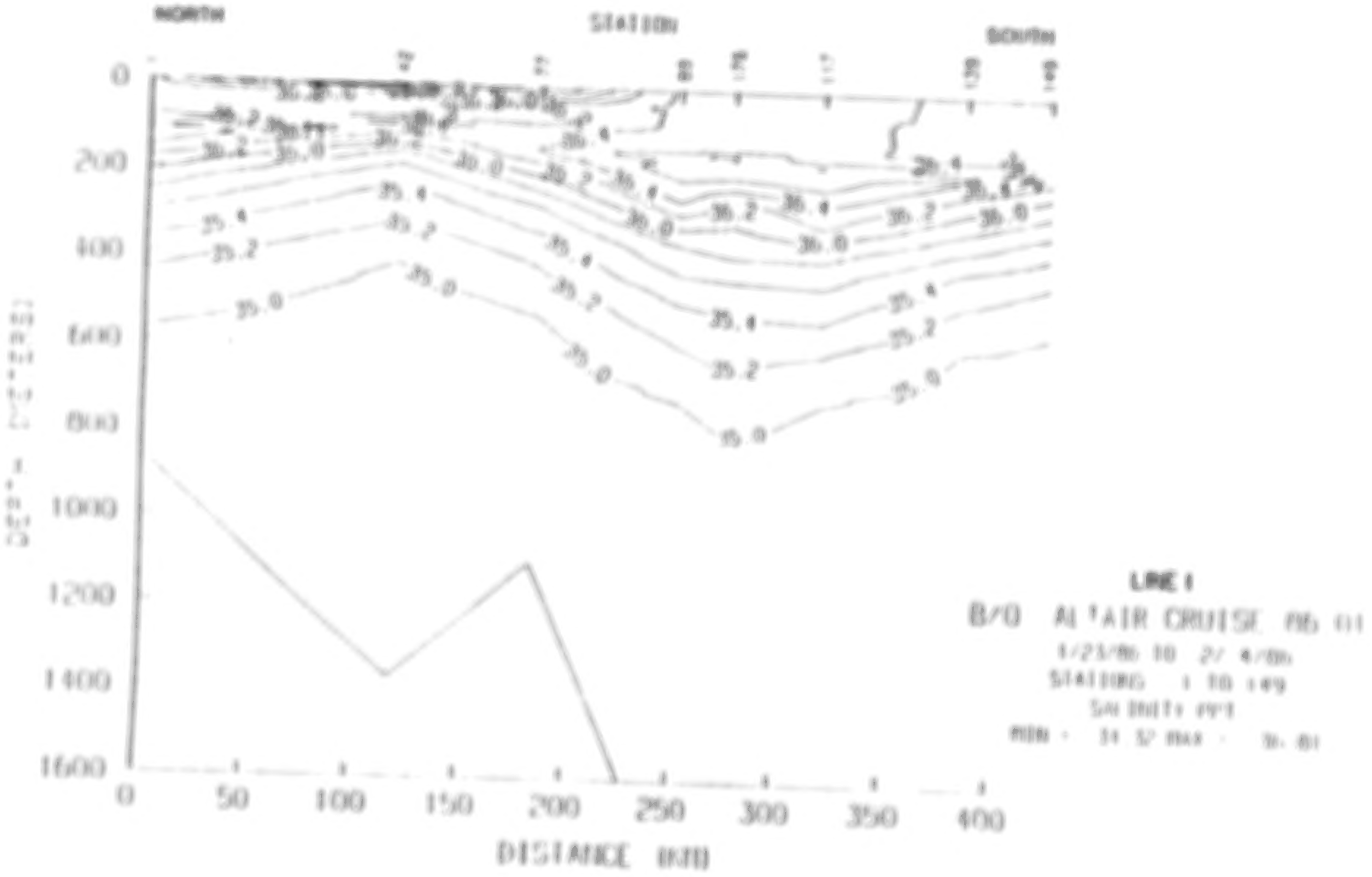

Figure 4.4-22. Vertical section of salinity to 1500m along Line 1 of the January 1986 B/O ALTAIR cruise. See Figure 2.3-3 for location of Line I.

172

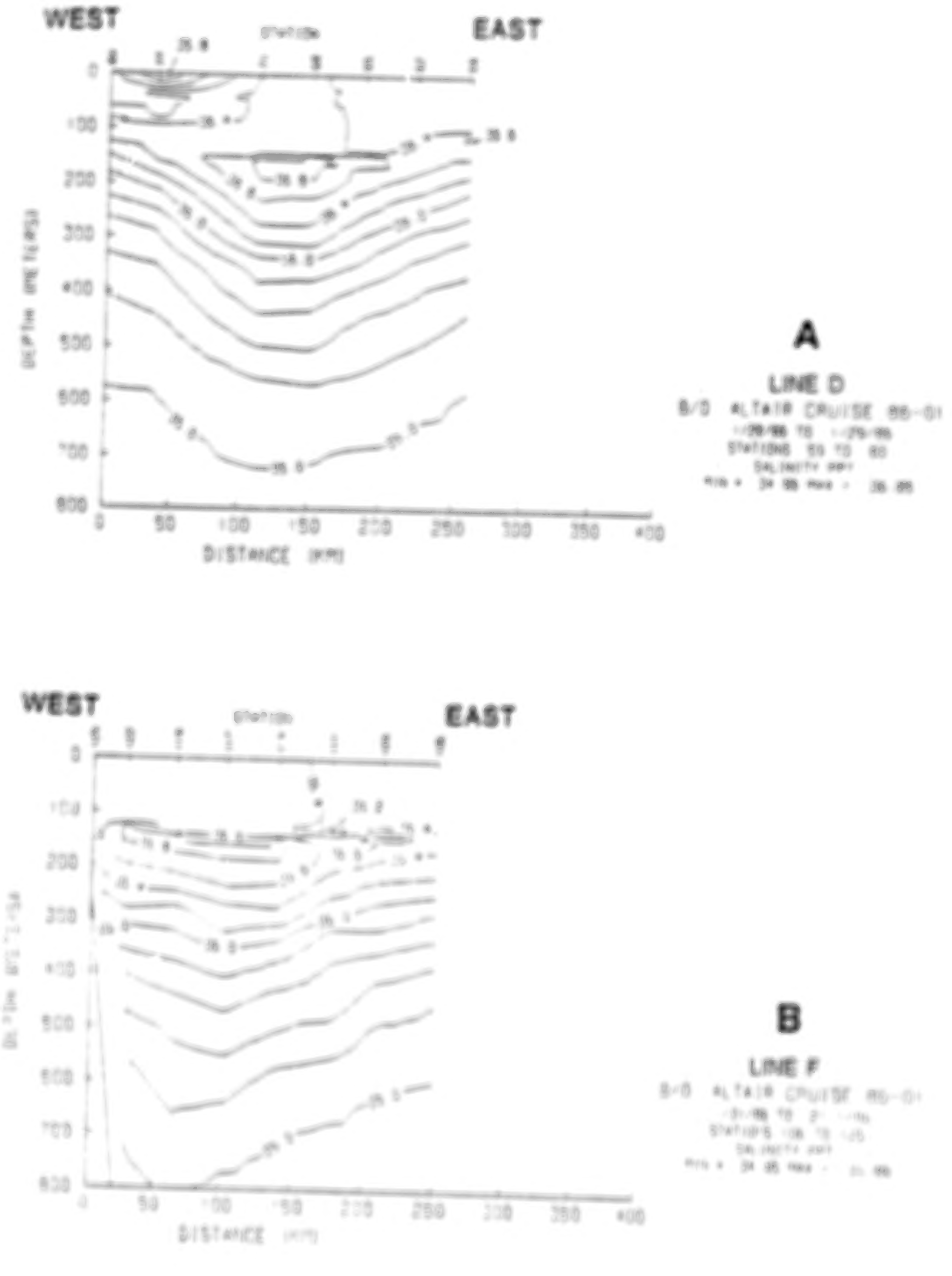

Figure 4.4-23. Vertical section of salinity to 800m along (a) Line D and (b) Line F of the January 1986 B/O ALTAIR cruise. See Figure 2.3-3 for locations.

coast and the major axis of the eddy and demonstrate the structure of the high salinity core. In Line F (Figure 4.4-23b) it is more than 150 km wide and extends almost onto the continental shelf. Figure 4.4-24 shows the salinity at 200m, which is slightly below the core of the maximum. The 36.6 ppt contour gives a good idea of the lateral extent of the high salinity water.

To see the change in time of the vertical position and extent of the high salinity core, compare Figure 4.4-23a with the vertical salinity section from the October 1985 cruise (Figure 4.3-14, p. 85) Like the isotherms, the isohalines in the upper part of the eddy in January are shallower by about 100m and less concave. The subsurface maximum is about 40m thinner and flat on the top because of vertical mixing. The winter surface mixed layer is about 150m thick in both cases. Thus the rising high salinity core is gradually eroded at its top as the eddy decays. Elliott (1979) found this process to occur more rapidly in the eddies he studied. It is possible, relatively speaking, that the winter of 1985-1986 was mild, thus increasing the longevity of the subsurface salinity maximum.

At the surface at the western end of Line D (Figure 4.4-23a), there is low salinity water from the shelf that is being drawn off the shelf by the northeastward flow between Eddy Z and Eddy B. This shelf water is also visible in Figure 4.4-22. This was also seen in historical thermal imagery.

Figure 4.4-25 shows the T-S plot for all CTD stations for the January 1986 B/O ALTAIR cruise. The plot forms a thin line below 16°C. Above it, the T-S relation broadens. The high salinity side (right) corresponds to stations in the center of Eddy B, and the low salinity side (left) to stations near the shelf. Figure 4.4-26 shows T-S diagrams for stations in (a) the center of the Loop Current in 1984, (b) the center of Eddy B in October 1985 and (c) the center of Eddy B in January 1986. These curves are identical below about 22°C. Above it they differ only in the extent to which mixing has eroded the top of the salinity maximum. The figures also indicate the high quality of the data, since the data were collected on different cruises using different instruments.

4.4.4.2.3 Nutrients

Figure 4.4-27 contains the vertical sections along Line I for: (a) dissolve oxygen, (b) silicate and (c) phosphate. Figure 4.4-28 shows composite plots for all stations of sigma-t versus (a) silicate and (b) phosphate. Oxygen values are greatest in the near-surface waters where values reach 5.0 ml l^{-1}. Oxygen content decreases with depth to a minimum of less than 2.6 ml l^{-1} near 400m and then increases with depth. Lowest values occur in the centers of Eddy B and Eddy Z. Between them, oxygen values in the minimum layer are slightly elevated at Station 77, which is in the region of strong northeastward flow. Silicate values increase monotonically from minimum values near the surface to maximum values of about 27 ug-at l^{-1} between 1000m and 1200m. Sigma-t at the silicate maximum is 27.7 (Figure 4.4-28a). Phosphate values also increase downward from the near surface to a maximum between about 600m and 800m. Sigma-t at the phosphate maximum is 27.4 (Figure 4.4-28b). Phosphate values in the maximum layer are greatest north of Station 176, but this may be an artifact caused by instrument drift since the values decrease with increasing station number.

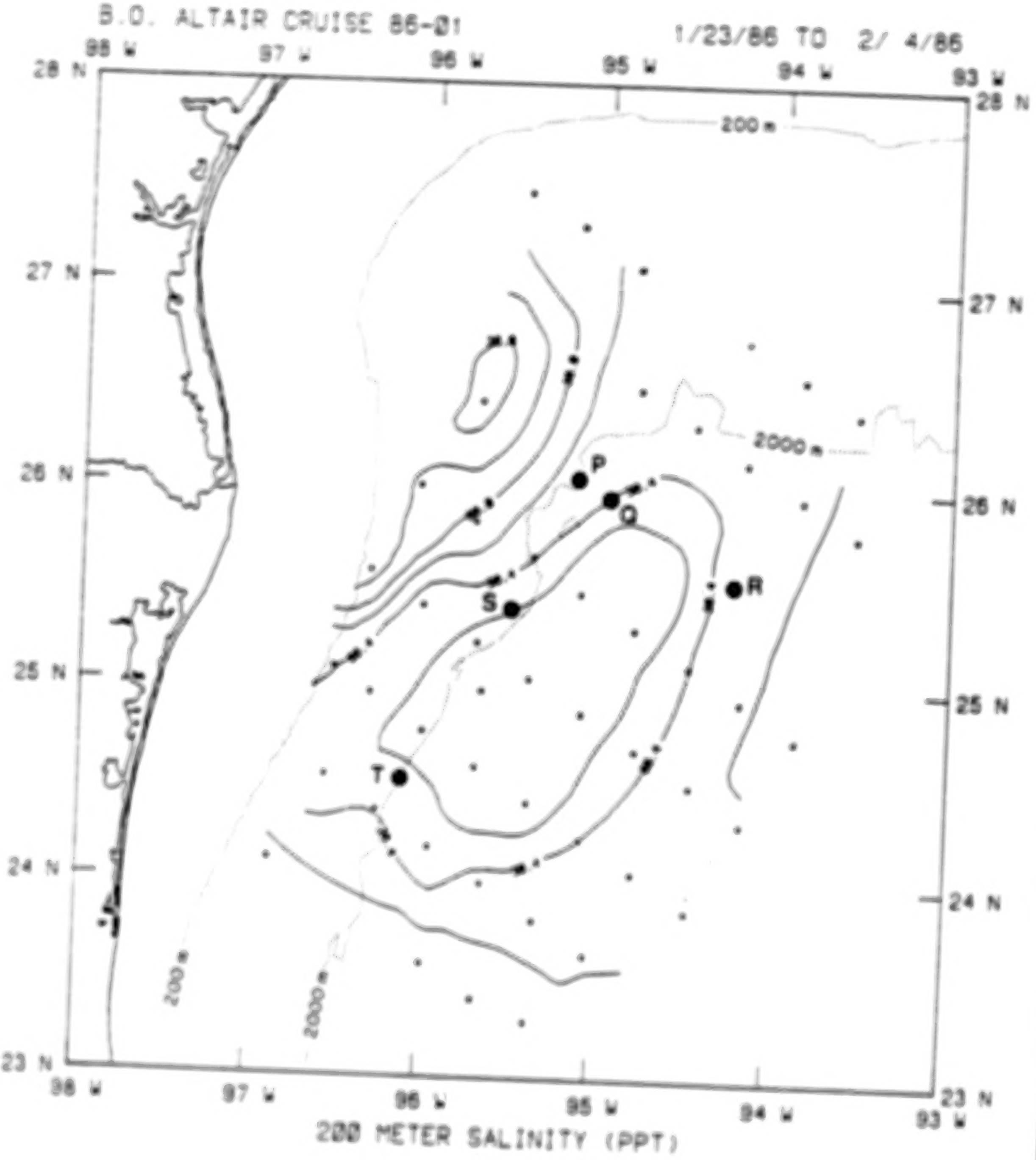

Figure 4.4-24. Salinity distribution at 200m during the January 1986 B/O ALTAIR cruise.

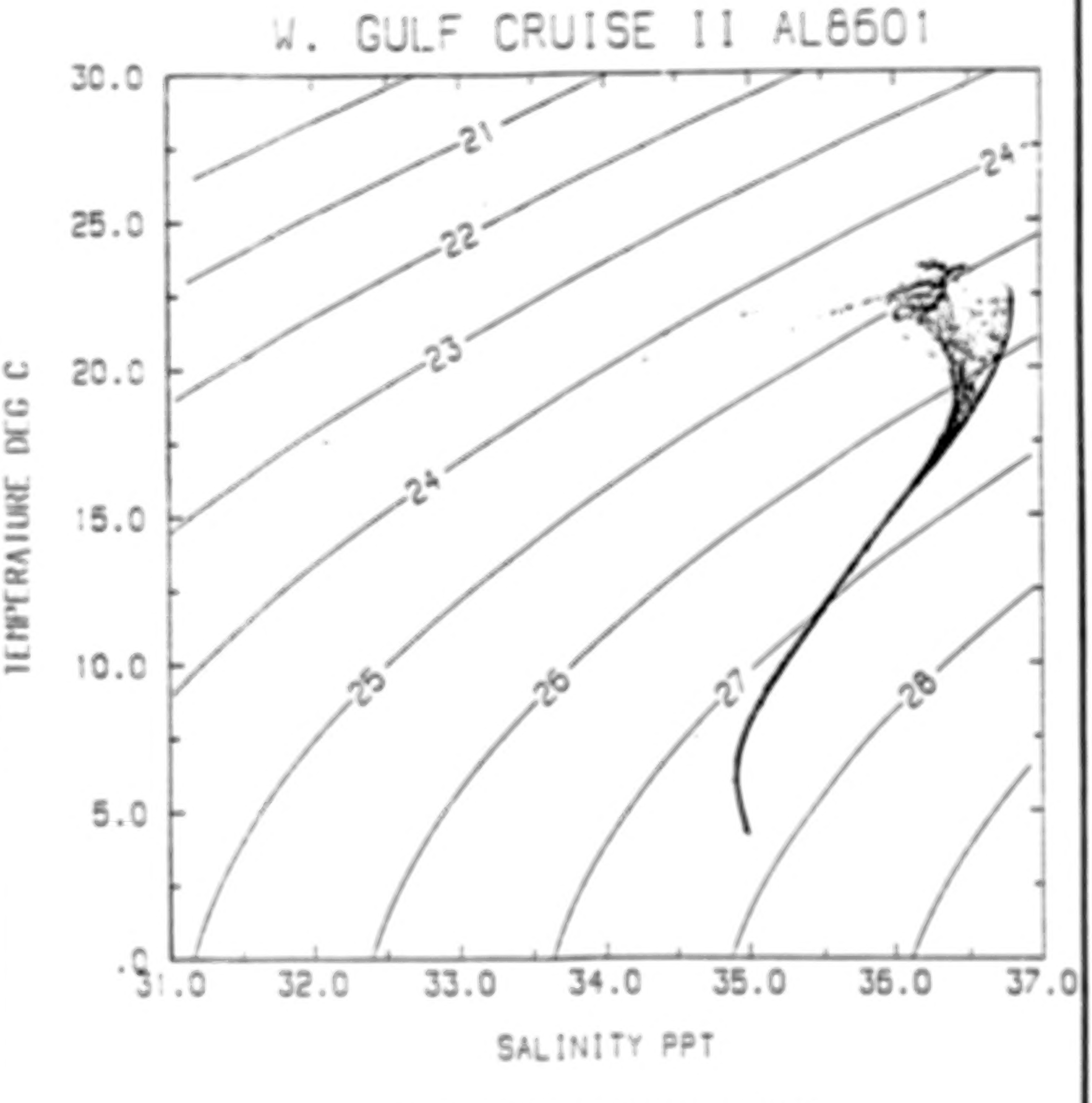

Figure 4.4-25. Composite T-S plot of all CTD data collected during the January 1986 R/O ALTAIR cruise.

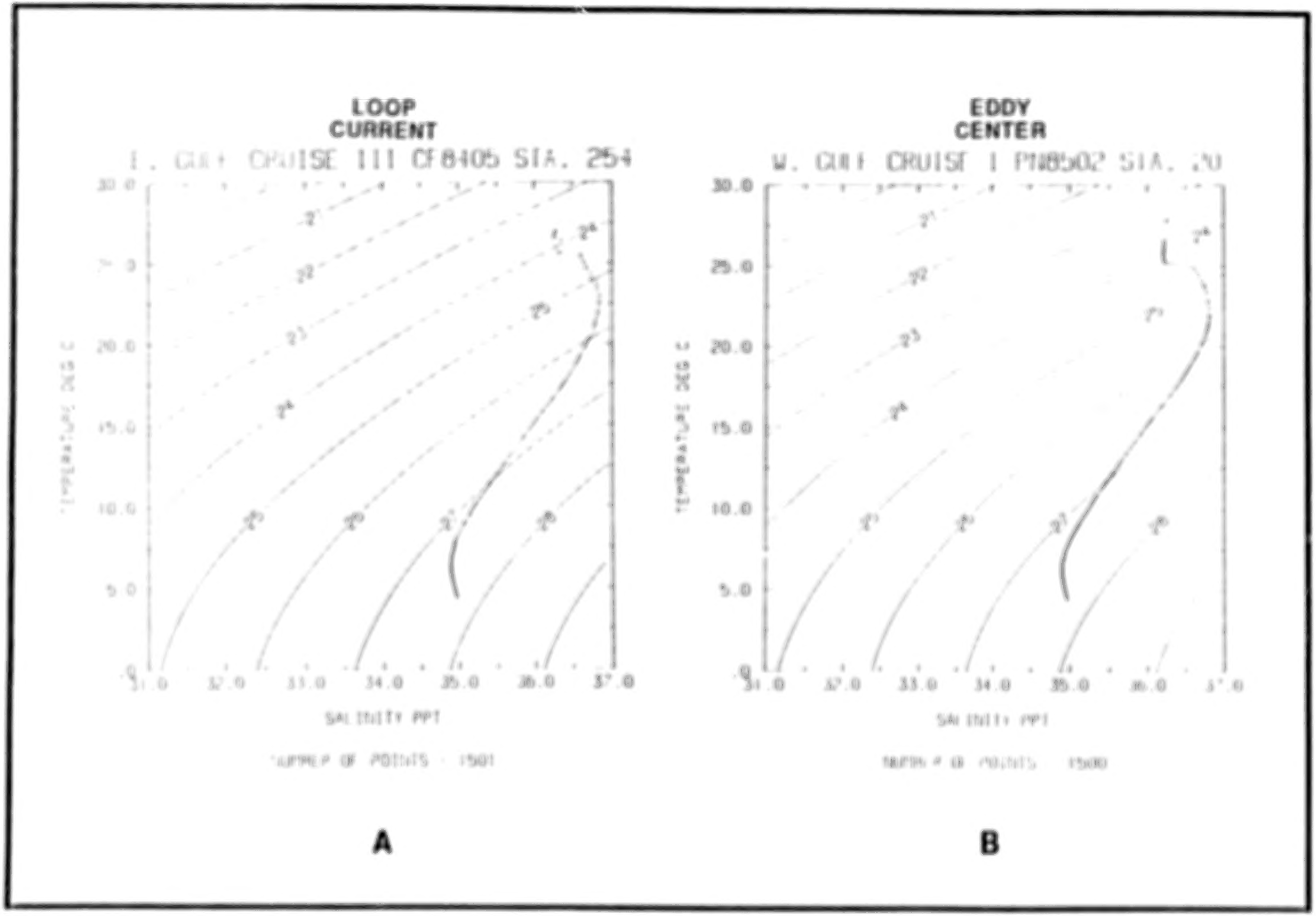

Figure 4.4-26a-b. T-S diagram of: (a) Station 254 in the Loop Current from an eastern Gulf cruise in May 1984 and (b) Station 20 in the center of Eddy B in October 1986.

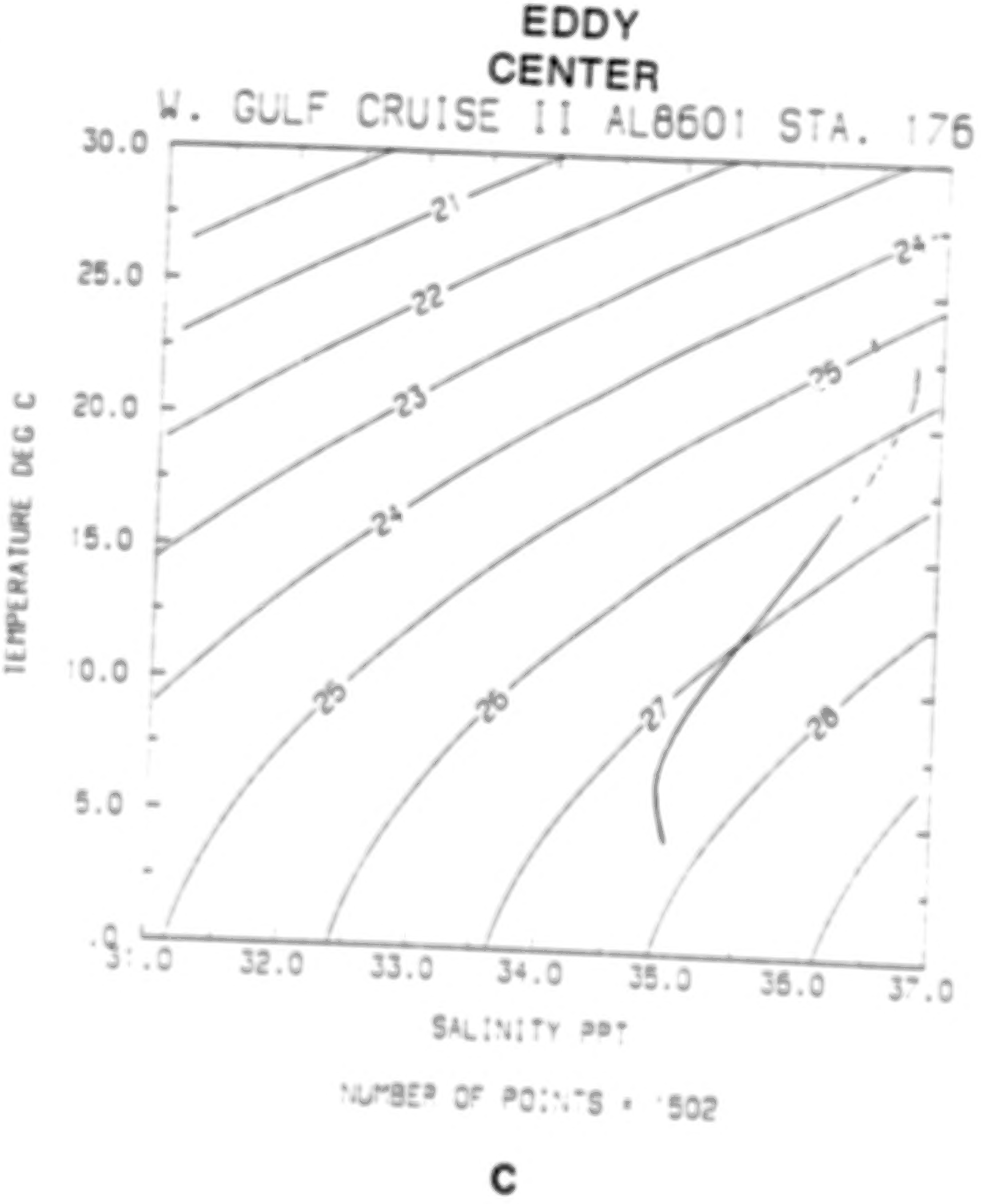

Figure 4.4-26c. T-S diagram of Station 176 in the center of Eddy B in January 1986.

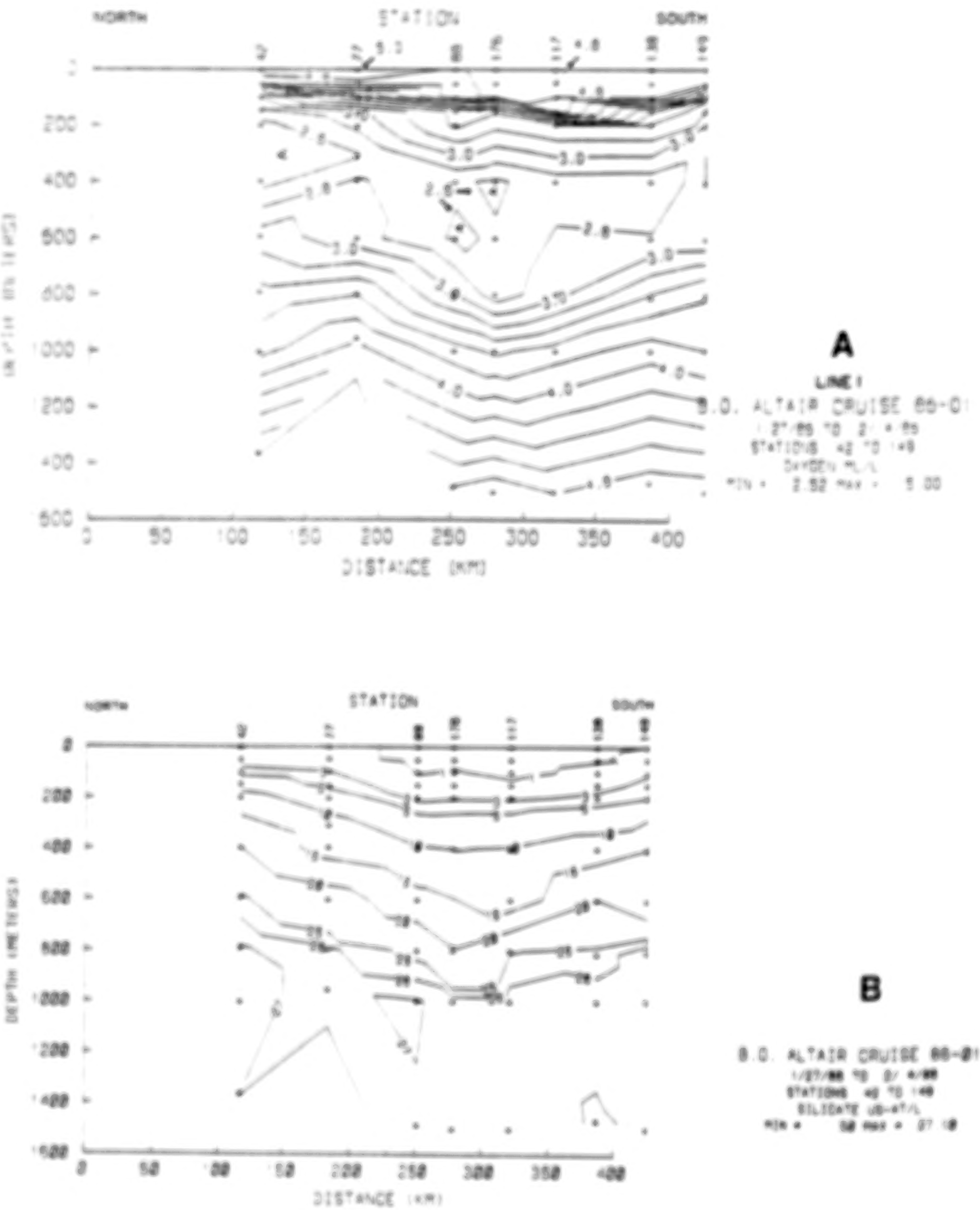

Figure 4.4-27a-b. Vertical section of: (a) dissolved oxygen and (b) silicate to 1500m depth along Line I for January 1986.

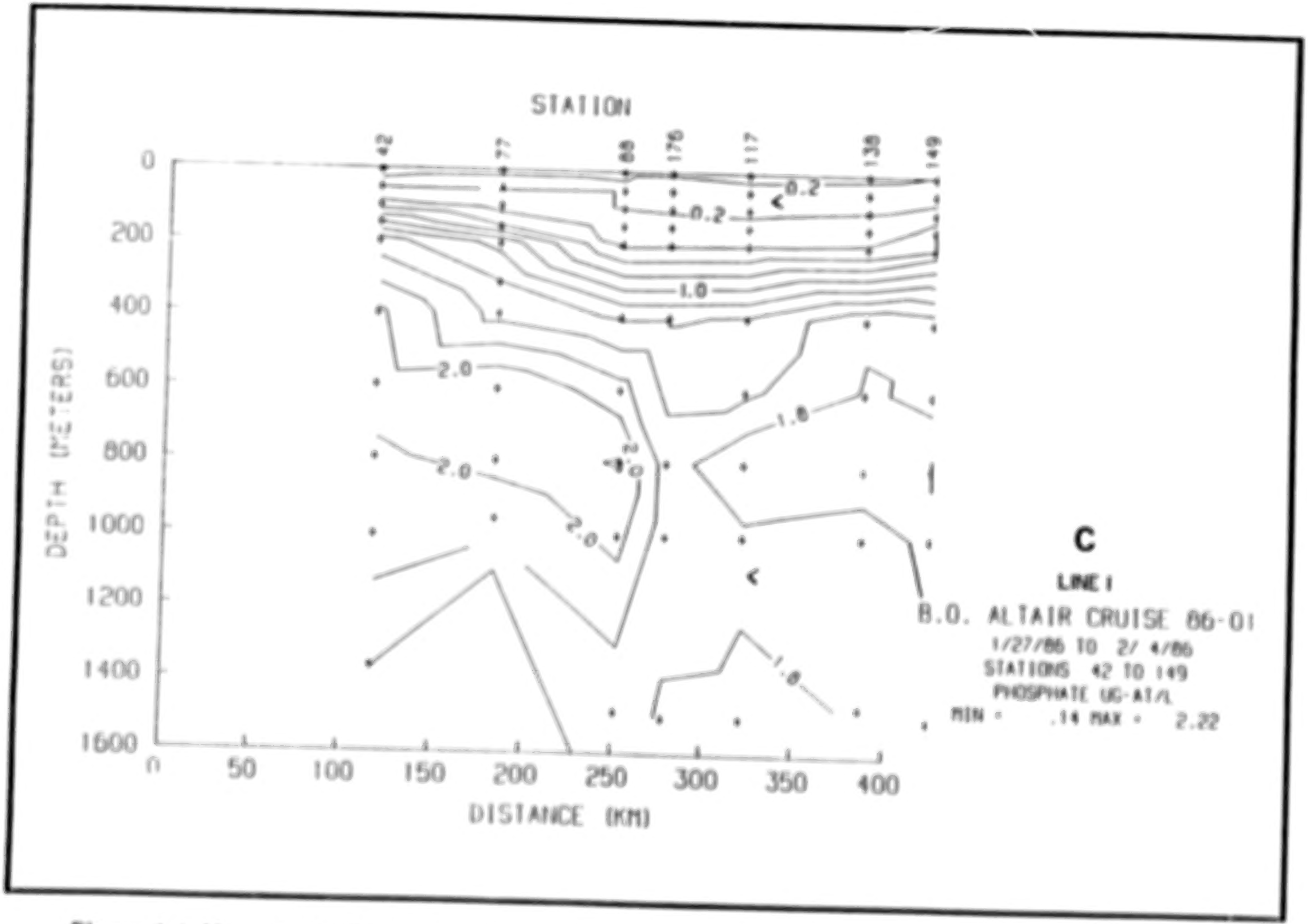

Figure 4.4-27c. Vertical section of phosphate to 1500m depth along Line I for January 1986.

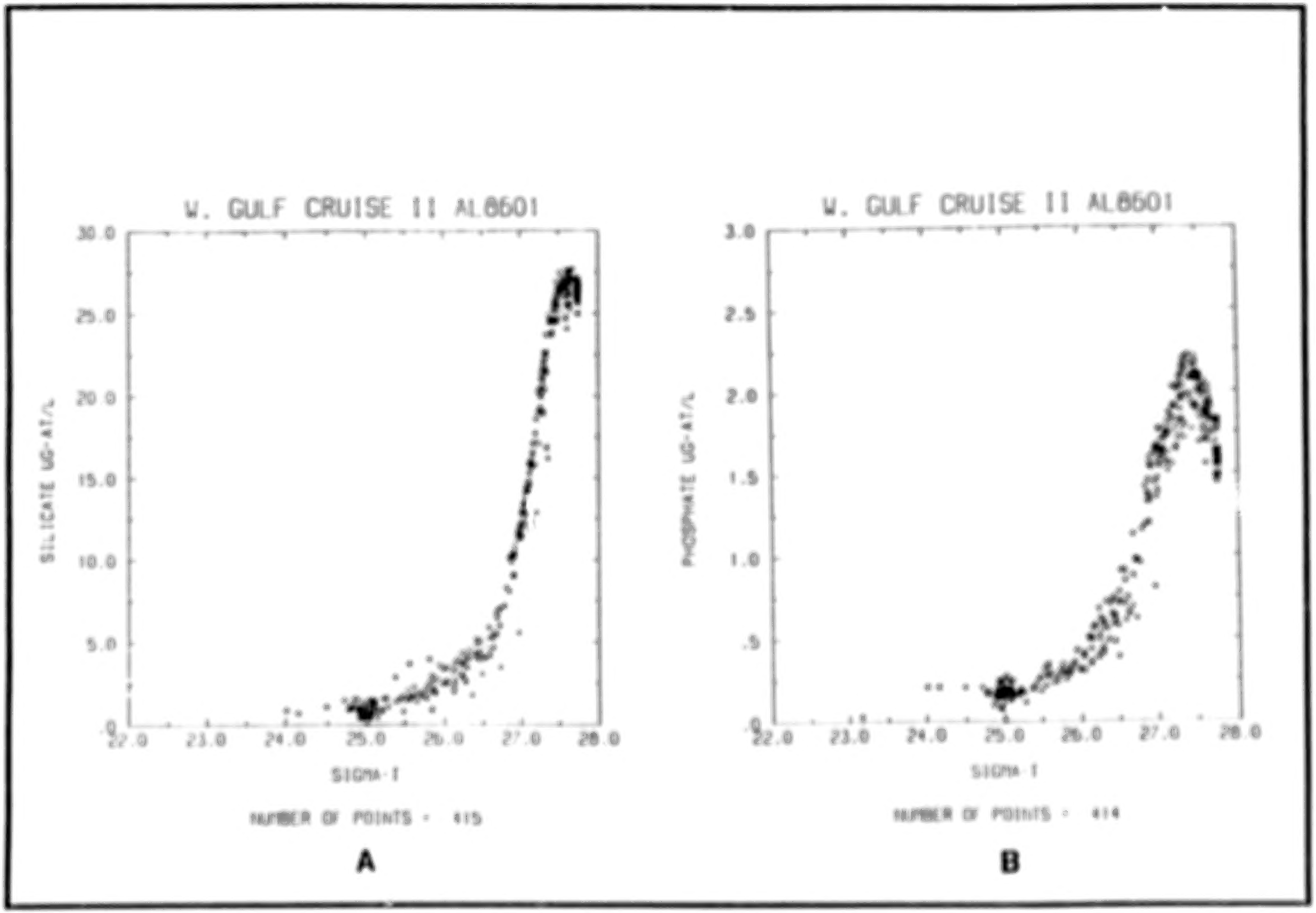

Figure 4.4-28. Composite plots of: (a) silicate versus sigma-t and (b) phosphate versus sigma-t for all data from the January 1986 R/O ALTAIR cruise.

4.4.4.2.4 The Question of Interaction between Eddy A and Eddy B

Figure 4.4-29 shows the trajectory of ARGOS Drifter 3353 from the time it was placed in Eddy A to the end of the January 1986 R/V ALTAIR cruise. After making a partial revolution around Eddy A, it became entrained in a cyclonic feature. It made one cyclonic revolution and then escaped, becoming entrained in Eddy B. During the first part of January, the orbits of Drifter 3353 and Drifter 3378 (Figure 4.2-7, p. 58) passed as far south as 23°N, near the position of Eddy A in November 1985. The behavior of the drifters and sea- surface temperature patterns suggest a merging of the eddies (Section 4.4.3, p. 152). This is highly speculative since there are no subsurface hydrographic observations in the region of Eddy A before or after the hypothesized event. The original structure and hydrographic properties of Eddy A are unknown, and after Drifter 3353 left it in November there is no information about its location or its existence. Some of the material printed above argues against a merging. It has been shown in this section that the deep core of Eddy B was relatively constant in size through January and that its outer part actually eroded away. In the upper part of Eddy B the structure of the core of high salinity also indicates no change except that due to very gradual mixing at the base of the mixed layer. A merging of Eddies A and B would seem to have to occur in the upper periphery if it occurred. Drifter data is consistent with this.

4.4.5 Subsurface Currents

4.4.5.1 Time Domain Description

During the second deployment period, the experiment yielded data in the upper layer at 300m at Moorings Q and T (Figure 4.4-30). With insight provided by the information from Drifter 3378 (Figures 4.2-5, p. 56; 4.2-7, p. 58; 4.2-9, p. 61 and 4.2-10, p. 62) and the two surveys of Eddy B (Figures 4.2-8, p. 59 and 4.2-11, p. 63), it is easier to understand the patterns of upper level currents than it was for the first deployment period, even though data was available at more locations during the first deployment period. For example, during the last half of November and the first half of December, the center of Eddy B lay offshore of Mooring T and an elliptical northward extension is indicated; the flow was northward at Mooring T on the eddy's west side and southward at Mooring Q on the east side of the extension.

Between mid-December and late January, Eddy B pressed closer to the slope and its major axis rotated slightly clockwise. The currents at Mooring T accelerated strongly, reaching a maximum speed at 300m of about 65 cm sec^{-1}, while at Mooring Q they rotated counterclockwise as the elliptical extension passed to the east side of the mooring. From February to the end of the record the main part of Eddy B moved offslope, then southward and then back towards the slope to a point just south of Mooring T. The currents at Mooring T accordingly decreased then increased and rotated clockwise, eventually becoming eastward on the north side of Eddy B. At Mooring Q the currents rotated clockwise as the elliptical extension retreated southward and rotated slightly counterclockwise (cf. Figures 4.2-8, p. 59 and 4.2-11, p. 63).

The currents at Mooring Q give no indication of behavior, such as occurred at Mooring S during the first deployment period (Figure 4.3-27, p. 105), that would indicate the presence of a cyclone. Therefore, the origins of the cyclone indicated in the survey in early May are unknown.

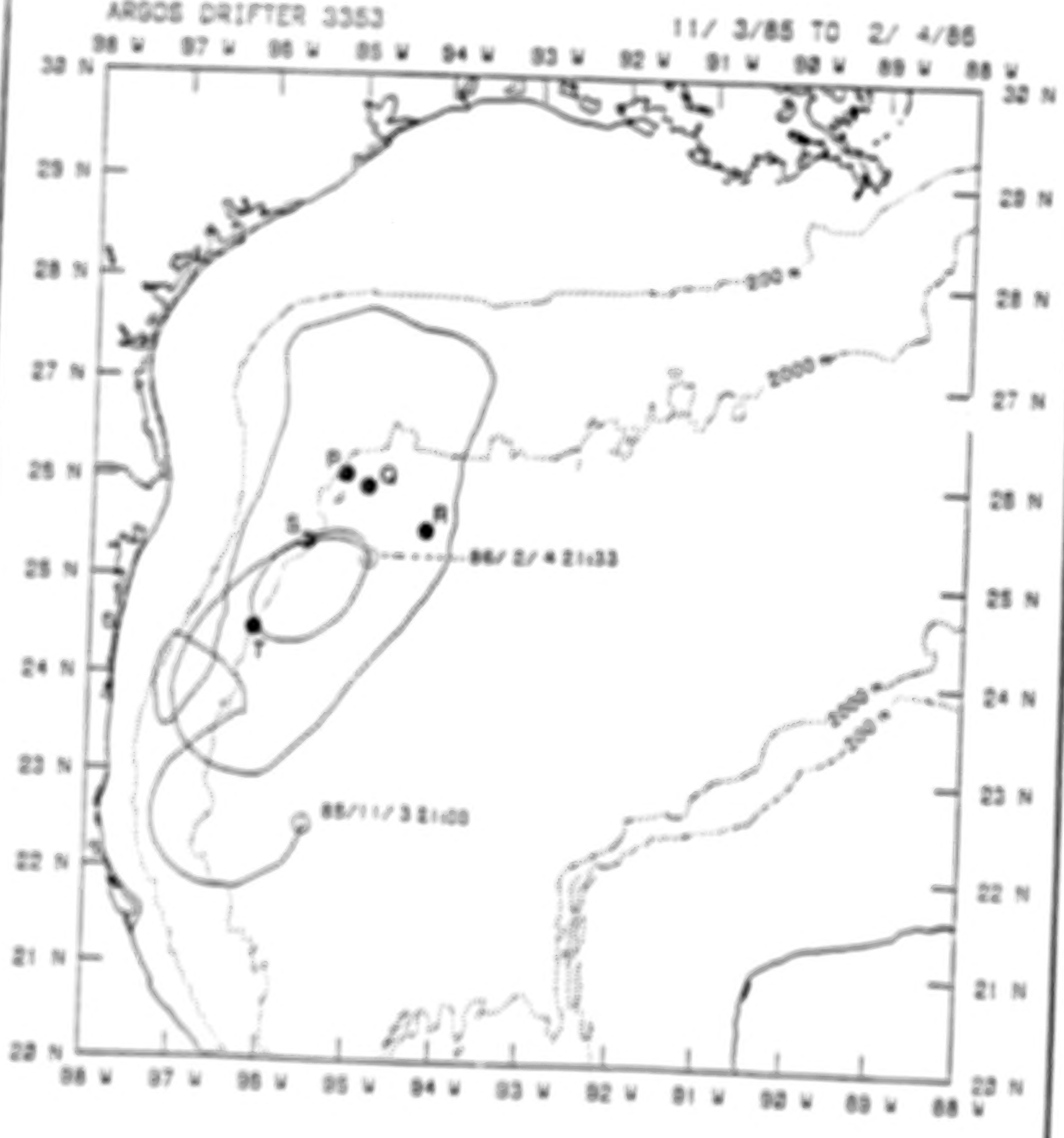

Figure 4.4-29. Trajectory of Drifter 3353 from November 3, 1985 to February 4, 1986.

BLANK

PAGE

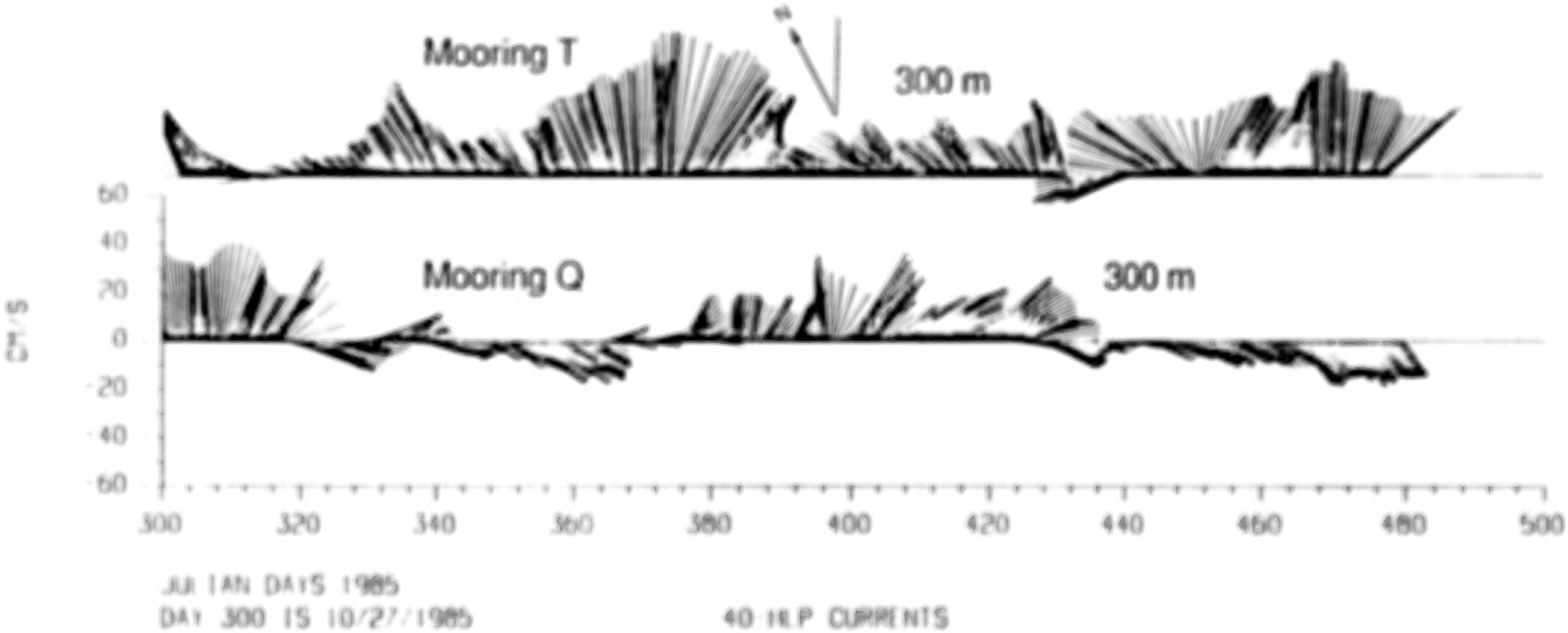

Figure 4.4-30. Stick plots of 40-hour, low-passed currents at 300m at Moorings Q and T for the second deployment period. Vertically up (+V) is towards 30°.

The time-series of the second deployment period were joined to those of the first, where possible, and filtered with a 7-day, low-pass filter to present them in a compact form for comparison. In Figure 4.4-31, which shows the current vectors in stick form, vertically up is also towards 30°T. The currents in the lower layer do not reflect to any great degree the influence of the strong baroclinic flow in the upper layer associated with Eddy B except, perhaps, at Moorings T and P at 1000m during late December and early January (Days 360-380). The lower layer currents also do not exhibit much visual correlation between moorings, suggesting that either the data sets have low signal-to-noise ratios or the observations are linearly independent.

At any given instrument location, however, the time-series of each deployment period are strikingly similar in nature. At Mooring P at 1500m, for instance, the currents are predominantly in the negative V direction and have a weak 40-day periodicity. The currents at 1500m at Mooring Q show a distinct clockwise rotation from the positive V direction. The currents at 1000m at Mooring S are weak throughout the record, and fluctuations occur at a gross 20-day interval. Such self-similarity in the records suggests that the processes in the lower layer at a given location were the same during both deployment periods despite the differences in the strength and location of the baroclinic eddy events occurring in the upper layer.

Figure 4.4-32 shows the time-series of temperature in the same format as Figure 4.4-31. The warming at 300m at Mooring T from mid-November through early March (Days 320-435) reflects the persistent presence of Eddy B. Figures 4.4-32 and 4.4-33 show the effect of the northward elongation of Eddy B at 1000m at Mooring P as elevated temperature values from November 21 through January 25 (Days 325-390). The temperature records at 1000m reveal two events that propagated along the continental slope. (They are marked in Figure 4.4-32 by dashed lines). The first began at Mooring T on November 4 (Day 308), when the temperature rose to a maximum and then moved past Mooring S, reaching Mooring P on December 2 (Day 336), which translates into a rate of 6.8 km day^{-1}. The source of the event can be seen in Figure 4.2-6 (p. 57) as the lobe protruding westward towards Mooring S. The second event was caused by the southward movement of Eddy Z that caused temperature to decrease, reaching a minimum first at Mooring P on February 26 (Day 422) and finally at Mooring T on March 23 (Day 447), a rate of 7.6 km day^{-1}.

As during the first deployment period, the currents of the second period frequently exhibit persistent periods of strong inertial oscillation. To emphasize this characteristic, the time-series from Mooring P at 1000m are shown in Figure 4.4.33 (in the same format as Figure 4.3-33, p. 113). Again, it is not clear what excites the oscillations, but eddies are the principal forcing mechanism in the study region and an obvious candidate. As an example of one line of investigation that future analyses of the data might take, it is noted that Cushman-Roisin (1987) studied the exact analytical solutions for a highly idealized model of elliptical warm eddies and found, among other modes, a pulsating mode in which the vortex alternatively contracts and deepens and then expands and shallows. The frequency of the pulsation is exactly inertial.

4.4.5.2 Basic Characteristics of the Velocity Fields

Statistics of the time-series during the second deployment period are listed in Table 4.4-3. At the 300m and 1000m levels, the vectors reflect the effects of the clockwise rotation of Eddy B that resided in the region for 3-4 months

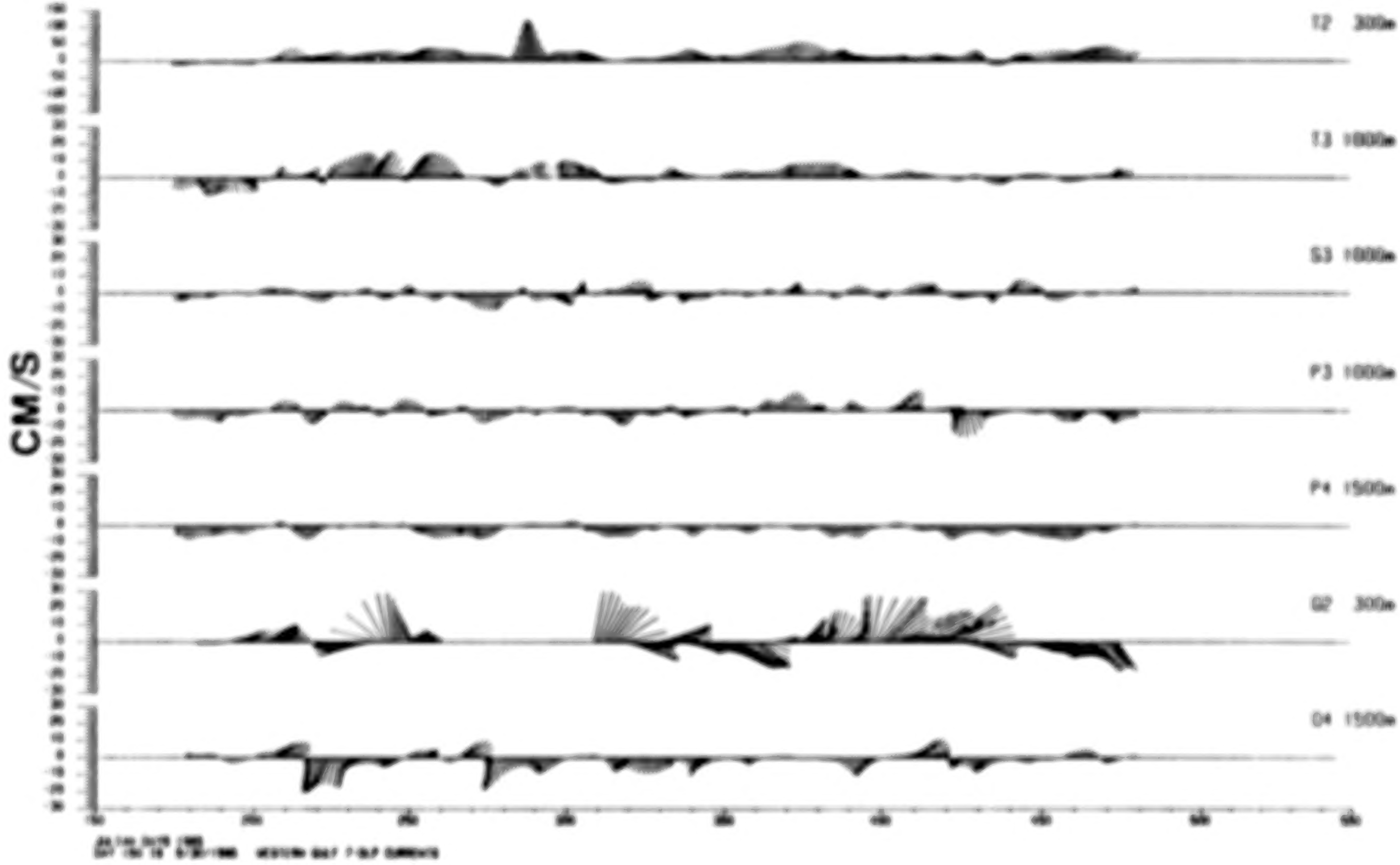

Figure 4.4-31. Stick plots of 7-day, low-passed currents at Moorings T (300m and 1000m), S (1000m), P (1000m and 1500m), and Q (300m and 1500m) for both deployment periods combined. Vertically up (+V) is towards 30°.

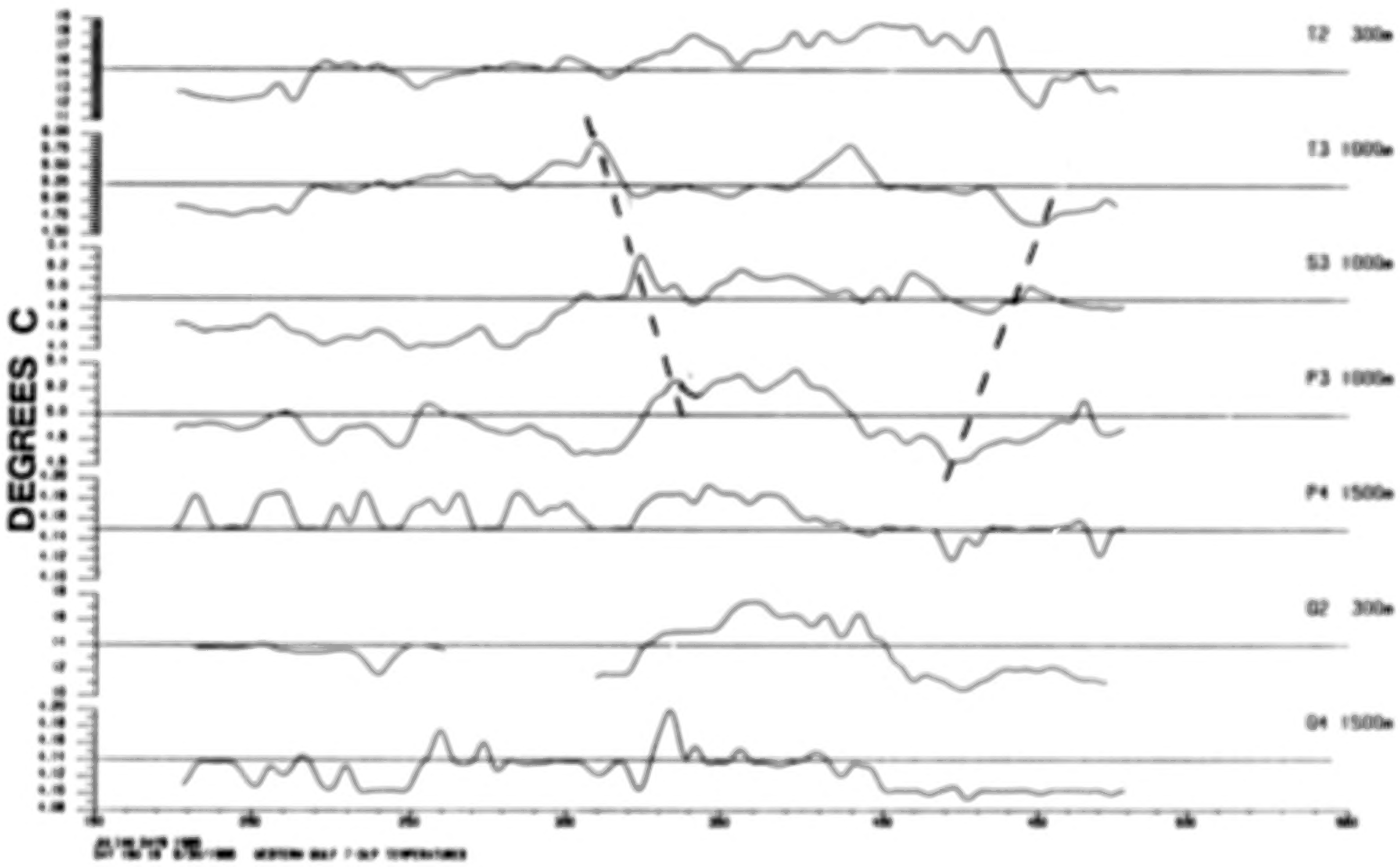

Figure 4.4-32. Plots of 7-day, low-passed temperature at Moorings T (300m and 1000m), S (1000m), P (1000m and 1500m), and Q (300m and 1500m) for both deployment periods combined.

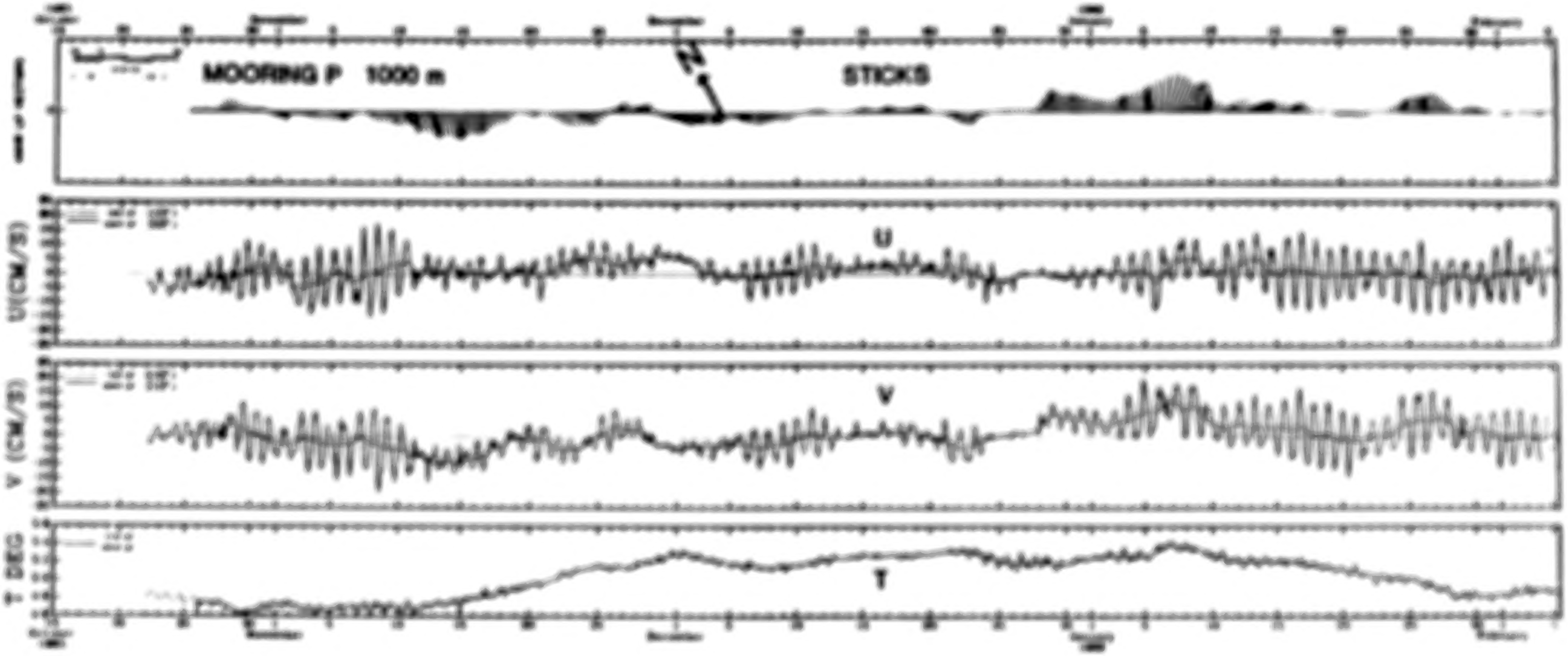

Figure 4.4-33. Time-series plots of 40-hour, low-passed stick vectors, and 3-hour (light line) and 40-hour (heavy line), low-passed U and V components and temperature for the second deployment period at Mooring P at 1000m. Vertically up (+V) is toward 30°.

METER ID	DEPTH(M) WATER DEPTH	DIRECTION OF V-COMPONENT	VARIABLE U,V (CM/S) T(C),P(DB)	MAXIMUM (3-HLP)	MINIMUM (3-HLP)	MEAN	VARIANCE (U'**2)ETC. (3-HLP)	VARIANCE (U'**2)ETC. (40-HLP)	RATIO 40-HLP : 3-HLP KE	ORIENTATION OF PRINCIPAL AXES (DEGREES TRUE)
M2P3	1000 2000	00	U	26.4	-15.1	1.91	29.24	13.41	.541	47.8
			V	26.1	-23.3	-.87	40.08	21.38		
			T	7.44	6.56	6.857	.043	.043		
M2P4	1500	00	U	7.3	-6.3	.22	2.87	1.51	.772	96.9
			V	8.2	-16.3	-2.96	9.87	8.38		
			T	6.23	6.11	6.158	.000	.000		
M2Q2	300 1000	00	U	58.4	-19.3	16.43	137.78	119.80	.869	15.4
			V	67.8	-36.3	3.05	248.85	233.51		
			T	17.74	10.88	13.318	4.655	4.337		
M2Q4	1500	00	U	17.3	-13.4	.22	15.28	14.36	.916	71.6
			V	16.8	-15.3	-1.82	18.51	17.37		
			T	6.21	6.06	6.122	.001	.001		
M2S3	1000 1400	00	U	26.1	-14.1	1.34	16.18	8.36	.612	65.1
			V	15.7	-13.3	.43	19.56	13.80		
			T	5.38	4.69	4.961	.017	.016		
M2T2	300 2200	00	U	49.7	-47.4	-8.66	337.52	347.71	.969	91.6
			V	66.3	-16.3	21.58	187.48	180.86		
			T	19.12	12.50	16.486	2.306	2.010		
M2T3	1000	00	U	14.2	-21.0	-1.50	17.58	11.88	.703	61.8
			V	18.3	-11.6	2.54	35.24	19.64		
			T	6.00	4.83	5.207	.083	.081		

Table 4.4-3. Basic statistics of the U and V components of current and of temperature over the available record lengths at Moorings P, Q, S and T for the second deployment period: October 22, 1985 through May 1, 1986.

of the deployment period. At 1500m the mean flow at Moorings P and Q is parallel to the topography and is directed southwest, just as it was during the first deployment period (Figure 4.3-34, p. 115).

The ratio of the variance of the U and V components at Mooring P in the lower layer also reflects topographic steering. At Moorings Q, S and T, however, the component variances are similar in magnitude, unlike those of the first period. In the upper layer the V component is twice the U component at Mooring Q, while the opposite is true at Mooring T.

As illustrated in Table 4.4-3, the ratio of 40-hour, low pass kinetic energy to 3-hour, low pass kinetic energy is less for instruments at depths of 1000m or greater on moorings placed on or near the 2000m isobath. During the first deployment, the proportion of kinetic energy at periods shorter than 40 hours was less than during the second deployment because the inertial period fluctuations were more vigorous during the second deployment when Eddy B was closer to the moorings.

4.4.5.3 Frequency Domain Description

4.4.5.3.1 Autospectra

Autospectra of U and V components of current velocity and temperature for Mooring Q at 300m and 1500m are shown in Figure 4.4-35. The spectra follow the pattern stated in Section 4.3.5.3 (p. 116). Minor peaks occur for all three components at periods of 3-5 days and 5-10 days. In the temperature spectra, the variance near the diurnal period is much weaker than for the first deployment period, deviating from the pattern somewhat. The kinetic energy at 1500m is uniformly about one order of magnitude less than that at 300m (note the decade offset). The autospectra of the other time series from the second deployment period are briefly described, but plots are not shown because of their similarity to Figure 4.4-35 and to the first deployment period.

The autospectrum of the U component at 1500m at Mooring P shows numerous peaks at periods of 2-10 days, but fluctuations corresponding to them in the time domain (Figure 4.4-31) are not apparent because their amplitudes are small compared to those of the V component. On the other hand, the long period fluctuations on the order of 40 days in the V component, noted in the time-domain discussion, are not readily apparent in the autospectrum, except as a plateau, because they are not quite periodic and the record length is only 171 days. Energy near the diurnal period is, as during the first deployment, very high. The temperature autospectra at both the 1000m and 1500m levels are similar to those of the first deployment.

As the time series plots (Figures 4.4-31 and 4.4-32) would suggest, the autospectra of U, V and T at 1000m at Mooring S are similar to those of the first deployment period. The autospectra of U, V and T at both levels at Mooring T follow the pattern, decreasing by three orders of magnitude as period decreases and rising by one to two orders near the diurnal period, except for temperature at 300m.

4.4.5.3.2 Rotary Spectra

Figure 4.4-36 shows the rotary spectra at 1000m for all three moorings along the continental slope. The dominant feature is the large amount of inertial

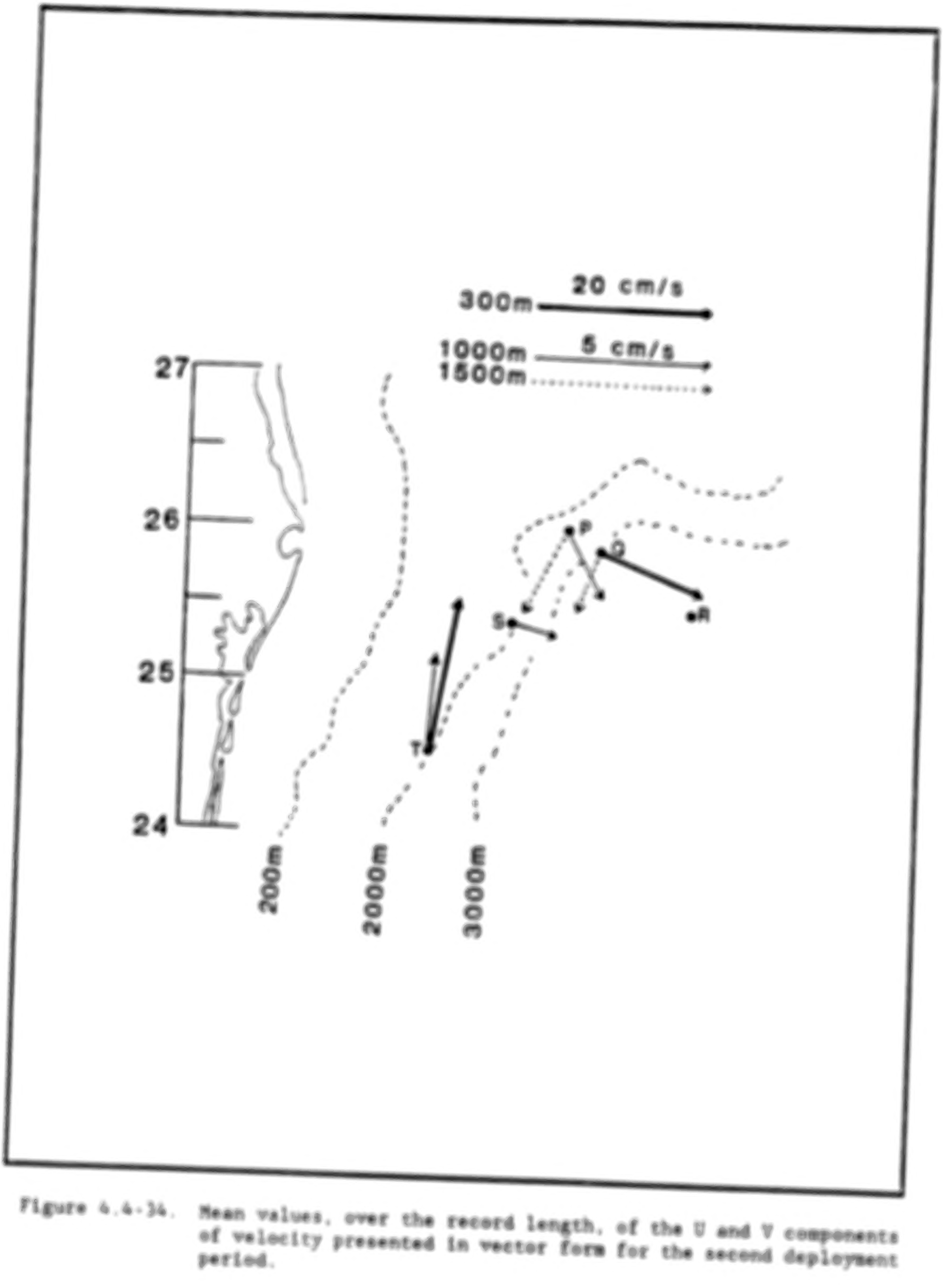

Figure 4.4-34. Mean values, over the record length, of the U and V components of velocity presented in vector form for the second deployment period.

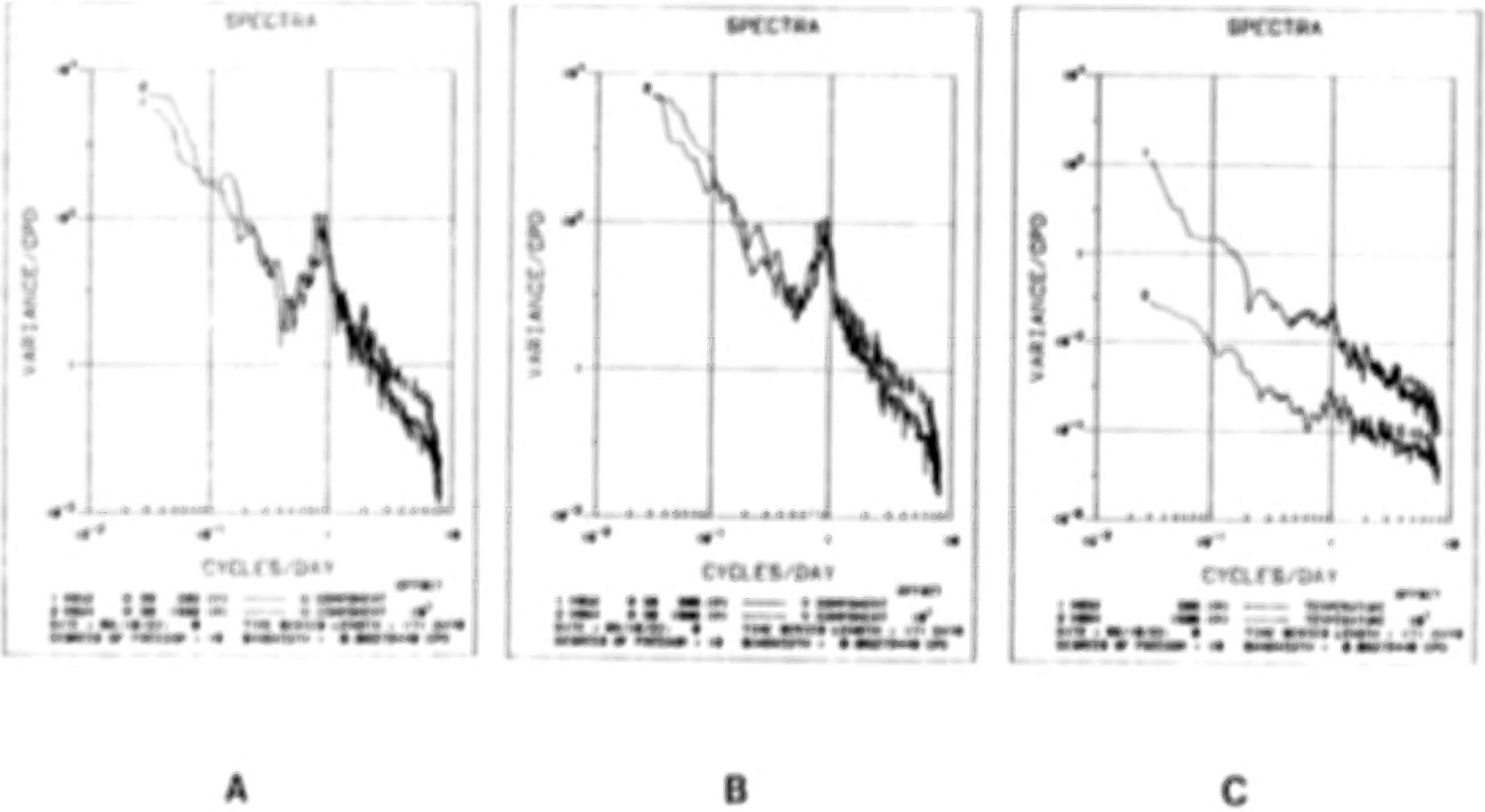

Figure 4.4-35. Spectra for Mooring Q at 300m and 1500m: (a) U velocity components, (b) V velocity components and (c) temperature for the 171-day period beginning October 22, 1985.

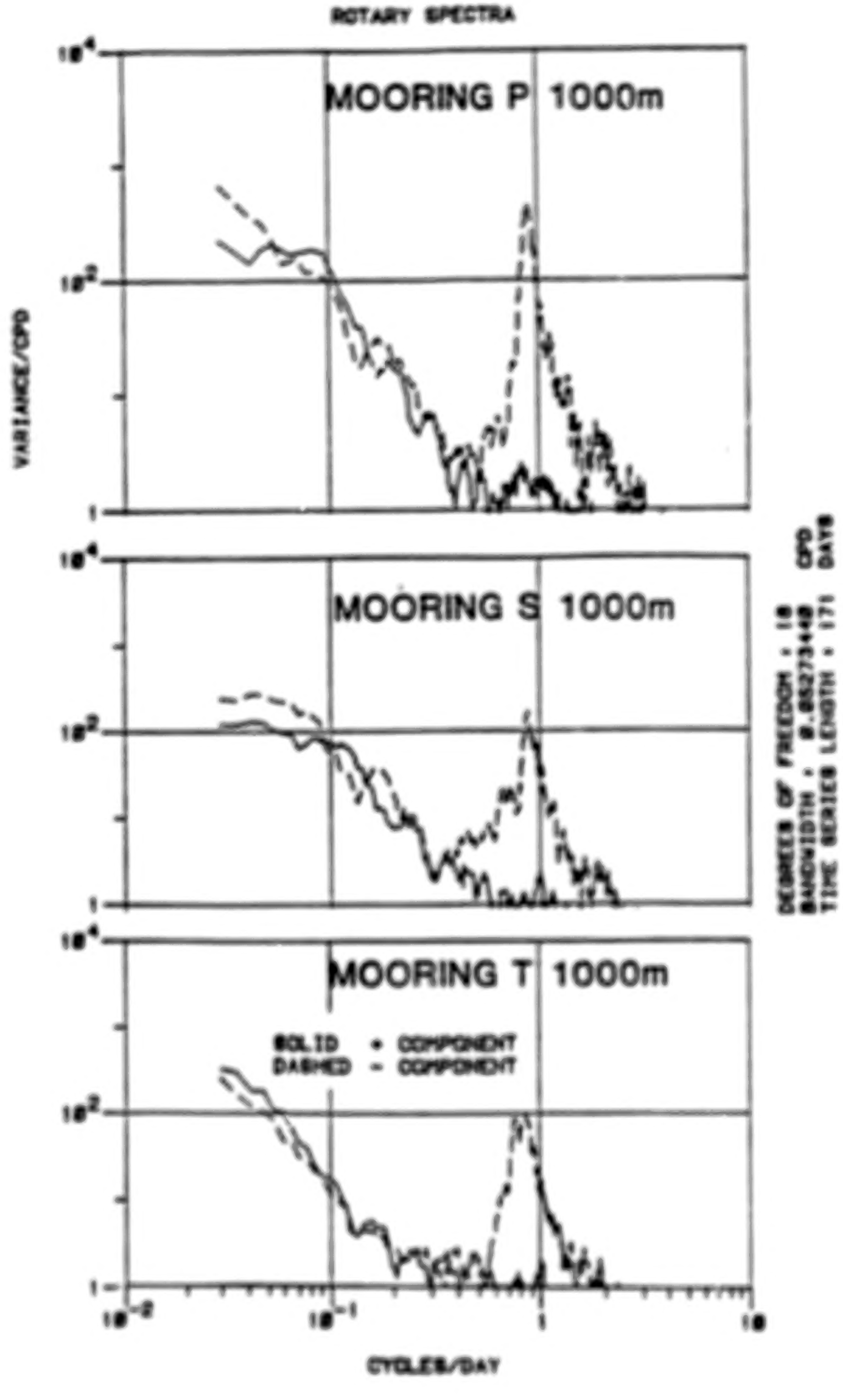

Figure 4.4-36. Rotary spectra emphasizing the inertial energy at 1000m for Moorings P, S and T using 3-hour, low-passed currents for the 171-day period beginning October 22, 1985. Dashed line is clockwise component.

energy in a broad band near the diurnal period. Tidal components are very much smaller than the inertial signal. The inertial peak is highest at Mooring P where it is as great as the long-period variance, and it is only slightly smaller at Moorings S and T. Although it is difficult to estimate energy content by visually integrating under the curve on a logarithmic scale, it is clear that the energy of the inertial motion is a substantial fraction of the total variance.

Figures 4.4-37, 4.4-38 and 4.4-39 show the rotary spectra for the above moorings at periods longer than 2 days, plotted to the same scale that is used later in the rotary cross-spectral analysis of pairs of vector series. In all three there is a CCW peak at periods of 10-12 days. Motion is elliptical at periods longer than about 20 days, CCW at Mooring T and CW at Moorings P and S.

4.4.5.3.3 Vertical and Horizontal Coherence

Information about vertical coherence between the upper and lower layers is available only for Moorings Q and T. Between 300m and 1500m at Mooring Q, the U components are weakly coherent at a period of 25 days with a phase not statistically different from zero, and the V components are incoherent. The temperatures are coherent only at a period of 4 days (0.25 cycles per day) with a phase of 180°. Between 300m and 1000m at Mooring T (Figure 4.4-40), the U components are strongly coherent at periods longer than about 15 days (0.07 cycles per day), with zero phase lag. At periods longer than 12 days, the V components exhibit coherence, albeit weaker. Temperatures are not coherent. For the lower layer at Mooring P, the U components at 1000m and 1500m are weakly coherent at periods near 10 and 25 days, while the V components are strongly so at periods near 5 and 25 days.

Currents but not temperatures are coherent horizontally at periods near 25 days between Moorings P and Q at 1500m (Figure 4.4-41). At 300m the U components of Moorings Q and T are weakly coherent at a period of 25 days, but not the V components or temperatures.

Between Moorings S and P at 1000m, both currents and temperatures are incoherent in the Cartesian representation at the 95% significance level. Coherence was also computed by the rotary method, and weak coherence was indicated only if the significance level was lowered to 90%.

Between Moorings S and T at the same level, the U components are coherent at a period of 10 days, and the V components are coherent at periods of 3-5 days and 9-14 days (Figures 4.4-42a and b). Temperatures exhibit strong coherence at a period of 25 days (Figure 4.4-42c). The rotary method (Figure 4.4-43) also finds coherences at period of 3-5 days and 9-14 days.

Finally, at the largest separation, between Moorings P and T, the rotary cross-spectra show some coherence at periods between 30 and 50 days (0.03 and 0.02 cycles per day), 10 days and 3-5 days (Figure 4.4-44), even though Moorings P and S are basically coherent. Also, recall that during the first deployment period, coherence was found between Moorings P and S but not between Moorings S and T.

To recapitulate, the time-series records at any given location in the lower layer are self-similar over the combined deployment periods, based on qualitative comparisons in the time domain and on the structure of the

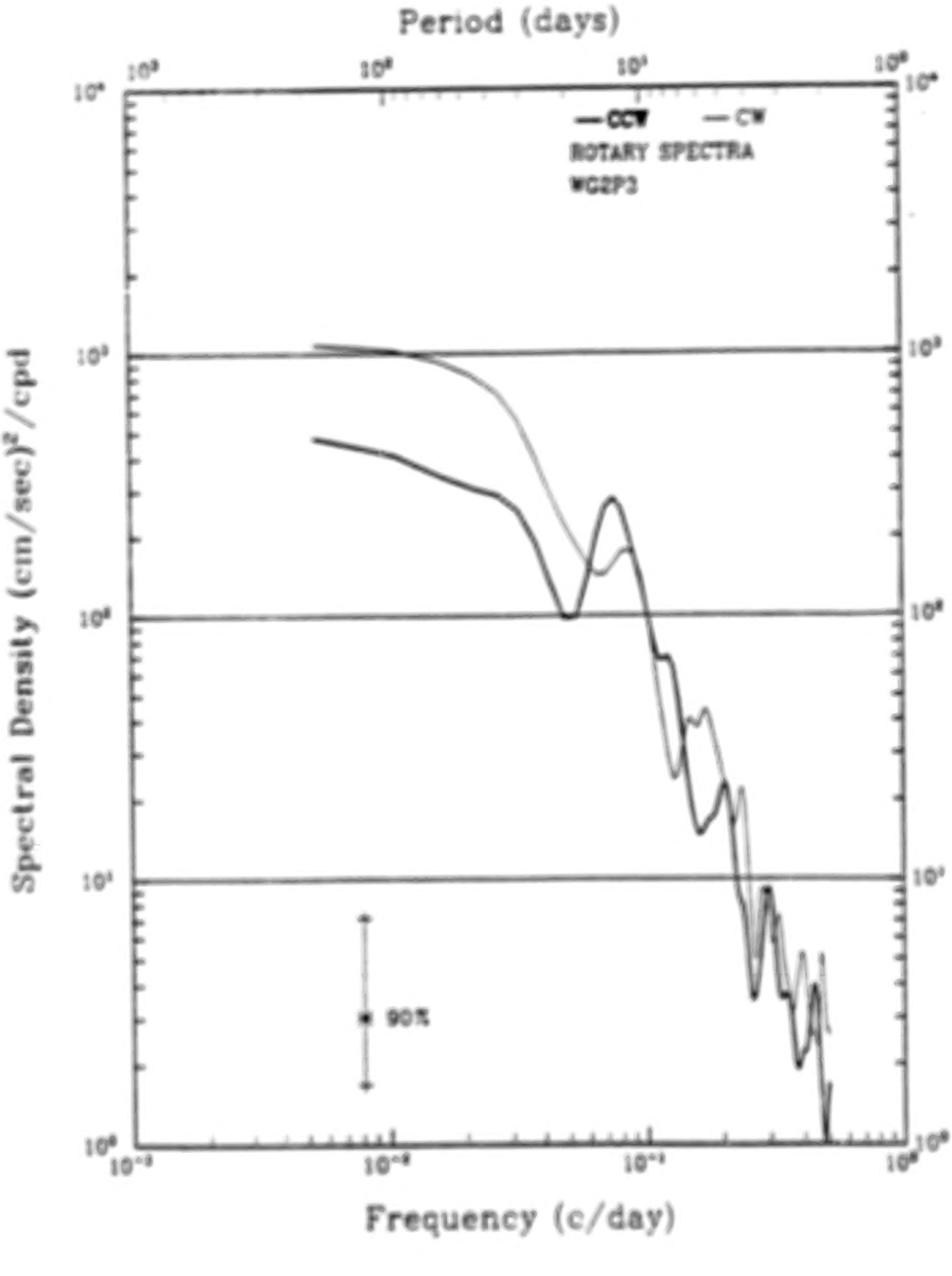

Figure 4.4-37. Rotary spectra at 1000m for Mooring P using 40-hour, low-passed currents for the 186-day period beginning October 24, 1985.

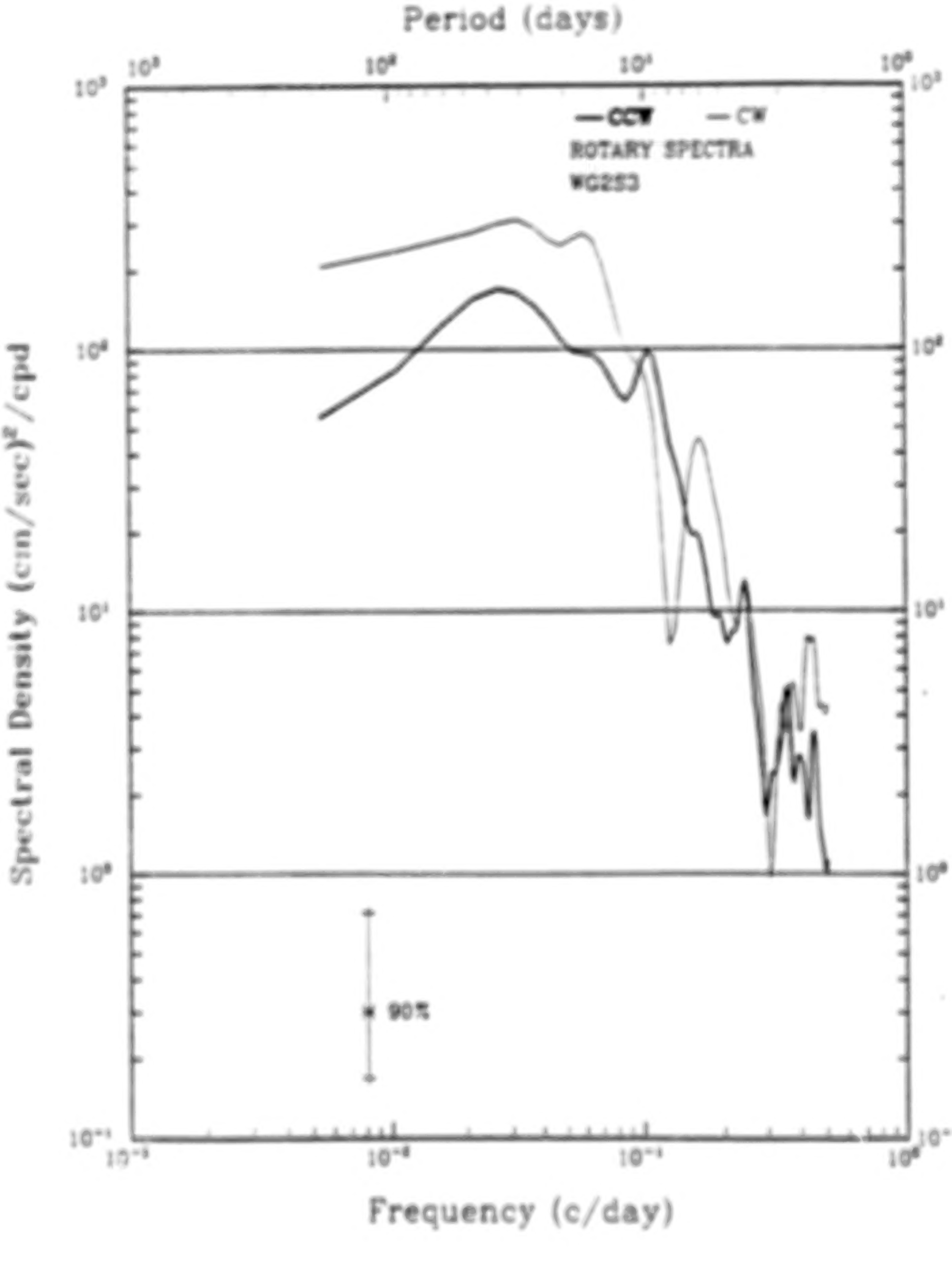

Figure 4.4-38. Rotary spectra at 1000m for Mooring S using 40-hour, low-passed currents for the 186-day period beginning October 24, 1985.

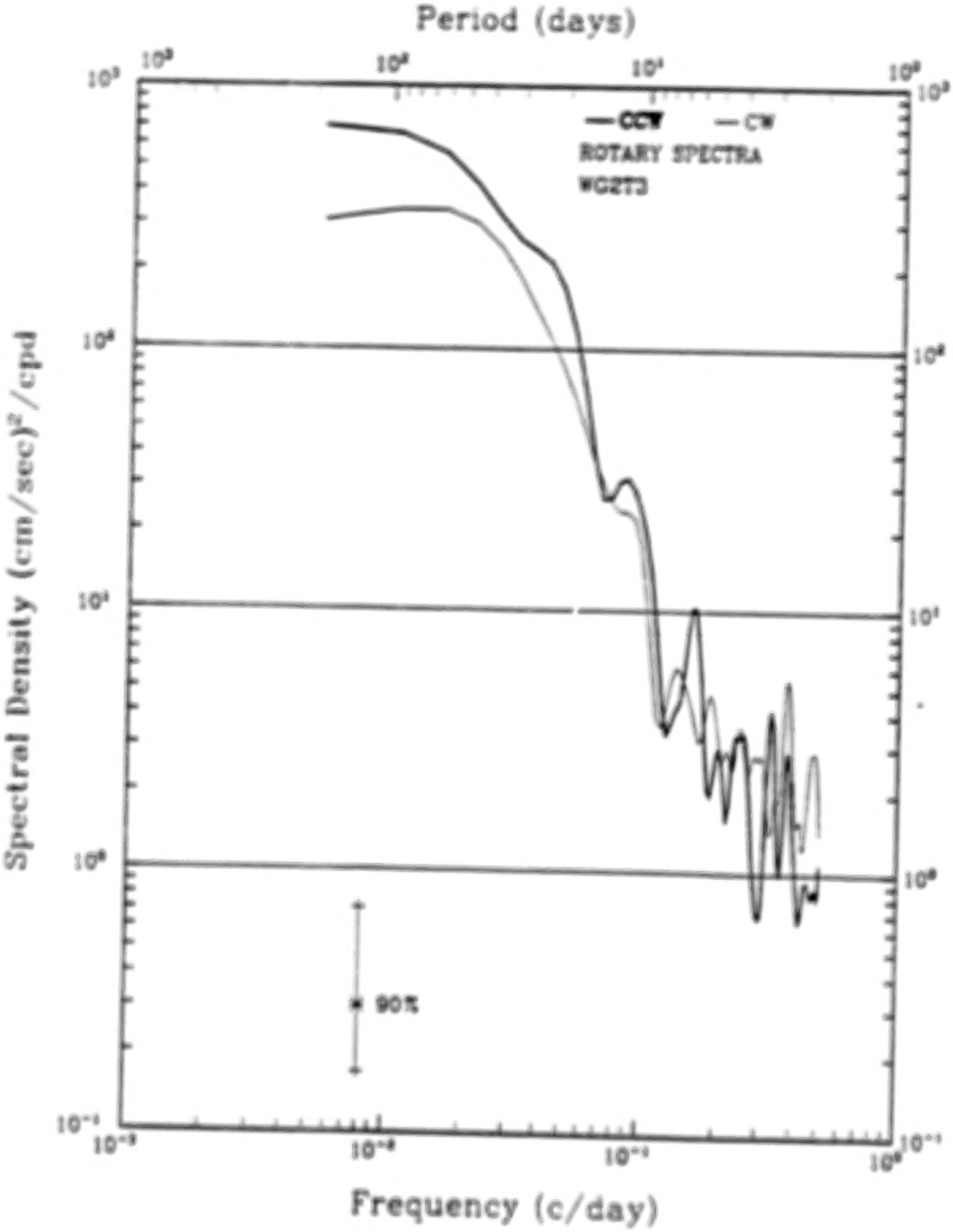

Figure 4.4-39. Rotary spectra at 1000m for Mooring T using 40-hour, low-passed currents for the 186-day period beginning October 24, 1985.

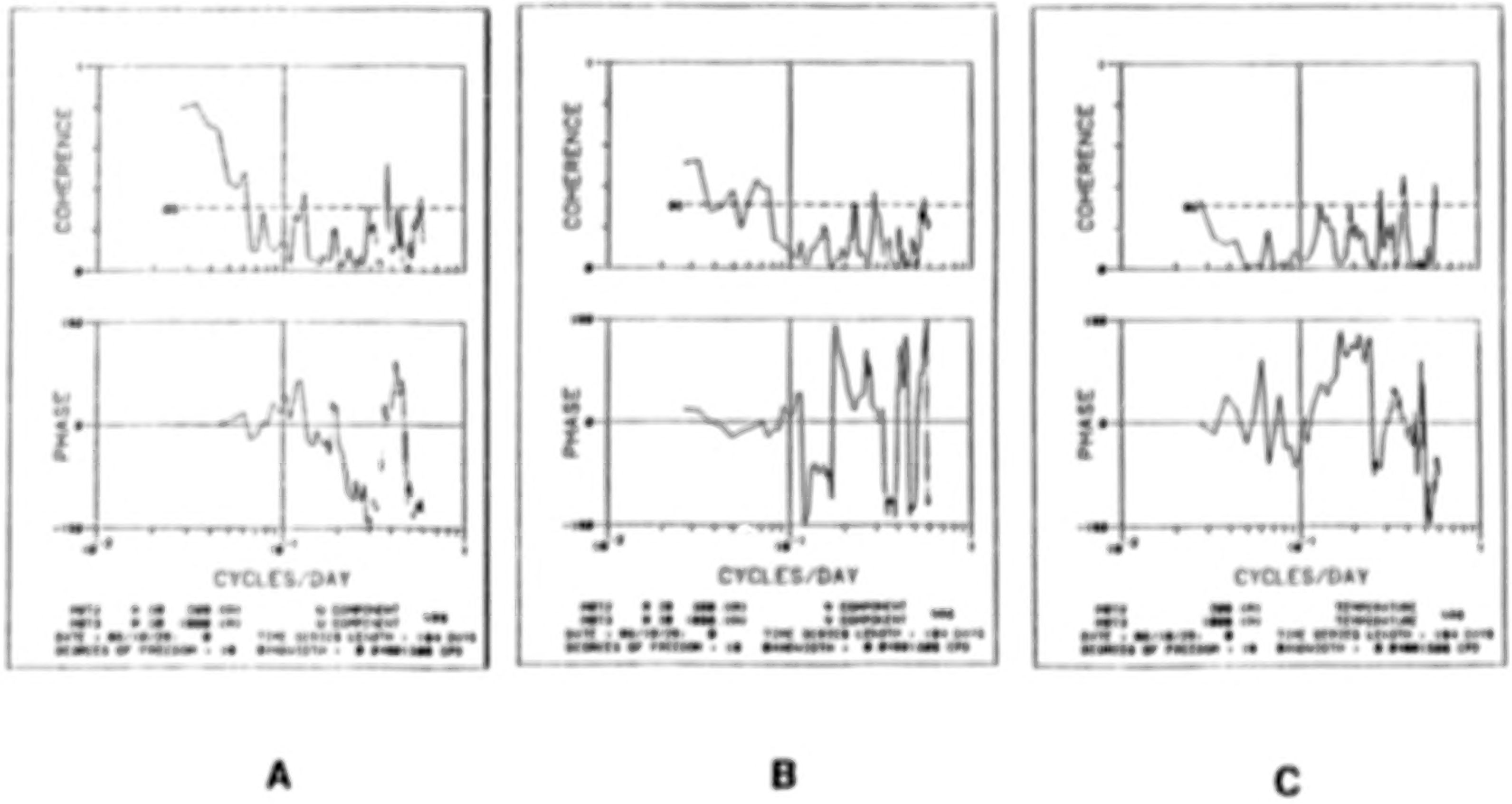

Figure 4.4-40. Vertical, cross-spectral coherence and phase at Mooring T between 300m and 1000m: (a) U components of velocity, (b) V components of velocity and (c) temperature for the 184-day period beginning October 26, 1985.

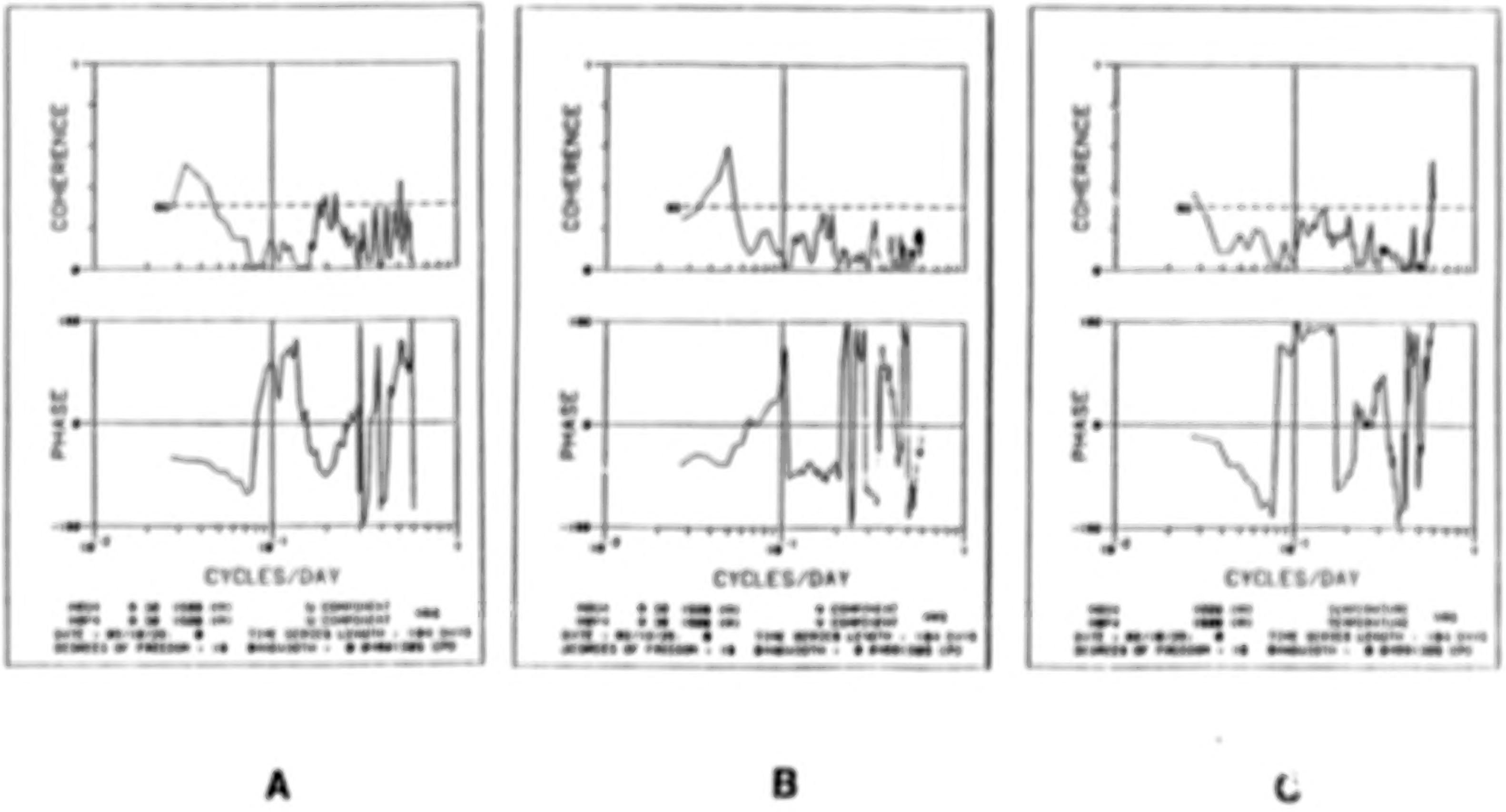

Figure 4.4-41. Horizontal, cross-spectral coherence and phase at 1500m between Moorings Q and P: (a) U component of velocity, (b) V component of velocity and (c) temperature for the 184-day period beginning October 26, 1985.

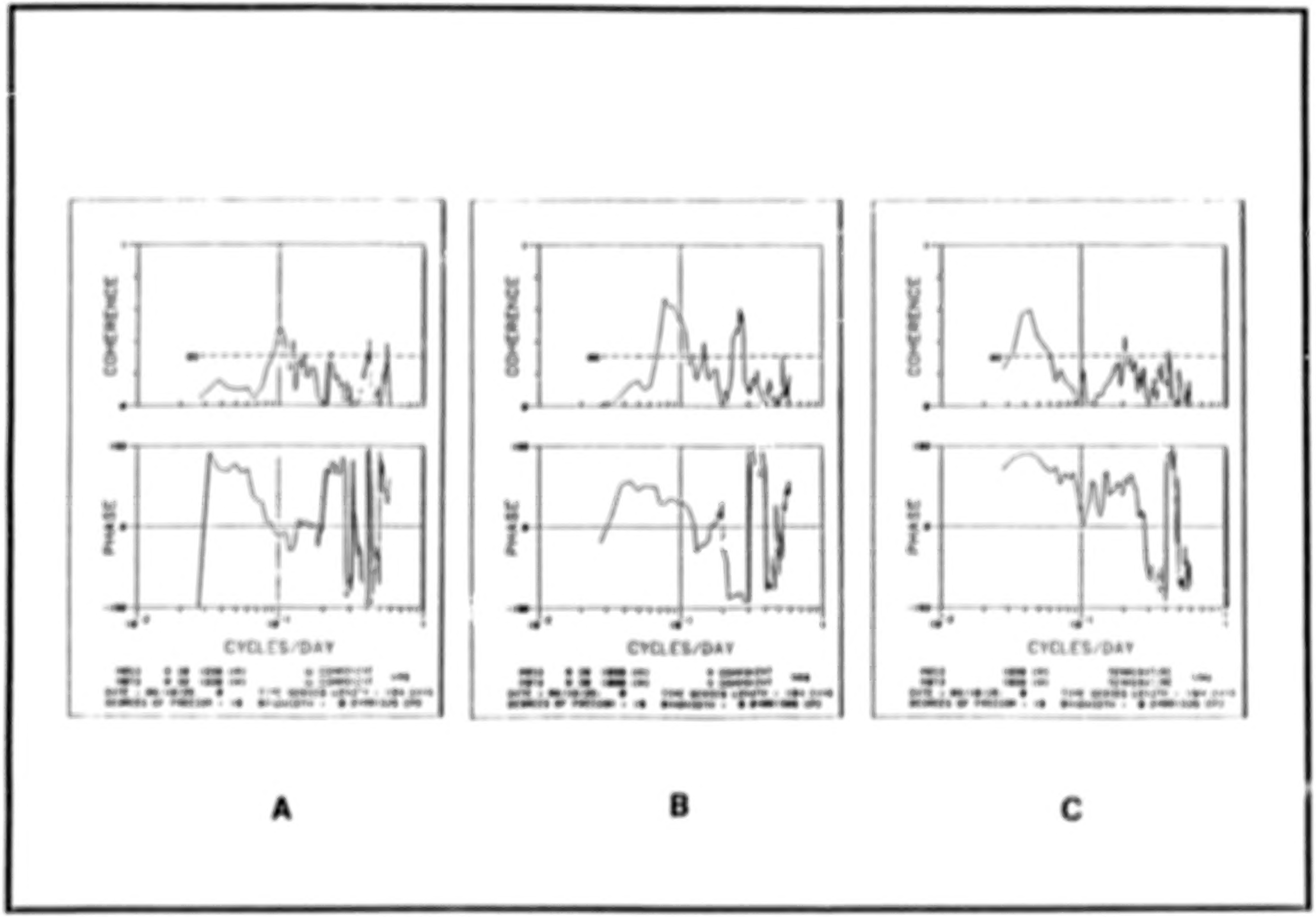

Figure 4.4-42. Horizontal, cross-spectral coherence and phase at 1000m between Moorings S and T: (a) U component of velocity, (b) V component of velocity and (c) temperature for the 184-day period beginning October 26, 1985.

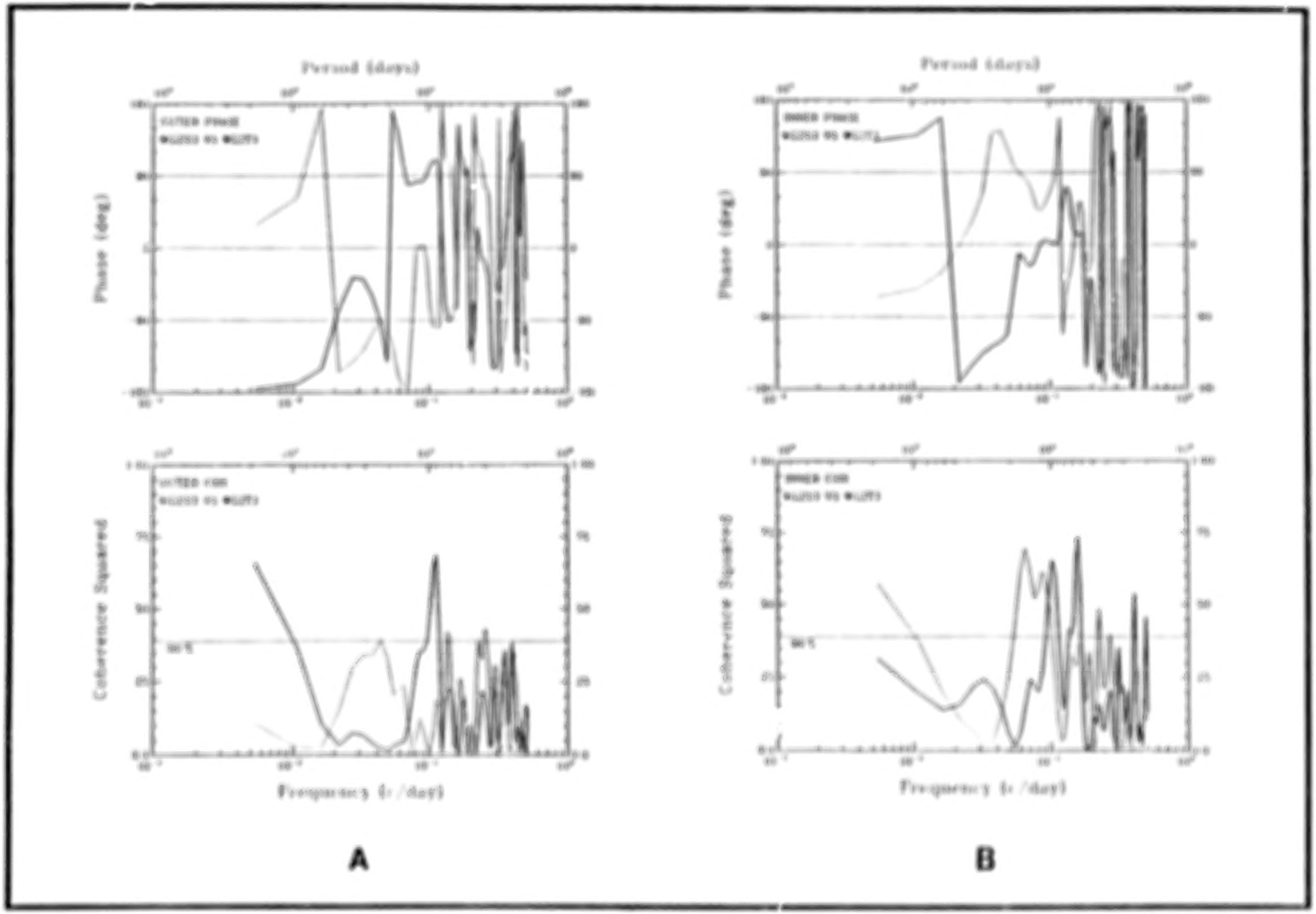

Figure 4.4-43. Rotary cross-spectral coherence and phase at 1000m between Moorings S and T: (a) outer phase and coherence and (b) inner phase and coherence. See text for explanation of rotary method.

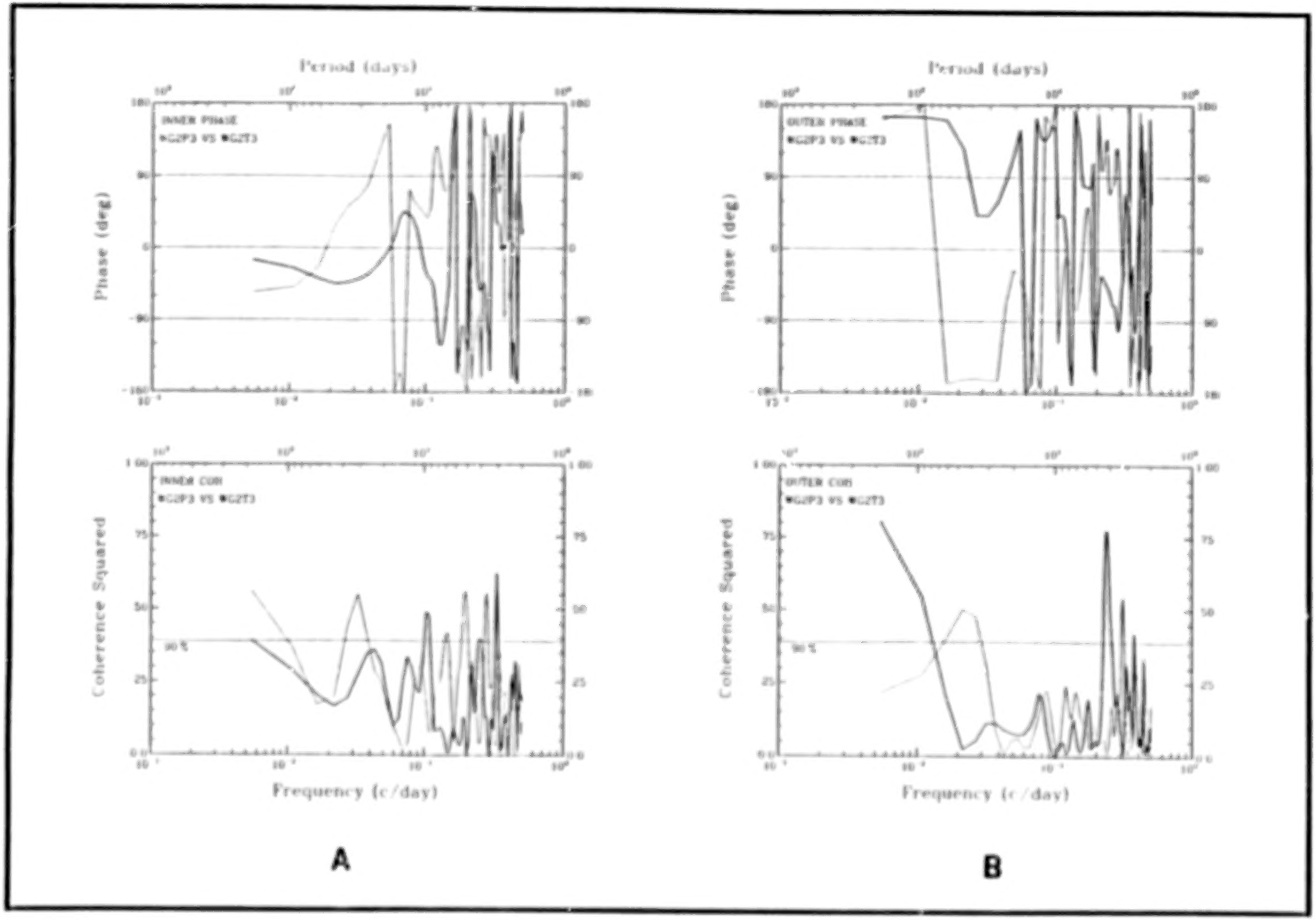

Figure 4.4-44. Rotary cross-spectral coherence and phase at 1000m between Moorings P and T: (a) inner phase and coherence and (b) outer phase and coherence. See text for explanation of rotary method.

autospectra. This suggests that at a given location the same processes are at work during both deployment periods, despite the differences in the locations and strengths of the eddies active in the upper layer. Between locations, however, there are significant differences in the nature of the flow, as reflected in the often weak and frequently nonexistent coherence. Coherence, when it is significant, is usually confined to periods of 3-5 days, 9-14 days and 25 days. The most consistent feature of the time-series is the large fraction of variance or energy contributed by oscillations with a near-inertial period.

4.5. Eddy Reflection and Dissipation

4.5.1 Introduction

Following the previous period of substantial eddy-slope interaction, the anticyclone-cyclone pair moved away from and then back toward the slope. The surface flow field appeared to become less well organized and the overall energy of the eddy pair diminished with time.

4.5.2 Surface and Near-Surface Currents

4.5.2.1 Sea-Surface Temperature and Surface Processes

This section presents satellite SST data combined with *in-situ* data in February and March 1986 when the eddy moved away from the western wall of the Gulf. The SST pattern for late February 1986 (Figure 4.5-1) shows that Eddy C which separated from the Loop Current in January had penetrated further into the western Gulf. The center of Eddy C was at approximately 25.2°N, 90.0°W. The SST pattern in the western Gulf more clearly indicates that there were two eddies in that region. A warm-core eddy (W) was located in the northwestern corner of the Gulf, centered at 27.0°N, 95.6°W, which is defined by the closed 20°C isotherm in that region. The second eddy (Eddy B) was found immediately to the south, and the sea-surface isotherm patterns suggest that it was centered at about 24.8°N, 95.2°W, east of the late January position (Section 4.4.2, p. 138). The sea-surface isotherm pattern suggested that Eddy B was elliptic in shape and that the major axis was oriented east to west. At this time, there was no indication from the available data that Eddy A was in the southern part of the western Gulf.

There also was no indication in the satellite SST pattern for February of a cyclonic perturbation. A cyclonic shear zone should have existed between the warm water masses (Eddy B and warm water to the north). A temperature section (Figure 4.5-2) from hydrographic data collected on February 13 and 14, 1986, however, indicates the presence of a cold dome feature centered at approximately 26.5°N, 95.8°W (i.e., in the cyclonic shear zone between the two warm eddies noted in Figure 4.5-1). It is not clear that this cold dome is the cyclonic perturbation previously noted or simply a manifestation of the shear zone.

The satellite SST analyses also indicate the presence of a cold lens (C) centered at approximately 24.0°N, 94.4°W. This may be the same lens noted in January (Figure 4.4-6, p. 141). The configuration of this lens suggests that it was associated with a cyclonic perturbation; however, no *in-situ* evidence was available to confirm this notion.

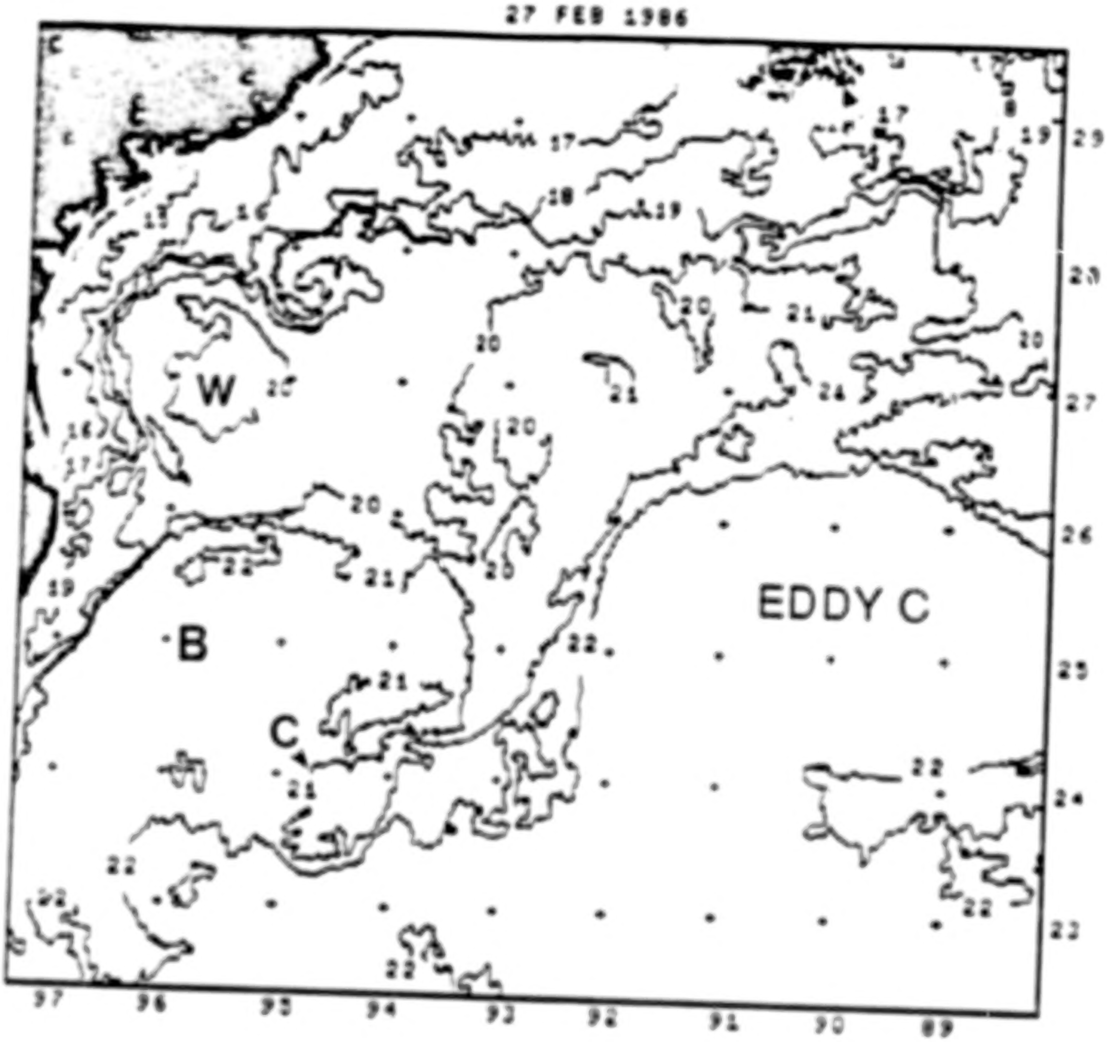

Figure 4.5-1. NOAA-9 SST (°C) analysis in the western Gulf of Mexico for February 27, 1986.

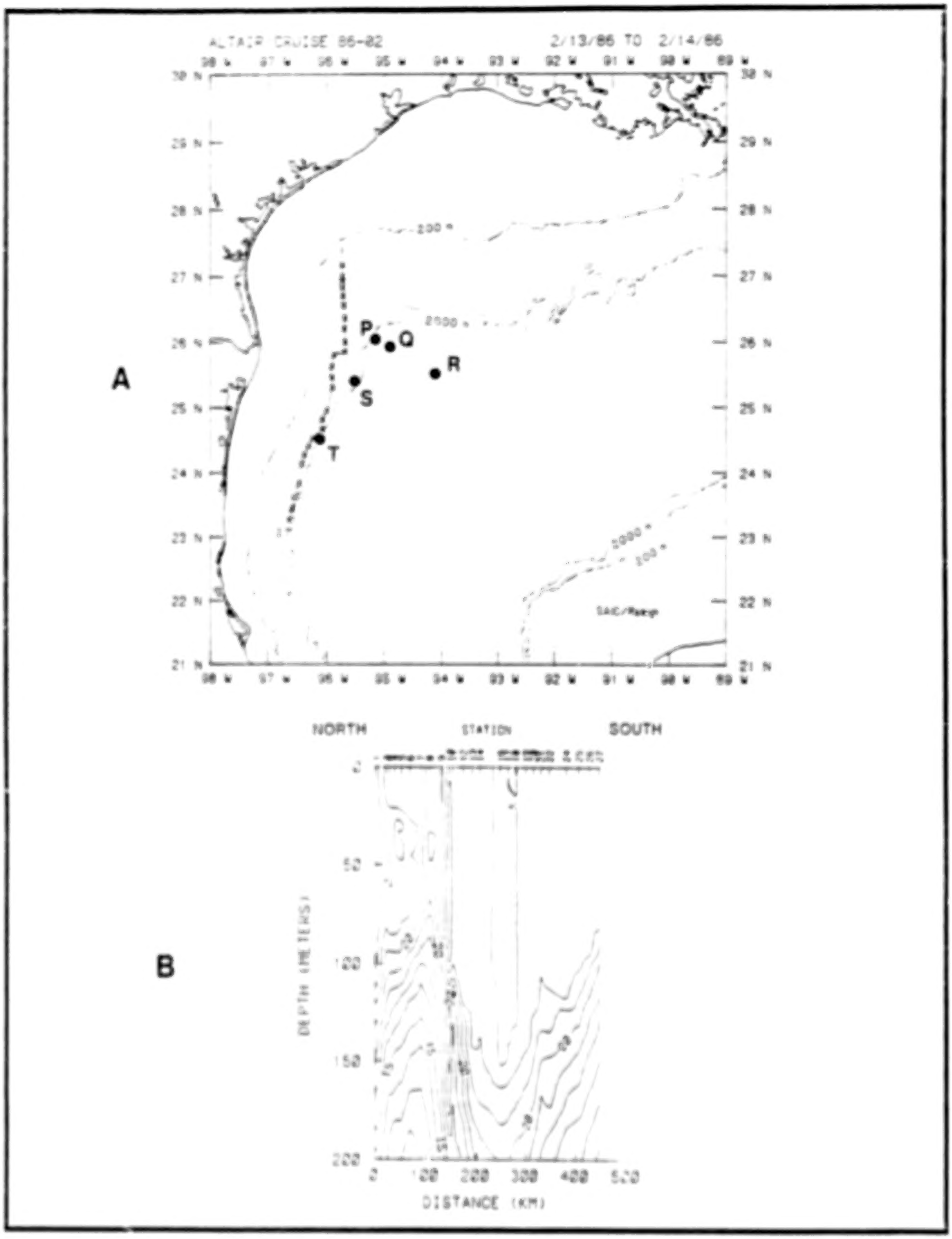

Figure 4.5-2. (a) Location of stations for the SOOP transect performed in the period of February 13-14, 1986 and (b) vertical section of temperature (°C) from the data collected in (a).

The satellite SST analysis for late March 1986 (Figure 4.5-3) shows a broad warm zone having temperatures greater than 23°C in the eastern portion of the analysis. This is Eddy C, which separated from the Loop Current in January 1986. The warmest waters, having temperatures greater than 24°C, were located in the southern portion of this warm zone and it is believed that Eddy C was embedded in that portion of the zone. The SST analyses suggest that there may have been another warm feature immediately north of that eddy.

A tongue of warm water (T) emanated from the region occupied by Eddy B and extended into the northwestern Gulf (Figure 4.5-3). The orientation of this tongue suggests anticyclonic motion, advecting warm water into that region. There was no indication in the SST pattern of any of the cyclonic perturbations previously detected.

Figure 4.5-4 is a representation of the flow field near the surface at the center of Eddy B from February 1 to March 31, 1986 that is based on drifter position data from Drifters 3353 and 3378. The near-surface flow field remained elliptically shaped during this period. The center of the ellipse moved smoothly in a southeasterly direction with displacements of not much more than 30 km in 15 days. Furthermore, the orientation of the ellipse changed from northeast-southwest to southeast-northwest, maintaining an anticyclonic rotation about the major axis. The rotational displacements of the major axis during this period were not as large as those noted in the December 1985 through January 1986 period (Figure 4.4-11, p. 151). This evidence suggests that any oscillations that were set up by the eddy's encounter with the western slope had dampened considerably.

4.5.2.2 SST and Path Data

For 3 and 1/2 months (February to mid-May 1986), Eddy B was located off the Mexican coast. Maximum swirl speeds were 75 cm sec^{-1} at a radius of 80 km, but this occurred in mid-February 1986. During March through May, Eddy B became less energetic and less well organized. By late February 1986 (Figure 4.5-5a), Eddy B had moved eastward, and Drifter 5678 had become entrained in the flow field of Eddy C. Over the next 2 weeks, Eddy B became quite elliptical as Eddy C approached. Conditions for March 12 to 18, 1986 (Figure 4.5-5b) show a distinct east-west elongation for the flow field of Eddy B. The motion of Drifter 5678 indicates the extent of Eddy C, a relatively large eddy. These data suggest that the flow fields of the two eddies may have begun to interact.

Eddy C continued moving southwestward across the deepest regions of the Gulf. The flow field of the older Eddy B became irregular, as depicted for March 19 through 25, 1986 shown in Figure 4.5-6a. At that time, Eddy B appeared to have moved even further offshore, becoming elongated in a north-south direction. Over the next 3 weeks, neither Drifter 3378 nor Drifter 3353 revealed any organized anticyclonic flow in the western Gulf. By April 16 through 22, 1986 (Figure 4.5-6b), the center of Eddy C had reached 25.0°N, 91.0°W. Drifters 3353 and 5678 appeared influenced by the newer eddy's western and northern flow fields, respectively, and Drifter 3378 was moving south into the Campeche Bay region.

A set of XBT data were collected in the western Gulf during the period of April 26 through May 14, 1986. The depth of the 8°C isotherm is shown in Figure 4.5-7. The results indicate a smaller but still intense anticyclone-cyclone pair centered at about 24.0°N, 95.5°W. Drifter 3378, however, made a

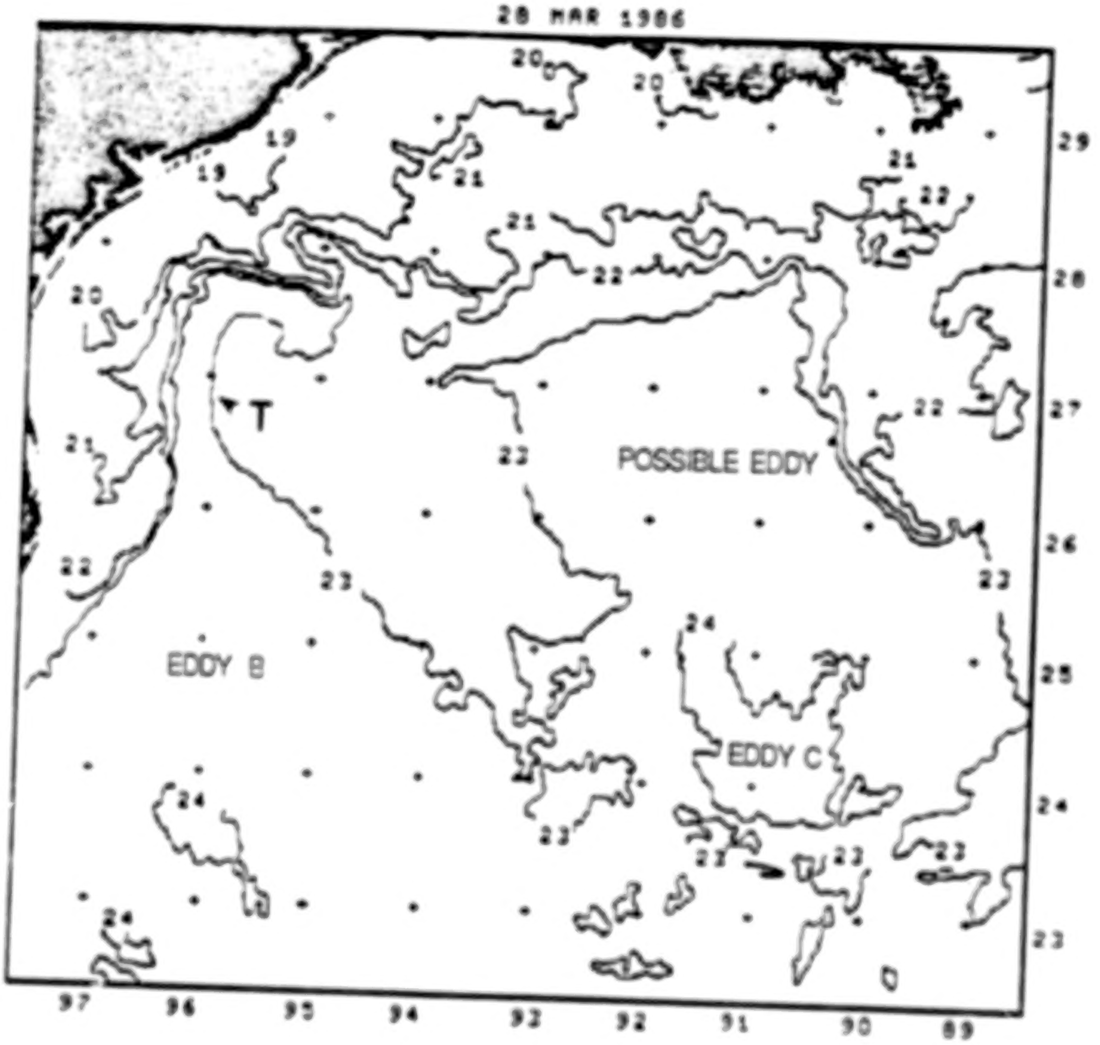

Figure 4.5-3. NOAA-9 SST (°C) analysis in the western Gulf of Mexico for March 28, 1986.

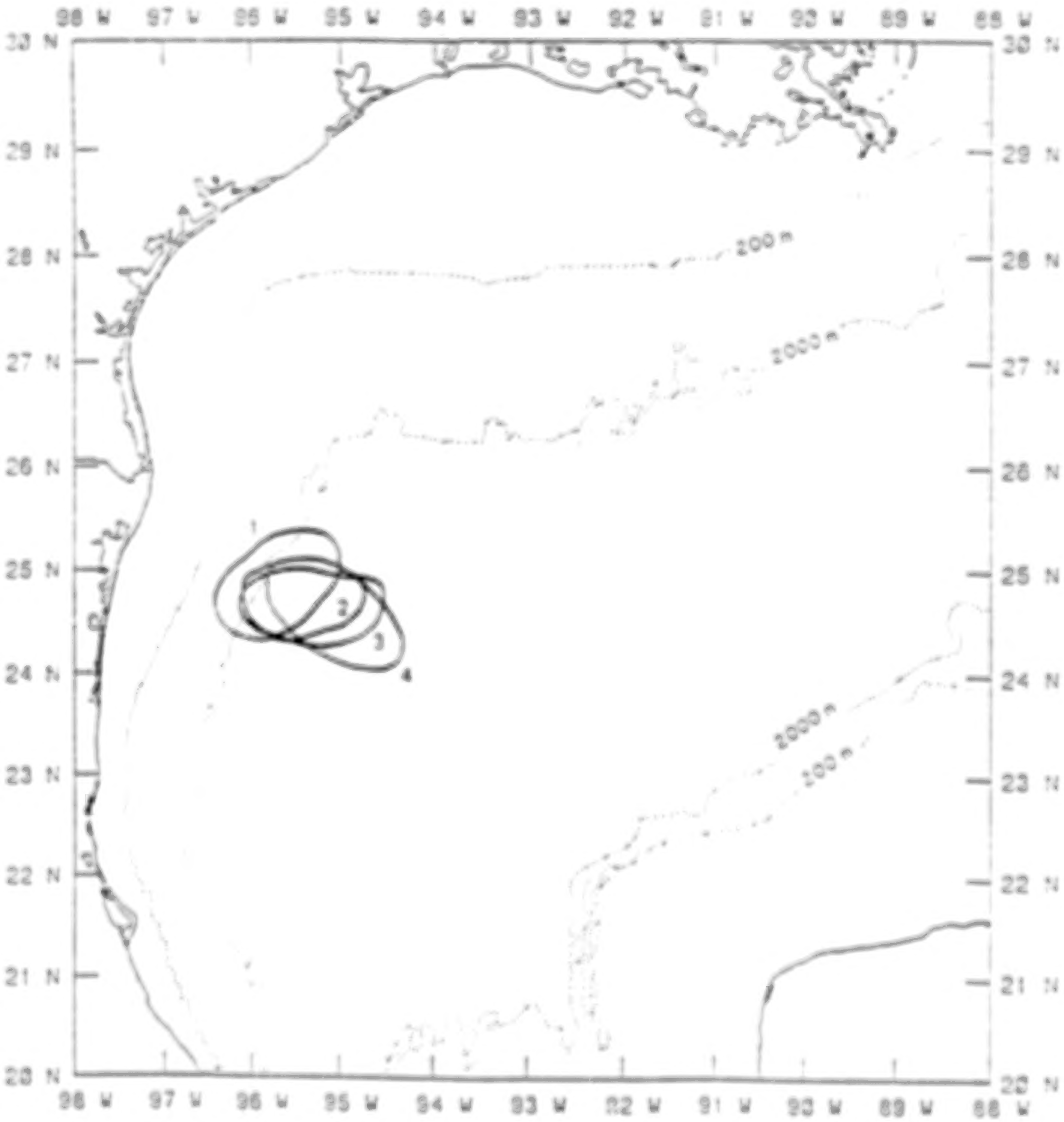

Figure 4.5-4. Stylized representation of the paths of Drifters 3353 and 3378 during the period of February through March 1986. Path 1 occurred in the first half of February, Path 2 in the last half of February, Path 3 in the first half of March and Path 4 in the last half of March. See text for further information.

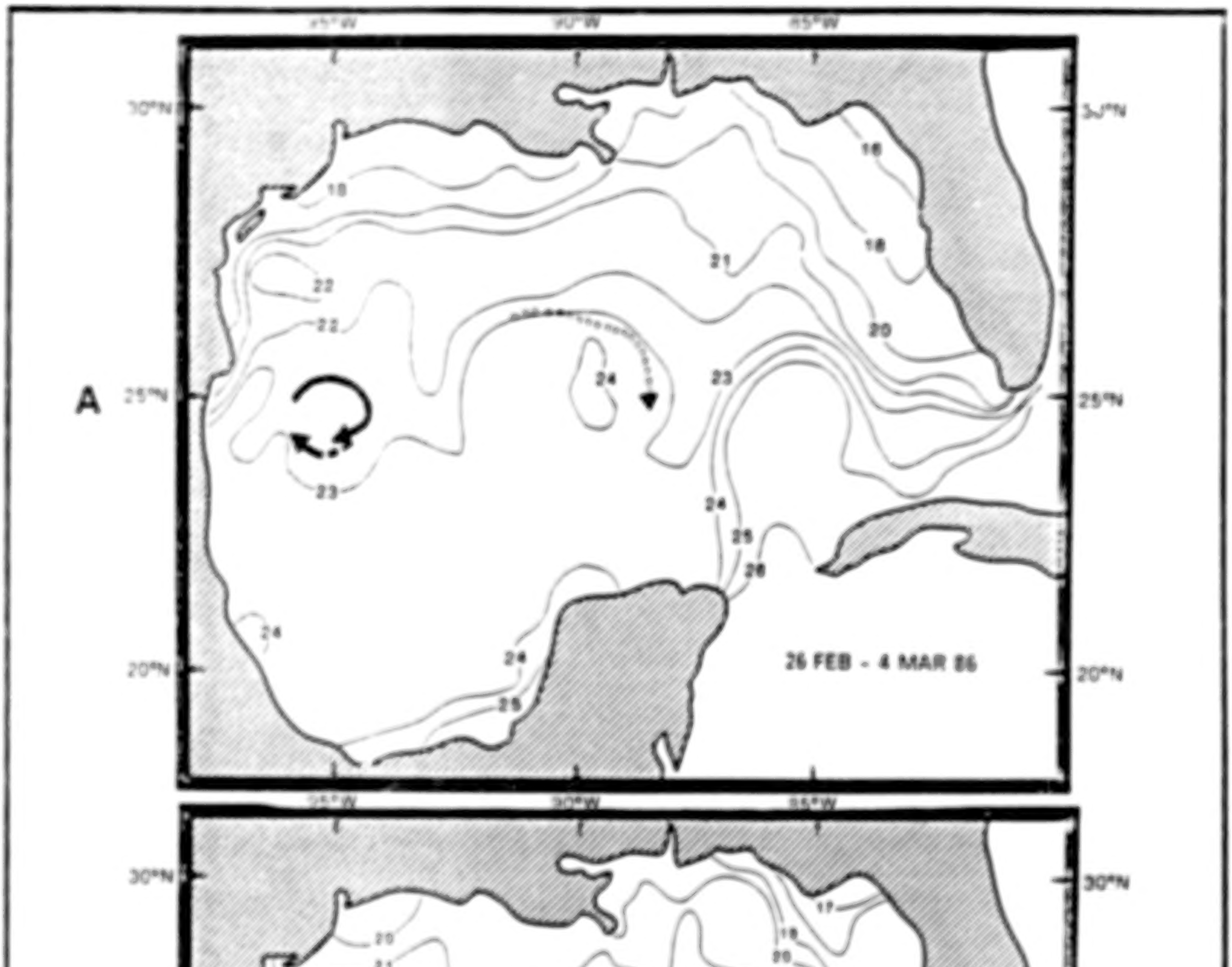

Figure 4.5-5. SST data (°C) for: (a) February 26 through March 4, 1986 and (b) March 12-18, 1986. The drifter trajectories, shown by arrows, are identified in Table 2.2-1.

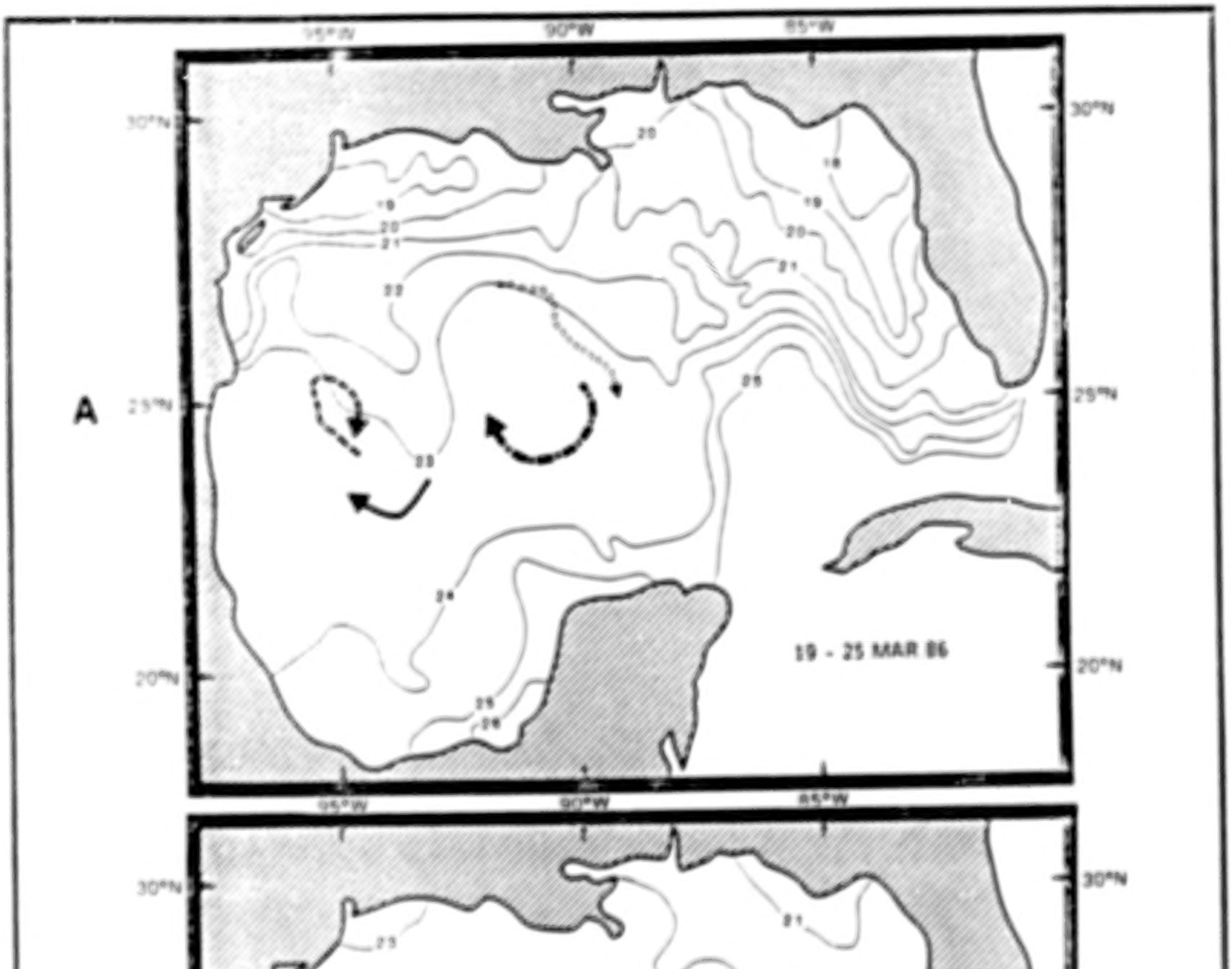

Figure 4.5-6. SST data (°C) for: (a) March 19-25, 1986 and (b) April 16-22, 1986. Shorter arrows denote the flow at the edges of Eddy B while dotted lines indicate the locations of eddy waters (based on XBT data). The drifter trajectories, shown by arrows, are identified in Table 2.2-1.

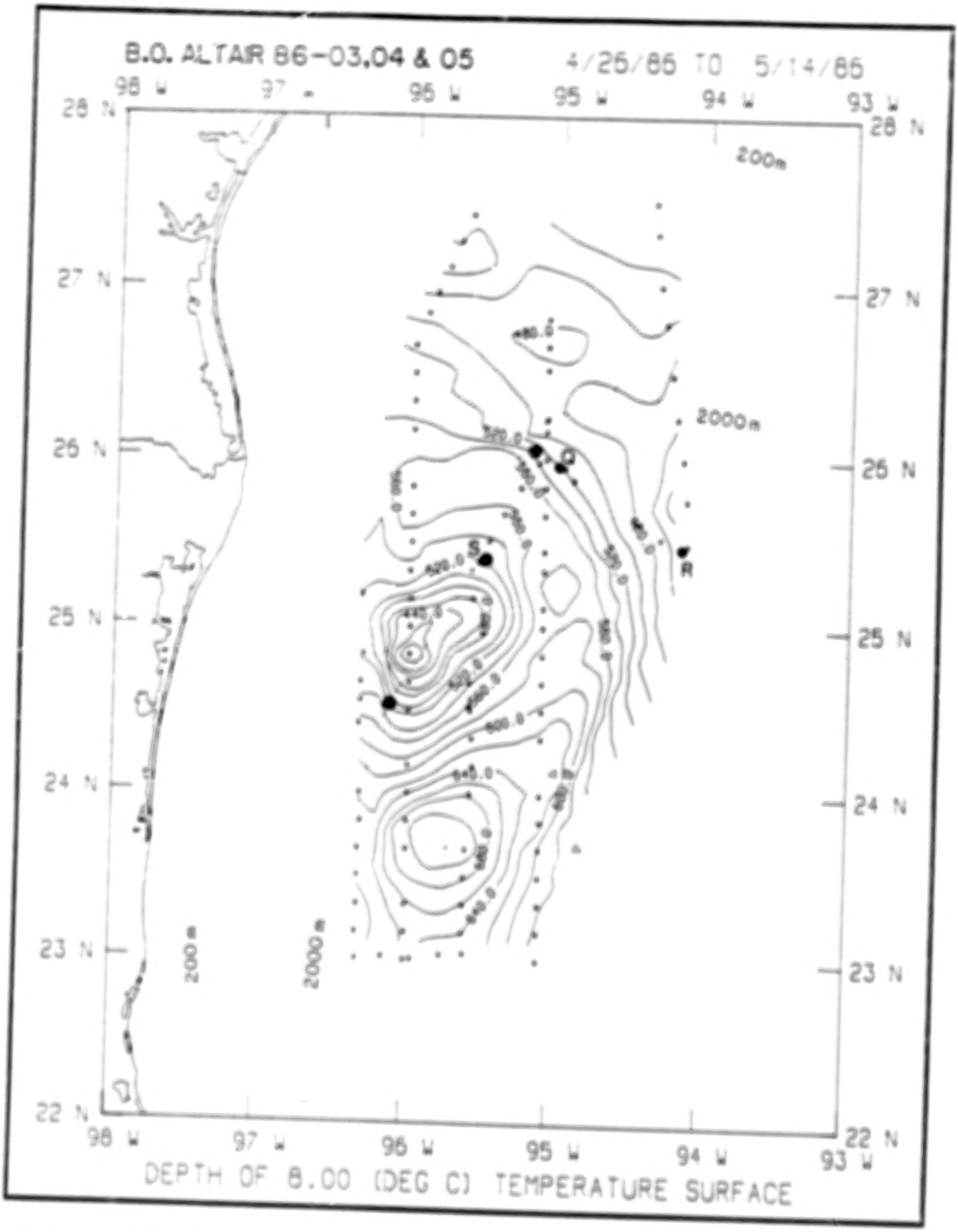

Figure 4.5-7. Topography of the 8°C temperature surface based on the April 26 to May 14, 1986 B/O ALTAIR XBT surveys.

large anticyclonic loop in the western Gulf with no apparent relationship to the subsurface anticyclone indicated in the XBT data. It went as far south as 22.0°N, then moved northward along the western side of the anticyclone-cyclone pair, finally turning eastward at about 25.5°N.

4.5.3 Temperature Fields

Figures 4.5-7 and 4.5-8 show the 8°C, 15°C and 21°C temperature surfaces from the XBT data collected by the R/O ALTAIR on three separate cruises during the period April 26 to May 14, 1986. At 8°C, Eddy B and a companion cyclone are still well defined. Eddy B is now located about one degree farther south than in January, and most of its structure lies east of the 2000m isobath. As noted in Section 4.2 (p. 49) and in the discussion of Table 4.4-2 (p. 170) and Figure 4.5-7, the size of Eddy B is about half that of January. A trough in the 8°C topography extends northeastward from the deep core of Eddy B and wraps around the eastern and northern sides of the cyclone, implying elongated anticyclonic or clockwise flow. This trough separates the cyclone from another region to the north where there is also cyclonic circulation.

The cyclone (Eddy Z) is also diminished in size but not as markedly as Eddy B. The core of Eddy Z is on the 2000m isobath, so it has moved into substantially deeper water compared to January. The centers of Eddy B and Eddy Z are about 50 km closer together than in January, primarily because of the smaller size of Eddy B. Thus, the two features are still strongly coupled.

At 15°C (Figure 4.5-8a), Eddy B is weakly defined and its core is farther south. Eddy Z is still evident. The deep and shallow regions north of Eddy Z are better defined than at 8°C. At 21°C (Figure 4.5-8b), Eddy B has the same form as at 15°C. Eddy Z is not well defined, but the anticyclonic feature to the north of it is quite evident.

Figure 4.5-9 shows a vertical temperature section along the north-south line that passes through the center of Eddy Z (the second line from the west in Figure 4.5-7). The section falls slightly west of the centers of Eddy B and the features north of Eddy Z, which exaggerates the strength of Eddy Z relative to these other features. Note that the isotherms above 11°C in Eddy B slope downward from north to south. This trend extends across most of the section in the shallower layers. It suggests a weak, large-scale, anticyclonic circulation superposed on the mesoscale eddy field, possibly an indication of wind forcing.

4.6 Eddy-Eddy Interaction (May 1986 and Onward)

4.6.1 Introduction

Once in the western Gulf and after having been substantially affected by the interaction with the western Gulf slope, Eddy B came into contact with Eddy C which was shed by the Loop Current well after Eddy B. The interaction of these large energy and mass fields had a controlling influence on circulation patterns in the central and western Gulf for many months. The mechanism for eddy-eddy interaction is not readily apparent; however, there can be no doubt that the influence was substantial. Presented below is a discussion using available information. Note that this episode relies primarily on SOOP cruises and drifting buoy data with limited historical satellite imagery in support.

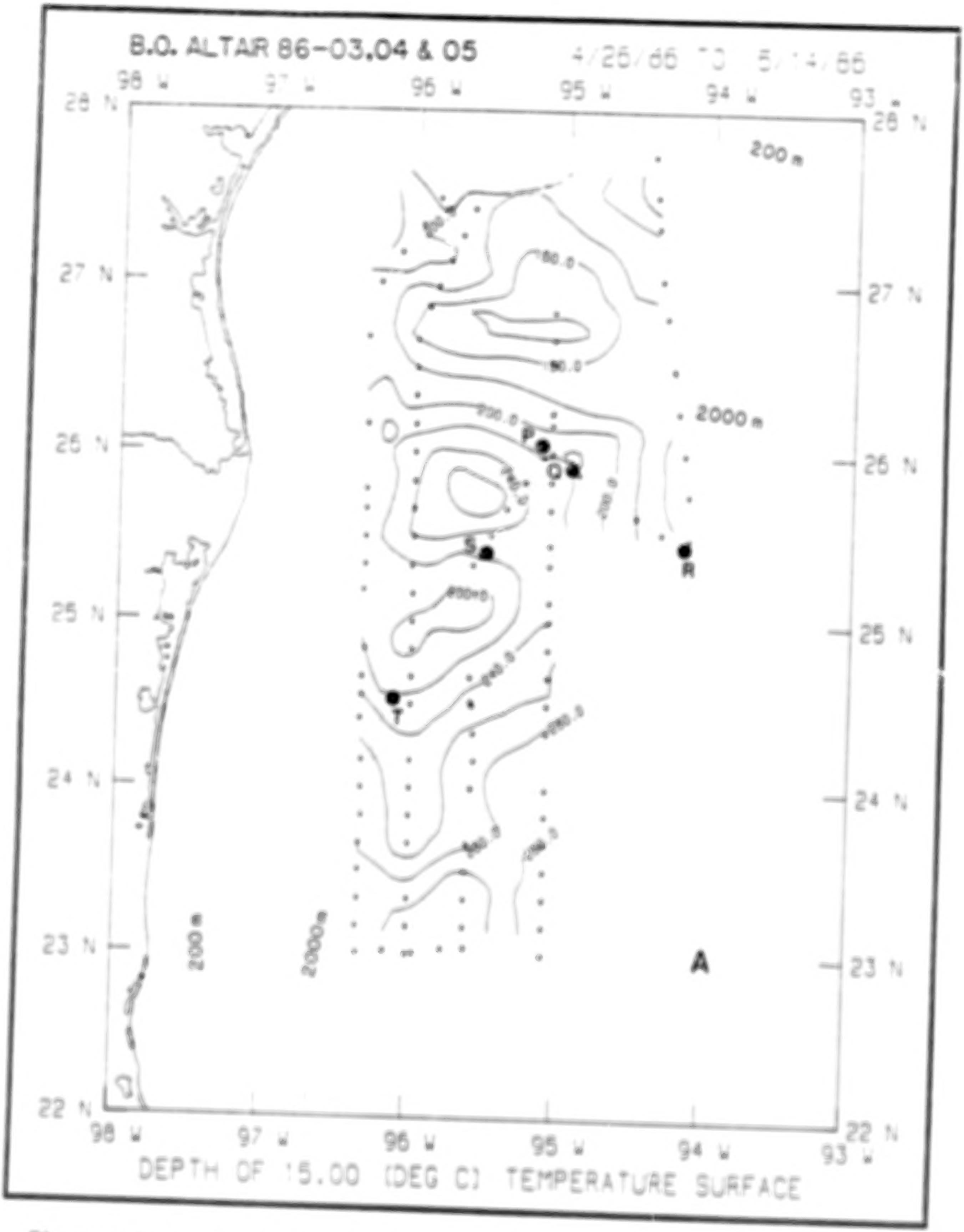

Figure 4.3-8a. Topography of the 15°C temperature surface based on the April 26 to May 14, 1986 B/O ALTAIR XBT surveys.

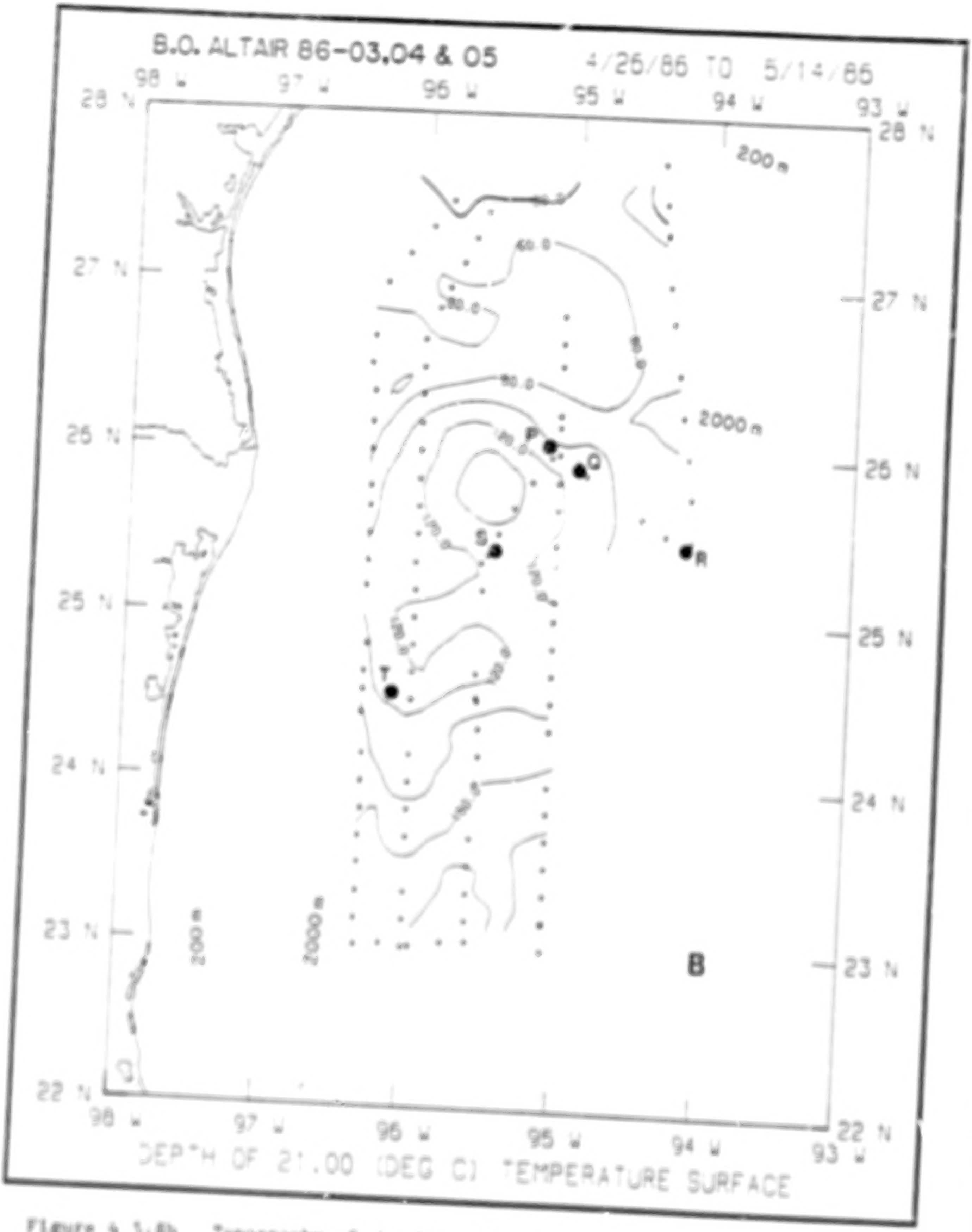

Figure 4.5-8b. Topography of the 21°C temperature surface based on the April 26 to May 14, 1986 B/O ALTAIR XBT surveys.

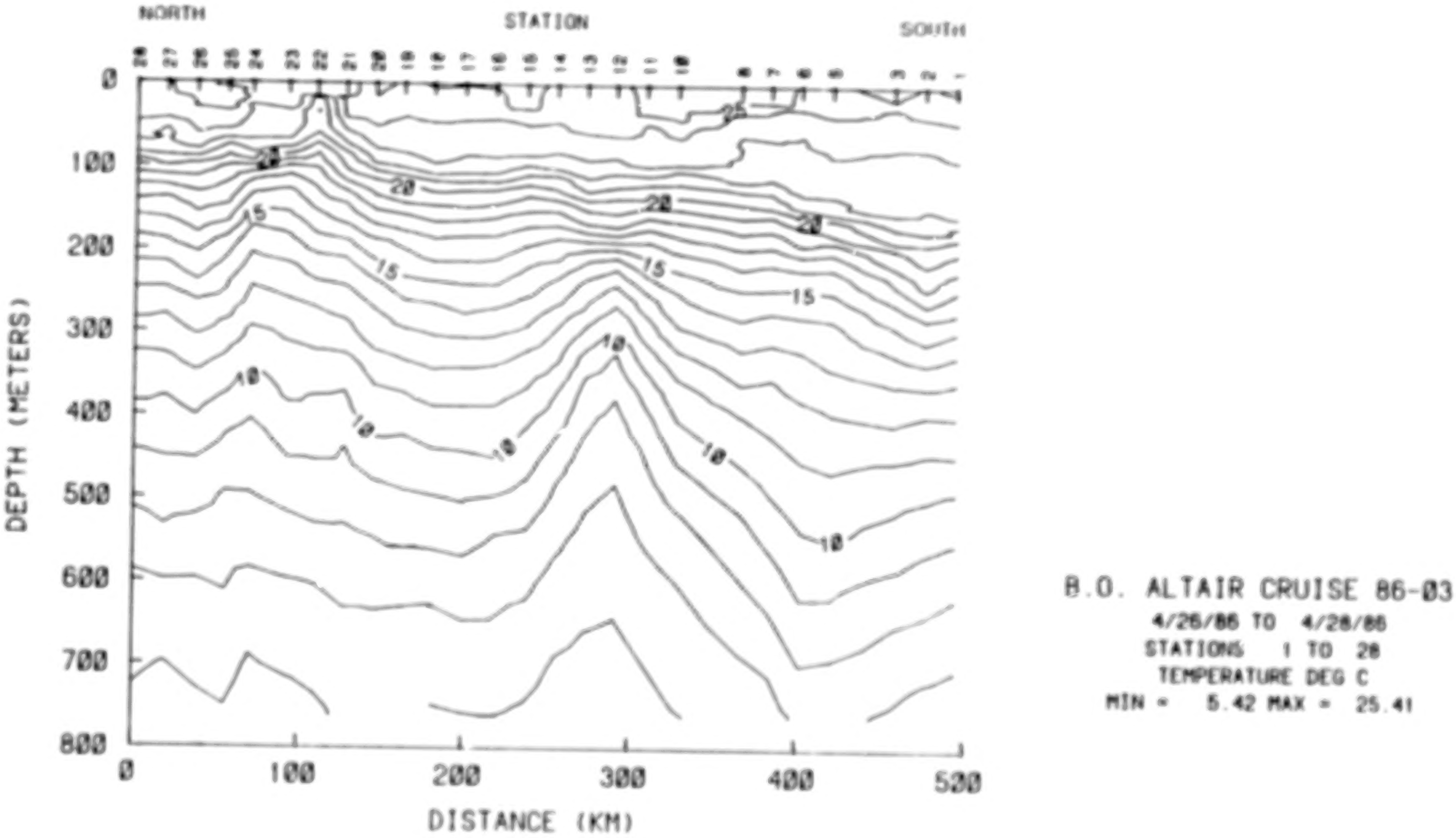

Figure 4.5-9. Vertical section of temperature to 800m between Station 1 and Station 28 for B/O ALTAIR XBT cruise AL-86-03 in April 1986.

4.6.2 Surface Currents

4.6.2.1 Interaction with Eddy C

At the time that Drifter 3378 turned eastward, a curious event which involved Eddy C occurred. Conditions for May 14 through 20, 1986 are shown in Figure 4.6-1a. As Drifter 3378 moved eastward, Drifter 3379 began to move towards the west at ~24.0°N. At about 94.0°W, Drifter 3379 abruptly turned northward (Figure 4.6-1b) to complete the outline of an elongated ellipse with an east-west orientation. Drifter 3379 then continued its anticyclonic rotation, but Drifter 3378 kept moving eastward toward the Loop Current. By June 15 to 21, 1986 (Figure 4.6-2), Drifter 3378 had moved northward around the Loop Current and had left the Gulf through the Florida Straits in mid-July 1986. Eddy C reached the Mexican coast at ~24.0°N (Figure 4.6-3a) 3 weeks later. At that time, Drifter 3379 began making large anticyclonic loops in the western Gulf (Figure 4.6-3b) and continued this type of motion through August 1986. These loops covered almost 4° in latitude and longitude. An XBT survey was conducted during August 17 through 22, 1986 (Figure 4.6-4), and the 8°C isothermal surface indicated a large, elongated anticyclone centered at about 23.0°N.

The XBT survey of April 26 through May 14, 1986 (Figure 4.5-7, p. 211) shows a distinct, closed, anticyclonic vortex in the western Gulf, the remnants of Eddy B. As Eddy C approached this vortex, Drifter 3378 made a large, anticyclonic loop and passed on the western side of the anticyclone shown in the XBT data. At this point, the two anticyclones began an interaction as depicted in Figure 4.6-1. The peculiar factor of this interaction was the elongated elliptical path taken by Drifter 3379. This "peanut"-shaped path had an east-west orientation, and the track occurred at the same time as Drifter 3378 made a sharp eastward turn and began tracking eastward. This apparently is not an unusual phenomenon, being seen in the trajectories of two previous drifter-tracked Gulf eddies (Kirwan et al., 1984a and b; Lewis and Kirwan, 1985). The XBT data from August 16 through 22, 1986 (Figure 4.6-4) give some indication of an elongated, east-west anticyclone in the western Gulf. Although the depth of the 8°C isotherm was shallower relative to the previous survey (Table 4.3-1, p. 96), the volume of the anticyclone appears to have grown substantially. Thus, speculation is that the interaction of Eddies B and C resulted in some coalescence.

The data set is not sufficiently extensive to determine how the two anticyclones may have coalesced. However, during the earlier hypothesized coalescence of Eddies A and B there was no indication of the "peanut" phenomenon in any of the drifter trajectories. It is true, however, that exaggerated elliptical trajectories were possibly made during that process. The elongated ellipses occurring during the interaction of Eddy B and Eddy A went beyond and well north of the center of rotation of Eddy B. In the case of Eddy B and Eddy C, the "peanut" occurred in between the centers of rotation.

The other form of coalescence for vortices of the same sign is the gradual joining of streamlines as the eddies touch (Chang, 1983). In such a case, a more central streamline remains closed (around one center of rotation) until all outlying streamlines have merged with those of the other center of rotation. At that time, the streamlines can merge with the corresponding streamlines of the other vortex. The general shape of a recently merged streamline is that of a dumbbell or peanut.

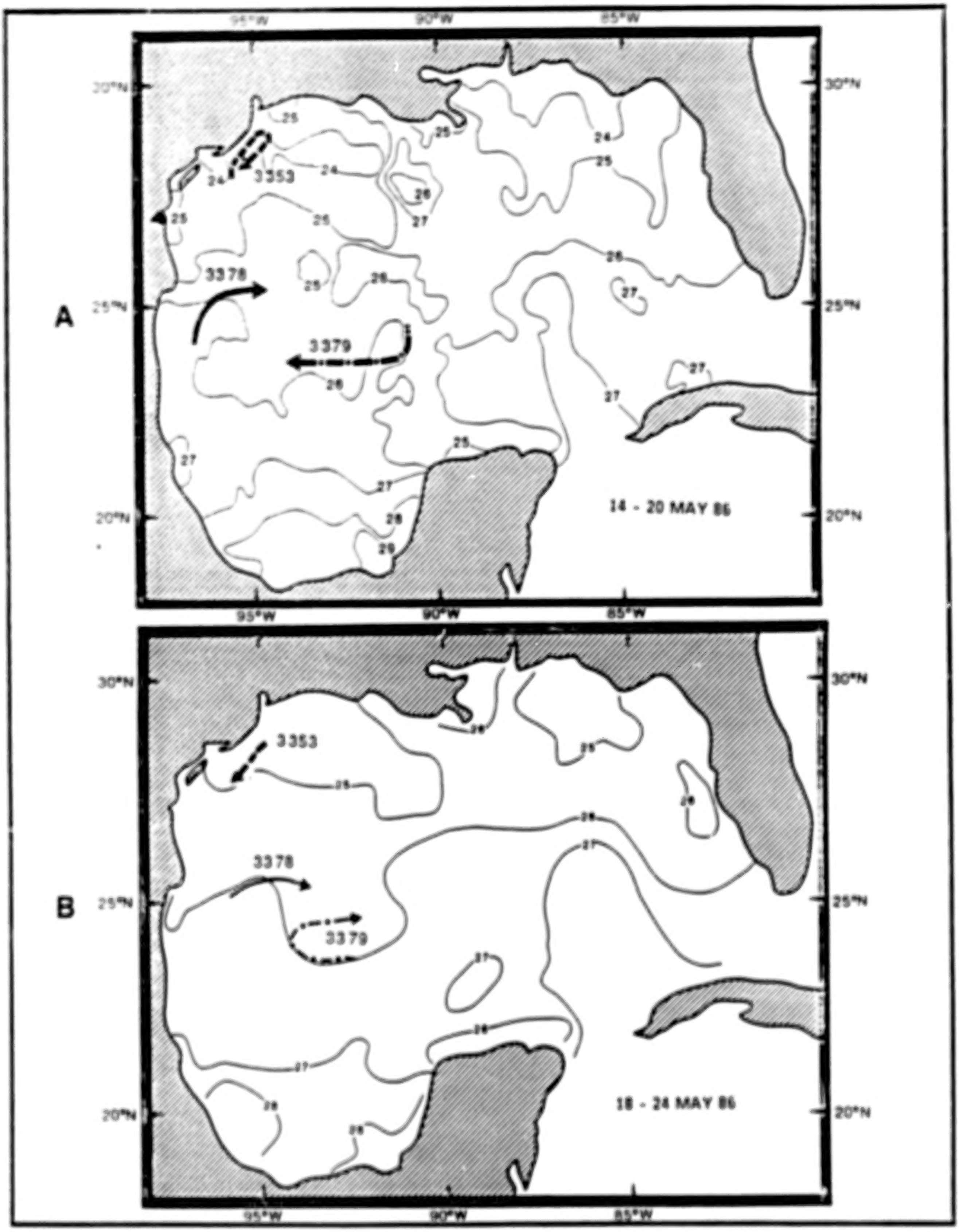

Figure 4.6-1. SST data (°C) for: (a) May 14-20, 1986 and (b) May 18-24, 1986. The drifter trajectories, shown by arrows, are identified in Table 2.2-1.

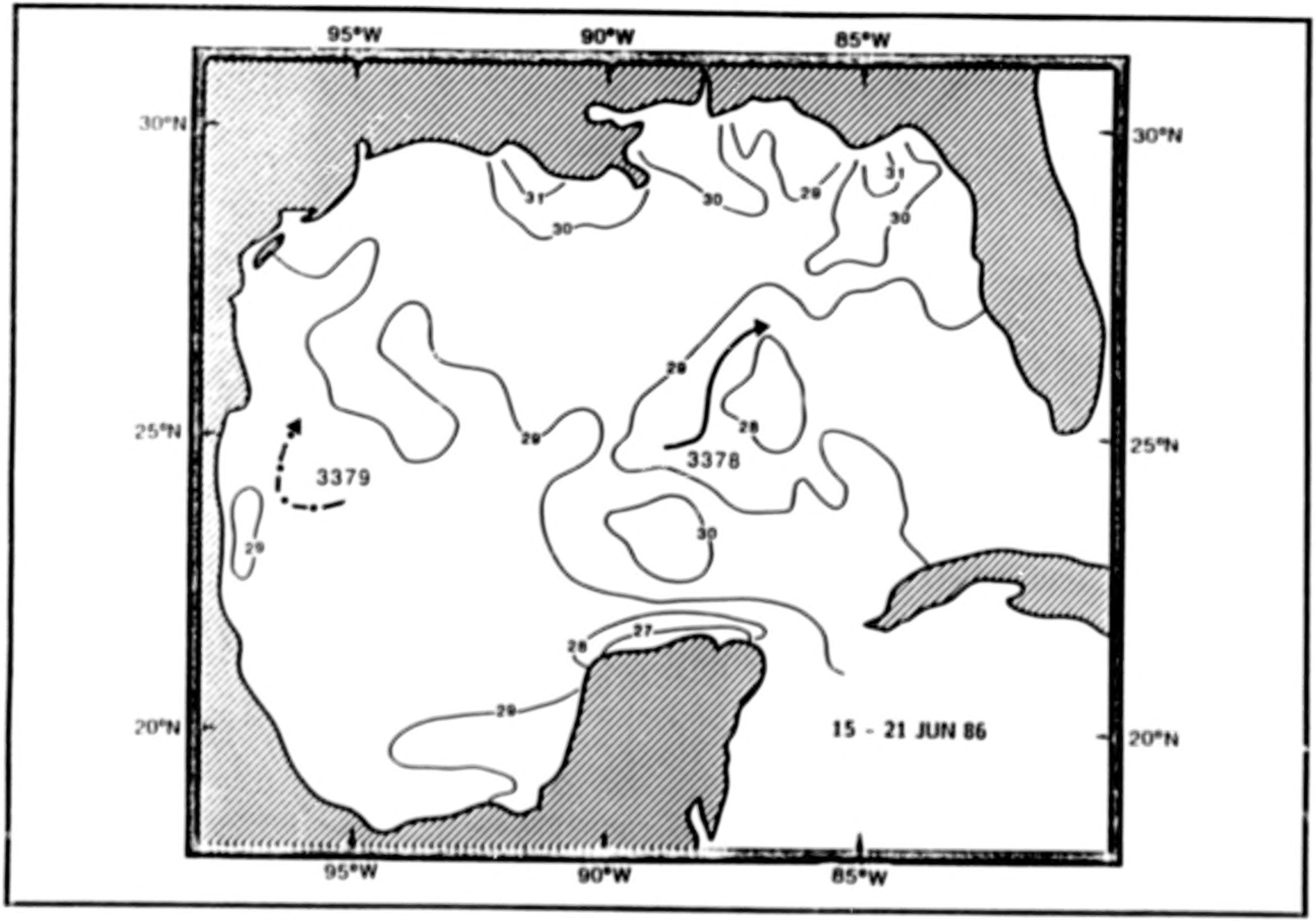

Figure 4.6-2. SST data (°C) for June 15-21, 1986. The drifter trajectories, shown by arrows, are identified in Table 2.2-1.

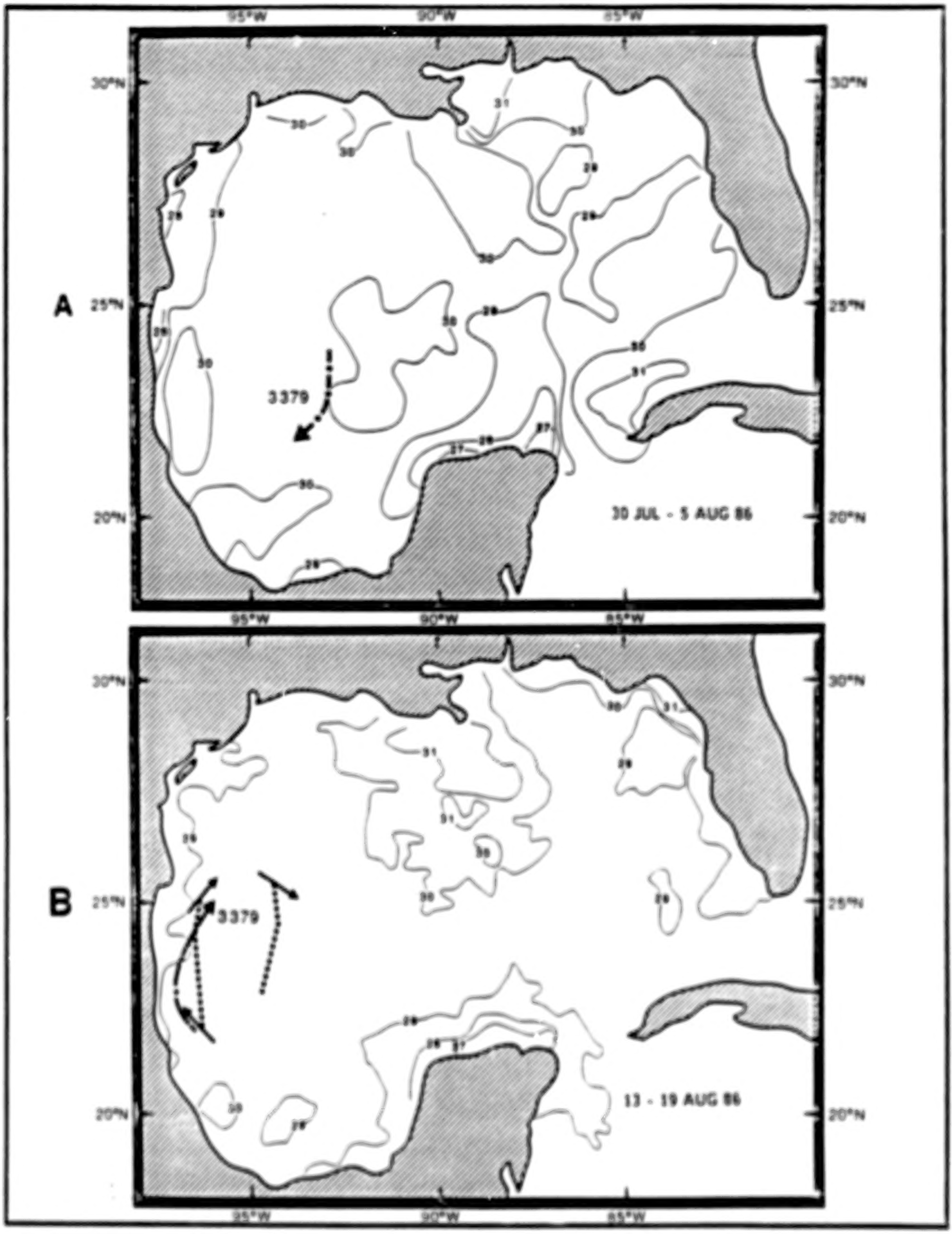

Figure 4.6-3. SST data (°C) for: (a) July 30 through August 5, 1986 and (b) August 13-19, 1986. Shorter arrows denote the flow at the edges of Eddy B while dotted lines indicate the locations of eddy waters (based on XBT data). The drifter trajectories, shown by arrows, are identified in Table 2.2-1.

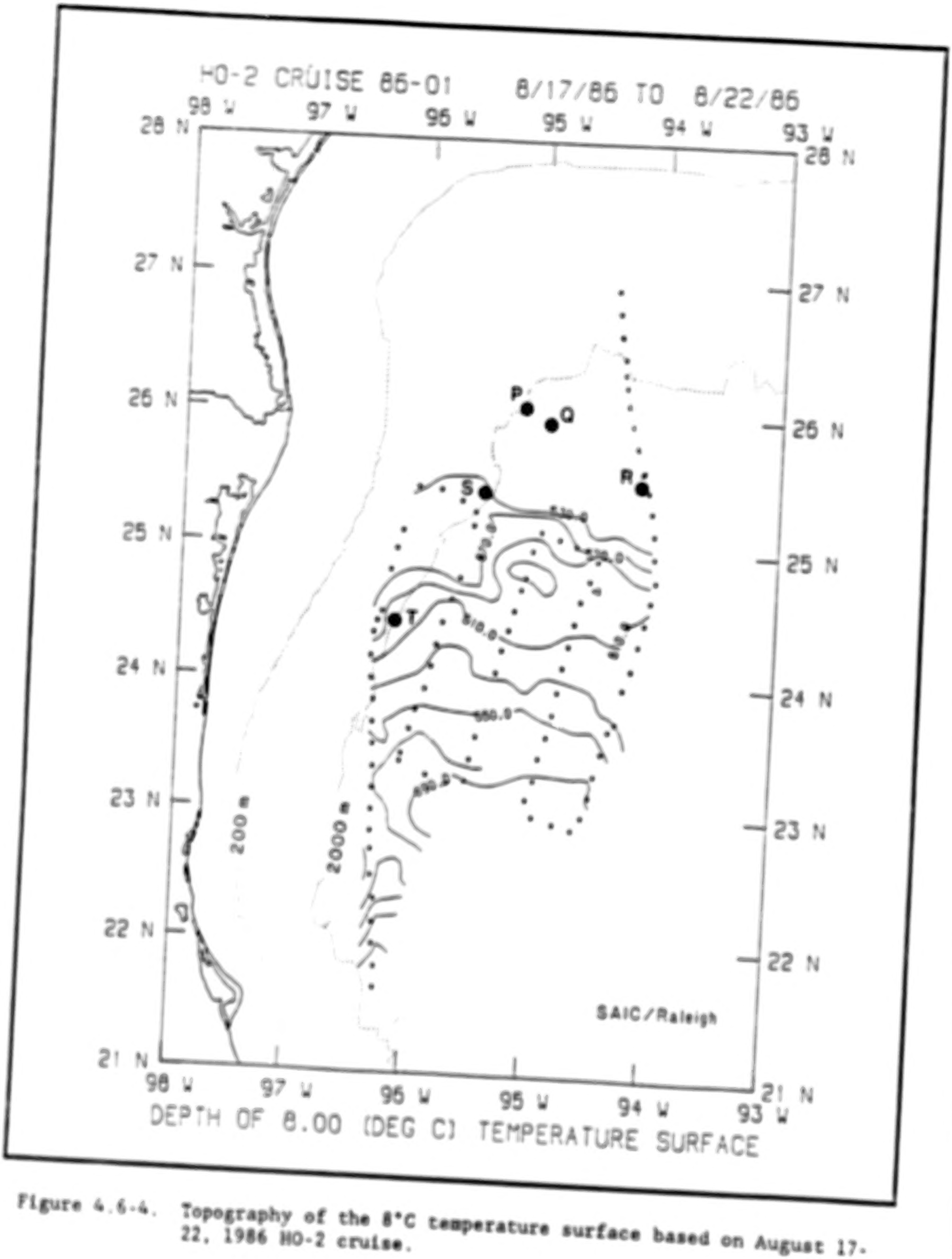

Figure 4.6-4. Topography of the 8°C temperature surface based on August 17-22, 1986 HO-2 cruise.

4.6.3 Temperature Fields

4.6.3.1 Consolidation of Eddies B and C

Following separation from the Loop Current in February 1985, Eddy C moved westward and southwestward across the Gulf. A position of Eddy C relative to Eddy B is shown in Figure 4.6-5 which is based on data from a sequence of B/O ALTAIR cruises in conjunction with temperature profiles taken from the EXXON JAMESTOWN. XBT's released by the EXXON JAMESTOWN provided information to a depth of 460m while the B/O ALTAIR obtained data to 760m. Conditions adjacent to the slope are best illustrated in Figure 4.5-7 (p. 211) which shows the 8°C isotherm representation of the anticyclone-cyclone pair. Higher in the water column, the associated temperature patterns are not as well resolved. The data from Figure 4.5-7 were used to locate the general area of the paired mesoscale circulation patterns in Figure 4.6-5. Figure 4.6-5 also shows that Eddy C had moved to the southwest after moving westward past the Yucatan shelf and slope. From these various data sets, it would appear that Eddies B and C were at approximately the same latitude with their centers separated by approximately 240 nautical miles.

The single XBT transect in mid-July (Figures 4.6-6 and 4.6-7) illustrates that an anticyclone-cyclone pair was still well developed adjacent to the western slope. However, reliance on such a single line does not provice information concerning possible interaction of Eddies B and C. As shown in Figure 4.2-13 (p. 65), Drifter 3379, which was originally released in Eddy C, begins in June to move clockwise around the region believed to contain Eddy B as shown in Figure 4.5-7 (p. 211). This process continued during July and August 1986. It is not clear whether the anticyclone seen in July 1986 is Eddy B, Eddy C or a combination of the two. The anticyclones shown in Figure 4.5-7 (Eddy B) and Figure 4.6-7 have comparable central depths of the 8°C isotherm. Note also that the cyclone on the northern end of this transect does not have appreciable signal above approximately 225m depth, and the surface-mixed layer (i.e., above the seasonal thermocline) is approximately 50m deep. Thus, there would be no temperature signature of the two features above 50m depth.

Figures 4.6-4, 4.6-8 and 4.6-9 present results of an XBT survey conducted in mid-August 1986 by the Mexican Navy Ship HO-2 in cooperation with MMS. Figures 4.6-4 and 4.6-9 contain contour plots of the 8°C, 15°C and 21°C isotherm depths. Comparison of the 8°C temperature contours from April to May (Figure 4.5-7, p. 211) and July (Figure 4.6-6) with these August observations shows that the cyclonic feature has changed location substantially or dissipated. Depths of the various isothermal surfaces suggest that a general area of warmer water may have been present south of 25°N. In Figure 4.6-4, the 8°C isotherm goes to 680m which is the same seen in previous cruises. However, the survey showed the gradient of isotherm depth to be much more gradual than seen previously. This could be explained in part by the apparent absence of the cyclone to the north. During previous cruises, the isotherm doming associated with the cyclone tended to intensify lateral thermal gradients. Based on a combination of drifter data and the XBT cruise data, it is probable that Eddies B and C interacted and possibly merged to form a large but more diffuse region of warm water (depressed isotherms).

4.6.3.2 Western Gulf of Mexico XBT Surveys in 1987

In 1987, Mexican scientists from the Instituto de Investigaciones Electricas conducted two major hydrographic surveys of the western Gulf south of 26°N

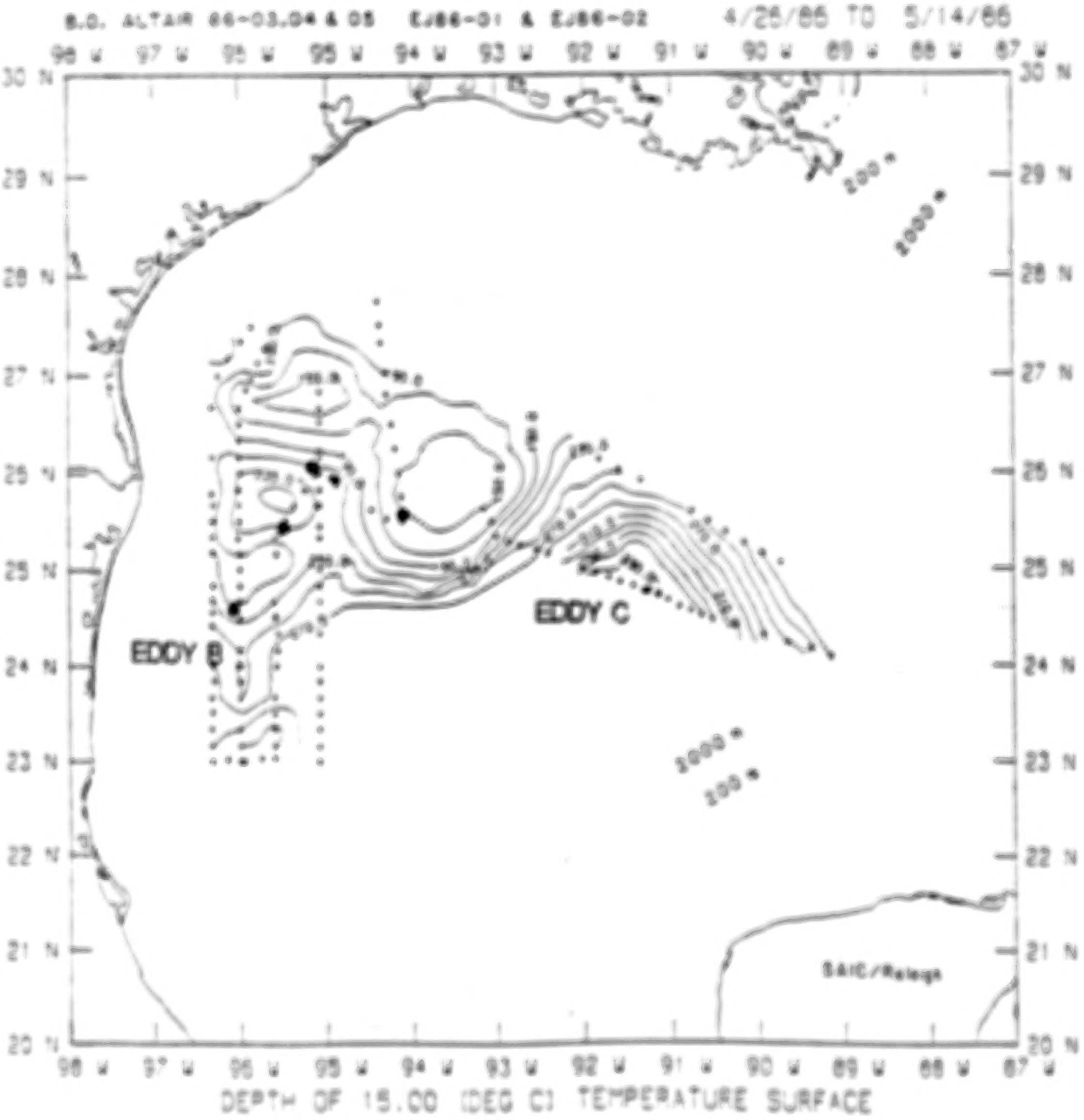

Figure 4.6-5. **Topography of the 15°C temperature surface in late April and early May 1986 based on SOOP cruises AL-86-03, AL-86-04, AL-86-05, EJ-86-01 and EJ-86-02.**

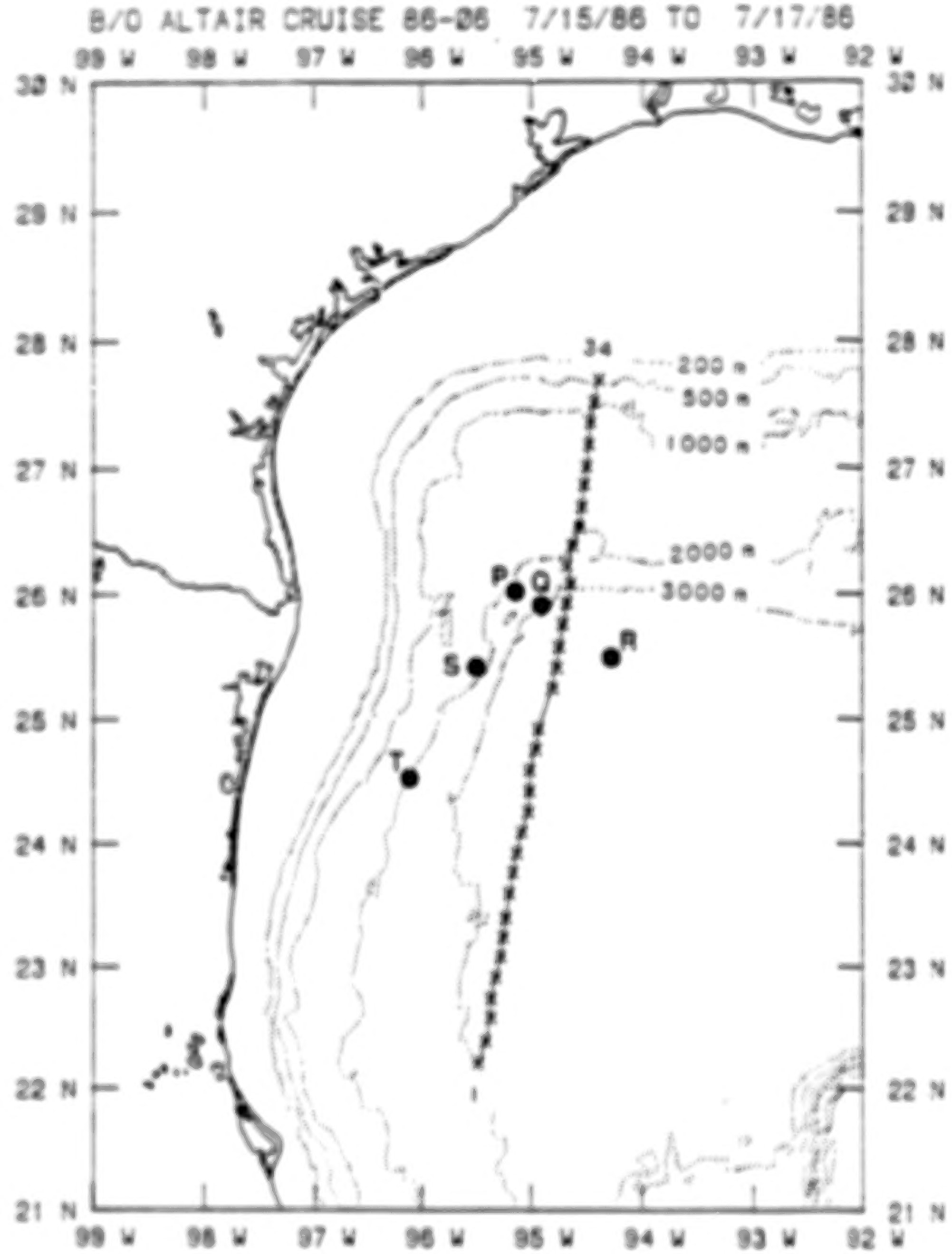

Figure 4.6-6. Cruise track for B/O ALTAIR cruise AL-86-06 in mid-July 1986.

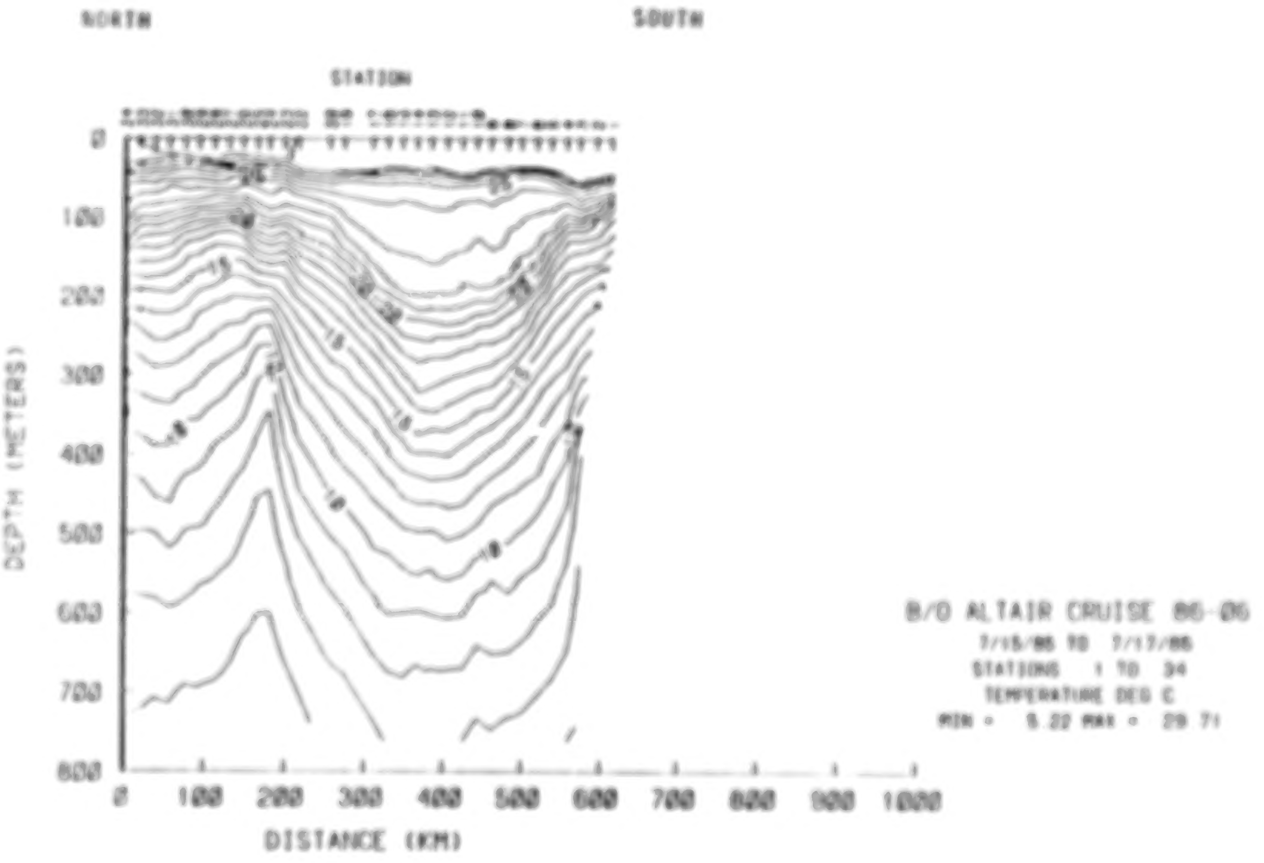

Figure 4.6-7. Vertical section of temperature to 800m between Station 1 and Station 34 for B/O ALTAIR XBT cruise AL-86-06 in mid-July 1986.

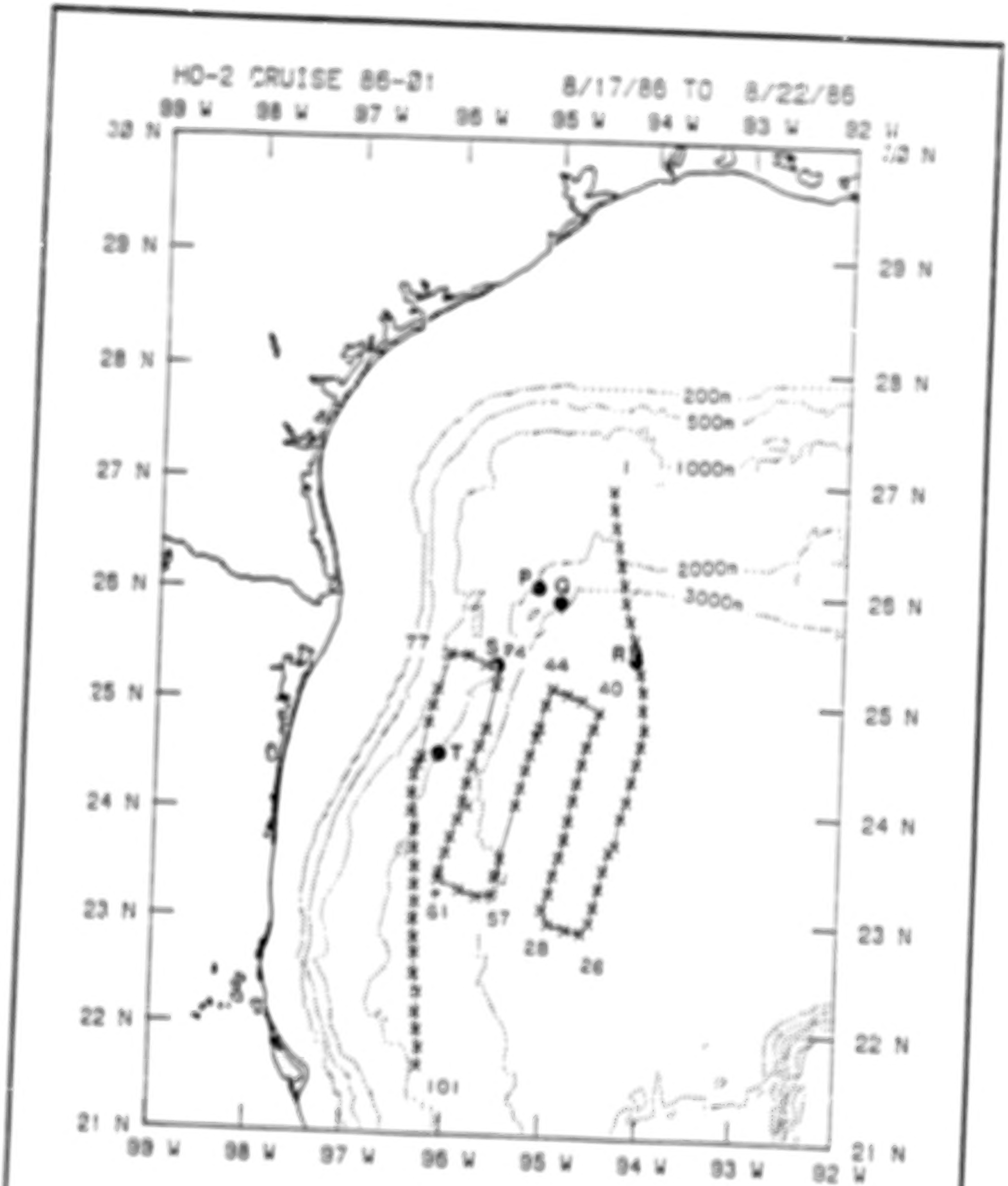

Figure 4.6-8. Cruise track for the HO-2 cruise and the location of all XBT stations occupied during the period from August 17-22, 1986.

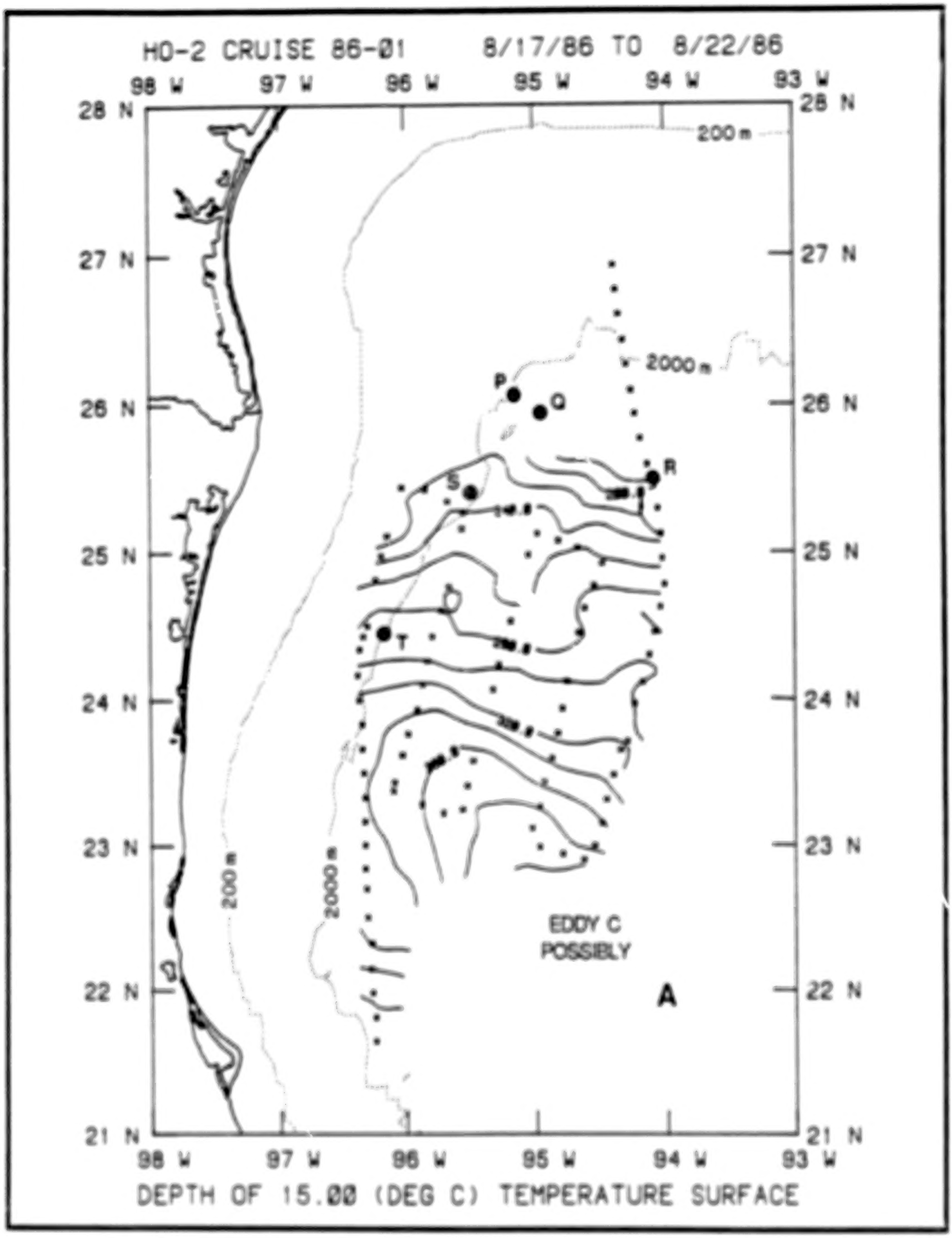

Figure 4.6-9a. Topography of the 15°C temperature surface based on the August 17-22, 1986 HO-2 cruise.

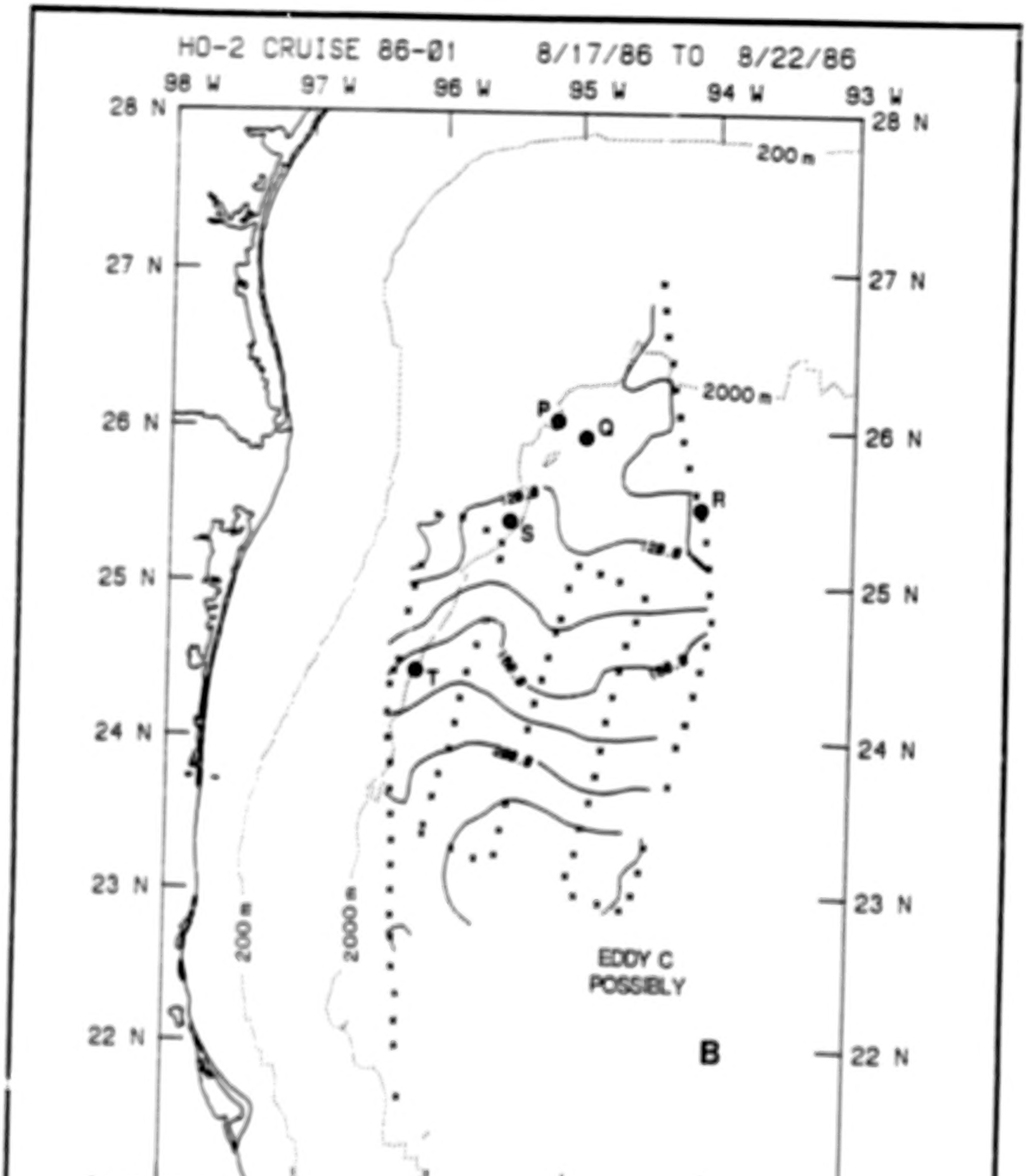

Figure 4.6-9b. Topography of the 21°C temperature surface based on the August 17-22, 1986 HO-2 cruise.

aboard the R/V JUSTO SIERRA. They also collected XBT data as part of the MMS SOOP program that are available for use in this study. Figure 4.6-10 shows the positions of the XBT stations for the May 1987 cruise, and Figures 4.6-11a and b show the depths of the 15°C and 21°C temperature surfaces. There is no temperature surface for 8°C for the May 1987 cruise because type T-4 XBT probes, which have a maximum depth capability of 450m, were used. The positions of the XBT stations for the second cruise in October 1987 are shown in Figure 4.6-12, and the depths of the 8°C, 15°C and 21°C temperature surfaces are shown in Figures 4.6-13a-c.

The prominent feature in the figures for the May 1987 cruise is a large Loop Current eddy that is believed to have separated in early 1987. Like Eddy A, this one followed a more westerly than southwesterly path across the Gulf. The May cruise mapped it before it began to interact strongly with the continental slope. The 280m depth contour of the 15°C isotherm in Figure 4.6-11a indicates that this eddy is very large--on the order of 450 km in diameter. Its core is slightly elliptical, with the major axis oriented north-south. Lobes protrude to the northeast and south in its outer portion. Some of this structure may, however, be an artifact of the several weeks over which the data were collected. Figure 4.6-14 shows the path of ARGOS drifter 7234 which was trapped in the eddy during April and May. The centers of the clockwise orbits migrate westward, and the diameters of the orbits increase until the drifter is ejected in early June, at which time the western side of the eddy appears to have reached the continental slope.

On the eastern or trailing side there is a partially resolved cyclonic feature. The spacing between the latitudinal lines of XBT stations is too wide to define the internal structure of the cyclonic feature. It is possible that instead of a single feature, there are two or more smaller ones. Figures 4.6-15 and 4.6-16 show the paths of ARGOS drifters 5839 and 5837, respectively. Drifter 5839 goes southward during June and July while undergoing a series of small cyclonic loops. The motion suggests the drifter is trapped in a small cyclone that is advecting clockwise along the southeastern periphery of the large anticyclone. Drifter 5837 is in the same region at the same time and exhibits small cyclonic revolutions as it moves anticyclonically around the major LC eddy. These drifter trajectories and XBT data strongly suggest the presence of cyclonically rotating features which are moving anticyclonically about the primary mesoscale eddy.

During August, the paths of ARGOS drifters 5839 and 5837 make similar, large anticyclonic orbits that indicate that the western edge of the anticyclone is located next to the continental shelf. The October 1987 cruise data show a very elliptical anticyclone oriented northeast-southwest. The western side of the anticyclone is located east of the 2000m isobath, and a cyclone lies over the continental slope. Although there are no drifrter data for the anticyclone during September, it is reasonable to speculate, given the behavior of Eddy B that was observed in great detail, that during September the anticyclone moved eastward off the topography and that the cyclone was spun up during the interaction of the anticyclone with the continental slope. If the anticyclone was moving during the 4 weeks of the October cruise, its ellipticity and some of the smaller scale features in Figures 4.6-13a-c may be artifacts.

In Figure 4.6-13, a small, weak anticyclone is centered near 24.5°N, 92.0°W. Its origin was not observed. It is also known, based on drifter data, that

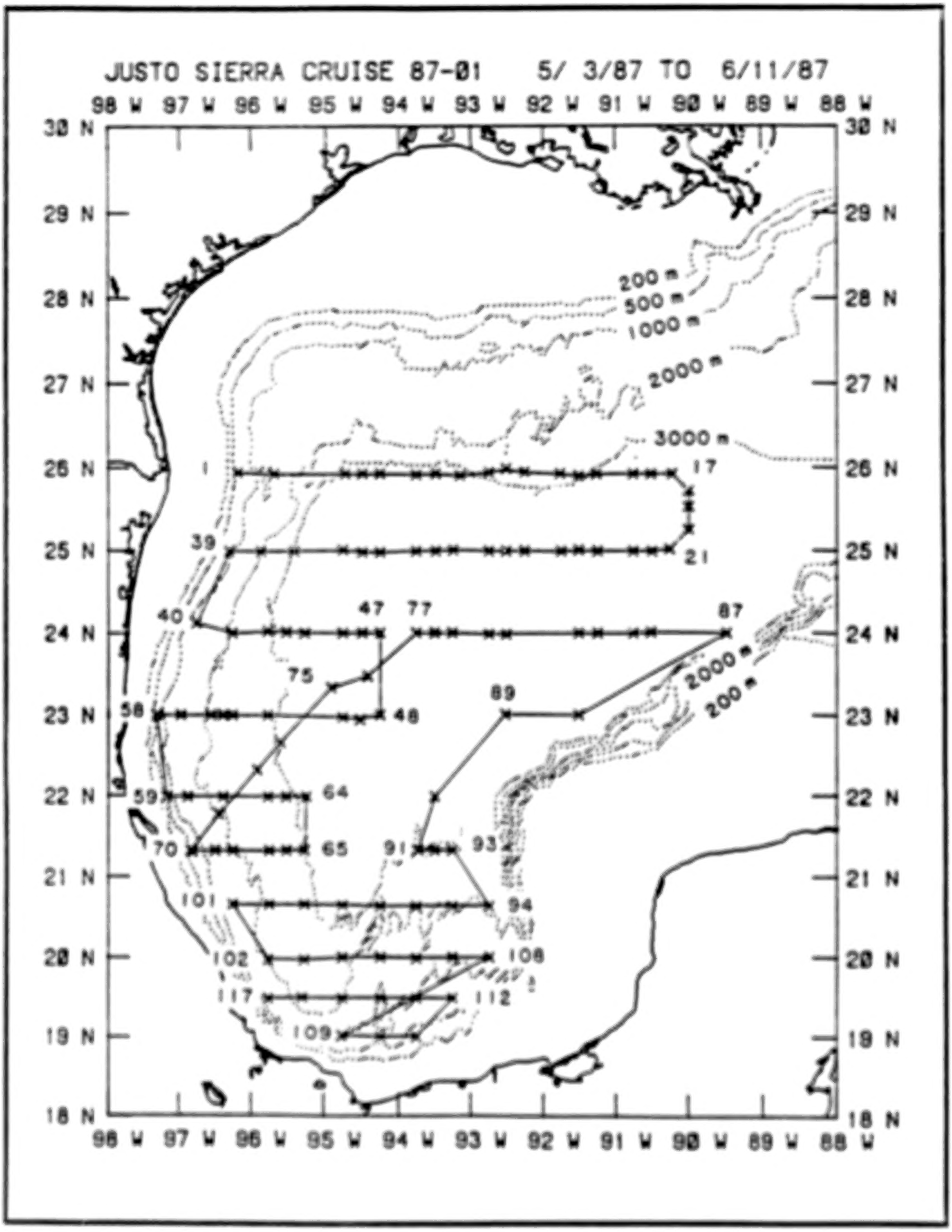

Figure 4.6-10. Cruise track of the R/V JUSTO SIERRA and the location of all XBT stations occupied during the period from May 3 through June 11, 1987.

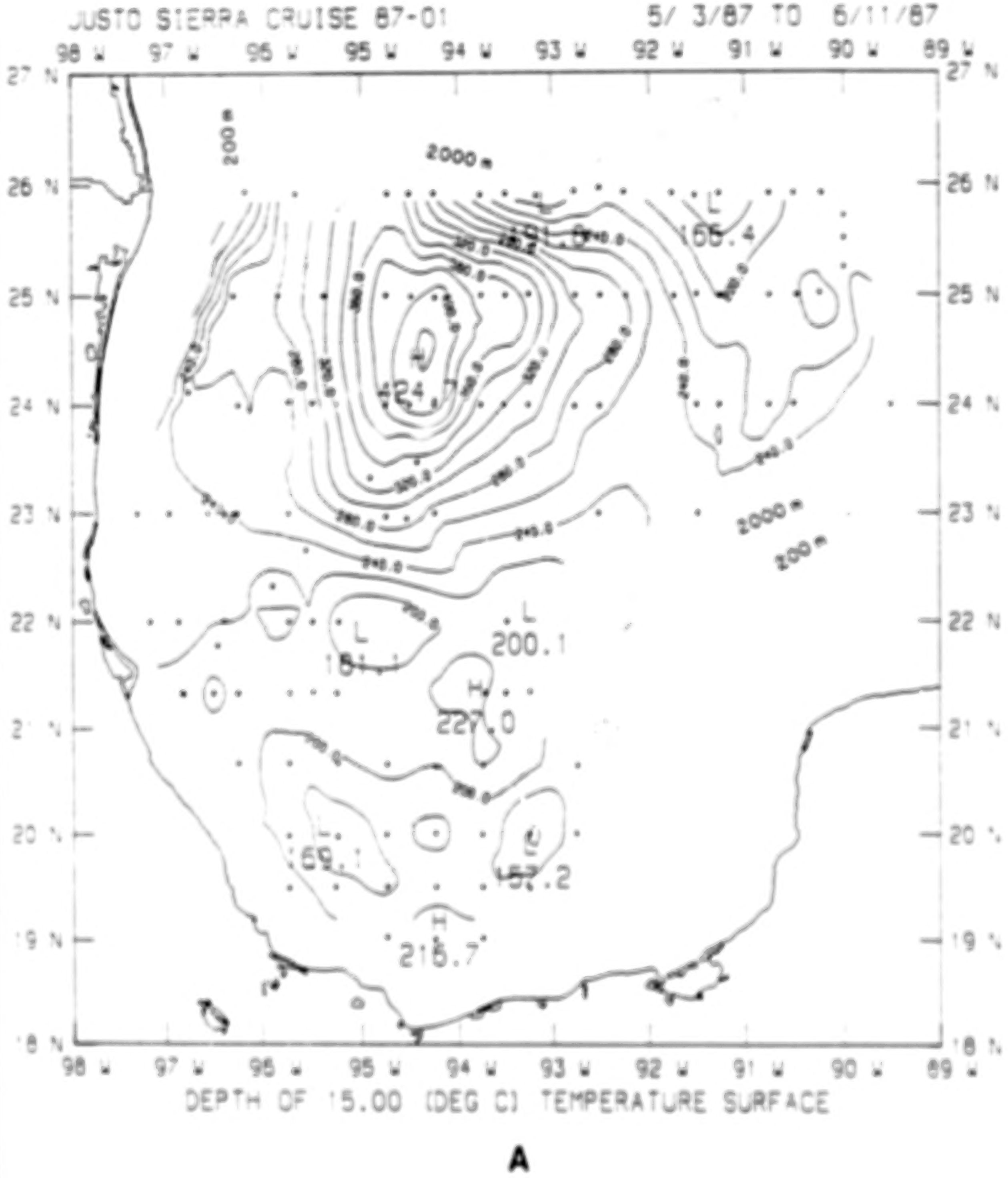

Figure 4.6-11a. Topography of the 15°C temperature surface based on XBT data for the May 1987 R/V JUSTO SIERRA cruise.

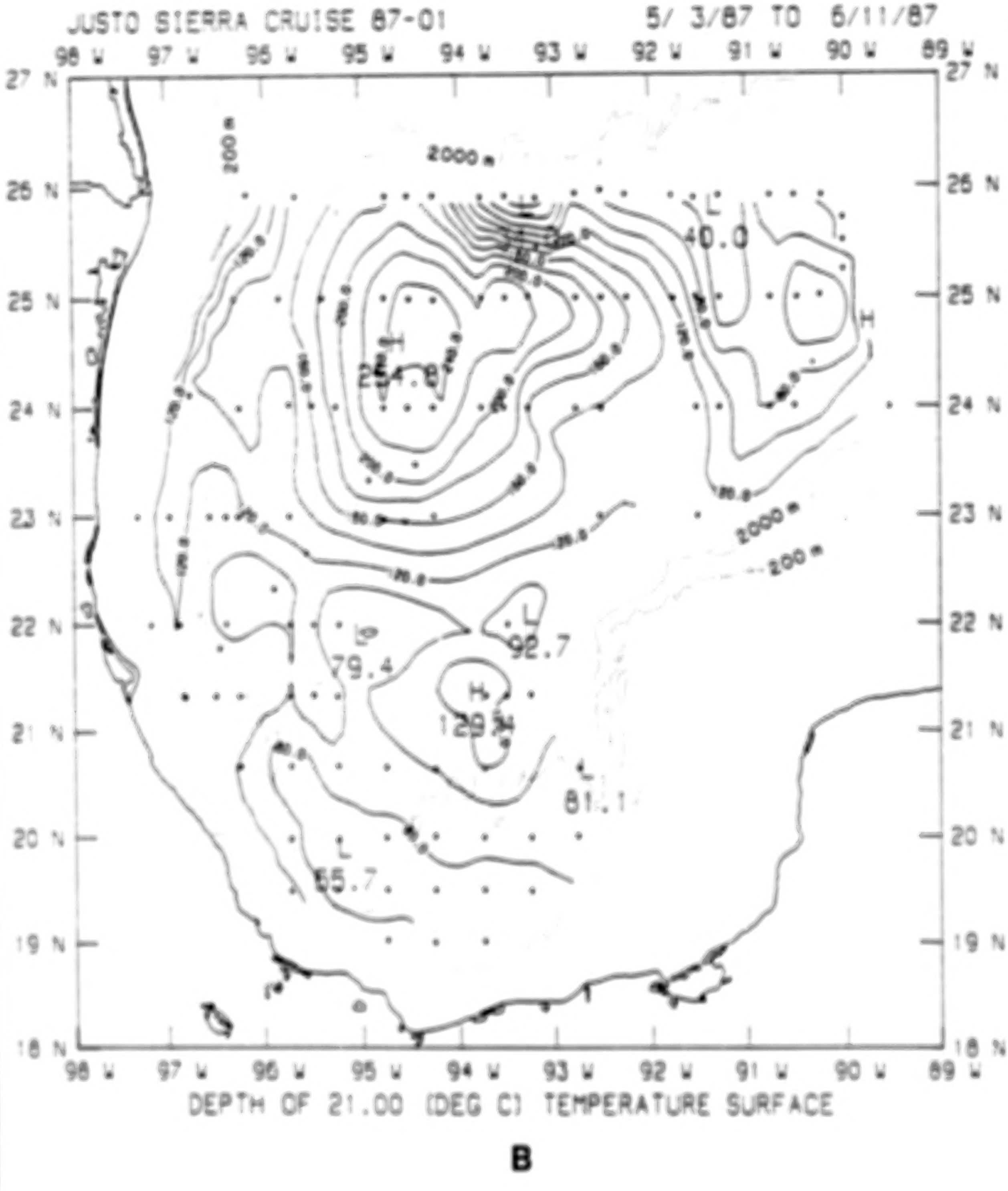

Figure 4.6-11b. Topography of the 21°C temperature surface based on XBT data for the May 1987 R/V JUSTO SIERRA cruise.

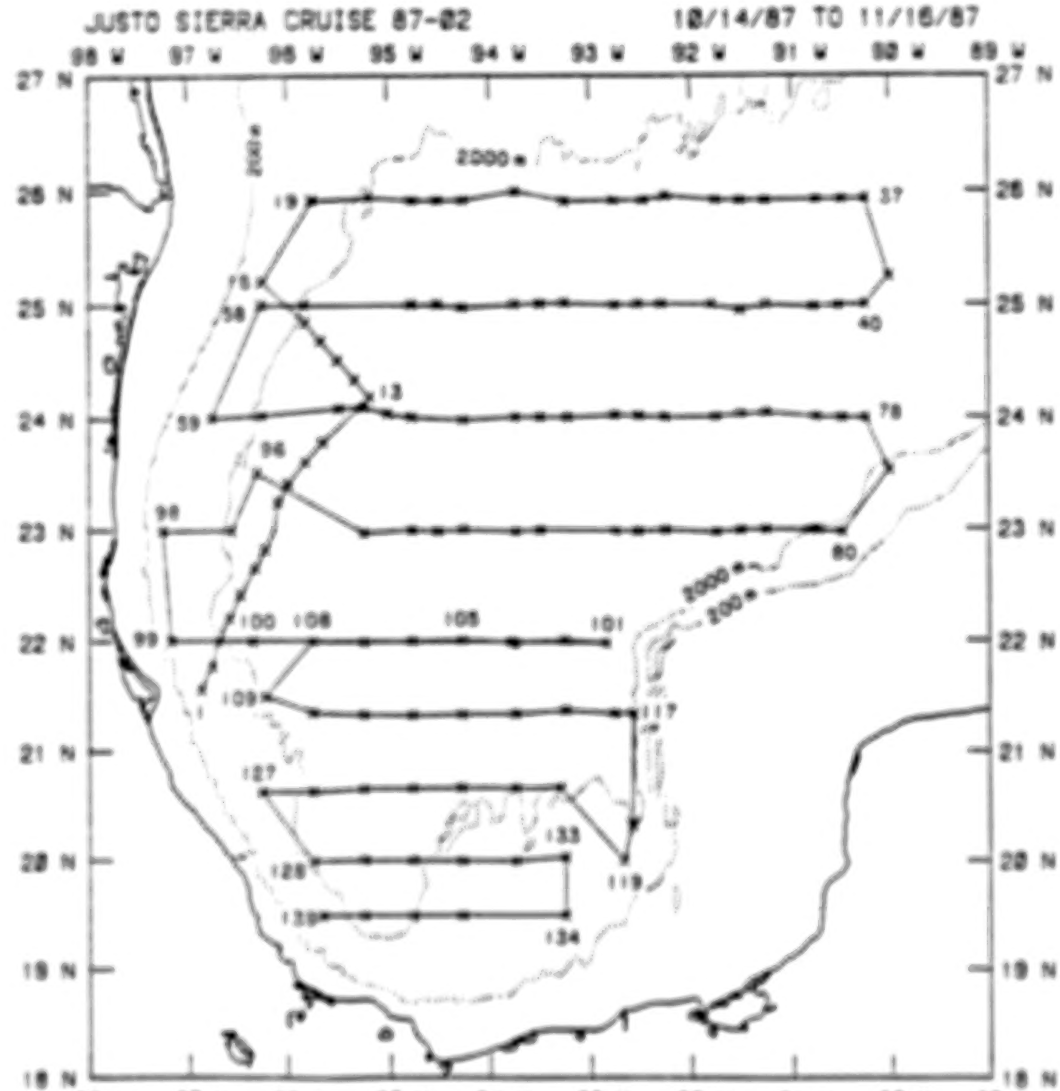

Figure 4.6-12. Cruise track of the R/V JUSTO SIERRA and the location of all XBT stations occupied during the period from October 14 through November 16, 1987.

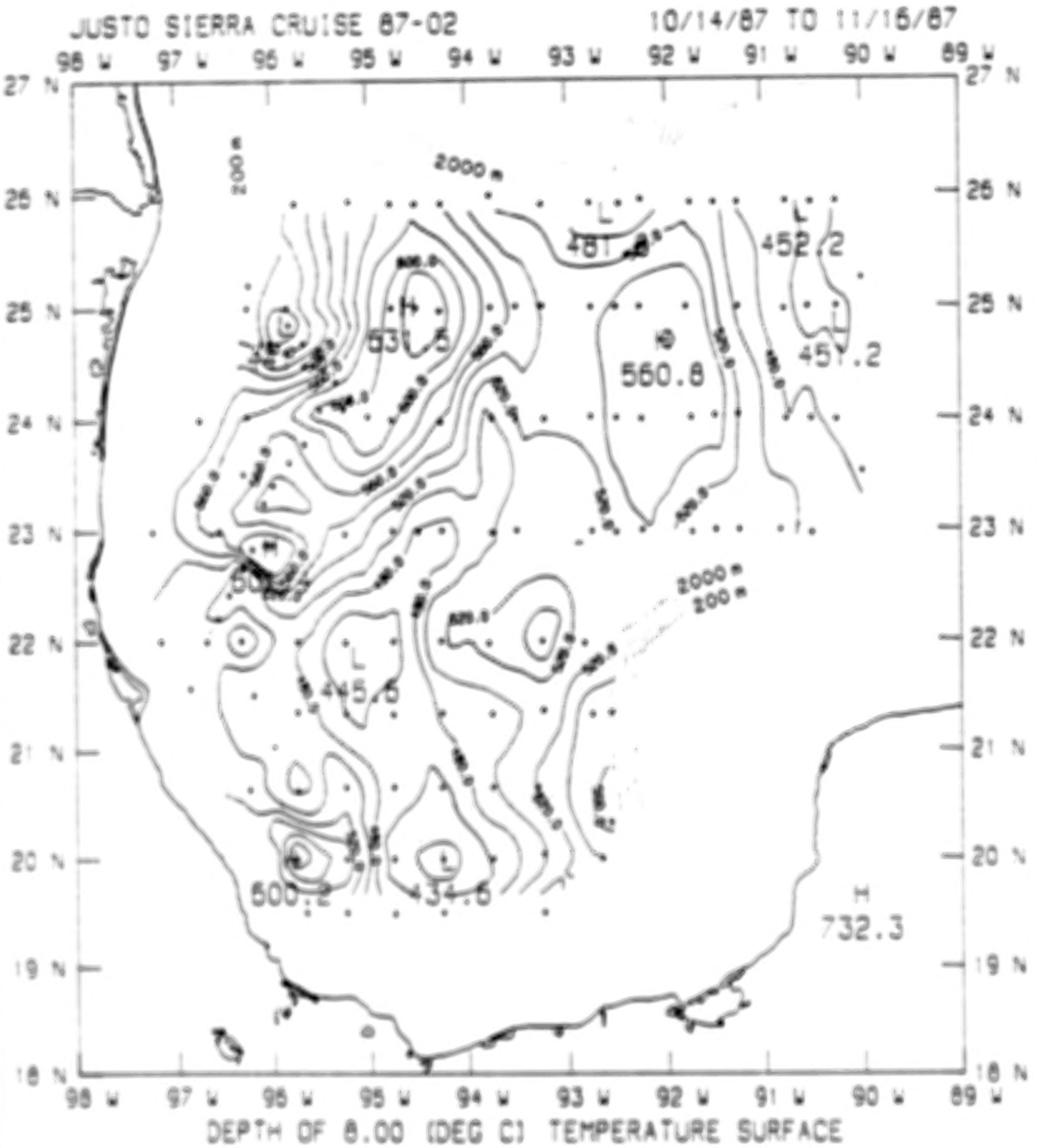

Figure 4.6-13a. Topography of the 8°C temperature surface based on XBT data for the October 1987 R/V JUSTO SIERRA cruise.

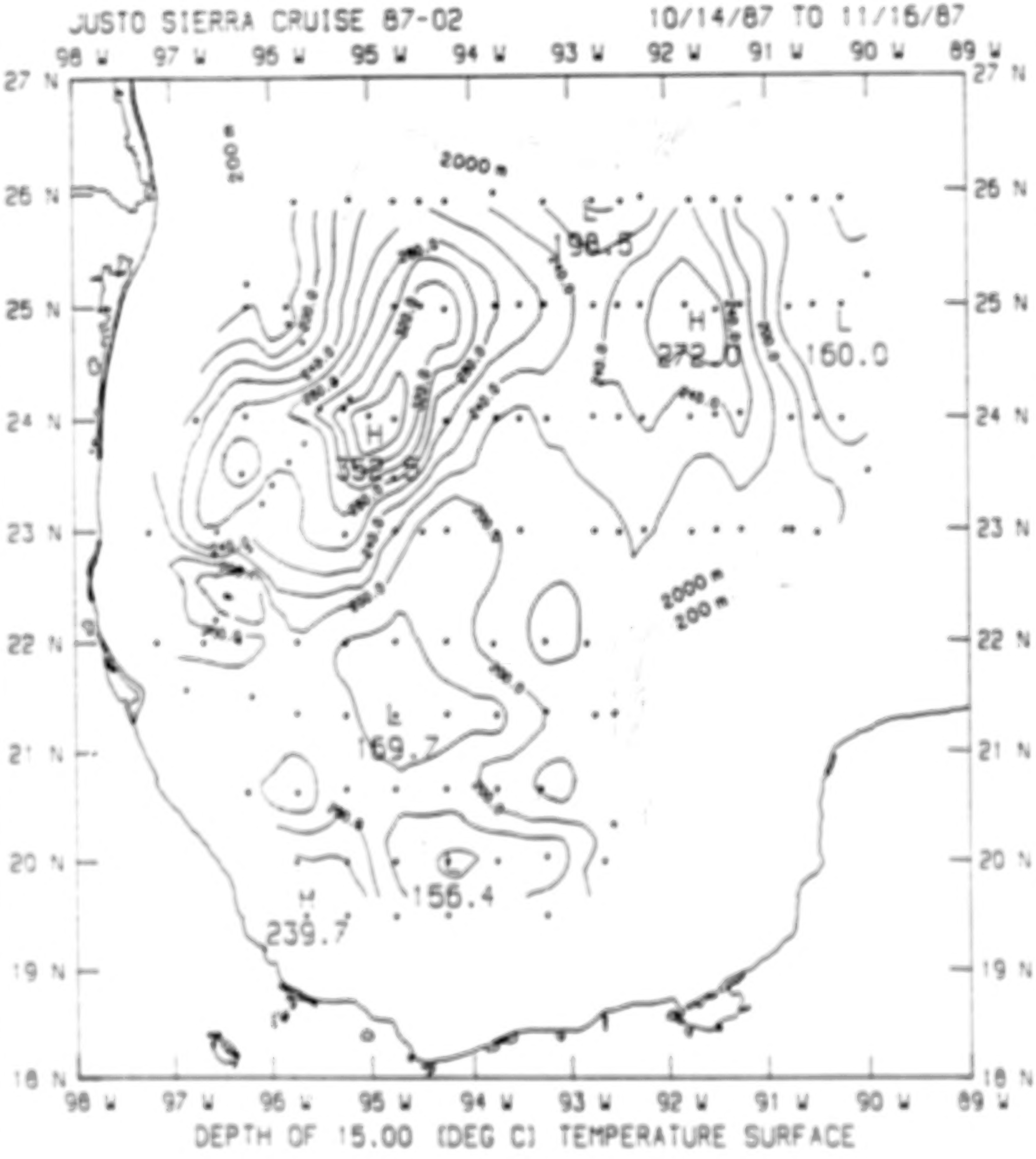

B

Figure 4.6-13b. Topography of the 15°C temperature surface based on XBT data for the October 1987 R/V JUSTO SIERRA cruise.

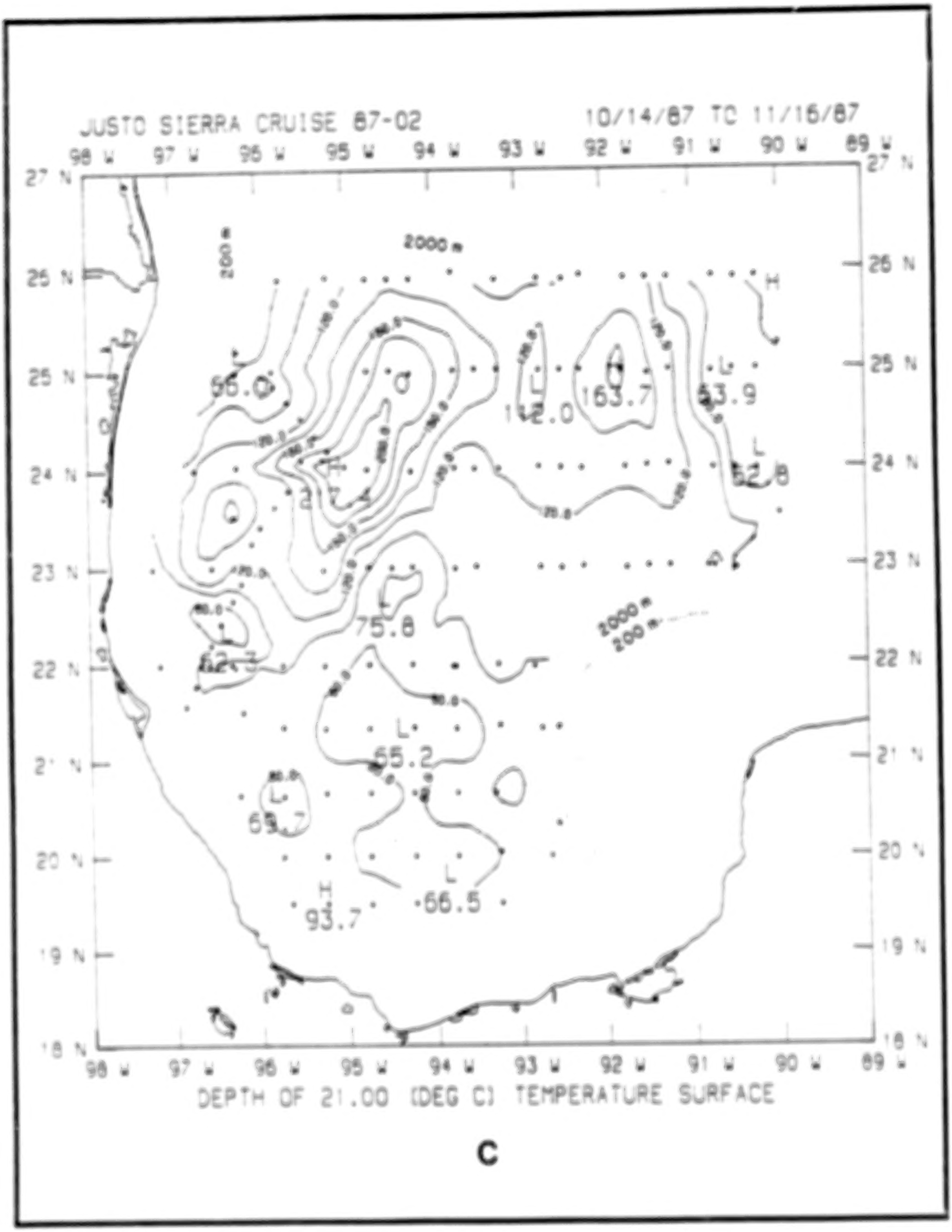

Figure 4.6-13c. Topography of the 21°C temperature surface based on XBT data for the October 1987 R/V JUSTO SIERRA cruise.

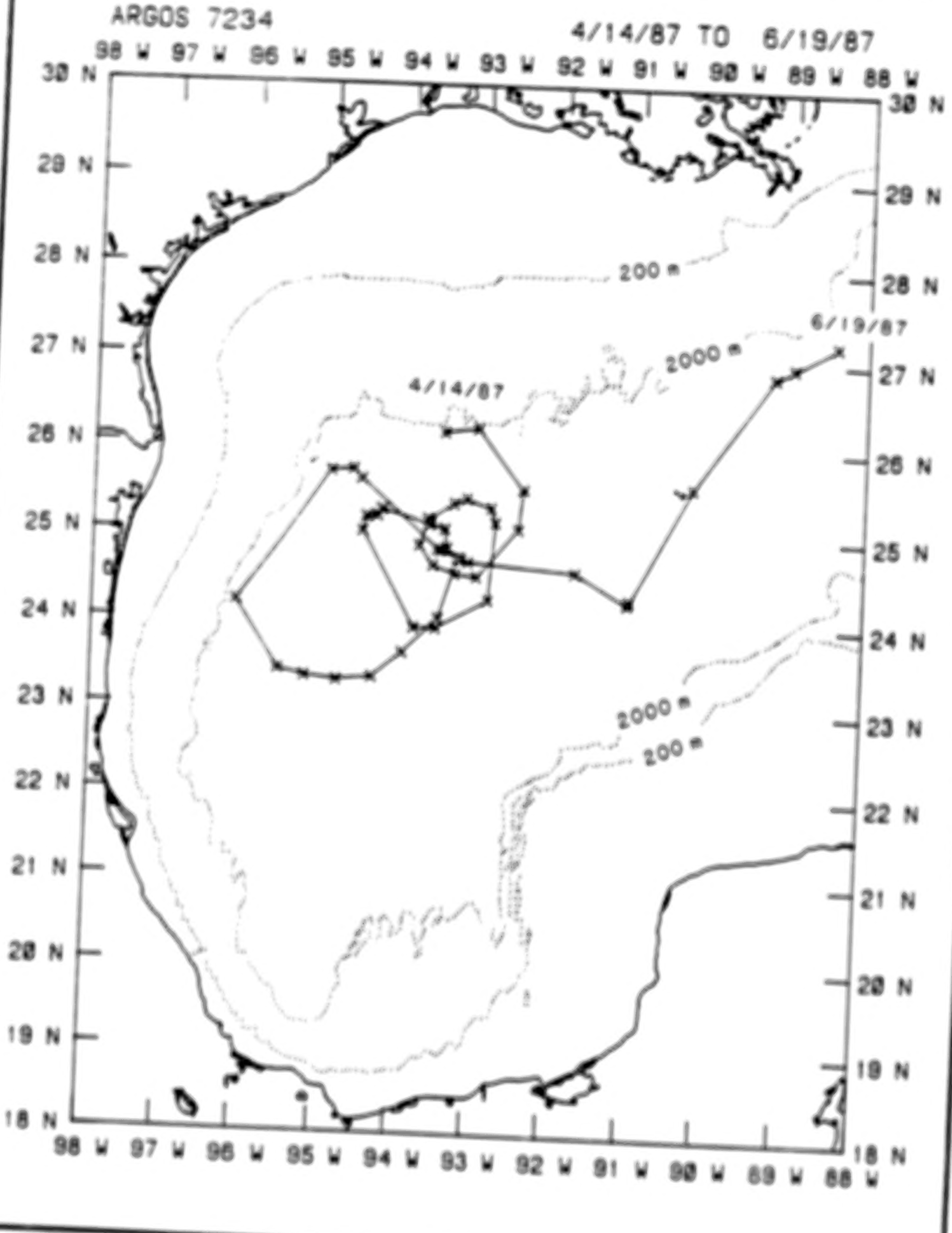

Figure 4.6-14. Trajectory of Drifter 7234 from April 14 to June 19, 1987. Each X indicates a one-day interval.

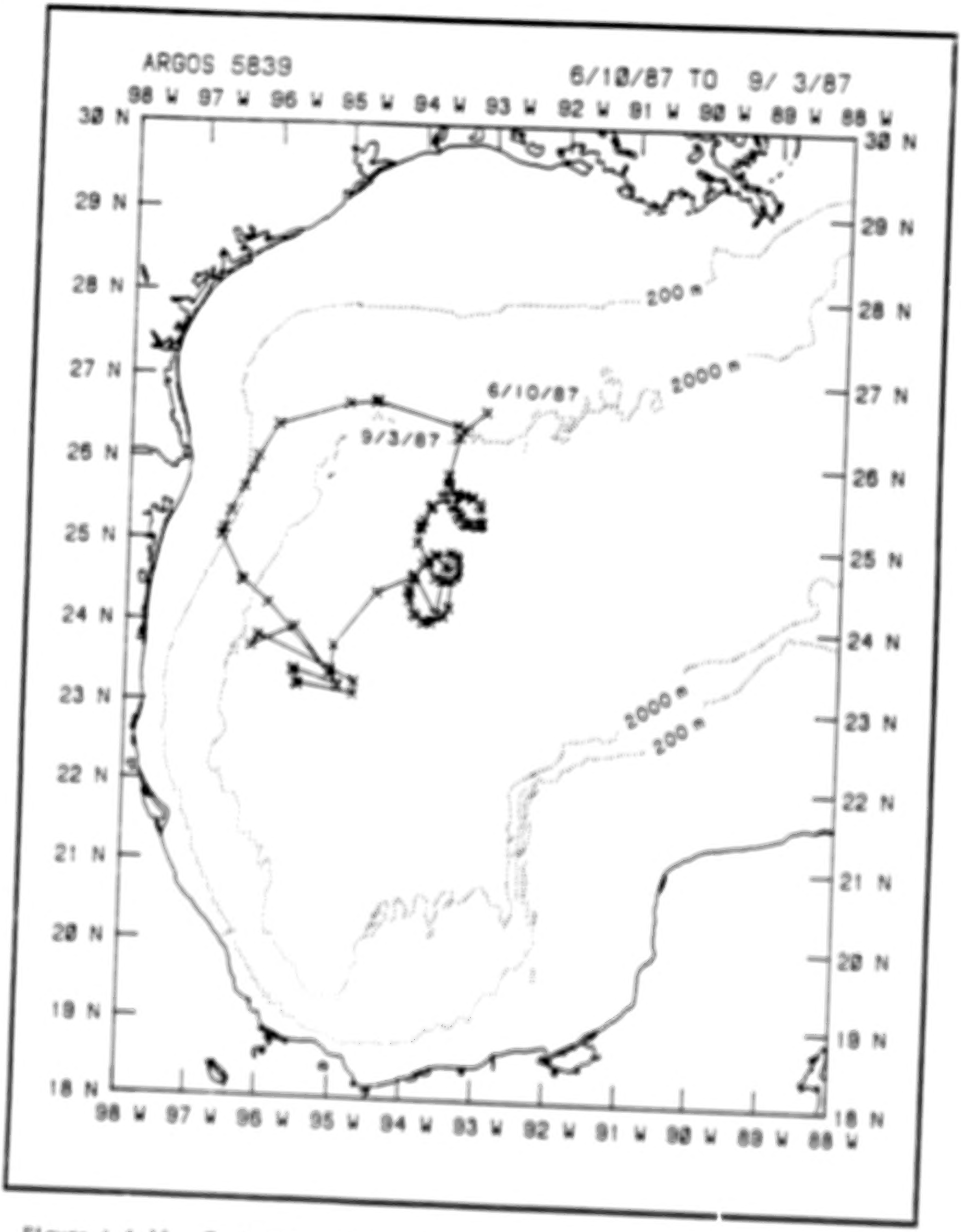

Figure 4.6-15. Trajectory of Drifter 5839 from June 10 to September 3, 1987. Each X indicates a one-day interval.

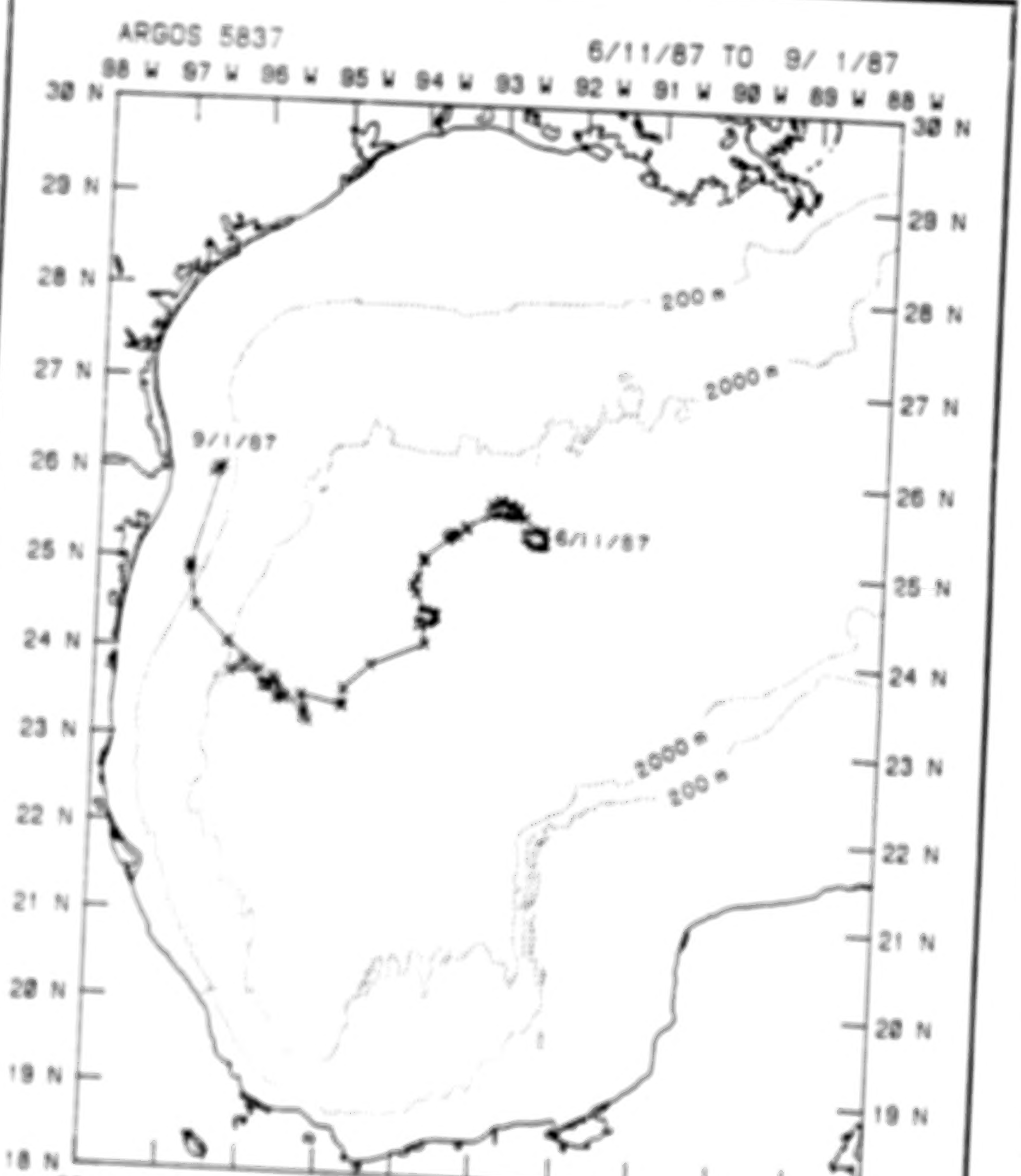

Figure 4.6-16. Trajectory of Drifter 5837 from June 11 to September 1, 1987. Each X indicates a one-day interval.

another anticyclone was centered with little change in position near 25.5°N, 88.5°W during the months of November and December.

The XBT surveys and drifter data during 1987 clearly suggest that a large eddy separated from the Loop Current, followed a path similar to that of Eddy B and evolved in a manner similar to Eddy B, at least through the reflection stage.

4.7 References for Chapter 4

Auer, S.J. 1987. Five-year climatological survey of the Gulf Stream System and its associated rings. J. Geophys. Res. 92(C11): 11709-11726.

Bane, J.M., Jr., D.A. Brooks and K.R. Lorenson. 1981. Synoptic observations of the three-dimensional structure and propagation of Gulf Stream meanders along the Carolina continental margin. J. Geophys. Res. 86(C7): 6411-6425.

Brooks, D.A. 1983. The wake of Hurricane Allen in the western Gulf of Mexico. J. Phys. Oceanogr. 13(1): 117-129.

Brooks, D.A. 1984. Current and hydrographic variability in the northwestern Gulf of Mexico. J. Geophys. Res. 89: 8022-8032.

Brooks, D.A. and J.M. Bane, Jr. 1978. Gulf Stream deflection by a bottom feature off Charleston, South Carolina. Science 201: 1225-1226.

Brooks, D.A., and R.V. Legeckis. 1982. A ship and satellite view of hydrographic features in the western Gulf of Mexico. J. Geophys. Res. 87: 4195-4206.

Chang, S.W. 1983. A numerical study of the interactions between two tropical cyclones. Mon. Wea. Rev. 111: 1806-1817.

Cresswell, G.R. 1982. The coalescence of two East Australian Current warm-core eddies. Science 215: 161-164.

Cushman-Roisin, B. 1987. Exact analytical solutions for elliptical vortices of the shallow water equations. Tellus 39A: 235-244.

Elliott, B.A. 1979. Anticyclonic rings and the energetics of the circulation of the Gulf of Mexico. Ph.D. Dissertation, Texas A&M University, College Station, Texas. 188 pp.

Hofmann, E.E., and S.J. Worley. 1986. An investigation of the circulation of the Gulf of Mexico. J. Geophys. Res. 91(C12): 14221-14236.

Hooker, S.B. 1987. Mesoscale eddy dynamics by the method of point vortices. Ph.D. Dissertation, Univ. of Miami, Coral Gables, Fla. 158 pp.

Kirwan, A.D., Jr., W.J. Merrell, Jr., J.K. Lewis and R.E. Whitaker. 1984a. Lagrangian observations of an anticyclonic eddy in the western Gulf of Mexico. J. Geophys. Res. 89(C3): 3417-3424.

Kirwan, A.D., Jr., W.J. Merrell, Jr., J.K. Lewis, R.E. Whitaker and R. Legeckis. 1984b. A model for the analysis of drifter data with an application to a warm core eddy in the Gulf of Mexico. J. Geophys. Res. 89(C3): 3425-3438.

Legeckis, R.V. 1979. Satellite observations of the influence of bottom topography on the seaward deflection of the Gulf Stream off Charleston, South Carolina. J. Phys. Oceanogr. 9(3): 483-497.

Lewis, J.K., and A.D. Kirwan, Jr. 1985. Some observations of eddy topography and ring-ring interactions in the Gulf of Mexico. J. Geophys. Res. 90(C5): 9017-9028.

Merrell, W.J., Jr., and J.M. Morrison. 1981. On the circulation of the western Gulf of Mexico with observations from April 1978. J. Geophys. Res. 86: 4181-4185.

Merrell, W.J., Jr., and A.M. Vazquez. 1983. Observations of changing mesoscale circulation patterns in the western Gulf of Mexico. J. Geophys. Res. 88: 7721-7723.

Mooers, C.N.K. 1973. A technique for the cross-spectrum analysis of pairs of complex-valued time series, with emphasis on properties of polarized components and rotational invariance. Deep-Sea Res. 23: 613-628.

Morrison, J.M., W.J. Merrell, Jr., R.M. Key and T.C. Key. 1983. Property distributions and deep chemical measurements within the western Gulf of Mexico. J. Geophys. Res. 88(C4): 2601-2608.

Nof, D., and L. M. Simon. 1987. Laboratory experiments on the merging of nonlinear anticyclonic eddies. J. Phys. Oceanogr. 17: 343-357.

Nowlin, W.D., Jr. 1972. Winter circulation patterns and property distributions. In: L.R.A. Capurro and J.L. Reid (eds.), Texas A&M University Oceanog. Stud., Vol. 2. Gulf Publishing Co., Houston, pp 3-51.

Pequegnat, W.E. 1972. A deep bottom current on the Mississippi cone. In: L.R.A. Capurro and J.L. Reid (eds.), Contributions on the Physical Oceanography of the Gulf of Mexico. Gulf Publishing Co., Houston, pp 65-87.

Pond, S. and G.L. Picard. 1983. Introductory Dynamical Oceanography. Pergamon Press, Oxford.

Rao, P.K., A.E. Strong and R. Koffler. 1971. Gulf Stream meanders and eddies as seen in satellite infrared imagery. J. Phys. Oceanogr. 2: 237-239.

Science Applications International Corporation. 1987. Gulf of Mexico physical oceanography program, final report, year 4. Volume II: technical report. MMS Contract No. 14-12-0001-29158, SAIC Report No. SAIC-87/1027. 226 pp.

Smith, D.C., IV. 1986. A numerical study of Loop Current eddy interaction with topography in the western Gulf of Mexico. J. Phys. Oceanogr. 16: 1260-1272.

Smith, D.C., and J.J. O'Brien. 1983. The interaction of a two layer isolated mesoscale eddy with topography. J. Phys. Oceanogr. 13: 1681-1697.

Vukovich, F.M., and B.W. Crissman. 1980. Some aspects of gulf stream western boundary eddies of the east coast of Florida. J. Phys. Oceanogr. 9: 1214-1222.

Vukovich, F.M., and B.W. Crissman. 1986. Aspects of warm rings in the Gulf of Mexico. J. Geophys. Res. 91(C2): 2645-2660.

Wallcraft, A.J. 1986. Gulf of Mexico circulation modeling study, annual progress report: year 2, progress report by JAYCOR submitted to the Minerals Management Service, Metairie, LA. MMS Contract No. 14-12-0001-30073. 94 pp.

As the Nation's principal conservation agency, the Department of the Interior has responsibility for most of our nationally owned public lands and natural resources. This includes fostering the wisest use of our land and water resources, protecting our fish and wildlife, preserving the environmental and cultural values of our national parks and historical places, and providing for the enjoyment of life through outdoor recreation. The Department assesses our energy and mineral resources and works to assure that their development is in the best interest of all our people. The Department also has a major responsibility for American Indian reservation communities and for people who live in Island Territories under U.S. Administration

242

N 95/ 19391

END

12-16-91